



Characterizing quantum systems based on non-classical correlations

By

EKTA PANWAR

Supervisor: DR HAB. INŻ. MARCIN WIEŚNIAK

Institute of Theoretical Physics and Astrophysics,
Faculty of Mathematics, Physics and Informatics
UNIVERSITY OF GDAŃSK

ACKNOWLEDGEMENT

This work would not have been possible without the guidance and invaluable insights provided by my supervisor, Marcin Wieśniak. I thank him for giving me the time and freedom I needed to explore and develop a passion for what I wanted to pursue further in science. I am indebted to him for all the opportunities he has given me.

I am immensely grateful to Mracin Pawłowski for introducing me to the field of device and semi-device independent theory, which I thoroughly enjoyed exploring and working on during my PhD. I also sincerely appreciate his financial support during this time.

My deepest gratitude goes to my wonderful co-workers Tushita Prasad, Paweł Mazurek, Chithra Raj, Giuseppe Viola, Pedro Ruas-Diequez, Giovanni Scala, Palash Pandya, Ray Ganardi, Mahasweta Pandit, and Paulo J. Cavalcanti for fostering a supportive and peaceful work environment. Profound thanks also to Marek Żukowski, Nicolás Gigena, Máté Farkas, and Tomasz Paterek for their invaluable scientific discussions.

Support from beyond my professional field has been incredibly valuable, and mere words cannot fully capture my gratitude. I have received immense love and encouragement from my friends Nidhi, Sujata, Manisha, Heena, Pooja, Akriti, and Jyoti from my undergraduate days at Kalindi College, University of Delhi, as well as Devandar, Rakesh, Jaspreet Kaur, Piyali Biswas, and Amrapali Chaudhary from my time at the Indian Institute of Technology, Jodhpur. I am profoundly grateful for your presence in my life and for all the support you have provided.

I also owe a deep gratitude to my family, whose steadfast support and love have been pivotal throughout this journey. A special thank you to my brother, Sagar Panwar, for being my source of relief and strength when I needed it most. I also thank Vinita Chaturvedi, Anupam Chaturvedi, Apoorv Chaturvedi, and Riya Lodha for your kind words and thoughtful gestures. Your support has been comforting and encouraging, making this journey all the more meaningful.

I am also immensely grateful to my partner, Anubhav Chaturvedi, whose support and companionship have been my stronghold. Your encouragement has been crucial in helping me maintain my focus and perseverance throughout this journey. His passion for science has inspired me countless times to put forth my best efforts in the field, shaping me into the scientist I am today.

Lastly, special thanks to Ewa Kaszewska, Marta Krzyżkowska, and Małgorzata

Szczekocka, thank you for your invaluable assistance in the office and for making Gdansk feel at home.

I am particularly grateful for the financial support from the NCN grant SONATA-BIS grant (No. 2017/26/E/ST2/01008) as well as the NCBiR through the QuantEra grant (No.2/2020). I also want to express my appreciation to the University of Gdańsk and the ICTQT for providing an optimal research environment.

I attribute creative support to <https://youtu.be/h2h1GyOEPic?si=3HMoTJw1tTdM9DCh>

This work has indeed been a collaborative effort, and I am fortunate to have had such a supportive circle during this journey. Thank you all.

DEDICATION

*I dedicate this work to my parents with all my love
and gratitude.*

Sunita Panwar & Pradeep Panwar

ABSTRACT

Quantum systems exhibit non-classical correlations that go beyond the capabilities of classical physics, making these correlations a central focus of research in quantum information science. This thesis addresses a seemingly simple yet profound question: *what can we infer about the underlying physics when we observe non-classical correlations?* Specifically, how can we characterize non-classical correlations and certify the underlying quantum systems? Accurate characterization and certification of quantum systems are of fundamental and practical significance for advancing quantum information theory. In this thesis, we develop novel theoretical models for the characterization of non-classical correlations and the certification of underlying quantum systems. Despite the precision of the theoretical models, their implementation in experimental setups often requires consideration of additional factors. Experimentalists must contend with noise and imperfect devices, which can obscure the certification of the underlying quantum systems. Consequently, this thesis also addresses an experimentally significant question: *how can we effectively certify underlying quantum systems in experimental settings despite the presence of imperfections and noise?*

The first two articles derive novel *robust analytical* self-testing statements, which form the most accurate certification of quantum systems underlying the maximum violation of Bell inequalities. The first article deals with the self-testing of Bell inequalities in the sparsely explored multipartite Bell scenarios. We present a novel self-testing technique, which is very simple yet effective in that it can be applied to a substantially large class of multipartite Bell inequalities. The second article addresses the practical challenge of finding the optimal strategies that yield the maximum violation of Bell inequalities in the presence of imperfect devices. We show that the optimal strategies maximally violate a tilted version of the Bell inequality. We derive self-testing statements for the tilted versions of the Clauser-Horne-Shimony-Holt (CHSH) inequality, demonstrating that the optimal strategies are unique. Beyond providing analytical and robust self-testing statements, the articles uncover several pivotal features of quantum correlations in Bell scenarios. In particular, the results in both articles highlight the impracticality of the traditional methods, such as the sum-of-squares (SOS) decomposition method and the Navascués–Pironio–Acín (NPA) hierarchy of semi-definite programming relaxations, for obtaining the self-testing statements. Both articles leverage Jordan’s lemma as a crucial component of the self-testing technique.

The third article investigates the relationship between non-classical correlations and mediated dynamics (dynamics generated by a mediator that couples non-interacting systems). We concentrate on the non-classical characteristics of the interactions involved. We derive conditions that solely use correlations between the coupled systems, excluding the need to measure the mediator, to certify the non-commutativity and non-decomposability of mediated interactions. We also discuss the implications of this formalism, including constraints on possible theories of gravity within a Hilbert space framework and within the theory of quantum simulators.

ABSTRAKT

Ukady kwantowe wykazuj nieklasyczne korelacje wykraczajce poza moliwoci fizyki klasycznej, co czyni te korelacje przedmiotem intensywnych bada w teorii informacji kwantowej. Niniejsza praca dotyczy pozornie prostego, ale gbokiego pytania: *co moemy wywnioskowa na temat podstawowej fizyki, obserwujc nieklasyczne korelacje?* a w szczególności w jaki sposób moemy scharakteryzowa korelacje nieklasyczne i powiadczy nieklasyczno danego urzdzenia? Dokadna charakterystyka i certyfikacja systemów kwantowych jest konieczna do fundamentalnego i praktycznego rozwoju kwantowej teorii informacji. W niniejszej pracy opracowujemy nowatorskie modele teoretyczne do charakteryzacji korelacji nieklasycznych oraz certyfikacji wybranych ukadów kwantowych. Pomimo ich precyzyjnego opisu teoretycznego, ich implementacja w ukadach eksperymentalnych czsto wymaga rozwaenia dodatkowych czynników. W dowiadzeniach musimy zmaga si z szumem i innymi niedoskonaymi urzdzeniami, które mog utrudnia lub uniemoliwia certyfikacj kwantowoci scenariuszy. W zwizku z tym niniejsza rozprawa dotyczy take m.in pytania istotnego dla eksperymentu: *w jaki sposób moemy skutecznie certyfikowa scenariusze kwantowe pomimo obecności niedoskonaoci i szumów?*

Pierwsze dwa artykuy wywodz si z nowatorskich analitycznych stwierdze samotestujcych, które stanowi najdokadniejsz certyfikacj systemów kwantowych lec u podstaw maksymalnego amania nierównoci Bella. Pierwszy artyku dotyczy samotestowania wieloczkowych scenariuszy Bellowskich, dotychczas mao zbadaych. Przedstawiamy nowatorsk technik samotestowania, która jest bardzo prosta, a jednoczenie ogólna, poniewa mona j zastosowa do zasadniczo duej klasy rodzin nierównoci wieloczkowych. Drugi artyku dotyczy praktycznego wyzwania, jakim jest znalezienie optymalnej strategii, która prowadzi do maksymalnego amania pewnej nierównoci Bella w obecności niedoskonaoci pomiarowych. Pokazujemy, e optymalne strategie prowadz do maksymalnego amania przechylonej nierównoci Bella (tilted, z czonem prawdopodobieństw brzegowych). Wyprowadzamy dowód samotestowania dla pochylonej nierównoci Clausera-Horne’a-Shimony’ego-Holta (CHSH), pokazujc, e optymalne strategie s unikalne. Poza tymi dowodami, artykuy pokazuj kilka kluczowych cech korelacji kwantowych w rozwaanym scenariuszu Bella. W szczególności wyniki w obu artykuach podkreli niepraktyczno tradycyjnych metod dowodzenia samotestowania, takich jak rozkad operatora Bella na sum kwadratów (SOS), czy hierarchia Navascuésa Pironio Acína (NPA). Obydwa artykuy odwouj si do lematu Jordana jako kluczowego elementu dowodu. W trzecim artykule zbadano zwizek pomidzy korelacjami nieklasycznymi i oddziazywaniem przez porednika.

Wyprowadzamy warunki wykorzystujce wycznie korelacje pomidzy posprzonymi systemami, z wyczeniem konieczności pomiaru ukadu mediatora, na nieprzemienno i nierozkadalno oddziaywa z porednikiem. Omawiamy take implikacje tego formalizmu, w tym ograniczenia dotyczce moliwych teorii grawitacji kwantowych oraz symulatorów kwantowych.

PUBLICATIONS INCLUDED IN THE DISSERTATION

- [A] Panwar E, Pandya P, Wieniak M. An elegant scheme of self-testing for multipartite Bell inequalities. *npj Quantum Information*. 2023; 9(1): 71.
- [B] Gigena N, Panwar E, Scala G, Araújo M, Farkas M, Chaturvedi A. Robust self-testing of Bell inequalities tilted for maximal loophole-free nonlocality. *arXiv:2405.08743*. 2024.
- [C] Ganardi R, Panwar E, Pandit M, Woloncewicz B, Paterek T. Quantitative nonclassicality of mediated interactions. *PRX Quantum*. 2024; 5 (1): 010318.

TABLE OF CONTENTS

	Page
1 Introduction	1
2 Preliminaries	9
2.1 The postulates of quantum mechanics	9
2.2 Entanglement as a quantum property of composite systems	12
2.2.1 Entanglement measures	12
2.3 Mediated dynamics	13
2.4 Mathematical foundations for nonlocal correlations	15
2.4.1 Bell nonlocality	15
2.4.2 No-signalling correlations	17
2.4.3 Properties of the three correlation sets \mathcal{L} , \mathcal{Q} and \mathcal{NS}	18
2.4.4 Polytopes and facet inequalities	18
2.4.5 Bell functionals and Bell inequalities	19
2.4.6 The quantum set and semidefinite relaxations (NPA) hierarchy	20
2.4.7 Upper bound on the quantum value of Bell operator W	21
2.5 Bell scenarios	22
2.5.1 The CHSH Scenario	22
2.5.1.1 Local bound of CHSH inequality	23
2.5.1.2 The Tsirelson's bound	23
2.5.1.3 Popescu Rohrlich (PR) boxes	24
2.5.2 Multipartite Scenarios	24
2.5.2.1 Linear inequalities	25
2.5.2.2 Uffink's Quadratic inequalities	26
2.6 Inefficient detectors	27
2.6.1 Post-processing strategies	28
2.6.2 Effect of inefficient detectors with local assignment strategy on Bell inequalities	29
2.6.3 Effect of inefficient detectors with local assignment strategy on CHSH inequality	30

TABLE OF CONTENTS

2.7	Device-independent certification	30
2.7.1	Self-testing	30
2.7.2	SOS and maximal violation of the CHSH inequality	32
2.7.3	Duality between SOS and NPA relaxation	33
2.7.4	Jordan’s lemma	35
2.7.5	Self-testing based on Jordan’s lemma	36
3	Summary of dissertation	37
3.1	An elegant scheme of self-testing for multipartite Bell inequalities	37
3.2	Robust self-testing of Bell inequalities tilted for maximal loophole-free nonlocality	40
3.3	Quantitative non-classicality of mediated interactions	43
4	Outlook	47
	Bibliography	51

INTRODUCTION

“Everything we call real is made of things that cannot be regarded as real. ”

—Niels Bohr

In 1927, when the field of quantum theory was still at a pivotal moment, a historical 5th Solvay Conference in Brussels highlighted the conflict between Einstein’s realism, which sought a deterministic underpinning of quantum phenomena through hidden variables, and Bohr’s instrumentalist perspective, which embraced the quantum theory’s probabilistic nature. The debate between Einstein and Bohr set the stage for decades of philosophical and experimental explorations into the nature of reality. Later, Expanding on his concerns, Einstein, alongside collaborators Boris Podolsky and Nathan Rosen, further articulated his critique in the 1935 Einstein-Podolsky-Rosen (EPR) paper [1]. The article unveiled the EPR paradox (a thought experiment showing that measuring one particle in an entangled quantum system can instantaneously influence another particle, no matter how far apart they are) and reflected Einstein’s discomfort with the probabilistic nature of quantum theory and challenged its completeness. Einstein described the phenomenon of quantum entanglement (when two or more particles share a strong correlation, and any measurement made on one particle instantaneously influences the state of its entangled counterpart, regardless of the distance separating them) as something that defies the conventional understanding of spatial separation and violates the principle of causality and locality, cornerstones of classical physics. Einstein famously criticized it as "spooky action at a distance" [1, 2].

Quantum theory distinguishes itself from theories based on local causality through its inherent Bell non-local characteristics. Unlike classical theories, quantum theory features entangled

states and fundamentally incompatible measurements. When performed on the local subsystems of an entangled quantum state, these incompatible measurements unearth correlations stronger than what is possible under local causal theories. This is recognized as Bell nonlocality and underscores the profound difference between quantum and theories based on local causality. Moreover, Bell's pivotal work in 1964 [3] also introduced inequalities, a set of criteria that serve as benchmarks that any theory based on local causality must satisfy. Quantum theory, however, violates these inequalities, marking a significant departure from classical physical theories. From an experimental perspective, suppose a Bell experiment (a foundational experimental setup intended to demonstrate quantum non-locality by violating Bell inequalities, which are expressions of observed probabilities) does not result in any violations of the Bell inequalities. In that case, the observed statistics can be interpreted through a deterministic framework as long as no extra assumptions about the underlying system are introduced.

Despite many challenges, quantum theory has triumphed over numerous obstacles. It has stood the test of time, consistently proving its validation through numerous experimental tests that underscore its probabilistic nature, compelling us to reject the concept of local hidden variable theories. However, it was not until 2015 that a significant milestone was achieved in this direction. Several research groups across the globe successfully executed Bell tests that were "loophole-free" [4–6]. These loophole-free experiments have not only reinforced the quantum mechanical view of the world by discarding local hidden variable models but also implied profound implications for developing quantum technologies, such as quantum computing and secure quantum communication. By landing a robust experimental foundation, they affirmed the strange, counterintuitive, yet powerful phenomena of quantum entanglement and nonlocality.

In the past thirty years, the field of quantum information science has significantly heightened interest in the concept of Bell Nonlocality. This surge in interest has spurred the development of a broad spectrum of concepts and technical tools aimed at probing and understanding quantum theory's nonlocal characteristics. The thorough investigation into this area is well written in several publications listed in the review article [7]. The more we delve into the nonlocal features of quantum theory, the more captivating the journey becomes. The existence of nonlocal correlations, which are more potent than classical correlations, stands at the heart of this excitement. The extremes of such nonlocal correlations empower us to deduce microscopic behaviors solely from the observed statistical data. This aspect of quantum mechanics is inconceivable in local-causal theories and is called *self-testing* of quantum systems, where the properties of the microscopic world are entanglement and measurement incompatibility.

The term *self-testing* was officially introduced to the academic world in 2004 by Mayers and Yao [8]; they showcased its utility in bipartite Bell scenarios, focusing on the self-testing of maximally entangled qubits. While Mayers and Yao are credited for coining the word self-testing, the seeds of this idea can be traced back to 1992 [9]. Since its formal introduction, self-testing has emerged as a vibrant area of research within quantum information science. The research in self-

testing has just not been confined to bipartite systems. It has extended to various scenarios, such as those involving multipartite systems, prepare and measure scenarios and steering scenarios, and many others [10]. This prompts the question: *why self-testing has become the preferred method for certifying quantum systems, as opposed to other available techniques?*

In this era, there is convincing evidence that suggests quantum devices have performed better than classical devices in various aspects. However, as the complexity of quantum devices is growing, verifying that they are behaving as expected has also become increasingly difficult. To tackle this issue, one can use a conventional approach such as *quantum tomography*. However, this technique faces significant challenges as the complexity of quantum systems grows [11, 12]. More specifically, quantum tomography requires an exponential increase in resources as the system size grows. Consequently, this situation highlights the quest for feasible certification methods for quantum devices, which is essential in order to advance the construction of large-scale, practical quantum technologies. Self-testing stands out as a promising alternative that can effectively overcome the challenges faced by traditional methods [8, 13].

Self-testing allows a classical user to deduce the microscopic behavior of a quantum system based solely on the observed macroscopic experimental statistics. This technique is an approach aimed at unraveling the intricate structure of the quantum correlation set. Moreover, the implications of self-testing extend beyond the theoretical aspect; it offers a cornerstone for *device-independent* quantum information processing [14, 15]. Specifically, self-testing empowers any classical user to understand quantum systems without a comprehensive understanding of the internal mechanisms of quantum devices; it treats the quantum devices as a "black box" (precisely, the user does not need to know the internal workings of the device to verify its quantum properties). It is the power of this method that it maintains its integrity even under the assumption that some adversaries might try to cheat by constructing quantum devices. Moreover, self-testing has proven useful in numerous areas of quantum information science, such as quantum key distribution [16, 17], quantum channels [18], randomness expansion [19], and the coarse-graining of many-body singlet states [20].

Indeed, a significant amount of work in self-testing has been concentrated only on bipartite quantum scenarios, indicating that the realm of "multipartite scenarios" (those involving more than two parties) remains relatively underexplored [10]. The complexity and diversity of multipartite scenarios offer unique challenges and prospects for a self-testing framework, suggesting that existing methodologies either fail to apply or need significant adaptation [10, 21]. The need to explore self-testing in multipartite scenarios is not merely a theoretical exercise but a necessity for advancing quantum computing and communication technologies, which require bigger quantum systems than bipartite scenarios for practical functionality [22, 23].

The *First* article attempts to progress in this direction by introducing a straightforward yet broadly applicable method for self-testing in the context of multipartite Bell inequalities. This method's beauty lies in its simplicity and broad applicability to self-test within multipartite

Bell scenarios, distinctively not relying on the traditional sum-of-square decomposition method [24]. More specifically, the sum-of-squares method is intricately tied to the specific structure of the Bell inequalities and the hermiticity of the associated Bell operators. However, with the scaling complexity of multipartite scenarios, identifying a sum-of-square decomposition for the corresponding Bell operators became more mathematically demanding and computationally intensive. This complexity barrier presents a significant hurdle in applying traditional proof techniques. Therefore, there is a pressing need to find a novel self-testing approach in multipartite Bell scenarios that can sidestep these complexities [25].

The *first* article introduces a new methodology in this direction. In the article, we showcase the practicality and effectiveness of our proof technique by retrieving self-testing statements for N-party Mermin-Ardehali-Belinskii-Klyshko (MABK) [26, 27] and Werner-Wolf-Weinfurter-Żukowski-Brukner (WWWŻB) [28–30] families of linear Bell inequalities. Additionally, the article expands on this by providing the self-testing proofs of N-party Uffink’s quadratic Bell inequalities [31] and complex-valued Bell expression. Notably, these inequalities retain the crucial permutational symmetry (the property of a system or equation remaining unchanged when its components are rearranged or permuted), which makes them stringent indicators of genuine multipartite non-locality. The genuine N-partite non-locality is crucial for quantum information processing tasks that require all participating parties’ involvement, specifically in scenarios where all parties are required and no subset of parties can achieve success independently such as quantum secret sharing (enables the secure division of a secret among multiple parties), social welfare games (which explore the allocation of resources among the parties securely), device-independent randomness generation (DIRG) (secure random numbers without relying on the trustworthiness of the devices used) and conference key distribution schemes (enable secure communication among the parties) [32–35]. However, when translating these theoretical protocols into practical applications, a degree of caution is necessary. In the real world, there is the possibility of deviation from the idealized conditions assumed by theoretical formulations, which can introduce avenues for "loopholes" [21].

These loopholes can allow measurement statistics to be interpreted in a way that supports local realism, thereby undermining the integrity of the protocols. Addressing and closing these loopholes is crucial to prove the non-local nature of quantum correlations and to improve the security and effectiveness of quantum information processing tasks. Among the various operational loopholes, the detection loophole is particularly significant. Detection loophole arises primarily due to imperfect detectors used in the experiment. The inadequacy of these inefficient detectors in experiments can introduce loopholes that a local classical model could leverage to mimic the experimental statistics that one would expect from a quantum system. Moreover, the detection loophole is the main obstacle to achieving practical, long-distance device-independent (DI) cryptography [36–40].

The most prevailing strategy to overcome the detection loophole involves determining the

critical detection efficiency, denoted as η , for the detectors used in a Bell test. Here, the word critical detection efficiency denotes the minimum required performance of a detector to ensure the observed violation of a Bell inequality and reflects the presence of quantum nonlocality in the experiment. In the context of bipartite Bell scenarios, where each of the two parties has two dichotomic (binary outcome) measurements, for the maximal violation of the Clauser-Horne-Shimony-Holt (CHSH) inequality that could confidently indicate Bell nonlocality in the experiment, the critical detection efficiency must be $\eta = 2(\sqrt{2} - 1) \approx 0.8284$, when using maximally entangled state [41, 42].

Interestingly, for quantum states that are partially entangled, the required threshold efficiency for detecting nonlocality can drop to as low as $\frac{2}{3}$ [43]. Moreover, significant advancements in the field have indicated the potential to reduce further the critical detection efficiency threshold in more complex Bell scenarios. Specifically, the work from Massar and collaborators has demonstrated that within larger Bell setups, the required efficiency threshold for closing the detection loophole can decrease exponentially [44]. Subsequently, several studies have focused on reducing critical detection efficiency, highlighting the importance of lower detection efficiency for loophole-free certification of nonlocality [45–47]. However, real-world implementation of quantum technologies demands not just evidence of nonlocality but a high degree of nonlocality [48]. This requirement stems from the fact that many quantum information processing tasks, such as secure communication, rely on the strength of nonlocality to ensure their effectiveness and security. This motivates an important question: *which quantum strategies yield the maximum loophole-free nonlocality in the presence of inefficient detectors?*

The *second* article attempts to answer this question using self-testing as the key method. Violation of Bell inequality indicates the presence of nonlocality; the more violations there are, the further these correlations are from the local polytope. This measure of nonlocality narrows our question to identifying the quantum strategies that achieve the maximal loophole-free violation of a given Bell inequality for specific detection efficiencies. In experiments when detectors fail to click, resulting in a "no-click" event, to address this challenge and achieve a loophole-free violation of Bell inequalities, it is crucial to incorporate these "no-click" the most general way is to treat them as an additional outcome of the measurement [49]. However, the additional outcome enlarges the Bell scenario. One can avoid this problem and the fair-sampling assumption by employing a more convenient post-processing method that assigns a pre-existing outcome to each no-click event while staying within the same scenario [50]. In the *second* article, we demonstrate that for any Bell inequality and any given detection efficiencies, the optimal strategies are those that achieve the maximum violation of a tilted version of the Bell inequality under ideal conditions. Considering the simplest Bell scenario, the quantum strategies that achieve the maximum loophole-free violation are unique (up to local isometries), which means the maximal violation of the tilted inequality *self-tests* the optimal strategy for any given detection efficiencies [51].

However, in the scenario where only one detector is imperfect, the set of tilted CHSH inequalities, as studied in reference [24], reveals that the maximum violation of these inequalities self-tests a partially entangled two-qubit state alongside a distinctive pairing of measurements: one party employs maximally incompatible local observables, while the other uses non-maximally incompatible observables. In particular, they used the sum-of-squares decomposition method, with polynomials of measurements operators of degree $(1+AB)$ corresponding the level of Navascués–Pironio–Acín (NPA) hierarchy enough to saturate the maximum quantum value of these inequalities. Our article, however, demonstrates that when we consider the scenario where both detectors are imperfect, retrieving the maximum violation of tilted CHSH inequalities becomes significantly more challenging; even higher levels of NPA are not enough. As a result, self-testing using the conventional sum-of-squares decomposition approach becomes exceedingly complex. The article underscores the intricate difficulty characterizing the set of quantum correlations, even within the simplest Bell scenario. As the main result, we derive analytical self-testing statements for the family of double-tilted Bell inequalities (inequalities as the result of imperfect detectors of both parties). Furthermore, In *second* article, we also show the robustness of our self-testing results via numerical. This work not only delves into the significance of our results but also opens up new pathways for further investigations in this direction [51].

The phenomenon of nonlocality in quantum mechanics, indicated by the violation of some Bell inequalities, presents an exhilarating aspect of quantum theory. One can also ask *what additional insight can be gleaned from the non-local correlations in quantum theory?* The *third* article ventures in this direction, offering some intriguing answers. In the microscopic realm, quantum objects exhibit behaviors that defy classical intuitions. For example, particles can exist in multiple states simultaneously (superposition) and can be instantly correlated with each other regardless of the distance separating them (entanglement). However, in the framework of classical physics, the interaction between distant systems can be explained through the concept of a field, which permeates space and acts as an *mediator* (a system that couples others, non-interacting, systems) for these systems. This concept adheres to the principles of locality, which says that a system can only be influenced by its immediate environment [52]. These mediator interactions are common and often, cannot be directly accessed or observed through experiments. However, exploring whether such fields possess nonclassical properties can be fascinating and vital.

In quantum theory, the approach to mediated interactions mirrors that of classical physics, with the vital distinction being that instead of the field, we use operators. A notable example that is gathering significant interest involves two quantum masses that interact through a gravitational field [53, 54]. It has been posited that the entanglement gain between these masses exhibits the nonclassical characteristic of the states of the entire tripartite system and also what we can say about the mediator. The *third* article delves into quantifying the nonclassicality of such mediated interactions, focusing on the nonclassical characteristics at play rather than the state themselves. We introduced inequalities whose violation signifies noncommutativity

and nondecomposibility (open system generalization of noncommuting unitaries) in mediator-based interactions, offering a new avenue to explore the quantum characteristics of mediator interactions. The derivation we employ hinges on the principles of quantum mechanics and is grounded in minimal assumptions about the systems under investigation. This minimal-assumption framework provides the advantage of applicability across various scenarios, making our method quantitative and experiment-ready. It is independent of the initial state and the systems' dimensions or the interactions' specific nature. In the article we also demonstrate that amount of violations places a lower bound on a suitably defined degree of nondecomposability[55].

In our article, we illustrate our theoretical findings with two examples. The first example delves into the field of quantum simulations, specifically, the use of the Suzuki-Trotter expansion for simulating arbitrary sums of local Hamiltonians, a technique referenced in several studies [56, 57]. Recent advancements have revealed that the number of Trotter steps required to obtain the required simulation error is proportional to the spectral norm of the commutator. We draw a connection between this norm and the system's correlations, illustrating a quantitative link between simulation complexity and the amount of correlations. In the second instance, our method can detect and measure the noncommutativity in the gravitational interaction between two quantum masses. Our approach reveals that the correlations observed among these masses indicate that gravity cannot be modeled as a commutative interaction between particle and field. Furthermore, from Reference [58], any system interacting with a quantum system must also be quantized. Thus, our framework offers a novel way to identify gravitational interaction's nonclassical nature.

Finally, all the above articles collectively address a fascinating question *how can we certify the underlying quantum systems based on non-classical correlations?* in quantum theory, with each offering unique insights and advancements. The *third* article explores nonlocal correlations in quantum theory even beyond the violation of Bell inequalities, mainly focusing on *mediated interactions*. The *first* and *second* article centers around the concept of Bell Nonlocality and its significant influence on the evolution of quantum information science by the advent of *self-testing*. Specifically, the *first* article ventures into the realm of *multipartite scenarios*, underscoring the complexity and potential to extend self-testing beyond bipartite scenarios. It highlights the necessity of such advancements for the practical realization of *quantum communication* technologies, which depend on larger quantum systems. The article presents a new methodology for self-testing for multipartite Bell scenarios, which steps away from the traditional sum-of-squares method [25]. The *second* article delves into the question of which quantum strategies yield the maximum *loophole-free nonlocality* in the presence of *imperfect detectors*. Moreover, *second* article systematically addresses the challenge of certifying quantum systems under practical conditions, specifically when detectors are imperfect [51]. Both *First* and *second* article employs Jordan's lemma to characterize the measurements, highlighting the methodological consistency. Finally, *third* article offers a different perspective on understanding and exploiting

the quantum characteristics of mediator-based interactions. Specifically, this article sheds light on the *noncommutativity* in the gravitation interactions [55]. Together, these articles stitch a comprehensive narrative on theoretical progress and practical inquiries into nonlocal correlations in quantum mechanics, showcasing the depth and breadth of current research in this area.

PRELIMINARIES

“I state my case, even though I know it is only part of the truth, and I would state it just the same if I knew it was false because certain errors are stations on the road of the truth. I am doing all that is possible on the definite job at hand”

— Robert Musil

In chapter 2, we provide a brief introduction to the theoretical and mathematical framework necessary for understanding non-classical correlations in quantum theory, setting the stage for more detailed discussions in the subsequent chapters. The chapter is divided into the following sections: We begin with an introduction to quantum formalism, entanglement, mediated dynamics and the mathematical foundations of Bell nonlocal correlations. Next, we explore Bell scenarios, followed by a discussion of the challenges posed by inefficient detectors in Bell experiments. The final section focuses on device-independent certification or self-testing method.

This section introduces the fundamental postulates of quantum mechanics. The postulates of quantum mechanics provide the bridge between the physical phenomena we observe and the framework of quantum mechanics.

2.1 The postulates of quantum mechanics

The first postulate of quantum mechanics introduces the concept of Hilbert space, a complex vector space with an inner product. This space, denoted as \mathcal{H} , functions as the state space for the quantum systems,

Postulate 1- Wave Function : A quantum system's state is fully described by a state vector $|\psi\rangle$ situated in a complex vector space equipped with an inner product, known as Hilbert Space \mathcal{H} . This state vector encapsulates all necessary information to fully describe the system's physical properties [22].

While Postulate 1 deals with the single systems, let us consider a scenario involving a composite system comprising two or more distinct physical systems. We need to understand how the states of these individual systems merge to represent the state of the entire composite system. The subsequent postulate clarifies this by describing how the state space of a composite system is constructed from the state spaces of its constituent systems.

Postulate 1.1-Composite systems: The state space of a composite physical system is formed by the tensor product of the state spaces of its individual components. Additionally, if we have several systems numbered from 1 to n , with each system i prepared in the state $|\psi_i\rangle$, then the state of the entire composite system is expressed as:

$$(2.1) \quad |\psi_1\rangle \otimes |\psi_2\rangle \otimes \dots \otimes |\psi_n\rangle.$$

Postulate 1 and 1.1 describes quantum mechanics using state vectors. However, a more general approach employs the concept of density operator, which is especially useful for dealing with systems characterized by mixed states or those that are components of larger systems. The density operator approach is invaluable when the exact state of a quantum system is unknown. For instance, imagine a quantum system that might be in any of several potential states $|\psi_i\rangle$, each indexed by i , and occurring with a certain probability p_i . This collection of states and their probabilities forms what is known as an ensemble of pure states. The density operator, or density matrix, for such a system is defined by the equation:

$$(2.2) \quad \rho \equiv \sum_i p_i |\psi_i\rangle \langle \psi_i|.$$

While Postulate 1 describes the system's state at any given initial time, the following postulate describes how it evolves with time [22, 59].

Postulate 2-Time Evolution : The evolution of a closed quantum system is governed by a unitary transformation. Specifically, the state $|\psi_1\rangle$ of the system at a certain time, t_1 , is transformed into the state $|\psi_2\rangle$ at another time, t_2 , by using the unitary operator \mathcal{U} . This unitary operator \mathcal{U} depends solely on the times t_1 and t_2 , such that:

$$(2.3) \quad |\psi_2\rangle = \mathcal{U}|\psi_1\rangle.$$

The above postulate established the fact that closed quantum systems evolve according to unitary evolution. Postulate 2 describes the relationship between the quantum states of a closed quantum system at two distinct points in time. However, a more refined iteration of this postulate can be the evolution of quantum systems continuously over time [60, 61].

Postulate 2.1 : The time evolution of the state of a closed quantum system follows the Schrödinger equation, i.e., $i\hbar \frac{d|\psi\rangle}{dt} = \mathcal{H}|\psi\rangle$.

It is very natural to ask how the dynamics described by the Hamiltonian in Postulate 2.1 relate to the unitary operator outlined in Postulate 2; this relationship is clearly illustrated in the following equation:

$$(2.4) \quad |\psi(t_2)\rangle = \exp\left[\frac{-i\mathcal{H}(t_2-t_1)}{\hbar}\right]|\psi(t_1)\rangle = U(t_1, t_2)|\psi(t_1)\rangle.$$

Postulates 2 and 2.1 provide insights into the dynamics of quantum mechanics. Up till now we were considering evolution of closed quantum systems lets now consider the system interacting with a local environment. In this scenario, the system's evolutions cannot be solely governed by unitary evolution; instead, its evolution is described by a dynamical map denoted as $\{\Lambda_t\}_{t \geq 0}$. When the initial state of the system is ρ_0 , the state of the system at time t is given by $\rho_t = \Lambda_t(\rho_0)$. However, dynamics exist where systems do not interact directly but instead through a mediator [cite]. We will explore this topic further in the section on mediated dynamics.

Next, we introduce Postulate 3, which describes how measuring affect quantum systems. *Postulate 3- Measurement*: Quantum measurements are described using a set of measurement operators, denoted as $\{\mathcal{M}_m\}$. These operators act on the state space of the system being measured with the subscript m indicating the possible outcomes. If the state of the quantum system is $|\psi\rangle$ prior to measurement, then the probability of obtaining the outcome is given by:

$$(2.5) \quad p(m) = \frac{\langle \psi | \mathcal{M}_m^\dagger \mathcal{M}_m | \psi \rangle}{\langle \psi | \psi \rangle},$$

where \mathcal{M}_m^\dagger represents the adjoint (or Hermitian conjugate) of \mathcal{M}_m . After the measurement, the state of the system collapses to a new state given by:

$$(2.6) \quad |\psi\rangle = \frac{\mathcal{M}_m |\psi\rangle}{\langle \psi | \mathcal{M}_m^\dagger \mathcal{M}_m | \psi \rangle}.$$

Moreover, the measurement operators must fulfill the completeness relation $\sum_m \mathcal{M}_m^\dagger \mathcal{M}_m = \mathbb{I}$, ensuring that the sum of the probabilities of all possible outcomes is equal to one. The set of necessarily positive semi-definite operators $\{E_m = \mathcal{M}_m^\dagger \mathcal{M}_m \geq 0\}$ are POVMs and suffice to describe measurements when we are not interested in the post-measurement state. If the POVM elements satisfy the orthogonality condition $E_m E_{m'} = \delta_{mm'} E$ then the measurement is projective [22].

It is interesting to observe that these local measurements when performed on an entangled state, generate correlations among outcomes that cannot be accounted for by any local causal theory. We will further explore this in the upcoming section on mathematical foundations for nonlocal correlations.

Having familiarized ourselves with the postulates of quantum mechanics, we are now prepared to explore the fascinating phenomenon of entanglement.

2.2 Entanglement as a quantum property of composite systems

Replacing the classical concept of phase space with the more abstract Hilbert space introduces a notable shift in how composite systems are described. To grasp this, consider a multipartite system made up of n subsystems. In classical mechanics, the total state space of the system is defined as the Cartesian product of the state spaces of the n subsystems, implying that the overall state is simply a product state of the individual subsystems [62, 63].

In contrast, quantum mechanics prescribes that the total Hilbert space, \mathcal{H} , is the tensor product of the individual subsystem spaces, represented as $\mathcal{H} = \bigotimes_{k=1}^n \mathcal{H}_k$. Utilizing the density matrix formalism, the complete state of the system can be expressed as:

$$(2.7) \quad \rho = \sum_{I_n, J_n} C_{I_n, J_n} |I_n\rangle \langle J_n|,$$

where $I_n = i_1, i_2, \dots, i_n$ and $J_n = j_1, j_2, \dots, j_n$ form multi-indices, and $|I_n\rangle = |i_1\rangle \otimes |i_2\rangle \otimes \dots \otimes |i_n\rangle$ and $\langle J_n| = \langle j_1| \otimes \langle j_2| \otimes \dots \otimes \langle j_n|$. Generally, this density matrix ρ could be entangled, i.e., cannot be decomposed into a product of density matrices from the individual subsystems [64] illustrating that it is not generally feasible to assign a single-density matrix to any of the n subsystems. This framework underscores the concept of entanglement, a fundamental aspect of quantum mechanics. Furthermore, states that do not exhibit entanglement, such that $\rho = \sum_i p_i \rho_1^i \otimes \rho_2^i \otimes \dots \otimes \rho_n^i$ are referred to as separable [22, 62, 63].

Entanglement is a crucial component for the progression of quantum technologies based on quantum information science. The exploration of entanglement can be framed around three primary questions: First is its characterization, which involves determining whether a quantum state is entangled or separable. Second is the manipulation of entanglement, exploring how it can be altered or utilized. Lastly, the quantification of entanglement aims to measure the degree of entanglement which is essentially the theory of entanglement measures. In the next section, we revisit a few significant entanglement measures.

2.2.1 Entanglement measures

Over the years, a wide variety of entanglement measures have been introduced, each providing substantial mathematical and conceptual contributions. These measures are deeply connected to different aspects of quantum information processing. While theoretically, the number of such measures could be infinite, some are particularly significant for specific applications [65–67].

For instance, in the context of bipartite systems, two notable entanglement measures are the entanglement cost E_c and the distillable entanglement E_D . The entanglement cost E_c measures the rate at which entanglement can be created using other resources, whereas the distillable entanglement E_D quantifies the maximum amount of pure entanglement that can be extracted from a state through local operations and classical communication (LOCC) [68]. Initially, it was unclear whether these measures were equivalent or if there were other measures that could

fill the gaps between them. The relative entropy of entanglement is one such measure that fits this intermediate space [69]. The relative entropy of entanglement is an elegant and powerful instrument within entanglement theory, grounded in the concept of relative entropy, which is a fundamental quantity in quantum information theory.

Relative entropy of entanglement: Let us first consider the concept of total correlations, quantified by the quantum mutual information, given by:

$$(2.8) \quad I(\rho_{AB}) = S(\rho_A) + S(\rho_B) - S(\rho_{AB}).$$

Where $S(\rho) = -\text{Tr}\{\rho \ln \rho\}$ is von Neumann entropy using the quantum relative entropy, which measures the distinguishability between two quantum states (ρ, σ) , defined as:

$$(2.9) \quad S(\rho||\sigma) := \text{Tr}\{\rho \log \rho - \rho \log \sigma\},$$

This allows us to express the quantum mutual information (2.9) as:

$$(2.10) \quad I(\rho_{AB}) = S(\rho_{AB}||\rho_A \otimes \rho_B).$$

Given that total correlations are quantified by comparing the state ρ_{AB} with the uncorrelated state $\rho_A \otimes \rho_B$, it is logical to measure the specifically quantum part of these correlations by comparing ρ_{AB} with the closest separable state. This perspective leads to the general definition of the relative entropy of entanglement with respect to a set X as:

$$(2.11) \quad E_R^X(\rho) := \inf_{\sigma \in X} S(\rho||\sigma).$$

In the bipartite scenario, this infimum is taken over all separable states or those with positive partial transpose, serving as an effective indicator of entanglement in the sense that relative entropy of entanglement is always positive if and only if ρ_{AB} is entangled [70, 71].

Furthermore, the condition of a positive partial transpose is necessary for separability. This leads to another significant entanglement measure.

Negativity: Negativity is a convex entanglement monotone that aims to quantify the negativity in the spectrum of the partial transpose. It is defined as:

$$(2.12) \quad N(\rho) \equiv \frac{\|\rho^{T_B}\| - 1}{2},$$

where $\|X\| = \text{Tr}\sqrt{X^\dagger X}$ is the trace norm. From here, we transition from examining the non-classicality of states to developing tools for quantifying the amount of non-classicality in mediated interactions [70, 72].

2.3 Mediated dynamics

Let us consider the simplest and most straightforward scenario in mediator dynamics involving two objects, A, B interacting through a mediator M (see Fig. 2.1). Notably, systems A and B do

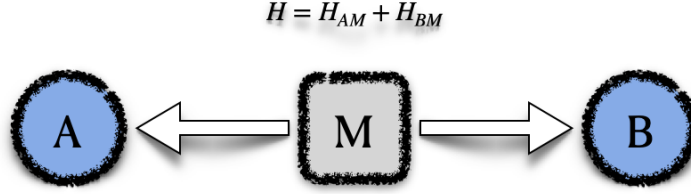


Figure 2.1: *Mediated interactions*:- Systems A and B interact indirectly through a mediator M i.e. the underlying Hamiltonian is $H_{AM} + H_{BM}$, explicitly excluding any direct interaction H_{AB} between the systems A and B.

not interact directly; rather, their interactions are mediated solely through the mediator M . It is assumed that all three systems are fully described by quantum theory, implying each has its own associated Hilbert space. This setup raises several compelling questions, particularly concerning the mediator. The first question to consider is: what characteristics must the mediator possess for us to categorize the interaction as quantum? Additionally, is it possible to identify certain quantum properties of the mediator without directly measuring it? These inquiries prompt a deeper exploration into the quantum dynamics of mediated interactions. Furthermore, our primary interest in exploring these questions stems from the desire to impose constraints on potential theories of quantum gravity. However, beyond theoretical considerations, this framework also bears practical significance, particularly in the realm of quantum simulators [20, 56].

One approach to addressing the previously mentioned question about the quantum nature of interactions is by examining the non-commutativity of the interaction Hamiltonians. This is a viable method to assess the quantumness of interactions because any interaction characterized by non-commuting terms cannot be emulated using a classical mediator. An interaction is considered classical if the commutator of the Hamiltonians H_{AB} and H_{BM} equals zero i.e., $[H_{AM}, H_{BM}] = 0$. This indicates that the unitary operator $e^{-itH_{ABM}}$ can be decomposed as $e^{-itH_{ABM}} = e^{-itH_{AM}} e^{-itH_{BM}} = e^{-itH_{BM}} e^{-itH_{AM}}$ [73]. This decomposability characteristic proves to be crucial in identifying nonclassical interactions. In the context of mediated dynamics an interaction is considered classical if it is decomposable, defined as,

Decomposable evaluation: Consider U as a unitary operator acting on a tripartite system $H_A \otimes H_B \otimes H_M$. We classify $U = e^{-itH_{ABM}}$ as decomposable if there exist unitary operators $U_{AM} = e^{-itH_{AM}}$ and $U_{BM} = e^{-itH_{BM}}$ such that $U(\rho_{ABM}) = U_{BM}U_{AM}(\rho_{ABM})$. In essence, decomposable unitaries are those that can be simulated by initially coupling system A to the mediator M, followed by coupling system B to the mediator. Now suppose your system is not closed anymore, to articulate decomposability in the context of open systems, we define the decomposability of the

quantum map as,

Decomposability of the quantum map: Let Λ be a map acting on a tripartite system $H_A \otimes H_B \otimes H_M$. We say Λ is decomposable if there exists maps ϕ_{AM} and ϕ_{BM} such that $\Lambda(\rho_{ABM}) = \phi_{BM}\phi_{AM}(\rho_{ABM})$. We denote the set of all decomposable maps as DEC [74].

Up till now we have described non-classicality based on quantum formalism now we will define non-classicality based on the observed experimental statistics between distant observers.

2.4 Mathematical foundations for nonlocal correlations

In statistics, correlations indicate the strength of the interdependence between two variables or systems, measuring the extent to which changes in one are associated with changes in the other. In quantum theory, correlations typically refer to the distant connections between two or more local subsystems. When these subsystems are subjected to appropriate measurements, they exhibit behaviors that defy classical physics. Unlike classical correlations, which can be entirely explained through classical probability distributions, quantum correlations exhibit phenomena such as entanglement and nonlocality that challenge classical explanations. In the next part of the chapter, we will provide a brief overview of the key concepts and tools used to characterize nonlocal correlations in Bell experiments. This discussion will set the stage for introducing certification schemes (self-testing) later in the chapter.

2.4.1 Bell nonlocality

In this section of the chapter, we will provide a brief introduction to the mathematical definition of Bell nonlocality within the context of a typical *Bell experiment* [75, 76]. Consider a scenario where two devices are controlled by two parties, known as Alice and Bob, who are situated at distant locations. These devices might have possibly interacted in the past; for example, they may share quantum systems emitted from the same source and can exhibit correlations. However, during the Bell experiment, they are not allowed to communicate in any way, typically referred to as the no-signaling. Each device has several buttons, each linked to a distinct measurement [7].

Let us assume that Alice and Bob can each select one of k possible measurements, with Alice's measurement setting denoted by $x \in [n_X] = \{1, 2, \dots, n_X\}$ and Bob's by $y \in [n_Y]$. More specifically, x could represent a setting on a dial of her measurement device. Similarly, y denotes Bob's choice of measurement on his device. When Alice and Bob perform these measurements on their respective systems, they each produce outcomes $a \in [n_A]$ and $b \in [n_B]$.

Note that Alice and Bob's interaction with these devices is purely classical. However, the underlying processes within the devices may extend beyond classical physics. Their only means of investigation are the classical actions of pressing buttons and observing the resulting outcomes. Additionally, it is assumed that they can repeat the experiment multiple times, with each iteration of the devices operating consistently under the same conditions. This ensures that for each pair of

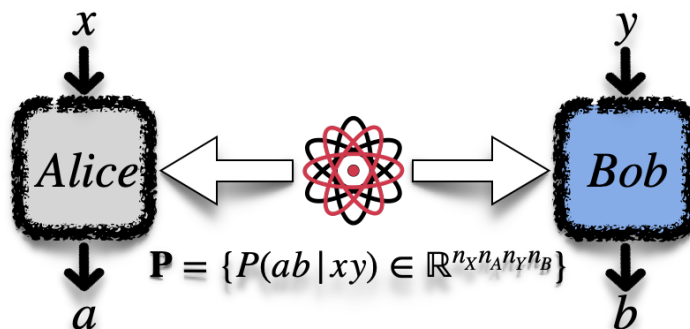


Figure 2.2: *Schematic of bipartite Bell experiment*:- A source sends two physical systems to distant observers, Alice and Bob. Alice performs measurement $x \in n_X$ and gets outcome $a \in n_A$, and Bob performs measurement $y \in n_Y$ and gets outcome $b \in n_B$. The experimental observations are specified by the joint probability distribution $\mathbf{P} = \{P(a, b|x, y) \in \mathbb{R}^{n_X n_Y n_A n_B}\}$, which represents the probability of outcomes a and b given measurements x and y chosen by Alice and Bob, respectively.

measurement settings (x, y) , there is a well-defined probability distribution over the outcome pairs (a, b) . This probability distribution will be presented as $P(a, b|x, y)$ for a given pair of settings (x, y) and a *probability point* is represented by $\mathbf{P} = \{P(a, b|x, y) \in \mathbb{R}^{n_X n_Y n_A n_B}\}$ (see Fig. 2.2). Where $\mathbb{R}^{n_X n_Y n_A n_B}$ can be visualized as a real vector space, this space arises from the fact that there are $n_X n_Y$ distinct pairs of settings, and $n_A n_B$ possible outcomes. The probability distribution \mathbf{P} corresponds to a valid probability distribution, if : (a) $P(a, b|x, y) \geq 0$ for all possible values of a, b, x, y , and (b) the sum of all probabilities over all outcomes a and b for any measurement settings x and y equals 1, i.e. $\sum_{a,b} P(a, b|x, y) = 1$

Observe that $P(a, b|x, y) \neq P(a|x)P(b|y)$, where $P(a|x) = \sum_b P(ab|x, y)$, $P(b|y) = \sum_a P(ab|x, y)$ implies that the outcomes from both sides are not statistically independent. Despite the fact that both systems are significantly distanced apart, the presence of such correlations is quite intriguing. They may suggest a dependency between the two systems stemming from their past interactions, an idea that is consistent with the expectations of a *classical (local causal) theory* [77]. The assumption of locality entails two key points:

- A prior to the Bell experiment, systems have been selected from the probability distribution $q(\lambda)$, having a joint causal effect on both outcomes
- During the experiment the outcomes are determined locally through response schemes $P(a|x, \lambda)$ and $P(b|y, \lambda)$, based on the hidden variables λ and the specific measurement settings chosen independently by each observer.

with these factors, the statistical outcomes can be expressed as:

$$(2.13) \quad P(a, b|x, y, \lambda) = P(a|x, \lambda)P(b|y, \lambda).$$

To consider all the possible values of variable λ encountered during each experimental run, it should be represented by a probability distribution $q(\lambda)$. The statistics can then be modeled as given below:

$$(2.14) \quad P(a, b|x, y) = \int_{\lambda} d\lambda q(\lambda)P(a|x, \lambda)P(b|y, \lambda),$$

when a probability point \mathbf{P} can be described using (2.14), it belongs to the set of *local realistic correlations*, mostly referred to as the *local set* generally denoted by \mathcal{L} and, λ is often called a *local hidden variable* (LHV), and this factorability condition is known as a LHV model [2, 78–80]. This fundamental mathematical equation, (2.14), was formulated by John Bell in 1964 and established a verifiable criterion, widely recognized as *Bell's theorem* [3]. The theorem proves that experiments involving entangled quantum particles cannot be explained by the local hidden variable model, highlighting that quantum theory is incompatible with the local hidden variable (LHV) model.

Now that we've covered the local hidden variable (LHV) model, we can transition our discussion from classical to quantum devices. In the most general cases, quantum devices share a quantum state, represented as ρ_{AB} . On Alice's side, her choice of measurement x corresponds to a set of measurement operators $\{\hat{M}_a^x\}_{x,a}$ such that $\hat{M}_a^x \leq 0, \sum_a \hat{M}_a^x = \mathbb{1}$. Similarly, Bob's measurement choice y corresponds to a set of measurement operators $\{\hat{N}_b^y\}_{y,b}$ such that $\hat{N}_b^y \leq 0, \sum_b \hat{N}_b^y = \mathbb{1}$. According to the Born rule [22, 81, 82], the probability of obtaining outcomes a and b for their respective measurement settings x and y is given by $P(a, b|x, y) = \text{Tr}(\hat{M}_a^x \otimes \hat{N}_b^y \rho_{AB})$. The triple consisting of ρ_{AB} , $\{\hat{M}_a^x\}_{x,a}$, and $\{\hat{N}_b^y\}_{y,b}$ is commonly referred as the *quantum realization or strategy*. The set of probability distribution which admit a quantum realization is denoted by \mathcal{Q} . It is important to note here that the quantum set \mathcal{Q} is determined based on a specific Bell scenario, which is characterized by the number of settings and outcomes of each party. However, this set is completely independent of the dimensionality of the quantum realization. One can easily verify that quantum realization can accurately replicate the statistics of the LHV models. Therefore, it directly implies that $\mathcal{L} \subseteq \mathcal{Q}$. However, there exists a nonlocal probability distribution $\mathbf{P} \in \mathcal{Q} \setminus \mathcal{L}$ which possesses quantum realizations but is not explainable by LHV models (2.14).

As mentioned earlier in the section on Bell nonlocality, 2.4.1 both parties, Alice and Bob, are restricted by a rule prohibiting communication between them. This introduces a crucial constraint known as *no-signaling*, a key characteristic shared by both local and quantum sets. In the upcoming part of the chapter, we will delve deeper into this concept.

2.4.2 No-signalling correlations

A key feature that both local \mathcal{L} set and quantum set \mathcal{Q} shared is that they both obey the no-signaling conditions. The concept of no-signaling says that neither Alice nor Bob can determine

the measurement choices of the other based on their own inputs and outcomes. Mathematically, this principle is expressed as follows:

$$(2.15) \quad \sum_b P(a, b|x, y) = \sum_b P(a, b|x, y') \text{ for any } a, x, y, \text{ and } y',$$

$$(2.16) \quad \sum_a P(a, b|x, y) = \sum_a P(a, b|x', y) \text{ for any } b, y, x, \text{ and } x'.$$

(2.15), (2.16) implies that Alice's marginal probabilities $P(a|x) = \sum_{b=1}^{n_B} P(ab|xy)$ are independent of Bob's choice of measurement setting y , and similarly, Bob's marginal probabilities $P(b|y) = \sum_{a=1}^{n_A} P(ab|xy)$ do not depend on Alice's settings. This prevents any possibility of communication between Alice and Bob via their choice of inputs. Moving forward, We represent the no-signaling set of correlations as \mathcal{NS} . A probability point belongs to the no-signaling set if it adheres to the valid probability distribution rules outlined earlier in the section on Bell nonlocality 2.4.1 paragraph 2 and the no-signaling conditions [7, 83].

So far, we have discussed three sets of correlations: the local set \mathcal{L} , the quantum set \mathcal{Q} , and the no-signalling set \mathcal{NS} . These sets are related as follows: $\mathcal{L} \subseteq \mathcal{Q} \subseteq \mathcal{NS}$, and each inclusion is strict. Moving forward, we will review the fundamental properties of these *correlation sets*.

2.4.3 Properties of the three correlation sets \mathcal{L} , \mathcal{Q} and \mathcal{NS}

The sets \mathcal{L} , \mathcal{Q} and \mathcal{NS} are characterized as *closed*, *bounded*, and *convex* [84, 85]. In order to discuss these correlation sets further, we must first understand these properties, starting with convexity. The set \mathcal{S} is a subset of \mathbb{R}^n and is defined as convex if, for any points p_1 and p_2 within this subset, then the linear combination $\mu p_1 + (1 - \mu)p_2$, with μ ranging from 0 to 1, also falls within \mathcal{S} . This means that the set must include all the convex combinations of its points. Notably, if we have a non-convex set \mathcal{S} , it can be transformed into a convex set by incorporating all possible convex combinations of points within \mathcal{S} . This process is termed as taking the *convex hull* (or convex envelope) of \mathcal{S} [86–88].

Remember, a subset of \mathbb{R}^n is compact if it satisfies two criteria: it must be both closed and bounded. Demonstrating compactness involves showing that the set fits within a unit ball according to the vector ∞ norm, which implies that the absolute value $|P(a, b|x, y)|$ must not exceed 1 for any possible value of a , b , x and y [89–91].

2.4.4 Polytopes and facet inequalities

A notable category of compact convex sets are those with only a finite number of *extremal points*, known as *polytopes*. These extremal points are often referred to as vertices [88]. Interestingly, among the three correlation sets discussed earlier, two classify as polytopes. The local set \mathcal{L} and the no-signaling set \mathcal{NS} are structured as polytopes, which implies that their geometry is relatively straightforward. On the other hand, the quantum set \mathcal{Q} does not conform to a polytope

structure as it may have continuously infinite extremal points. We now discuss a useful result concerning the membership of convex sets.

Theorem 1. Hyperplane separation theorem:- if S is close convex set within \mathbb{R}^n and x is point in \mathbb{R}^n that does not lie within S , then there exists a linear functional that separates x from S . Specifically, there exists $f \in \mathbb{R}^n$ and $c \in \mathbb{R}$ such that $\langle f, y \rangle \leq c$ for all $y \in S$, but $\langle f, x \rangle > c$.

According to this theorem, if a probability point $\mathbf{P} \in \mathbb{R}^n$ is not part of the closed convex sets \mathcal{L} , \mathcal{Q} or $\mathcal{N}S$, one can find a linear function of the form given below that separate this point:

$$(2.17) \quad \beta(\mathbf{P}) = \sum_{a,b,x,y} c_{abxy} P(ab|xy),$$

where c_{abxy} are real coefficient and (2.17) satisfied by all the points belong to set S [92, 93]. It is interesting to note that every polytope can be depicted in two equivalent yet complementary ways: (a) either by defining its vertices or (b) by specifying half-spaces. The local set's half-space description has two classes of conditions. It mandates that all probabilities must be non-negative i.e., $P(a, b|x, y) \geq 0$. These conditions are termed as *positivity facets*, which are somewhat not that interesting because all-natural and reasonable theories satisfy them. The other set of conditions is referred to as *facet Bell inequalities* [84, 88].

In the next part of the chapter, we will delve deeper into the Bell functionals and Bell inequalities in more detail as they play a crucial role in differentiating between quantum and classical correlations.

2.4.5 Bell functionals and Bell inequalities

A Bell functional $\beta(\mathbf{P})$ is a real linear functional defined over the space of probability points. The action of this functional on probability point is described as in (2.17). A Bell inequality has the following generic form:

$$(2.18) \quad \beta(\mathbf{P}) = \sum_{a,b,x,y} c_{abxy} P(ab|xy) \leq \beta_{\mathcal{L}},$$

where $\beta_{\mathcal{L}}$ represents the maximum upper bound of the local Polytope \mathcal{L} . However, it is crucial to understand that there may be Bell inequalities other than the facet Bell inequalities, which emerge from the half-space description of the local polytope. Nonetheless, computing the value of maximum upper bound of the local Polytope $\beta_{\mathcal{L}}$ is easy as it can be cast as a linear program. However, computing quantum values, which involve a quantum state $\rho_{A,B}$ and the measurement sets $\{\hat{M}_a^x\}_{x,a}$ for Alice and $\{\hat{N}_b^y\}_{y,b}$ for Bob is more complex. for instance, to find the optimal state given fixed measurements, we first need to formulate *Bell operator* as follows [7]:

$$(2.19) \quad \hat{\beta} = \sum_{abxy} S_{abxy} \hat{M}_a^x \otimes \hat{N}_b^y$$

It is evident that determining the optimal state requires calculating the maximum eigenvalue of the Bell operator and identifying its corresponding eigenspace. Optimizing measurements for one party, although more challenging, essentially constitutes a *semidefinite program (SDP)*, which is an extension of linear programming that can be solved with some efficiency [86, 94, 95].

While it's possible to optimize each of the three components (the state and both parties' measurements), achieving the global maximum is not guaranteed. Therefore, to enhance the reliability of the results, the process should be repeated multiple times, each starting from different initial configurations. This exhaustive search, however, becomes impractical even in smaller scenarios. As such, algorithms like the *see-saw* are primarily useful for establishing lower bounds on quantum values or identifying optimal realizations. For upper bounds, alternative strategies must be employed [96, 97].

Next, we will explore the semidefinite relaxations of the quantum set, focusing primarily on *Navascués-Pironio-Acín (NPA) relaxations* [98–100].

2.4.6 The quantum set and semidefinite relaxations (NPA) hierarchy

The Navascués-Pironio-Acín (NPA) criterion, was initially proposed by Navascués et al. in 2008 [100]. By 2012, its application had been extended to self-testing, which we will discuss in detail in the later part of the thesis. Given the complexity of precisely defining the quantum set, employing approximations becomes a practical approach. One straightforward approximation involves limiting the Hilbert space dimensions of the possible states or measurements. However, the resulting set of behaviors then becomes a subset of \mathcal{Q} . In the context of device-independent certification, it's preferable to consider supersets (or relaxations) of \mathcal{Q} . This approach ensures that if a property is demonstrated for one of these supersets, it is automatically valid for the entire quantum set. This section introduces such supersets using NPA hierarchy.

Suppose the probability distribution \mathbf{P} is underpinned by quantum theory, and given set of operators $\mathbf{O} = \{\mathcal{O}_i\}_{i=1}^n$ and $|\psi\rangle$ is the state of the system that satisfies $\sum_{i,j} a_{i,j}^k \langle \psi | \mathcal{O}_i^* \mathcal{O}_j | \psi \rangle = f_k(\mathbf{P})$, $k = 1, \dots, m$ with $a_{i,j}^k$ are real coefficient and f_k being linear functions of the moments, then there should be an $n \times n$ positive semi-definite matrix Γ such that $\Gamma \geq 0$, where Γ is the moment matrices with entries $(\Gamma)_{i,j} = \langle \psi | \mathcal{O}_i^* \mathcal{O}_j | \psi \rangle$. Now let's define $\{\mathcal{M}_k\}$ be basis of monomials for set \mathcal{P}^{2n} of class representatives and define $F_{\beta\alpha}^k$ as a tensor with elements specified by:

$$(2.20) \quad F_{\beta\alpha}^k = \begin{cases} 1 & \text{if } \mathcal{M}_k = \overline{R}_\alpha^\dagger \overline{R}_\beta \\ 0 & \text{otherwise} \end{cases}$$

. We can write $\mathcal{O}_i^* \mathcal{O}_j = F_{\beta\alpha}^k \mathcal{M}_k$. This enables a decomposition of the moment matrix Γ as:

$$(2.21) \quad \Gamma = F_{\beta\alpha}^0 + F_{\beta\alpha}^k m_k,$$

where $m_k = \text{Tr}\{\mathcal{M}_k \rho_{AB}\}$. We can set $\mathcal{M}_0 = \mathbb{1}$ which makes $m_0 = 1$. We take the other basis elements $\{\mathcal{M}_k\}$ to be the measurement operators $\{\{M_\alpha^x\}, \{N_\beta^y\}\}$, with this we can represent the

Bell functional β in terms of moments, such as $\beta = c^0 + c^k m_k$, where $c^k = C^{\beta\alpha} F_{\beta\alpha}^k$. This approach results in an n-level NPA relaxation for the bell functional as follows:

$$(2.22) \quad \begin{aligned} \max \quad & c^0 + c^k m_k \\ \text{s.t.} \quad & F_0 + \sum_k F_k m_k \geq 0. \end{aligned}$$

From this discussion, it's apparent that if the state and measurement settings were known, calculating all elements of Γ would be straightforward. However, in a device-independent scenario, we do not have prior knowledge of the state and measurements; we merely assume their existence. Nevertheless, we can determine some of the matrix entries of Γ , specifically those representing $P(a, b|x, y)$, $P(a|x)$ and $P(b|y)$. Entries that involve pairs of operators from either Alice or Bob, which are not directly observable in the Bell test, can be assumed to be such that $\Gamma \geq 0$. If, after populating the matrix Γ with the observed behavior, it turns out impossible to complete the remaining entries in such a way that $\Gamma \geq 0$, it is evident that $\mathbf{P} \notin \mathcal{Q}$. Essentially, the NPA criteria outline the necessary conditions for a behavior \mathbf{P} to be included in the quantum set \mathcal{Q} .

The set of behaviors that fulfill the condition $\Gamma \geq 0$ for $\mathbf{O} \equiv \{\mathcal{M}_k\}$ is labeled as \mathcal{Q}_1 . The set of behaviors meeting the condition $\Gamma \geq 0$ for \mathcal{O} containing strings of monomials from $\{\mathcal{M}_k\}$ of at most length n is denoted it as \mathcal{Q}_n . It naturally follows that $\mathcal{Q}_1 \supseteq \mathcal{Q}_2 \supseteq \mathcal{Q}_3 \supseteq \dots \supseteq \mathcal{Q}_n \supseteq \mathcal{Q}$ for all n . The NPA criterion also demonstrates that this hierarchy converges, implying that $\lim_{n \rightarrow \infty} \mathcal{Q}_n = \mathcal{Q}$. Additionally, in several instances, the quantum result is achieved at a finite n . The characteristic of the NPA conditions as semidefinite constraints $\Gamma \geq 0$ is specifically important, as it indicates the potential for their application within *semidefinite programming* (SDPs) [101]. In the upcoming thesis section, we will briefly now outline one of the straightforward approach known as *sum-of-squares* (SOS) decomposition used to drive an upper bound on the quantum value of a Bell functional [10, 102]. Although finding SOS in more complex scenarios is not straightforward; this we will discuss in greater detail in later sections of the thesis.

2.4.7 Upper bound on the quantum value of Bell operator \mathbf{W}

Now, let's discuss a basic technique for establishing an upper bound on the quantum value of Bell functional. Consider a Bell inequality represented as $\beta(\mathbf{P}) = \sum_{abxy} c_{abxy} P(a, b|x, y) \leq \beta_{\mathcal{L}}$. The maximum violation achievable with quantum resources can be calculated as $\beta_{\mathcal{Q}} = \text{tr}[\hat{\beta}\rho]$. We can then define a shifted Bell operator. By construction, every shifted operator $\beta_{\mathcal{Q}}\mathbb{1} - \hat{\beta}$ is positive semidefinite i.e., $\langle \psi | \hat{\beta} | \psi \rangle \leq \beta_{\mathcal{Q}}$ for any state $|\psi\rangle$. If the shifted, Bell operator permits a breakdown, of the form $\beta_{\mathcal{Q}}\mathbb{1} - \hat{\beta} = \sum_{\lambda} \mathcal{P}_{\lambda}^{\dagger} \mathcal{P}_{\lambda} \geq 0$, with \mathcal{P}_{λ} being a polynomial of the operators \hat{M}_a^x and \hat{N}_b^y , This form of decomposition, called the *sum-of-squares* (SOS) decomposition. The SOS technique establishes an upper bound on the maximum quantum value achievable. Then, we can identify quantum realization that reaches this upper bound. This decomposition provides valuable insights into the state $|\psi\rangle$ and the measurements employed to achieve the maximum violation of specific Bell inequalities.

So far, we have focused on introducing some basic tools that will be helpful in the upcoming sections for defining both bipartite and multipartite Bell scenarios. In the next section, let us start with the smallest scenario, known as the Clauser-Horne-Shimony-Holt (CHSH) scenario, and then proceed to the multipartite scenario.

2.5 Bell scenarios

Bell scenarios are characterized based on the number of parties, the range of inputs available to each participant, and the set of possible outcomes. For now, our focus is on bipartite scenarios, involving just two parties. We represent a bipartite Bell scenario specified by the tuple $(n_X, n_A; n_Y, n_B)$.

2.5.1 The CHSH Scenario

The most basic Bell scenario where the three correlation sets \mathcal{L} , \mathcal{Q} and \mathcal{NS} diverge involves a bipartite system, two measurement settings, and two outcomes for each party $(2,2;2,2)$, known as the *CHSH scenario*.

In the CHSH scenario, the parties are typically referred to as Alice and Bob. Notably, for practicality and to better align with experimental setups in Bell tests, we adopt the convention $x, y \in \{0, 1\}$ for inputs and $a, b \in \{+1, -1\}$ for outputs. In this scenario, Alice can perform one of two measurements ($x = 0$ or 1) with outcomes $a = +1$ or -1 . Similarly, Bob has two measurements ($y = 0$ or 1) with outcomes $b = +1$ or -1 . The probability of Alice and Bob obtaining outcomes a and b given measurements x and y is denoted by $P(ab|xy)$ [7, 103].

The expectation value of outcomes a and b for specific measurement settings x, y is denoted as $\langle A_x B_y \rangle$ and is defined by the equation below,

$$(2.23) \quad \langle A_x B_y \rangle = \sum_{a,b} abP(a, b|x, y).$$

$\langle A_x B_y \rangle$ are known as *correlators*. The *marginal* correlators of Alice $\langle A_x \rangle$ and Bob $\langle B_y \rangle$ are defined as,

$$(2.24) \quad \langle A_x \rangle = \sum_a aP(a|x), \quad \langle B_y \rangle = \sum_b bP(b|y).$$

The joint probabilities $P(ab|xy)$ in terms of the marginals and correlators can be expressed as:

$$(2.25) \quad P(ab|xy) = \frac{1}{4}(1 + a\langle A_x \rangle + b\langle B_y \rangle + ab\langle A_x B_y \rangle).$$

Note, here, that the observed statistics can be completely described by the set $\mathbf{P} = \{P(a, b|x, y)\} \in \mathbb{R}^{16}$. However, utilizing the no signaling conditions (as given in (2.15) and (2.16)) along with normalization condition, i.e., $\sum_{a,b} P(ab|xy) = 1$, we find that only 8 real parameters are sufficient

to reconstruct the entire distribution. Consequently, a probability distribution $\mathbf{P} \in \mathbb{R}^8$ can be completely specified in the following way,

$$(2.26) \quad \mathbf{P} = (\langle A_0 \rangle, \langle A_1 \rangle, \langle B_0 \rangle, \langle B_1 \rangle, \langle A_0 B_0 \rangle, \langle A_0 B_1 \rangle, \langle A_1 B_0 \rangle, \langle A_1 B_1 \rangle).$$

In the (2,2;2,2) scenario, the local polytope \mathcal{L} is characterized by 16 deterministic vertices and 24 facets. The 16 facets among these are positive constraints i.e., $P(ab|xy) \leq 0$ [84]. The remaining 8 facets correspond to the Clauser-Horne-Shimony-Holt (CHSH) inequality (up to local relabelling of inputs and outputs) [104],

$$(2.27) \quad \mathcal{C}(\mathbf{P}) = \langle A_0 B_0 \rangle + \langle A_0 B_1 \rangle + \langle A_1 B_0 \rangle - \langle A_1 B_1 \rangle \leq 2.$$

The CHSH inequality is a linear inequality that must be satisfied by all local theories. However, it can be violated by quantum theory through specific measurements performed on an entangled pair of states.

2.5.1.1 Local bound of CHSH inequality

We can express the CHSH functional (2.27) as given below:

$$(2.28) \quad \mathcal{C}(\mathbf{P}) = c_{00} \langle A_0 B_0 \rangle + c_{01} \langle A_0 B_1 \rangle + c_{10} \langle A_1 B_0 \rangle + c_{11} \langle A_1 B_1 \rangle,$$

where $c_{xy} = (-1)^{x \cdot y}$. Recall that the local set \mathcal{L} forms a polytope, and extremal points of this polytope are local deterministic points, taking values in $\{+1, 1\}$. In more detail, a deterministic point can be completely determined by specifying the outcomes for Alice and Bob in each measurement setting, with settings $(x, y) \in \{0, 1\}$ and outcomes $(a, b) \in \{+1, -1\}$. Such that $\langle A_x B_y \rangle = |1|$, and

$$(2.29) \quad \mathcal{C}(\mathbf{P}) = (-1)^{0 \cdot 0} + (-1)^{0 \cdot 1} + (-1)^{1 \cdot 0} + (-1)^{1 \cdot 1},$$

which gives us the the local value of the CHSH functional equals 2 [7, 104]. Given that the expectation value of $\langle A_x B_y \rangle$ within $\{-1, +1\}$, the local bound of $\mathcal{C}(\mathbf{P})$ is constrained to ≤ 2 . The subsequent section of this thesis will explore how quantum theory surpasses this bound.

2.5.1.2 The Tsirelson's bound

Several methods can be employed to derive the maximum quantum violation of the CHSH inequality, commonly referred to as Tsirelson's bound [105]. However, this section will focus solely on the approach using the Khalfin-Tsirelson-Landau identity [106, 107]. The Tsirelson bound represents the maximum eigenvalue of CHSH Bell operator \hat{C} , expressed as $\|\hat{C}\|_\infty = \max_\psi |\langle \psi | \hat{C} | \psi \rangle|$, where $\|\hat{C}\|$ is the spectral norm (largest eigenvalue) of \hat{C} . Optimization is done over all possible observables $A_x = M_1^x - M_{-1}^x$ and $B_y = N_1^y - N_{-1}^y$. For the CHSH scenario, the Bell operator is defined as $\hat{C} = A_0 \otimes B_0 + A_0 \otimes B_1 + A_1 \otimes B_0 - A_1 \otimes B_1$, the observables can always be taken to be projective measurements, hence $A_x^2 = B_y^2 = \mathbb{1}$. Utilizing the Khalfin-Tsirelson-Landau identity [106, 107], the Bell operator can be reformulated as $\hat{C}^2 = 4\mathbb{1} - [A_0, A_1][B_0, B_1]$.

This formulation leads to the observation that $\|\hat{\mathcal{C}}^2\|_\infty \leq 8$, which implies $\|\hat{\mathcal{C}}\|_\infty \leq 2\sqrt{2}$. The quantum strategy $|\psi\rangle = \frac{|00\rangle + |11\rangle}{\sqrt{2}}$, $A_0 = \sigma_x$, $B_0 = \frac{\sigma_x + \sigma_z}{\sqrt{2}}$, $A_1 = \sigma_z$, $B_1 = \frac{\sigma_x - \sigma_z}{\sqrt{2}}$ saturates this bound [75]. Notably, if $[A_0, A_1] = 0$ or $[B_0, B_1] = 0$, then $\hat{\mathcal{C}} \leq 2$, illustrating how joint measurability results in local behavior. This insight also provides a foundational basis for self-testing, as the maximum bound of a Bell operator can only be achieved with specific states and measurements, which will be explored more thoroughly in the upcoming sections of the thesis. Next, we will examine correlations that more powerful quantum theory, potentially violating the CHSH inequality up to a value of 4.

2.5.1.3 Popescu Rohrlich (PR) boxes

In the CHSH scenario (2,2;2,2) for Bell tests, the structure of the no-signaling polytope \mathcal{NS} consists of 16 facets, all of which are positivity constraints, and it includes 24 vertices. Among these vertices, 16 are deterministic local points, while 8 represent non-local vertices generally known as Popescu Rohrlich (PR) boxes [108]. These non-local vertices are equivalent under the relabeling of inputs and outputs, defined by the behavior,

$$(2.30) \quad P(ab|xy) = \begin{cases} \frac{1}{2} & \text{if } a \oplus b = xy, \\ 0 & \text{otherwise.} \end{cases}$$

PR-boxes notably violate the CHSH inequality to its maximum algebraic value of 4 [7, 21].

In the CHSH setup, there is an interesting duality: each facet of Bell inequality is uniquely maximally violated by a specific PR box. However, this clear correspondence between facet Bell inequalities and extremal no-signaling boxes is not generally observed in more complex multipartite scenarios. Up to this point, our discussion has focused on the simplest setups involving only two parties; we will now expand our discussion to include scenarios with more than two parties.

2.5.2 Multipartite Scenarios

While earlier sections focused on Bell scenarios with $N = 2$ systems for simplicity, it's crucial to recognize that the fundamental concepts, such as the no-signaling conditions, are applicable to any number of parties, $N > 2$. In this section, we will discuss some significant Bell inequalities in the context of multipartite scenarios. In particular, we consider tripartite Bell scenarios, specifically the Bell scenarios with the tuple $(n_X, n_A; n_Y, n_B; n_Z, n_C)$

The most basic example of a *multipartite Bell scenario* is the (2,2;2,2;2,2) configuration, which involves three parties, each having two possible inputs and outputs. Unlike the simpler bipartite case, the local polytope in this scenario is considerably more complex. Research has shown that the local polytope contains 53,856 extremal points, substantially increasing from the 16 extremal points observed in the bipartite CHSH scenarios [109, 110].

Multipartite Bell scenarios diverge significantly in complexity from the simpler bipartite case. While the principle of locality can be extended from bipartite to multipartite scenarios, the

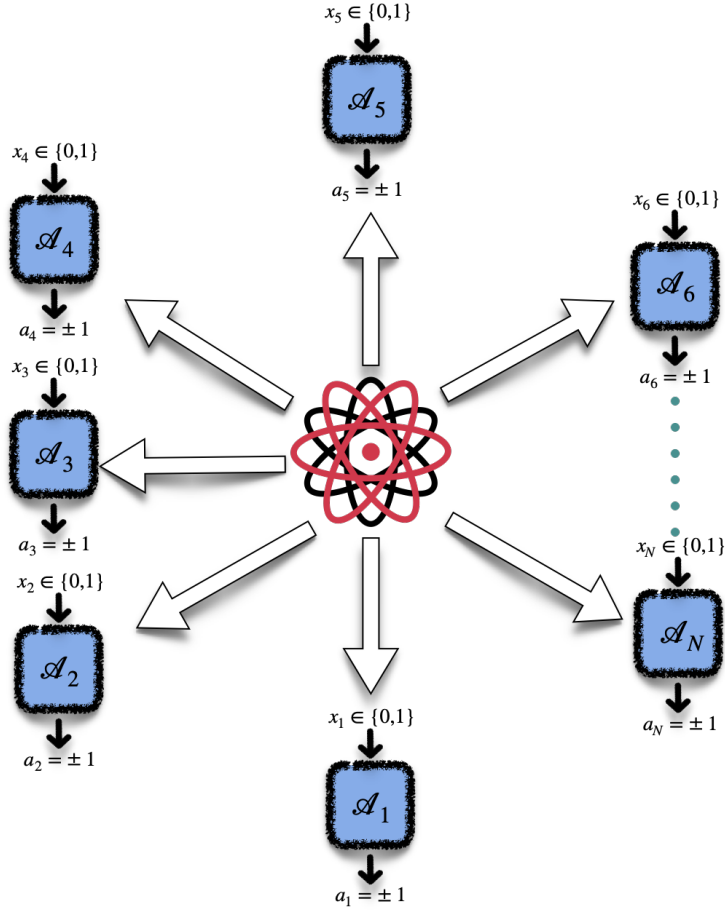


Figure 2.3: *Schematic of multipartite Bell scenarios*– A source sends physical systems to distant observers \mathcal{A}_i , with i ranging from 1 to N . Each party can perform measurement $x \in \{0,1\}$ and gets outcome $a \in \{\pm 1\}$.

manifestation of non-locality in multipartite systems is distinctively varied. One major challenge is that self-testing criteria for multipartite scenarios are harder to establish due to the lack of simplifications available in the bipartite context, such as the Schmidt decomposition of the shared entangled state. In the next part of this section, we will introduce various linear and quadratic *multipartite Bell inequalities* [111, 112]. In the next part of this section, we will introduce various linear and quadratic *multipartite Bell inequalities*.

2.5.2.1 Linear inequalities

The most commonly used Bell inequalities are those comprised of Bell expressions, which are linear combinations of observed probabilities. In this discussion, we only consider multipartite Bell scenarios involving N no-signaling spatially separated parties. We limit our discussion

only to the scenarios where each party \mathcal{A}_i , with i ranging from 1 to N , is equipped with two observables, $A_0^{(i)}$ and $A_1^{(i)}$, each yielding binary outcomes $\{+1, -1\}$ (see Fig. 2.3). Among these linear Bell inequalities, we particularly focus on the Werner-Wolf-Weinfurter-Żukowski-Brukner (WWWŻB) family of correlation Bell inequalities [14, 28–30]. The Bell operator for WWWŻB family of Bell inequalities has the following general form:

$$(2.31) \quad \hat{\mathcal{W}}_N = \frac{1}{2^N} \sum_{s_1, \dots, s_N = \pm 1} S(s_1, \dots, s_N) \bigotimes_{j=1}^N (A_0^{(j)} + s_j A_1^{(j)}),$$

Where $S(s_1, \dots, s_N)$ denotes a function determined by the indices s_1, \dots, s_N , which belong to the set $\{-1, 1\}$ with binary outcomes ± 1 . Every tight (WWWŻB) inequality is given by $\langle \hat{\mathcal{W}}_N \rangle \leq_{\mathcal{L}} 1$, where the notation $\leq_{\mathcal{L}}$ signifies that the inequality holds for all correlations which admit local hidden variable explanations (\mathcal{L}).

Next, we delve into a specific subset of the Werner-Wolf-Weinfurter-Żukowski-Brukner (WWWŻB) Bell inequalities, known as the Mermin-Ardehali-Belinskii-Klyshko (MABK) family of inequalities [21, 26, 27]. The N -party MABK operators can be obtained recursively as,

$$(2.32) \quad \begin{aligned} \hat{\mathcal{M}}_N &= \frac{1}{2} \left(\hat{\mathcal{M}}_{N-1} \otimes (A_0^{(j)} + A_1^{(j)}) + \hat{\mathcal{M}}'_{N-1} \otimes (A_0^{(j)} - A_1^{(j)}) \right) \\ &= \frac{1}{2^{\frac{N+1}{2}}} \left(\left(\frac{1-l}{\sqrt{2}} \right)^{(N-1) \bmod 2} \bigotimes_{j=1}^N (A_0^{(j)} + l A_1^{(j)}) + \left(\frac{1+l}{\sqrt{2}} \right)^{(N-1) \bmod 2} \bigotimes_{j=1}^N (A_0^{(j)} - l A_1^{(j)}) \right), \end{aligned}$$

where complementary Bell expression, $\hat{\mathcal{M}}'_{N-1}$, is equivalent to $\hat{\mathcal{M}}_{N-1}$ but with the observables $A_0^{(j)}$ and $A_1^{(j)}$ interchanged. The associated Bell inequalities are expressed as $\langle \hat{\mathcal{M}}_N \rangle \leq_{\mathcal{L}} 1$. The maximum achievable values of $\langle \hat{\mathcal{M}}_N \rangle$ for biseparable states \mathcal{Q}_{N-1} and general quantum correlations \mathcal{Q} are $2^{\frac{N-2}{2}}$ and $2^{\frac{N-1}{2}}$, respectively [21].

Finally, we present yet another relevant sub-family of the (WWWŻB) inequalities, referred to as Svetlichny inequalities [113, 114]. The Svetlichny operator can be formed of MABK operators (2.32) in the following way,

$$(2.33) \quad \hat{\mathcal{S}}_N^{\pm} = \begin{cases} 2^{k-1} (-1)^{\frac{k(k\pm 1)}{2}} \hat{\mathcal{M}}_N^{\pm}, & (\text{for } N = 2k); \\ 2^{k\pm 1} (-1)^{\frac{k(k\pm 1)}{2}} \hat{\mathcal{M}}_N \mp (-1)^{\frac{k(k\mp 1)}{2}} \hat{\mathcal{M}}'_N, & (\text{for } N = 2k + 1), \end{cases}$$

where $\hat{\mathcal{M}}_N^+$ is equivalent to $\hat{\mathcal{M}}_N$ (2.32) and $\hat{\mathcal{M}}_N^-$ is equivalent to $\hat{\mathcal{M}}'_N$. The corresponding Svetlichny inequalities are of the form, $\langle \hat{\mathcal{S}}_N^{\pm} \rangle \leq_{\mathcal{Q}_{N-1}} 2^{N-1} \leq_{\mathcal{Q}} 2^{N-\frac{1}{2}}$ [21].

2.5.2.2 Uffink's Quadratic inequalities

In bipartite Bell scenarios, it is typically sufficient to employ linear Bell inequalities to detect non-locality. This is because the set of behaviors that can be explained by local causal models

forms a convex polytope \mathcal{L} , characterized by linear facet inequalities. However, in multipartite settings, the landscape changes significantly; here, nonlinear Bell inequalities become essential for a thorough analysis of genuine multipartite non-locality. This distinction arises because the bi-separable quantum behaviors in multipartite scenarios do not constitute a polytope, making Uffink's quadratic Bell inequalities [31] more effective at witnessing genuine multipartite non-locality compared to their linear inequalities. There are two distinct families of N party quadratic Bell inequalities formed of the MABK (2.32) and Svetlichny (2.33), families of linear inequalities, \hat{U}_N^M and \hat{U}_N^S , respectively, which have the form

$$(2.34) \quad \hat{U}_N^M = \langle \hat{\mathcal{M}}_N \rangle^2 + \langle \hat{\mathcal{M}}'_N \rangle^2 \leq_{Q_{N-1}} 2^{N-2} \leq_Q 2^{N-1},$$

$$(2.35) \quad \hat{U}_N^S = \langle \hat{\mathcal{S}}_N^+ \rangle^2 + \langle \hat{\mathcal{S}}_N^- \rangle^2 \leq_{Q_{N-1}} 2^{2N-2} \leq_Q 2^{2N-1},$$

Genuine N -partite non-locality is crucial for quantum information processing tasks that require the active participation of all involved parties [32, 34, 35]. The certification of quantum nonlocality underpins practical applications such as device-independent quantum cryptography and random number generation protocols [33]. However, confirming nonlocality in practical scenarios is challenging due to experimental inaccuracies. In real-world experiments, deviations from the ideal conditions posited in theoretical models can lead to potential *loopholes* [14, 21]. In the following discussion, we will see how loopholes, particularly those caused by inefficient detectors, can impact the integrity of Bell experiment results.

2.6 Inefficient detectors

Bell inequalities provides a crucial benchmark for assessing the nature of correlations between measurements on entangled particles, with the foundational assumption that these measurements are unaffected by any distant actions. Over the years, numerous experiments have been conducted to test these inequalities by measuring correlations between entangled particles, demonstrating consistent violations of Bell inequality [14, 21]. Some of these experimental results have not been conclusively definitive, primarily due to the presence of "loopholes" that can allow local theories to potentially explain the observed statistics.

Several types of loopholes exist within Bell experiments [14, 21, 115, 116]. These include the *locality loophole*, which arises if the measurement on one particle could influence the measurement on another; the *freedom of choice loophole*, also known as the "free will" loophole, which pertains to the randomness in selecting measurement settings for each party; and the *detection loophole*, which occurs when not all particles involved in the experiment are detected [117]. Of these, the detection loophole is particularly significant. We will discuss this loophole in more detail in this section of the thesis and its impact on Bell inequalities.

The detection loophole arises because the detectors used in the Bell experiments' have poor detection efficiency. Detection efficiency, denoted as η , is the ratio of the number of particles

detected by a measurement device to the total number of particles emitted by the source. It is influenced by both the sensitivity of the measurement device and the distance of the device from the source [21].

For instance, in a bipartite Bell experiment testing the CHSH inequality with quantum strategy, the minimum required detection efficiency is $\eta = 0.828$. In photonic Bell experiments, the effective detection efficiency decreases exponentially with the increase in the length of the optical fiber l and can be modeled as $\eta = \eta_0 \exp\{-\alpha l\}$. Here, η_0 represents the intrinsic detection efficiency of the detectors, and α is the attenuation coefficient, typically around 0.2 dB/km for light at a wavelength of 1550 nm (used in the third telecom window) [41]. Consequently, the lower the required critical detection efficiency for observing nonlocal correlations, the greater the allowable distance between the measurement devices and the source for maintaining valid, loophole-free nonlocal observations [41–43].

2.6.1 Post-processing strategies

In Bell-type experiments, detector imperfections often lead to scenarios where one or more detectors fail to produce an outcome, known as a "no-click" event. Addressing how to handle these rounds is crucial. One common approach is to assign a different classical value, other than the pre-existing ones, to each no-click event. However, this approach requires developing a new form of Bell inequality to accommodate the additional outcomes [117]. Alternatively, more straightforward strategies which preserve the Bell scenario can be employed, such as

- **Discard Strategy:** In this strategy, any round where a detector fails to register an outcome is excluded from the statistical analysis. It's important to note, however, that using a discard strategy might introduce signaling into the estimated joint probability distribution, which can complicate the interpretation of the results.
- **Assignment Strategy:** During an experiment, if a detector fails to click, the corresponding party assigns a preexisting classical value, for that round.

The assignment strategy offers significant advantages over the discard strategy in managing "no-click" events within Bell experiments. Unlike the discard strategy, it preserves the no-signaling constraints and does not alter the local bound of the Bell inequality; instead, it primarily affects the quantum value, which typically decreases. This strategy is particularly useful for exploring the effects of imperfect detectors within the framework of established Bell inequalities. It maintains the dimensional integrity of the Bell scenario, simplifying analysis and interpretation [21, 118]. Next, we will discuss how the assignment strategy in the presence of inefficient detectors influences the violation of Bell inequality [5, 119, 120], examining its impact on the experimental results and theoretical interpretations.

2.6.2 Effect of inefficient detectors with local assignment strategy on Bell inequalities

Let's suppose the measurement device used by Alice and Bob has efficiencies denoted by η_A and η_B such that $\eta_A, \eta_B < 1$, respectively. When Alice's device fails to register a detection, she assigns a predefined outcome a with a certain probability $Q(a|x)$, and similarly, Bob assigns outcome b with probability $Q(b|y)$ when his device fails to click. The product of these probabilities, $Q(ab|xy) = Q(a|x)Q(b|y)$, defines a local strategy \mathbf{Q} .

Let $P(ab|xy)$ represent the ideal joint probability that would be observed with perfect detection efficiency. The actual measurement statistics, denoted as $\tilde{P}(ab|xy)$ are calculated based on a combination of the real detection outcomes and the probabilities assigned during "no-click" events as given below,

$$\begin{aligned} \tilde{P}(ab|xy) = & \eta_A \eta_B P(ab|xy) + \eta_A (1 - \eta_B) P(a|x) Q(b|y) \\ & + (1 - \eta_A) \eta_B Q(a|x) P(b|y) \\ & + (1 - \eta_A) (1 - \eta_B) Q(a|x) Q(b|y). \end{aligned} \quad (2.36)$$

This relationship describes how inefficient detectors impact the observed statistics through a linear transformation $\tilde{\mathbf{P}} = \Omega_{\eta_A, \eta_B}(\mathbf{P})$, mapping the ideal joint probabilities \mathbf{P} to the observed measurement statistics $\tilde{\mathbf{P}}$ such that,

$$\begin{aligned} \tilde{\mathbf{P}} = \Omega_{\eta_A, \eta_B}(\mathbf{P}) = & \eta_A \eta_B \mathbf{P} + \eta_A (1 - \eta_B) \mathbf{P}^A \\ & + (1 - \eta_A) \eta_B \mathbf{P}^B + (1 - \eta_A) (1 - \eta_B) \mathbf{Q}, \end{aligned} \quad (2.37)$$

where $\tilde{\mathbf{P}}$ includes the entries $\tilde{P}(ab|xy)$, and the vectors \mathbf{P}^A and \mathbf{P}^B are linear functions of the ideal marginal probabilities $P(a|x)$ and $P(b|y)$, respectively. Specifically, these vectors contain entries $P(a|x)Q(b|y)$ and $Q(a|x)P(b|y)$ for any values of η_A, η_B , and the local strategy \mathbf{Q} . Thus, by linearity, the value of a specific Bell functional β calculated over this effective behavior can be expressed as,

$$\begin{aligned} \beta(\tilde{\mathbf{P}}) = & \eta_A \eta_B \beta(\mathbf{P}) + \eta_A (1 - \eta_B) \beta(\mathbf{P}^A) + (1 - \eta_A) \eta_B \beta(\mathbf{P}^B) \\ & + (1 - \eta_A) (1 - \eta_B) \beta(\mathbf{Q}). \end{aligned} \quad (2.38)$$

As we have already discussed, assigning a pre-existing outcome to a "no-click" event cannot raise the local bound of Bell inequality. Therefore, using inefficient detectors in a Bell experiment that violate a given Bell inequality in a loophole-free way if the effective behavior $\tilde{\mathbf{P}}$ violates this same Bell inequality, i.e.,

$$\beta(\tilde{\mathbf{P}}) \leq \beta_L. \quad (2.39)$$

In the next section, we demonstrate the application of the discussion of this section for the simplest bipartite Bell scenario, involving two dichotomic measurements per party.

2.6.3 Effect of inefficient detectors with local assignment strategy on CHSH inequality

Let us now consider the simplest Bell scenario where Alice and Bob each perform one of two possible measurements $x, y \in \{0, 1\}$ and get binary outcomes, $a, b \in \{-1, +1\}$. We can express the behavior in terms of correlators (2.23) and marginals (2.24), such that the nonlocality of a given behavior can be detected by the violating of the CHSH inequality,

$$(2.40) \quad \mathcal{C}(\mathbf{P}) = \sum_{x,y} (-1)^{x \cdot y} \langle A_x B_y \rangle \leq 2.$$

This inequality is the only tight and complete Bell inequality for this scenario, subject to the relabeling of measurements and outcomes [7, 121]. To demonstrate the nonlocality of the effective behavior in (2.37) the ideal behaviour \mathbf{P} violates the following inequality for any local assignment strategy \mathbf{Q} and given detection efficiency η_A and η_B ,

$$(2.41) \quad \begin{aligned} \mathcal{C}(\tilde{\mathbf{P}}) = & \eta_A \eta_B \mathcal{C}(\mathbf{P}) + (1 - \eta_A)(1 - \eta_B) \mathcal{C}(\mathbf{Q}) \\ & + \eta_A(1 - \eta_B) \mathcal{C}(\mathbf{P}^A) + (1 - \eta_A) \eta_B \mathcal{C}(\mathbf{P}^B) \leq 2. \end{aligned}$$

With these foundational aspects clarified, we will now proceed to discuss one of the most robust methods of certification, known as *self-testing*, which was briefly introduced earlier. The upcoming section will detail this concept further.

2.7 Device-independent certification

For nonlocal correlations, two essential conditions are necessary: a) the quantum state involved must be entangled, and b) the measurements carried out by the participating parties must be incompatible. Observing these nonlocal correlations, therefore, serves as proof that the state is entangled and the measurements are indeed incompatible. This forms the basis for what is known as self-testing or device-independent certification of quantum devices (see Fig. 2.4). In the device-independent approach, all quantum devices involved in both the source and the measurement apparatus are treated as *black box*, implying that there are no presuppositions about their internal workings [10, 14, 21]. However, it's important to note that this form of certification still depends on certain assumptions regarding the Bell test itself, specifically the requirement for measurement independence and that the measurements by the parties should occur with a space-like separation to prevent any causal interaction.

2.7.1 Self-testing

In previous discussions, we've noted that certain statistics from measurement outcomes in nonlocal scenarios serve as evidence of the fundamentally quantum character of an experiment, demonstrating that it cannot be accounted for by local realism. Remarkably, these measurement

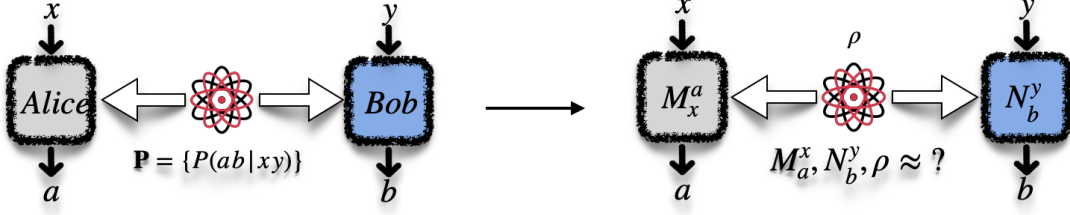


Figure 2.4: *Self-testing in bipartite systems*:- Self-testing schemes enable us to deduce the underlying physics of a Bell experiment i.e., quantum state ρ and the measurement operators M_a^x, N_b^y involved based solely on the observed statistics $\mathbf{P} = \{P(ab|xy)\}$.

statistics can sometimes allow us to draw even more conclusive insights. The most conclusive form of such insights is known as self-testing [10]. This method offers the most robust certification of the underlying physics i.e., the quantum state and the measurements involved in an experiment.

In a Bell scenario involving N parties, each denoted as $\{\mathcal{A}_j\}_{j=1}^N$, where every party measures two observables, $A_0^{(j)}, A_1^{(j)}$, and share a state $|\bar{\psi}\rangle\langle\bar{\psi}|$, *self-tests*, if we observed the quantum maximal value β_Q of the specific Bell operator $\hat{\beta}$, then the state $|\bar{\psi}\rangle$ used in the experiment must be transformable by local unitaries, $\otimes_j U_{\mathcal{A}_j}$, to a reference state, $|\psi\rangle$, combined with a separable "junk" part, $|\Psi\rangle$, on which the observables act trivially. This transformation can be mathematically represented as,

$$(2.42) \quad \otimes_j U_{\mathcal{A}_j} |\bar{\psi}\rangle = |\psi\rangle \otimes |\Psi\rangle.$$

Additionally, the local observables $\{A_0^{(j)}\}_{j=1}^N$ and $\{A_1^{(j)}\}_{j=1}^N$, must conform to the following transformations:

$$(2.43) \quad U_{\mathcal{A}_j} \bar{A}_0^{(j)} (U_{\mathcal{A}_j})^\dagger = A_0^{(j)} \otimes \mathbb{1},$$

$$(2.44) \quad U_{\mathcal{A}_j} \bar{A}_1^{(j)} (U_{\mathcal{A}_j})^\dagger = A_1^{(j)} \otimes \mathbb{1},$$

where the joint observables $\otimes_j O^{(j)}$ where $O^{(j)} \in \{A_0^{(j)}, A_1^{(j)}\}$ act on the Hilbert space of $|\psi\rangle$, and the tuple $\{|\psi\rangle, \{A_0^{(j)}, A_1^{(j)}\}_j\}$ maximizes the given Bell operator, i.e., $\langle\psi|\hat{\beta}(A_0^{(j)}, A_1^{(j)})|\psi\rangle = \beta_Q$.

Such characterization is typically referred to as device-independent certification. It operates under the assumption that the quantum devices involved do not communicate; no specific assumptions are made about their internal workings. Essentially, these devices are treated as black boxes, and their characterization is derived entirely from analyzing the statistics of their inputs and outputs. Another crucial concept is that of isometries. It is necessary to find the *local isometry* mapping that can map the physical realization $\{|\bar{\psi}\rangle, \{\bar{A}_0^{(j)}, \bar{A}_1^{(j)}\}\}$ to the desired one $\{|\psi\rangle, \{A_0^{(j)}, A_1^{(j)}\}\}$ [25].

An isometry $\Phi: \bar{\mathcal{H}} \rightarrow \mathcal{H}$ is a linear map such that $\Phi^\dagger \Phi = I_{\bar{\mathcal{H}}}$, where $I_{\bar{\mathcal{H}}}$ is the identity operator on $\bar{\mathcal{H}}$. This mapping preserves all inner products. On the other hand, a local isometry refers to an isometry that can be implemented locally i.e., A local isometry on the Hilbert space $\mathcal{H}_{\bar{A}_0^{(j)}} \otimes \mathcal{H}_{\bar{A}_1^{(j)}}$ is a map $\Phi: \bar{\mathcal{H}}_{\bar{A}_0^{(j)}} \otimes \bar{\mathcal{H}}_{\bar{A}_1^{(j)}} \rightarrow \mathcal{H}_{A_0^{(j)}} \otimes \mathcal{H}_{A_1^{(j)}}$, such that

$$(2.45) \quad V = V_{\bar{A}_0^{(j)}} \otimes V_{\bar{A}_1^{(j)}},$$

where $V_{\bar{A}_0^{(j)}}$ and $V_{\bar{A}_1^{(j)}}$ are isometries on $\bar{\mathcal{H}}_{\bar{A}_0^{(j)}}$ and $\bar{\mathcal{H}}_{\bar{A}_1^{(j)}}$, respectively. For instance $\otimes_j U_{A_j}$ constitute such a local isometries.

However, self-testing statements are based on experimental data is significant, their validation can faces two primary challenges. First, inevitable experimental noise can reduce the observed correlations. Second, exact statistics are never observed due to the finite number of experimental trials, resulting only in approximate representations of the true statistical outcomes. To overcome these challenges, the concept of robust self-testing has been developed, which focuses on proving self-testing statements in an approximate manner by acknowledging and accommodating the inherent noise in experimental setups [122–124].

While there are numerous schemes available for the robust self-testing of states and measurements, we can discuss the , the numerical SWAP method is particularly interesting. Detailed in studies such as [125, 126], this method is a numerical approach, predominantly employed in self-testing protocols where analytical methods are insufficient. Although its application is typically confined to simpler protocols due to computational limitations, it plays a crucial role in establishing the robust self-testing bounds that are essential for practical applications [127]. The core principle of this technique hinges on the use of local isometries, which transform the actual physical state $|\bar{\psi}\rangle$ into the desired reference self-testing state $|\psi\rangle$ and a junk state $|\Psi\rangle$ on local auxiliary systems. In many self-testing applications, these local isometries function similarly to partial SWAP gates. They effectively swap the actual physical state $|\bar{\psi}\rangle$ with the state $|0\rangle^{\otimes N}$ of the registers, such that the final state of the registers corresponds to the reference self-testing state $|\psi\rangle$. These local isometries can then be implemented through a swap circuit U_{SWAP} having the \hat{Z} and \hat{X} operators as gates so that the fidelity, $\mathcal{F}_n = \langle \psi | \rho_{SWAP}(\Gamma_n) | \psi \rangle$, of the final state of the register $\rho_{SWAP}(\Gamma_n)$ with the target state $|\psi\rangle$, as a function of the entries of the necessarily positive semi-definite NPA moment matrix Γ_n of level $n \in \mathbb{N}$, as well as of the target self-testing state $|\psi\rangle$ [10, 25, 128].

Self-testing is a dynamic field of research with extensive potential applications, though the current methods also have their limitations. In the following section, we will explore a novel approach to formulating self-testing statements using Jordan’s lemma.

2.7.2 SOS and maximal violation of the CHSH inequality

Self-testing aims to precisely verify the specific quantum states and measurements without relying on the internal mechanics of the devices involved, leveraging the maximum violation of a

Bell inequality. To understand it more clearly, let's start with an example of CHSH. We revisit the case of maximal violation of CHSH inequality, which is $2\sqrt{2}$, which can only be achieved by performing projective measurements on a two-qubit maximally entangled state, where the measurements are conducted in mutually unbiased bases.

Self-testing of CHSH inequality—The maximal violation of the CHSH inequality $\mathcal{C}(\mathbf{P}) = 2\sqrt{2}$, self-test the state to be maximally entangled i.e., $|\psi\rangle = \frac{1}{\sqrt{2}}(|0\rangle \otimes |0\rangle + |1\rangle \otimes |1\rangle)$ and the measurements corresponding to the observables i.e., $A_0^{(1)} = X$, $A_1^{(1)} = Z$, $B_0^{(2)} = \frac{\sigma_X + \sigma_Z}{\sqrt{2}}$, $B_1^{(2)} = \frac{\sigma_X - \sigma_Z}{\sqrt{2}}$.

To demonstrate this, one effective method is the Sum of Squares (SOS) decomposition. One can start by having an SOS decomposition of the shifted CHSH operators as,

$$(2.46) \quad 2\sqrt{2}\mathbb{1} - \hat{C} = \sum_{\lambda} \mathcal{P}_{\lambda}^{\dagger} \mathcal{P}_{\lambda},$$

where the polynomial \mathcal{P}_{λ} includes terms from the set $\{\mathbb{1}, A_x, B_y, A_x \otimes B_y\}$. The possibility of finding decomposition like the one in (2.46) for the CHSH operator \hat{C} confirms that this upper bound $2\sqrt{2}$ can be saturated by performing the following measurements i.e., $A_0 = X$, $A_1 = Z$, $B_0 = \frac{X+Z}{\sqrt{2}}$, $B_1 = \frac{X-Z}{\sqrt{2}}$ on the maximally entangled state i.e., $|\psi\rangle = \frac{1}{\sqrt{2}}(|0\rangle \otimes |0\rangle + |1\rangle \otimes |1\rangle)$ [10, 14].

Furthermore, the SOS method is a critical technique for identifying optimal states and measurements. Moreover, it shares a duality with the NPA relaxations. We will delve deeper into this relationship to gain a clearer understanding, and later in the thesis, we will see this connection further inspire us to seek alternative techniques like the one based on Jordan's lemma for self-testing.

2.7.3 Duality between SOS and NPA relaxation

Recall from the previous sections that the maximum violation achievable with quantum resources can be calculated as

$$(2.47) \quad \beta_Q = \text{Tr}\{\hat{\beta}\rho\},$$

where the optimization is carried over all possible quantum realizations. To show the duality between the SOS method and the NPA hierarchy, we can approach it first by setting a maximum degree n for the involved polynomials, allowing us to formulate:

$$(2.48) \quad \mathbf{f} = \beta_Q \mathbb{1} - \hat{\beta} = \sum_{\lambda} \mathcal{P}_{\lambda}^{\dagger} \mathcal{P}_{\lambda}$$

as a semidefinite program. Let \mathcal{T}_n represent the ring of a polynomial of degree at most n involving the measurement operators. Since these operators characterize quantum measurements, they must adhere to specific conditions that establish an equivalence relation within \mathcal{T}_n . This gives rise to a set \mathcal{P}_n of class representatives (substituting polynomials with their class representatives serves as a method to accommodate the constraints placed on quantum measurement operators when addressing the SDP relaxation of the quantum value problem). Now consider

$R = \{R_{i=1}^n, \dots, n\}$ set of linearly independent monomials within \mathcal{P}_n . Using these basis elements, we can express (2.48) as follows:

$$(2.49) \quad \mathbf{f} = \sum_i R_\alpha^\dagger p_i^{\alpha*} p_i^\beta R_\beta = M^{\beta\alpha} R_\alpha^\dagger R_\beta,$$

where we define $\mathcal{P}_\lambda = R_\alpha p_i^\alpha$ with $p_i^\alpha \in \mathbf{C}$ and summation over repeated indices is implied, and have defined the $n \times n$ complex matrix M as :

$$(2.50) \quad M = \sum_i p_i^\dagger p_i$$

Note that although R_i belong to \mathcal{P}_n , it does not guarantee that $R_\alpha^\dagger R_\beta$ belong to \mathcal{P}_{2n} . This indicates that the constraints on the measurement operators are not entirely captured. We can address this issue by substituting each factor $R_\alpha^\dagger R_\beta$ with its class representative $\bar{R}_\alpha^\dagger \bar{R}_\beta$. To implement this, let $\{\mathcal{M}_k\}$ be a basis of monomials for \mathcal{P}_{2n} , and define $F_{\beta\alpha}^k$ as a tensor with elements specified by (2.20). Using these newly defined tensors, we can express $R_\alpha^\dagger R_\beta$ as:

$$(2.51) \quad R_\alpha^\dagger R_\beta = F_{\beta\alpha}^k \mathcal{M}_k$$

Consequently, the operator \mathbf{f} can be expanded as:

$$(2.52) \quad \mathbf{f} = M^{\beta\alpha} F_{\beta\alpha}^k \mathcal{M}_k$$

Alternatively, we can expand \mathbf{f} as $\mathcal{V}\mathbb{1} - \hat{\beta} = w^k \mathcal{M}_k$ [cite] and it satisfied the conditions given below,

$$(2.53) \quad \min_{\mathcal{V} \in \mathbb{R}_{>0}} \quad \text{s.t.} \quad \mathbf{f} = \mathcal{V}\mathbb{1} - \hat{\beta} \geq 0,$$

it subsequently implies that $w^k = F_{\beta\alpha}^k M^{\alpha\beta}$. It is practical to set $\mathcal{M}_0 = \mathbb{1}$, which simplifies the expression for w^0 to $\mathcal{V}\mathbb{1} - F_{\beta\alpha}^0 M^{\alpha\beta}$. We are now prepared to formulate an n-level relaxation of the problem stated in (2.53) as a semidefinite program (SDP):

$$(2.54) \quad \begin{aligned} \min \quad & F_{\alpha\beta}^0 M^{\alpha\beta} \\ \text{s.t.} \quad & w^k = F_{\beta\alpha}^k M^{\alpha\beta} \quad \forall k \geq 1 \\ & M \geq 0 \end{aligned}$$

Duality:- We can write the lagrangian function for the Bell operator as $\beta = \text{Tr}\{\hat{\beta}\rho_{AB}\}$, as:

$$(2.55) \quad L(m_k, \mathcal{M}) = c^0 + c^k m_k + M^{\alpha\beta} (F^0 + F^k m_k)_{\alpha\beta}.$$

From the formulation, it follows that the dual function $g(\mathcal{M}) = \sup_{m_k} L(m_k, \mathcal{M})$, and the dual problem involves minimizing $g(\mathcal{M})$, which is expressed as:

$$(2.56) \quad \begin{aligned} \min \quad & F_{\alpha\beta}^0 M^{\alpha\beta} \\ \text{s.t.} \quad & c^k + F_{\beta\alpha}^k M^{\alpha\beta} = 0 \quad \forall k \geq 1 \\ & M \geq 0, \end{aligned}$$

From our discussion, it's evident that the level of the NPA hierarchy corresponds to the minimum degree of the polynomials utilized in a tight SOS method. This relationship suggests that in situations where the NPA does not converge, or converges at a very high level, the traditional SOS decomposition method may become impractical for deriving analytical self-testing statements. This difficulty is highlighted in the article [51] and is also apparent in multipartite scenarios, where finding an SOS decomposition can be particularly challenging [25]. In such situations, an alternative approach using Jordan's lemma is more suitable. We will discuss this method in more detail in the following section.

2.7.4 Jordan's lemma

Jordan's lemma asserts that for any two Hermitian matrices A_0, A_1 ($A_0 = A_0^\dagger, A_1 = A_1^\dagger$ where \dagger is complex conjugate) that have finite dimensions and eigenvalues ± 1 , can be applied to simultaneously block-diagonalize them into blocks of no more than 2×2 in size. We can further simplify by assuming that each block is 2×2 in size; as smaller one can be discarded as they do not contribute to Bell non-locality. Furthermore, additional unitary rotations can be applied to each block to ensure the observables are represented solely by real values. Based on this configuration, Alice's observables can be parameterized as follows,

$$(2.57) \quad A_0 = \bigoplus_k A_0^{(k)} = \bigoplus_k \sigma_Z$$

$$(2.58) \quad A_1 = \bigoplus_k A_1^{(k)} = \bigoplus_k (\cos \theta_k^A \sigma_Z + \sin \theta_k^A \sigma_X),$$

where index k iterates over the Jordan blocks, $\sigma_Z^{(i)}$ represents the Z-Pauli matrix and $\sigma_X^{(i)}$ represents the X-Pauli matrix applied to the k -th block. Similarly, Bob's observables can be expressed as

$$(2.59) \quad B_0 = \bigoplus_m B_0^{(m)} = \bigoplus_m \sigma_Z$$

$$(2.60) \quad B_1 = \bigoplus_m B_1^{(m)} = \bigoplus_m (\cos \theta_m^B \sigma_Z + \sin \theta_m^B \sigma_X),$$

with m iterating over the Jordan blocks [129]. Consequently, when represented in the Jordan bases, the Bell operator associated with Bell functional also adopted a block-diagonal structure. For instance the CHSH operator \hat{C} can be written as $\hat{C} = \bigoplus_{km} \hat{C}(\theta_k^A, \theta_m^B)$. Based on this representation, the Bell violation of the operator can be calculated using the following expression,

$$(2.61) \quad \beta = \sum_{km} P_{km} \text{tr}[\hat{C}(\theta_k^A, \theta_m^B) \rho_{km}].$$

Here, $P_{km} \rho_{km}$ are the projections of the physical state ρ onto the blocks corresponding to Alice's and Bob's observables [10, 21]. Fundamentally, Jordan's lemma suggests that all the essential characteristics of the interaction between two projectors can be observed within the qubit scenario, which can be used for self-testing [25, 51].

2.7.5 Self-testing based on Jordan's lemma

Jordan's lemma offers a key method for characterizing the local observables in scenarios involving two settings and two outputs per party, such as in the CHSH setup. By using Naimark's dilation theorem, we can always consider the observables of Alice (A_0, A_1) and Bob (B_0, B_1) to be projective. Jordan's lemma implies that local unitary transformations can be found that simultaneously block-diagonalize these observables into one- and two-dimensional blocks [10, 21, 25, 130, 131]. The maximal value of any Bell functional is achieved when, for every combination of Jordan Blocks, that is, across all the indices, the maximal value of the Bell functional is equivalent to the maximum value for a pair of two-dimensional Jordan blocks. Consequently, we can simplify the observables without any loss of generality as follows,

$$(2.62) \quad A_0 = \sigma_Z, \quad A_1 = \cos\theta_A \sigma_Z + \sin\theta_A \sigma_X,$$

$$(2.63) \quad B_0 = \sigma_Z, \quad B_1 = \cos\theta_B \sigma_Z + \sin\theta_B \sigma_X,$$

This observation forms the core of our proof technique in the first and second articles [25, 51]. Recall that, the maximum expectation value of an operator corresponds to its highest eigenvalue, attained when the state corresponds to the largest eigenvector of the Bell operator. Then, taking the expectation value of the Bell operator with respect to the eigenvector corresponding to the highest eigenvalue, we are left with a function of the angles θ_A, θ_B . The final step involves optimizing this expectation value to determine the maximum quantum violation by the Bell inequalities. If the optimizers θ_A^*, θ_B^* are unique, we say that maximal violation of the Bell inequality self-tests the optimal measurement angles. Moreover, if the maximum eigenvalue of the optimal Bell operator is non-degenerate, we say that the maximum violation of the Bell inequality self-tests the state, which is the corresponding eigenvalues [25, 51].

SUMMARY OF DISSERTATION

“All outstanding work, in art as well as in science, results from immense zeal applied to a great idea.”

— Santiago Ramón y Cajal

In this chapter, we present the findings from the articles [25, 51, 55] included in this thesis. Each section highlights the primary results and observations of these works.

3.1 An elegant scheme of self-testing for multipartite Bell inequalities

Quantum correlations that violate Bell inequalities can certify the shared entangled state and local measurements in a completely device-independent manner. This characteristic of quantum non-local correlations is known as self-testing. While numerous studies have focused on self-testing within the context of linear Bell inequalities, the exploration of self-testing in relation to non-linear Bell inequalities, particularly quadratic ones, has been relatively none.

Unlike the relatively straightforward bipartite Bell scenarios, multipartite Bell scenarios are inherently more complex due to the diverse forms of nonlocality (see Fig. 3.1). To ascertain whether a given correlation is genuinely multipartite nonlocal, it must be checked against the biseparable set of quantum correlations. In the biseparable set, any two of the three parties are allowed to share arbitrary bipartite quantum correlations, which do not form a convex polytope. Consequently, the convex biseparable set of quantum correlations also does not form a convex polytope. Therefore, quadratic Bell inequalities, such as those proposed by Uffink, serve as

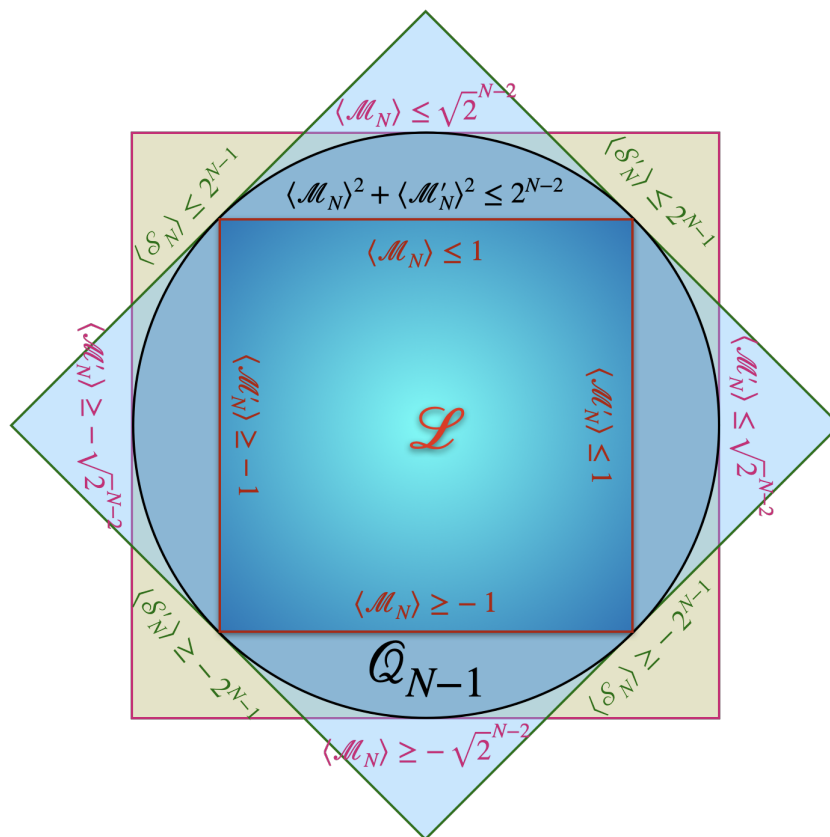


Figure 3.1: This graphic is a schematic representation of the correlations in multipartite Bell scenarios involving an arbitrary number N of spatially separated parties.

tighter witnesses of genuine multipartite nonlocality compared to linear Svetlichny and Mermin-type inequalities (see Fig 3.1), as they better approximate the boundary of the convex set of bi-separable quantum correlations.

In the first article, we introduce a straightforward and widely applicable proof technique that relies on Jordan's lemma (section 2.7.4) to derive self-testing statements for the maximum quantum violation of a significant class of multipartite Bell inequalities involving an arbitrary number N of spatially separated parties. Unlike traditional self-testing methods, such as those based on the SOS (sum of squares) decomposition of a linear Bell operator, which are designed for obtaining self-testing statements for linear Bell inequalities, our technique retrieves self-testing statements for the quadratic Bell inequalities and complex valued Bell functionals. Furthermore, numerically determining the maximum quantum violation of non-linear Bell inequalities is a challenging task, as standard semi-definite programming techniques, such as the Navascues-Pironio-Acin (NPA) hierarchy [98, 100] and the see-saw method, do not accommodate non-linear objective functions.

Additionally, we aimed to keep the mathematical complexity of our technique as simple as possible to further distinguish it from conventional techniques, whose complexity increases

3.1. AN ELEGANT SCHEME OF SELF-TESTING FOR MULTIPARTITE BELL INEQUALITIES

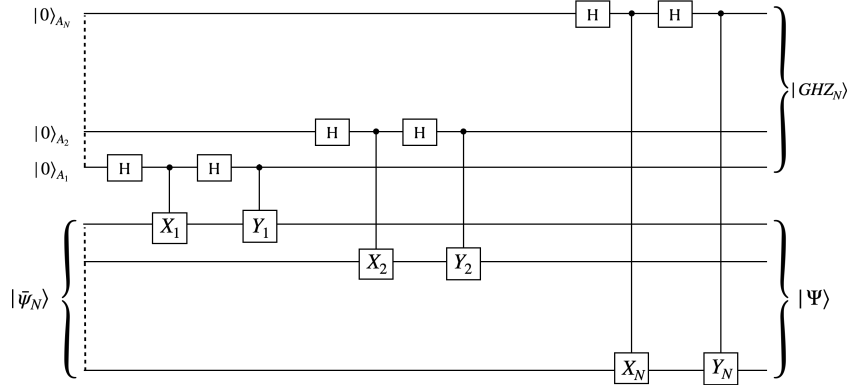


Figure 3.2: This graphic represents the partial SWAP gate isometry used to self-test maximally entangled N partite GHZ state $|GHZ_N\rangle = \frac{1}{\sqrt{2}}(|0\rangle^{\otimes N} + e^{i\phi(N)}|1\rangle^{\otimes N})$.

rapidly with the number of parties. For example, even for the MABK family of N -party Bell inequalities, the minimum degree $\lceil \frac{N}{2} \rceil$ of polynomials in an SOS decomposition increases with the number of parties.

The essence of the article can be understood through the following steps:

- *Characterising the local observables*:- We established a new way of proving Jordan's lemma by showing that in an N -partite binary input and output Bell scenario, it is sufficient to consider local observables of each party with a simultaneous anti-diagonal matrix representation. Specifically, we demonstrate that, without loss of generality, the first observable of each party can be taken as σ_x and the second observable can be taken as $\cos\theta_j\sigma_x + \sin\theta_j\sigma_y$.
- *Anti-diagonal form of observables and Bell operator*:- By virtue of our local observables being in an anti-diagonal form, any Bell operator linearly composed of tensor products of these observables will also be in an anti-diagonal form while being a function of $\{\theta_j\}_{j=1}^N$. This observation forms the core of our proof technique.
- *Eigenvector*:- Next, we observe that the eigenvectors of any anti-diagonal matrix are always of the generalized GHZ form, optimize $\alpha \otimes_{j=1}^N |i_j\rangle + \beta \otimes_{j=1}^N |\bar{i}_j\rangle$ where $i_j \in \{0, 1\}, \bar{i}_j = i_j \oplus 1$.
- *Expectation value*:- Now, taking the expectation value of the Bell operator with respect to any such eigenvector, we retain the weighted sum of two equidistant (from the top and the bottom) terms from the anti-diagonal Bell operator.
- *Optimization*:- Finally, all that remains is to optimize this expectation value over the complex coefficients $\alpha, \beta \in \mathbb{C}$ and N angles $\{\theta_j \in [0, \pi]\}_{j=1}^N$ to acquire the maximum quantum value of the Bell inequalities.

In the last to make the self-testing statements obtained in this work robust, one can use the numerical SWAP method (see Fig. 3.2). This method employs the Navascues-Pironio-Acin (NPA) hierarchy to obtain bounds on the closeness (fidelity) of the experimental measurements and the shared state to the ideal self-testing measurements and state.

To show the versatility of the proof technique we use this technique to obtain self-testing statements for the N partite family of linear MABK inequalities and quadratic Uffinks inequalities. While the self-testing results for the former exist in the literature, but serve as an easy benchmark for the verification of the technique, the latter, on the other hand, is a completely novel contribution. To showcase the various kinds of cases that could arise while using this technique we discuss key equivalence classes of tripartite WWWZB Bell inequalities in including one (unbalanced inequalities) whose maximum violation self-tests non-maximally anti-commuting observables and one (extended CHSH inequalities) for which strict self-testing statement does not exist. Apart from the linear inequalities considered here, it is easy to see that our proof technique, which relies on the anti-diagonal matrix representation of the Bell operator is directly applicable to all two settings binary outcome linear (on correlators) multipartite Bell inequalities, either yielding strict Mayers-Yao self-testing statements or pointing out limitations on them.

3.2 Robust self-testing of Bell inequalities tilted for maximal loophole-free nonlocality

Correlations arising from local measurements performed on entangled photons (quantum systems) resist classical (locally causal) explanations [3]. Such nonlocal correlations enable distant users to achieve classically inconceivable feats, the most significant of which is the ability to share an unconditionally secure secret key [38, 39]. However, the most persistent obstacle to large-scale adoption of these technologies is photon loss. Specifically, if the effective detection efficiencies fall below a critical threshold, the quantum systems, which are expected to be nonlocal, fail to produce effective nonlocal correlations. Consequently, extensive research has focused on developing quantum strategies with minimal critical efficiencies. Nonetheless, a crucial experimental question remains: what quantum strategies maximize effective nonlocality when detector efficiencies exceed these critical values? Despite its practical relevance, this question is still largely unexplored.

In the second article we tackled a specific aspect of this intriguing question: what quantum strategies maximize the loophole-free violation of a given Bell inequality in the presence of inefficient detectors?

The essence of the article can be understood through the following steps:

- First, we derive a pivotal result to address the central question: **Lemma 1** Consider a Bell experiment with inefficient detection with efficiencies η_A, η_B . For *any* given Bell inequality

of form,

$$(3.1) \quad \beta(\mathbf{p}) := \sum_{a,b,x,y} c_{ab}^{xy} p(ab|xy) \leq \beta_{\mathcal{L}},$$

with $c_{ab}^{xy}, \beta_{\mathcal{L}} \in \mathbb{R}$, which is satisfied by all local behaviors. The optimal quantum strategies which yield the maximum loophole-free violation of the Bell inequality are those that maximally violate a *tilted* Bell inequality of the form,

$$(3.2) \quad \begin{aligned} \beta_{\eta_A \eta_B}(\mathbf{p}) &= \beta(\mathbf{p}) + \frac{1-\eta_B}{\eta_B} \sum_{a,x} c_a^x p_A(a|x) \\ &\quad + \frac{1-\eta_A}{\eta_A} \sum_{b,y} c_b^y p_B(b|y) \\ &\leq \frac{\beta_{\mathcal{L}}}{\eta_A \eta_B} - \frac{1-\eta_A}{\eta_A} \frac{1-\eta_B}{\eta_B} \left(\sum_{x,y} c_{a_x b_y}^{x,y} \right), \end{aligned}$$

where $p_A(a|x)$, $p_B(b|y)$ are the ideal marginal probabilities of Alice and Bob, respectively, $q_A(a|x) = \delta_{a,a_x}$, $q_B(b|y) = \delta_{b,b_y}$ represent deterministic assignment strategies, and $c_a^x = \sum_y c_{ab}^{xy}$ and $c_b^y = \sum_x c_{ab}^{xy}$. The loophole-free value $\beta(\tilde{\mathbf{p}})$ of the Bell functional (2.38) is related to value of the Bell functional $\beta_{\eta_A \eta_B}(\mathbf{p})$ in the following way,

$$(3.3) \quad \beta(\tilde{\mathbf{p}}) = \eta_A \eta_B \beta_{\eta_A \eta_B}(\mathbf{p}) + (1-\eta_A)(1-\eta_B) \left(\sum_{x,y} c_{a_x b_y}^{x,y} \right).$$

- Then using the Lemma we analytically retrieve the optimal quantum strategies for maximum loophole-free violation of the CHSH inequality in presence of inefficient detectors,

Theorem 1 [*Self-testing of symmetrically tilted CHSH inequalities*] The maximum quantum violation $c_{\mathcal{Q}}(\alpha, \alpha)$ of the symmetrically ($\alpha = \beta$) tilted CHSH inequality,

$$(3.4) \quad C_{\alpha, \beta}(\mathbf{p}) = \sum_{x,y} (-1)^{x \cdot y} \langle A_x B_y \rangle + \alpha \langle A_0 \rangle + \beta \langle B_0 \rangle \leq 2 + \alpha + \beta,$$

is the largest root of the degree 4 polynomial,

$$(3.5) \quad f(\lambda) = \lambda^4 + (4 - \alpha^2)\lambda^3 + \left(\frac{11}{4}\alpha^4 - 12\alpha^2 - 4 \right)\lambda^2 \\ + (2\alpha^6 - \alpha^4 - 20\alpha^2 - 32)\lambda + 5\alpha^6 - 21\alpha^4 + 16\alpha^2 - 32.$$

$C_{\alpha\alpha}(\mathbf{p}) = c_{\mathcal{Q}}(\alpha, \alpha)$ *self-tests* a two-qubit quantum strategy with optimal (*) local observables of the form,

$$(3.6) \quad \hat{A}_0 = \sigma_Z, \quad \hat{A}_1 = c_A \sigma_Z + s_A \sigma_X$$

$$(3.7) \quad \hat{B}_0 = \sigma_Z, \quad \hat{B}_1 = c_B \sigma_Z + s_B \sigma_X,$$

such that the optimal cosines are equal, i.e., $c^*(\alpha) = c_A^*(\alpha) = c_B^*(\alpha) \in [0, 1]$, and satisfy the relation,

$$(3.8) \quad c^*(\alpha) = \frac{1}{8} \left[3\alpha^2 - 4 + \sqrt{16 + 9\alpha^4 + 8\alpha^2(2c_{\mathcal{Q}}(\alpha, \alpha) - 1)} \right].$$

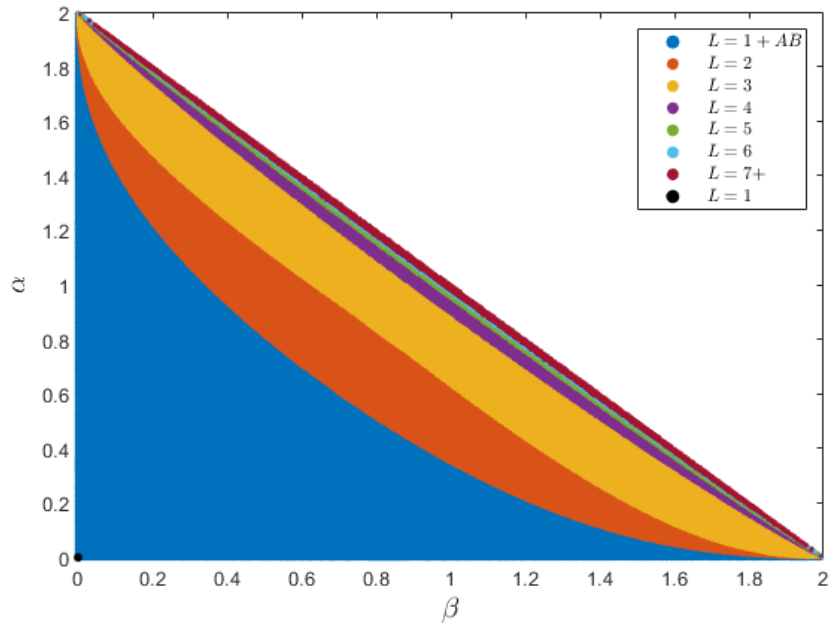


Figure 3.3: Increasing NPA upper bound in the CHSH scenarios. A plot depicting the minimum level $L \in \{1, 1 + AB, 2, 3, 4, 5, 6, 7+\}$ of the NPA hierarchy necessary to achieve saturation with machine precision.

- Impracticality of the SOS technique and NPA upper-bound convergence:*- The problem of determining the maximum quantum violation of a Bell inequality can be addressed using the NPA hierarchy of semi-definite programs, as discussed in section 2.7.3. This method provides a sequence of upper bounds that converge to the maximum quantum violation. In Fig. 3.3, we plot the minimum level L of the NPA hierarchy against the tilting parameters α and β , which are required to reach the maximum quantum violation of doubly-tilted CHSH inequalities (3.4), up to machine precision. Interestingly, as the tilting parameters α and β approach the critical boundary defined by, $\alpha + \beta = 2$, the level L of the NPA hierarchy increases rapidly. Our observation indicates that, even at level 12 of the NPA hierarchy, it remains insufficient to achieve the maximum violation for the symmetrically doubly-tilted CHSH inequality (see Fig. 3.4), this implies that the degree of the SOS polynomial would be extremely high, rendering the SOS approach impractical for self-testing statements. Therefore, we utilize Jordan's lemma as the tool for self-testing.
- We also observed that this unexpected phenomenon is observed at correlation points that achieve maximal loophole-free nonlocality with detection efficiencies close to the critical value, as shown in Fig. 3.3. These points are realized with nearly compatible measurements and almost product states.

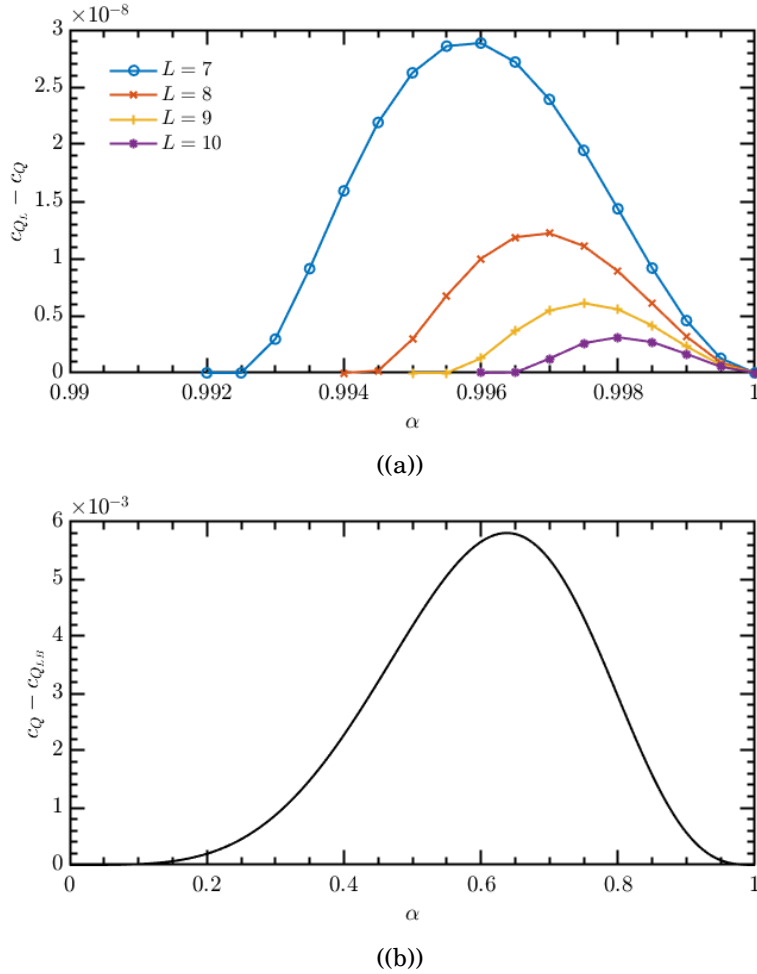


Figure 3.4: (a) This plot highlights the limitations of high levels of the NPA hierarchy in producing the tight bounds in the CHSH scenario. The curve in the plot (b) shows the difference between the maximum quantum violation and the lower bound from the sub-optimal analytical solutions presented in [46], against $\alpha \in [0, 1]$.

3.3 Quantitative non-classicality of mediated interactions

In mediated dynamics, methods have been developed to observe the nonclassicality of a mediator's state through the correlation dynamics between coupled probes. These methods are based on the premise that an increase in quantum entanglement indicates the mediator has transitioned through nonorthogonal states during the dynamics [132, 133]. One of the key strengths of these approaches is their minimalistic assumptions regarding the physical systems involved, which remain independent of the initial states, dimensions of the systems, or specific interactions and are effective even amidst local environmental influences. This broad applicability enhances their utility across diverse scientific domains.

In the third article, we used the nonclassicality of states to quantify the amount of nonclassi-

cality in mediated interactions while maintaining minimalistic assumptions about the physical systems under consideration. The concept of nonclassicality we use is based on the commutativity of interaction Hamiltonians in closed dynamics, which extends to the decomposability of dynamical maps, thus encompassing open systems as well. Our main contribution lies in developing methods to quantify nonclassicality. We derived conditions that provide a lower bound for the norm of the commutator and defined a specific distance to decomposable maps. The essence of the paper is divided into two main parts, as outlined below.

- *Accessible Mediator*:- First, we assume that the mediator is accessible to the experimentalist. In this scenario, we have provided a witness of decomposability in the form of the equation given below,

$$(3.9) \quad \mathcal{Q}_{A:MB}(\lambda(\rho_0)) \leq \sup_{\sigma_{AB}} \mathcal{Q}_{A:M}(\sigma_{AM}) + I_{AM:B}(\rho_0),$$

Here, the bound is derived for any correlation measure \mathcal{Q} that is monotonic under local operations, and σ_{AM} ranges over all possible joint states of AM and we assume $\rho_0 = \rho_{AM} \otimes \rho_B$. Additionally, a measure of the total correlations in the state $\rho = \lambda(\rho)$ where λ is the map that describes the state evolution at time t across the partition $AM : B$ is given by $I_{AM:B}(\rho) = \inf_{\sigma_{AM} \otimes \sigma_B} g(d(\rho, \sigma_{AM} \otimes \sigma_B))$. Furthermore, we demonstrate that the violation of 3.9 provides a lower bound on the degree of nondecomposability as follows,

$$(3.10) \quad d^{DEC}(\Lambda) \geq g^{-1}(\mathcal{Q}_{A:MB}(\Lambda(\rho_0)) - B(\rho_0)),$$

where $B(\rho_0)$ is the right-hand side of (3.9). Therefore, any violation of the decomposability criterion in terms of correlations establishes a nontrivial lower bound on the distance between the dynamical map and the set of decomposable maps.

- *Inaccessible Mediator*:- In the second part, we show the nonclassicality of evolution through a mediator without directly measuring the mediator. Here, we demonstrate that this is indeed possible. We begin by introducing the necessary concepts and related mathematical tools. Then, we present witnesses of non-decomposable evolution based solely on measurements of AB . Finally, we establish measures of non-decomposability along with their experimentally friendly lower bounds. Moreover, an interesting condition for witnessing non-decomposability follows from (3.9). Specifically, under the evolution generated by the set of all maps with a decomposable m -dilation $\lambda \in \overline{DEC}(m)$, any gd continuous correlation measure \mathcal{Q} can be upper-bounded in the following way,

$$(3.11) \quad \mathcal{Q}_{A:B}(\rho_t) \leq \sup_{\sigma_{XM}} \mathcal{Q}_{X:M}(\sigma) + I_{A:B}(\rho_0),$$

Here $\rho_t = \lambda(\rho)$ and we highlight that $\lambda \in \overline{DEC}(m)$ acts only on AB . Moreover, the supremum runs overall AM or BM states. Similarly, as in (3.10) we demonstrate the violation of (3.11)

also provides a lower bound on the degree of nondecomposability in case of inaccessible mediator as follows,

$$(3.12) \quad D^{\overline{DEC}(m)}(\Lambda_{AB}) \geq g^{-1}(Q_{A:B}(\rho_t) - \mathcal{B}(\rho_0)),$$

Here, \mathcal{B} is the right-hand side of (3.11). It is interesting to note that all these quantities pertain solely to states and maps on AB , not M , which means even though our mediator is not accessible to us, we can still deduce information about the system.

OUTLOOK

“Theoretical physicists live in a classical world, looking out into a quantum-mechanical world. The latter we describe only subjectively, in terms of procedures and results in our classical domain.”
— John Stewart Bell

Although these results enhance our understanding of device-independent certification and mediator dynamics, there is still much to explore. This chapter will summarize the most valuable insights and outline potential research directions that stem from all these works.

An elegant scheme of self-testing for multipartite Bell inequalities:— The technique presented in this paper offers a more straightforward approach than traditional methods like SOS decomposition. It can be applied to any binary input and output Bell scenarios with an arbitrary number N of spatially separated parties. Provided that the associated Bell operator has an anti-diagonal matrix representation, this technique can derive self-testing statements for any Bell inequality in such scenarios.

In the “*Characterizing Local Observables*” section, we demonstrated that in two-setting binary outcome multipartite Bell scenarios, the observables of each party can be represented as anti-diagonal matrices. This essentially provides an alternative approach to proving Jordan’s lemma. Consequently, with observables in anti-diagonal matrix form, the Hermitian Bell operators corresponding to all Bell inequalities composed of N correlators also possess an anti-diagonal matrix representation.

One of the most intriguing aspects of this work is the ability to operationally determine the relative phase $\phi(N)$ using Uffink’s complex-valued Bell expression. While the self-testing statements for the MABK and complementary MABK inequalities uniquely specify $\phi(N)$, the statements for Uffink’s quadratic Bell inequalities do not. Specifically, by fixing the local observables of

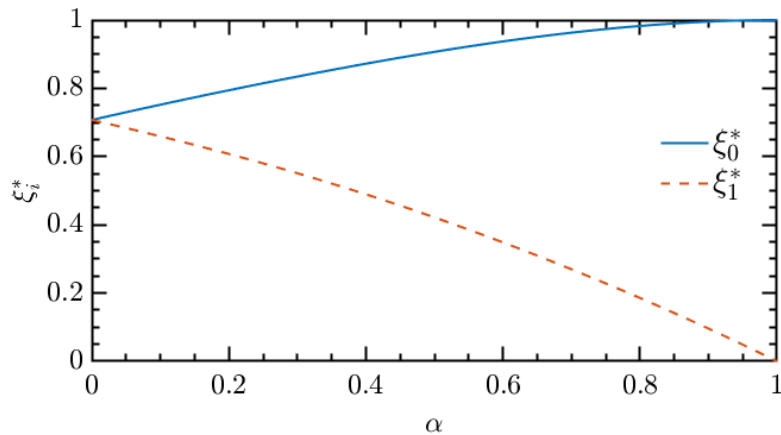


Figure 4.1: A plot of the Schmidt coefficients ξ_i^* of the optimal non-maximally entangled quantum state $|\psi\rangle = \xi_0^* |00\rangle + \xi_1^* |11\rangle$ (represented in the Schmidt basis) against $\alpha \in [0, 1]$.

each party to be σ_X and σ_Y , Corollary 7.1 establishes a one-to-one correspondence between the experimentally accessible extremal values of Uffink’s complex-valued Bell expressions and the relative phase $\phi(N)$ of the N -partite GHZ state. This effectively demonstrates the operational significance of the relative phase $\phi(N)$.

As Uffink’s quadratic inequalities and complex-valued Bell expression offer a more precise and robust certification of quantum devices. Consequently, replacing MABK with these expressions in device-independent applications can substantially improve performance and reliability.

Robust self-testing of Bell inequalities tilted for maximal loophole-free nonlocality:— This work provides valuable insights into the impact of decreasing detector efficiency on optimal quantum strategies. As illustrated in Fig. 4.1, when detectors are inefficient with $\eta_A, \eta_B < 1$ ($\alpha, \beta > 0$), the optimal strategy involves partially entangled states to achieve maximal loophole-free nonlocality. It has been observed that as the detector’s efficiencies approach near the critical values, the degree of entanglement decreases, with the state approaching an almost product form.

Additionally, we observe that when both detectors are inefficient, Alice’s measurements are affected by Bob’s detection efficiency η_B . As shown in Fig. 4.2, Alice’s optimal measurement trends towards compatible measurements as η_B approaches the critical boundary. Beyond the insights into achieving maximum effective nonlocality with inefficient detectors, the analytical results in Theorems 1 and 2 reveal a fascinating complexity in characterizing the set of nonlocal quantum correlations in the simplest Bell scenario using the NPA hierarchy.

These results raise both foundationally relevant and experimentally significant questions. In an upcoming article, we address the foundationally relevant question: whether the complexity of characterizing extremal nonlocal quantum correlation measured by the minimum saturating level of the NPA hierarchy is related to the partial incompatibility of the quantum measurements that realize them [134]. In another upcoming article, we address the experimentally motivated question: what quantum strategies are the best suited for DIQKD in presence of inefficient

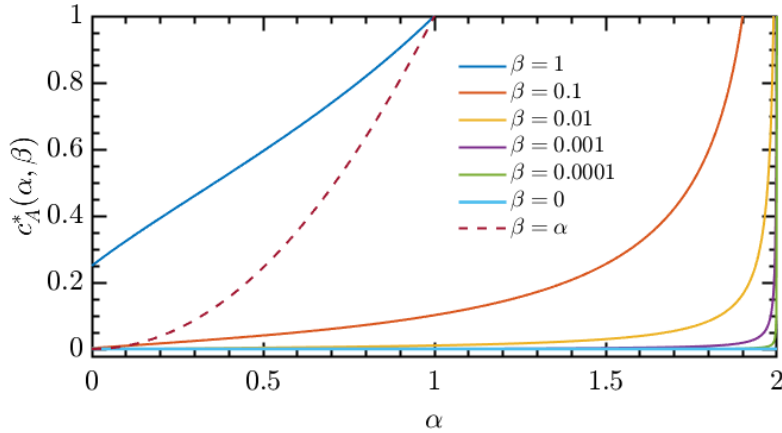


Figure 4.2: Increasing NPA upper bound in the CHSH scenarios. A plot depicting the minimum level $L \in \{1, 1 + AB, 2, 3, 4, 5, 6, 7+\}$ of the NPA hierarchy necessary to achieve saturation with machine precision.

detectors [135].

Quantitative non-classicality of mediated interactions:— In this work, we have demonstrated that accurate simulation of dynamics with high correlations necessitates a large number of Trotter steps. Additionally, we have shown that gravitational interactions cannot be accurately modeled using commuting particle-field couplings.

As the first application of our introduced measure, we have established a direct connection between system correlations and the number of Trotter steps necessary to keep the simulation error minimal. The degree of violation of (3.10) sets a lower bound on non-decomposability and the spectral norm of the commutator, thereby determining the required number of Trotter steps.

Our second application lies in foundational studies of gravitational interactions. Our method enables us to infer properties of the field based on the behavior of objects interacting through it. This approach is particularly intriguing for gravitational interactions, as there is currently no direct experimental evidence of their quantum properties. By driving nonclassicality witnesses, our approach provides a novel way of understanding this fundamental force, potentially leading to new insights into gravitational interactions inferred from the observation of the significant gravitational entanglement.

BIBLIOGRAPHY

- [1] A. Einstein, B. Podolsky, and N. Rosen, “Can quantum-mechanical description of physical reality be considered complete?,” *Physical Review*, vol. 47, no. 10, pp. 777–780, 1935.
- [2] D. Bohm, *A suggested interpretation of the quantum theory in terms of “hidden” variables. I*, vol. 85, 2. American Physical Society, 1952.
- [3] J. S. Bell, “On the einstein podolsky rosen paradox,” *Physics Physique*, vol. 1, no. 3, pp. 195–200, 1964.
- [4] B. Hensen, H. Bernien, A. Dréau, A. Reiserer, N. Kalb, M. Blok, J. Ruitenbergh, R. Vermeulen, R. Schouten, C. Abellán, *et al.*, “Loophole-free bell inequality violation using electron spins separated by 1.3 kilometres,” *Nature*, vol. 526, no. 7575, pp. 682–686, 2015.
- [5] M. Giustina, M. A. Versteegh, S. Wengerowsky, J. Handsteiner, A. Hochrainer, K. Phelan, F. Steinlechner, J. Kofler, J.-Å. Larsson, C. Abellán, *et al.*, “Significant-loophole-free test of bells theorem with entangled photons,” *Physical Review Letters*, vol. 115, no. 25, p. 250401, 2015.
- [6] L. K. Shalm, E. Meyer-Scott, B. G. Christensen, P. Bierhorst, M. A. Wayne, M. J. Stevens, T. Gerrits, S. Glancy, D. R. Hamel, M. S. Allman, *et al.*, “Strong loophole-free test of local realism,” *Physical Review Letters*, vol. 115, no. 25, p. 250402, 2015.
- [7] N. Brunner, D. Cavalcanti, S. Pironio, V. Scarani, and S. Wehner, “Bell nonlocality,” *Reviews of Modern Physics*, vol. 86, no. 2, pp. 419–478, 2014.
- [8] D. Mayers and A. Yao, “Self testing quantum apparatus,” *Quantum Info. Comput.*, vol. 4, no. 4, pp. 273–286, 2004.
- [9] S. Popescu and D. Rohrlich, “Which states violate Bell’s inequality maximally?,” *Physics Letters A*, 6 1992.
- [10] I. Šupić and J. Bowles, “Self-testing of quantum systems: a review,” *Quantum*, vol. 4, p. 337, Sept. 2020.

BIBLIOGRAPHY

- [11] M. G. A. Paris and J. Rehacek, *Quantum State Estimation*, vol. 649. Springer Science & Business Media, 2009.
- [12] A. I. Lvovsky and M. G. Raymer, “Continuous-variable optical quantum-state tomography,” *Reviews of Modern Physics*, vol. 81, no. 1, pp. 299–332, 2009.
- [13] A. Acín and L. Masanes, “Quantum certification and self-testing,” *Nature*, vol. 540, no. 7632, pp. 213–219, 2018.
- [14] V. Scarani, “The device-independent outlook on quantum physics,” *Acta Physica Slovaca*, vol. 62, no. 4, pp. 347–409, 2012.
- [15] V. Scarani, “Device-Independent Self-Testing,” in *Bell Nonlocality*, Oxford University Press, 2019, Oxford University Press, 08 2019.
- [16] A. Ekert and R. Renner, “The ultimate physical limits of privacy.” *Nature* 507, 443447 (2014). <https://doi.org/10.1038/nature13132>, 2014.
- [17] T. Vidick, “Parallel diqkd from parallel repetition,” 2017.
- [18] M. Christandl, N. G. Houghton-Larsen, and L. Mancinska, “An operational environment for quantum self-testing,” *Quantum*, vol. 6, p. 699, Apr. 2022.
- [19] B. W. Reichardt, F. Unger, and U. Vazirani, “Classical command of quantum systems via rigidity of chsh games,” 2012.
- [20] I. Frérot and A. Acín, “Coarse-grained self-testing,” *Physical Review Letters*, vol. 127, Dec. 2021.
- [21] V. Scarani, *Bell nonlocality*. Oxford University Press, 2019.
- [22] M. A. Nielsen and I. L. Chuang, *Quantum Computation and Quantum Information: 10th Anniversary Edition*. Cambridge University Press, 2010.
- [23] D. Gottesman, “Fault-tolerant quantum computation with local gates,” *Journal of Modern Optics*, vol. 47, no. 2-3, pp. 333–345, 1999.
- [24] C. Bamps and S. Pironio, “Sum-of-squares decompositions for a family of clauser-horne-shimony-holt-like inequalities and their application to self-testing,” *Phys. Rev. A*, vol. 91, p. 052111, 2015.
- [25] E. Panwar, P. Pandya, and M. Wieśniak, “An elegant scheme of self-testing for multipartite bell inequalities,” *npj Quantum Information*, vol. 9, p. 71, Jul 2023.

-
- [26] A. V. Belinskii and D. N. Klyshko, “Interference of light and bell’s theorem,” *Phys. Usp.*, vol. 36, no. 8, pp. 653–693, 1993.
- [27] M. Ardehali, “Bell inequalities with a magnitude of violation that grows exponentially with the number of particles,” *Phys. Rev. A*, vol. 46, pp. 5375–5378, Nov 1992.
- [28] M. Żukowski and i. c. v. Brukner, “Bell’s theorem for general n-qubit states,” *Phys. Rev. Lett.*, vol. 88, p. 210401, May 2002.
- [29] H. Weinfurter and M. Żukowski, “Four-photon entanglement from down-conversion,” *Phys. Rev. A*, vol. 64, p. 010102, Jun 2001.
- [30] R. F. Werner and M. M. Wolf, “All-multipartite bell-correlation inequalities for two dichotomic observables per site,” *Phys. Rev. A*, vol. 64, p. 032112, Aug 2001.
- [31] J. Uffink, “Quadratic bell inequalities as tests for multipartite entanglement,” *Phys. Rev. Lett.*, vol. 88, p. 230406, May 2002.
- [32] M. Banik, S. S. Bhattacharya, N. Ganguly, T. Guha, A. Mukherjee, A. Rai, and A. Roy, “Two-Qubit Pure Entanglement as Optimal Social Welfare Resource in Bayesian Game,” *Quantum*, vol. 3, p. 185, Sept. 2019.
- [33] F. Grasselli, G. Murta, H. Kampermann, and D. Bruß, “Entropy bounds for multiparty device-independent cryptography,” *PRX Quantum*, vol. 2, p. 010308, Jan 2021.
- [34] F. Grasselli, G. Murta, H. Kampermann, and D. Bruß, “Boosting device-independent cryptography with tripartite nonlocality,” *Quantum*, vol. 7, p. 980, Apr. 2023.
- [35] G. Murta, F. Grasselli, H. Kampermann, and D. Bruß, “Quantum conference key agreement: A review,” *Advanced Quantum Technologies*, vol. 3, no. 11, p. 2000025, 2020.
- [36] A. K. Ekert, “Quantum cryptography based on bell’s theorem,” *Phys. Rev. Lett.*, vol. 67, pp. 661–663, Aug 1991.
- [37] D. Mayers and A. Yao, “Quantum cryptography with imperfect apparatus,” in *Proceedings 39th Annual Symposium on Foundations of Computer Science (Cat. No.98CB36280)*, pp. 503–509, 1998.
- [38] J. Barrett, L. Hardy, and A. Kent, “No signaling and quantum key distribution,” *Phys. Rev. Lett.*, vol. 95, p. 010503, Jun 2005.
- [39] A. Acín, N. Brunner, N. Gisin, S. Massar, S. Pironio, and V. Scarani, “Device-independent security of quantum cryptography against collective attacks,” *Phys. Rev. Lett.*, vol. 98, p. 230501, Jun 2007.

BIBLIOGRAPHY

- [40] A. Acín, N. Brunner, N. Gisin, S. Massar, S. Pironio, and V. Scarani, “Device-independent security of quantum cryptography against collective attacks,” *Physical Review Letters*, vol. 98, no. 23, p. 230501, 2007.
- [41] “Optical fiber loss and attenuation.” <https://www.fiberoptics4sale.com/blogs/archive-posts/95048006-optical-fiber-loss-and-attenuation>, 2022.
- [42] A. Garg and N. D. Mermin, “Detector inefficiencies in the einstein-podolsky-rosen experiment,” *Phys. Rev. D*, vol. 35, pp. 3831–3835, Jun 1987.
- [43] P. H. Eberhard, “Background level and counter efficiencies required for a loophole-free einstein-podolsky-rosen experiment,” *Phys. Rev. A*, vol. 47, pp. R747–R750, Feb 1993.
- [44] S. Massar, “Nonlocality, closing the detection loophole, and communication complexity,” *Phys. Rev. A*, vol. 65, p. 032121, Mar 2002.
- [45] T. Vértesi, S. Pironio, and N. Brunner, “Closing the detection loophole in bell experiments using qudits,” *Phys. Rev. Lett.*, vol. 104, p. 060401, Feb 2010.
- [46] N. Miklin, A. Chaturvedi, M. Bourennane, M. Pawłowski, and A. Cabello, “Exponentially decreasing critical detection efficiency for any bell inequality,” *Phys. Rev. Lett.*, vol. 129, p. 230403, Nov 2022.
- [47] A. Chaturvedi, G. Viola, and M. Pawłowski, “Extending loophole-free nonlocal correlations to arbitrarily large distances,” *npj Quantum Information*, vol. 10, p. 7, Jan 2024.
- [48] M. Farkas, M. Balanzó-Juandó, K. Łukanowski, J. Kołodyński, and A. Acín, “Bell nonlocality is not sufficient for the security of standard device-independent quantum key distribution protocols,” *Phys. Rev. Lett.*, vol. 127, p. 050503, Jul 2021.
- [49] P. H. Eberhard and P. Rosselet, “Bell’s theorem based on a generalized EPR criterion of reality,” *Found. Phys.*, vol. 25, no. 1, pp. 91–111, 1995.
- [50] C. Branciard, “Detection loophole in bell experiments: How postselection modifies the requirements to observe nonlocality,” *Phys. Rev. A*, vol. 83, p. 032123, Mar 2011.
- [51] N. Gigena, E. Panwar, G. Scala, M. Araújo, M. Farkas, and A. Chaturvedi, “Robust self-testing of bell inequalities tilted for maximal loophole-free nonlocality,” 2024.
- [52] J. D. Thompson, B. M. Zwickl, A. M. Jayich, F. Marquardt, S. M. Girvin, and J. G. E. Harris, “Strong dispersive coupling of a high-finesse cavity to a micromechanical membrane,” *Nature*, vol. 452, pp. 72–75, Mar 2008.

-
- [53] S. Bose, A. Mazumdar, G. W. Morley, H. Ulbricht, M. Toroš, M. Paternostro, A. A. Geraci, P. F. Barker, M. S. Kim, and G. Milburn, “Spin entanglement witness for quantum gravity,” *Phys. Rev. Lett.*, vol. 119, p. 240401, Dec 2017.
- [54] C. Marletto and V. Vedral, “Gravitationally induced entanglement between two massive particles is sufficient evidence of quantum effects in gravity,” *Phys. Rev. Lett.*, vol. 119, p. 240402, Dec 2017.
- [55] R. Ganardi, E. Panwar, M. Pandit, B. Woloncewicz, and T. Paterek, “Quantitative nonclassicality of mediated interactions,” *PRX Quantum*, vol. 5, p. 010318, Feb 2024.
- [56] S. Lloyd, “Universal quantum simulators,” *Science*, vol. 273, no. 5278, pp. 1073–1078, 1996.
- [57] D. Poulin, M. B. Hastings, D. Wecker, N. Wiebe, A. C. Doherty, and M. Troyer, “The trotter step size required for accurate quantum simulation of quantum chemistry,” *Quantum Information and Computation*, vol. 15, no. 5-6, pp. 361–384, 2015.
- [58] L. Lami, J. S. Pedernales, and M. B. Plenio, “Testing the quantumness of gravity without entanglement,” *Phys. Rev. X*, vol. 14, p. 021022, May 2024.
- [59] R. Shankar, *Principles of Quantum Mechanics*. Springer, 2012.
- [60] D. J. Griffiths and D. F. Schroeter, *Introduction to Quantum Mechanics*. Cambridge University Press, 2018.
- [61] J. Goold, M. Huber, A. Riera, L. del Rio, and P. Skrzypczyk, “The role of quantum information in thermodynamics a topical review,” *Journal of Physics A: Mathematical and Theoretical*, vol. 49, no. 14, p. 143001, 2016.
- [62] L. Amico, R. Fazio, A. Osterloh, and V. Vedral, “Entanglement in many-body systems,” *Reviews of Modern Physics*, vol. 80, no. 2, p. 517, 2008, APS.
- [63] R. Horodecki, P. Horodecki, M. Horodecki, and K. Horodecki, “Quantum entanglement,” *Rev. Mod. Phys.*, vol. 81, pp. 865–942, Jun 2009.
- [64] R. F. Werner, “Quantum states with einstein-podolsky-rosen correlations admitting a hidden-variable model,” *Phys. Rev. A*, vol. 40, pp. 4277–4281, Oct 1989.
- [65] W. K. Wootters, “Entanglement of formation of an arbitrary state of two qubits,” *Physical Review Letters*, vol. 80, no. 10, pp. 2245–2248, 1998, APS.
- [66] V. Vedral, M. B. Plenio, M. A. Rippin, and P. L. Knight, “Quantifying entanglement,” *Physical Review Letters*, vol. 78, no. 12, pp. 2275–2279, 1997.

BIBLIOGRAPHY

- [67] C. H. Bennett, D. P. DiVincenzo, J. A. Smolin, and W. K. Wootters, “Mixed-state entanglement and quantum error correction,” *Physical Review A*, vol. 54, no. 5, pp. 3824–3851, 1996.
- [68] M. Horodecki, P. Horodecki, and R. Horodecki, “Distillability of inseparable quantum systems,” *Physical Review Letters*, vol. 78, no. 23, pp. 574–577, 2001.
- [69] M. B. Plenio, “Logarithmic negativity: A full entanglement monotone that is not convex,” *Physical Review Letters*, vol. 95, no. 9, p. 090503, 2005.
- [70] J. Eisert and M. B. Plenio, “Comparison of entanglement measures: Entropy of entanglement, entanglement of formation, and relative entropy of entanglement,” *Journal of Modern Optics*, vol. 46, no. 9, pp. 145–154, 1999.
- [71] V. Vedral, “The role of relative entropy in quantum information theory,” *Reviews of Modern Physics*, vol. 74, no. 1, pp. 197–234, 2002.
- [72] K. Zyczkowski, P. Horodecki, A. Sanpera, and M. Lewenstein, “Volume of the set of separable states,” *Physical Review A*, vol. 58, no. 2, pp. 883–892, 1998.
- [73] B. C. Hall, *Lie Groups, Lie Algebras, and Representations: An Elementary Introduction*. Graduate Texts in Mathematics, Cham: Springer International Publishing, 2 ed., 2015.
- [74] R. Ganardi, “Correlations in mediated dynamics,” *University of Gdask*, 2020.
- [75] J. F. Clauser, M. A. Horne, A. Shimony, and R. A. Holt, “Proposed experiment to test local hidden-variable theories,” *Physical Review Letters*, vol. 23, no. 15, pp. 880–884, 1969.
- [76] A. Aspect, J. Dalibard, and G. Roger, “Experimental test of bell’s inequalities using time-varying analyzers,” *Physical Review Letters*, vol. 49, no. 25, pp. 1804–1807, 1982.
- [77] A. Fine, “Hidden variables, local realism, and bell’s theorem,” *Physical Review Letters*, vol. 48, no. 21, p. 291, 1982.
- [78] J. S. Bell, “On the problem of hidden variables in quantum mechanics,” *Reviews of Modern Physics*, vol. 38, no. 3, pp. 447–452, 1966.
- [79] S. Kochen and E. P. Specker, “The problem of hidden variables in quantum mechanics,” *Journal of Mathematics and Mechanics*, vol. 17, no. 1, pp. 59–87, 1967.
- [80] J. S. Bell, “Introduction to the hidden-variable question,” *Foundations of Quantum Mechanics, Proceedings of the International School of Physics Enrico Fermi*, vol. 49, pp. 171–181, 1971.
- [81] A. M. Gleason, “Measures on the closed subspaces of a hilbert space,” *Journal of Mathematics and Mechanics*, vol. 6, no. 6, pp. 885–893, 1957.

-
- [82] W. H. Zurek, “Probabilities from entanglement, borns rule $p_k = |\psi_k|^2$ from envariance,” *Physical Review A*, vol. 71, no. 5, p. 052105, 2005.
- [83] A. Acín, N. Gisin, and L. Masanes, “Unitary operations, entanglement and no-signalling box,” *Physical Review Letters*, vol. 97, no. 12, p. 120405, 2006.
- [84] K. T. Goh, J. Kaniewski, E. Wolfe, T. Vértesi, X. Wu, Y. Cai, Y.-C. Liang, and V. Scarani, “Geometry of the set of quantum correlations,” *Physical Review A*, vol. 97, no. 2, p. 022104, 2018.
- [85] A. Rai, C. Duarte, S. Brito, and R. Chaves, “Geometry of the quantum set on no-signaling faces,” *Physical Review A*, vol. 99, no. 3, p. 032106, 2019.
- [86] S. Boyd and L. Vandenberghe, *Convex Optimization*. Cambridge University Press, 2004.
- [87] R. T. Rockafellar, *Convex Analysis*. Princeton University Press, 1970.
- [88] G. M. Ziegler, “Lectures on polytopes,” *Graduate Texts in Mathematics*, vol. 152, 1995.
- [89] W. Rudin, *Principles of Mathematical Analysis*. McGraw-Hill, 1976.
- [90] J. R. Munkres, *Topology*. Prentice Hall, 2000.
- [91] R. G. Bartle and D. R. Sherbert, *Introduction to Real Analysis*. John Wiley & Sons, 2011.
- [92] J. P. May and A. Peng, “The hahn-banach separation theorem and other separation results,” *University of Chicago REU*, 2014.
- [93] D. M. Kreps, “A note on "separating" hyperplanes,” *Journal of Economic Theory*, vol. 20, no. 2, pp. 412–415, 1979.
- [94] L. Vandenberghe and S. Boyd, *Semidefinite programming*, vol. 38, 1. SIAM, 1996.
- [95] L. Lóvasz and A. Schrijver, *Semidefinite Programming*, vol. 2. Elsevier, 2003.
- [96] K. F. Pal and T. Vertesi, “Quantum bounds on bell inequalities,” *Physical Review A*, vol. 82, no. 2, p. 022116, 2010.

BIBLIOGRAPHY

- [97] S. Pironio, M. Navascués, and A. Acín, “A convergent hierarchy of semidefinite programs characterizing the set of quantum correlations,” *New Journal of Physics*, vol. 12, p. 083026, 2010.
- [98] M. Navascués, S. Pironio, and A. Acín, “Bounding the set of quantum correlations,” *Physical Review Letters*, vol. 98, no. 1, p. 010401, 2007.
- [99] M. Navascués, S. Pironio, and A. Acín, “The power of semidefinite programming relaxations for noncommutative polynomial optimization and their applications,” *Proceedings of the Royal Society A: Mathematical, Physical and Engineering Sciences*, vol. 471, no. 2180, p. 20140898, 2015.
- [100] M. Navascués, S. Pironio, and A. Acín, “A convergent hierarchy of semidefinite programs characterizing the set of quantum correlations,” *New Journal of Physics*, vol. 10, p. 073013, 2008.
- [101] R. Murray, V. Chandrasekaran, and A. Wierman, “Foundations of semidefinite programming and sums-of-squares relaxations,” *arXiv preprint arXiv:2002.03074*, 2020.
- [102] A. A. Ahmadi, “Sum of squares (sos) techniques: An introduction.” https://www.princeton.edu/~aaa/Public/Teaching/ORF523/ORF523_Lec15.pdf, 2021.
Accessed: 2023-06-11.
- [103] A. Acín and S. Massar, “Randomness versus nonlocality and entanglement,” *Physical Review Letters*, vol. 108, no. 10, p. 100402, 2012.
- [104] J. F. Clauser, M. A. Horne, A. Shimony, and R. A. Holt, “Proposed experiment to test local hidden-variable theories,” *Phys. Rev. Lett.*, vol. 23, pp. 880–884, Oct 1969.
- [105] B. S. Tsirelson, “Quantum generalizations of bell’s inequality,” *Letters in Mathematical Physics*, vol. 4, no. 2, pp. 93–100, 1980.
- [106] L. A. Khalfin and B. S. Tsirelson, “Quantum and quasi-classical analogs of bell inequalities,” in *Symposium on the Foundations of Modern Physics 1985*, pp. 441–460, World Scientific Publishing, 1985.
- [107] L. A. Khalfin and B. S. Tsirelson, “Quantum/classical correspondence in the light of bell’s inequalities,” *Foundations of Physics*, vol. 22, no. 7, pp. 879–948, 1992.
- [108] S. Popescu and D. Rohrlich, “Quantum nonlocality as an axiom,” *Foundations of Physics*, vol. 24, no. 3, pp. 379–385, 1994.
- [109] E. G. Cavalcanti, Q. Y. He, M. D. Reid, and H. M. Wiseman, “Unified criteria for multipartite quantum nonlocality,” *Physical Review A*, vol. 84, p. 032115, 2011.

-
- [110] M. M. Taddei, T. L. Silva, R. V. Nery, G. H. Aguilar, S. P. Walborn, and L. Aolita, “Exposure of subtle multipartite quantum nonlocality,” *Physical Review A*, vol. 99, p. 052110, 2019.
- [111] M. Zukowski, “All multipartite bell correlation inequalities for two dichotomic observables per site,” *arXiv preprint quant-ph/0102024*, 2002.
- [112] T. Holz, H. Kampermann, and D. Bruß, “A genuine multipartite bell inequality for device-independent conference key agreement,” *arXiv preprint arXiv:1910.11360*, 2019.
- [113] G. Svetlichny, “Distinguishing three-body from two-body nonseparability by a bell-type inequality,” *Physical Review D*, vol. 35, no. 10, pp. 3066–3069, 1987.
- [114] J. L. Cereceda, “Violation of a bell-like inequality for three spin-1/2 particles,” *Physical Review A*, vol. 66, no. 2, p. 024102, 2002.
- [115] J.-A. Larsson, “Loopholes in bell inequality tests of local realism,” *Journal of Physics A: Mathematical and Theoretical*, vol. 47, no. 42, p. 424003, 2014.
- [116] M. Giustina, L. K. Shalm, E. Meyer-Scott, B. G. Christensen, P. Bierhorst, E. Knill, S. Glancy, Y. Zhang, A. Mink, N. Kirchner, *et al.*, “Tackling loopholes in experimental tests of bells inequality,” *Physical Review Letters*, vol. 123, no. 21, p. 210401, 2019.
- [117] C. Branciard, N. Gisin, and S. Pironio, “Detection loophole in bell experiments: How postselection modifies the requirements to observe nonlocality,” *Physical Review A*, vol. 83, no. 3, p. 032123, 2011.
- [118] M. Czechlewski and M. Pawłowski, “Influence of the choice of postprocessing method on bell inequalities,” *Phys. Rev. A*, vol. 97, p. 062123, Jun 2018.
- [119] V. Authors, “Revisited aspects of the local set in chsh bell scenario,” *arXiv preprint arXiv:2302.06320*, 2023.
- [120] V. Authors, “Entanglement versus bell violations and their behaviour under local filtering operations,” *arXiv preprint arXiv:quant-ph/0112012*, 2011.
- [121] N. Gigena, G. Scala, and A. Mandarino, “Revisited aspects of the local set in chsh bell scenario,” *International Journal of Quantum Information*, vol. 21, no. 07, p. 2340005, 2023.
- [122] M.-O. Renou, J.-D. Bancal, and A. Acín, “Robust self-testing of multipartite ghz states via homodyne detection,” *Physical Review A*, vol. 98, no. 6, p. 062111, 2018.
- [123] S. Sarkar, M. Horodecki, and M. J. Hoban, “Self-testing of multipartite ghz states of arbitrary local dimension,” *npj Quantum Information*, vol. 7, no. 1, p. 151, 2021.



BIBLIOGRAPHY

- [124] R. Schwonnek, K. T. Goh, and E. Wolfe, “Device-independent certification of quantum devices,” *Quantum*, vol. 5, p. 409, 2021.
- [125] T. H. Yang, T. Vértesi, J.-D. Bancal, V. Scarani, and M. Navascués, “Robust and versatile black-box certification of quantum devices,” *Phys. Rev. Lett.*, vol. 113, p. 040401, Jul 2014.
- [126] J.-D. Bancal, M. Navascués, V. Scarani, T. Vértesi, and T. H. Yang, “Physical characterization of quantum devices from nonlocal correlations,” *Phys. Rev. A*, vol. 91, p. 022115, Feb 2015.
- [127] T. Coopmans, J. m. k. Kaniewski, and C. Schaffner, “Robust self-testing of two-qubit states,” *Phys. Rev. A*, vol. 99, p. 052123, May 2019.
- [128] Y. Wang, X. Wu, and V. Scarani, “All the self-testings of the singlet for two binary measurements,” *New Journal of Physics*, vol. 18, p. 025021, feb 2016.
- [129] S. Pironio, A. Acín, N. Brunner, N. Gisin, S. Massar, and V. Scarani, “Device-independent quantum key distribution secure against collective attacks,” *New Journal of Physics*, vol. 11, p. 045021, apr 2009.
- [130] C.-E. Bardyn, T. C. H. Liew, S. Massar, M. McKague, and V. Scarani, “Device-independent state estimation based on bell’s inequalities,” *Phys. Rev. A*, vol. 80, p. 062327, Dec 2009.
- [131] P. Sekatski, J.-D. Bancal, S. Wagner, and N. Sangouard, “Certifying the building blocks of quantum computers from bell’s theorem,” *Phys. Rev. Lett.*, vol. 121, p. 180505, Nov 2018.
- [132] T. Krisnanda, M. Zuppardo, M. Paternostro, and T. Paterek, “Revealing nonclassicality of inaccessible objects,” *Phys. Rev. Lett.*, vol. 119, p. 120402, Sep 2017.
- [133] S. Pal, P. Batra, T. Krisnanda, T. Paterek, and T. S. Mahesh, “Experimental localisation of quantum entanglement through monitored classical mediator,” *Quantum*, vol. 5, p. 478, June 2021.
- [134] E. Panwar, N. Gigena, and A. Chaturvedi, “Incompatibility of self-testing measurements and complexity of characterizing quantum correlations,” *In-preparation*, 2024.
- [135] E. Panwar, A. Chaturvedi, S. Leonard, and H. Karol, “Optimal strategies for diqkd with inefficient detectors,” *In-preparation*, 2024.

ARTICLE OPEN



An elegant scheme of self-testing for multipartite Bell inequalities

Ekta Panwar^{1,2} , Palash Pandya¹ and Marcin Wieśniak^{1,2} 

Self-testing is the most accurate form of certification of quantum devices. While self-testing in bipartite Bell scenarios has been thoroughly studied, self-testing in the more complex multipartite Bell scenarios remains largely unexplored. We present a simple and broadly applicable self-testing scheme for N -partite correlation Bell inequalities with two binary outcome observables per party. To showcase the versatility of our proof technique, we obtain self-testing statements for the MABK and WWWŻB family of linear Bell inequalities and Uffink's family of quadratic Bell inequalities. In particular, we show that the N -partite MABK and Uffink's quadratic Bell inequalities self-test the GHZ state and anti-commuting observables for each party. While the former uniquely specifies the state, the latter allows for an arbitrary relative phase. To demonstrate the operational relevance of the relative phase, we introduce Uffink's complex-valued N partite Bell expression, whose extremal values self-test the GHZ states and uniquely specify the relative phase.

npj Quantum Information (2023)9:71 ; <https://doi.org/10.1038/s41534-023-00735-3>

INTRODUCTION

One of the most striking features of quantum theory is the deviation of its predictions for Bell experiments from the predictions of classical theories with local casual (hidden variable) explanations¹. This phenomenon is captured by quantum violation of statistical inequalities, which are satisfied by all local realistic theories, referred to as Bell inequalities². Experimental demonstrations of the loophole-free violation of such inequalities (e.g., refs. 3–5) imply the possibility of sharing intrinsically random private numbers among an arbitrary number of spatially separated parties which power unconditionally secure private key distribution schemes (for more information on Device-independent quantum cryptography see refs. 6–10). Such applications of Bell non-locality follow from the fact that the extent of Bell inequality violation can uniquely identify the specific entangled quantum states and measurements, a phenomenon referred to as *self-testing* (see refs. 11,12 for initial contributions and the recent review of the progress till now see ref. 13).

Self-testing statements are the most accurate form of certifications for quantum systems. Self-testing schemes allow us to infer the underlying physics of a quantum experiment, i.e., the state and the measurements (up to local isometry), without any characterization of the internal workings of the measurement devices, and based only on the observed statistics, i.e., treating the measurement devices as black boxes with classical inputs and outputs. Self-testing has found many applications in several areas like *device-independent randomness generation*^{8,14}, *quantum cryptography*⁹, *entanglement detection*¹⁵, *delegated quantum computing*^{16,17}. While self-testing in the bipartite Bell scenarios has been thoroughly studied, self-testing in more complex multipartite Bell scenarios (see Fig. 1) remains largely unexplored.

In a multipartite setting, self-testing has been demonstrated for graph states using stabilizer operators¹⁸. Self-testing of multipartite graph states and partially entangled Greenberger-Horne-Zeilinger (GHZ)¹⁹ states has been demonstrated using a stabilizer-based approach, and Bell inequalities explicitly constructed for the

state²⁰. In general, multipartite Bell inequalities explicitly tailored for self-testing of a multipartite entangled state can be obtained using convex optimization techniques such as linear programming and semi-definite programming (SDP)^{17,21–23}. However, the Bell inequalities obtained in this way are just suitable candidates for the self-testing of the given multipartite states, and the potential self-testing statements must be verified using numerical techniques (such as the Swap method), which tend to be computationally expensive for multipartite scenarios with more than four parties. Completely analytical self-testing statements have also been obtained for multipartite states such as the W and the Dicke states by reprocessing self-testing protocols of bipartite states^{24–26}. Furthermore, parallel self-testing statements for multipartite states can be obtained using categorical quantum mechanics²⁷. Finally, the Mayers-Yao criterion can also be utilized for self-testing of graph states when the underlying graph is a triangular lattice²⁸.

In this article, we prove self-testing statements for multipartite Bell scenarios without relying on the Bell-operator dependent sum-of-squares decomposition²⁹. Consequently, our methodology immediately extends to all multipartite Bell scenarios, where each spatially separated party has two observables with binary outcomes ± 1 . To exemplify our proof technique, we obtain self-testing statements for N party Mermin-Ardehali-Belinskii-Klyshko (MABK)^{30,31} and Werner-Wolf-Weinfurter-Żukowski-Brukner (WWWŻB)^{32–34} family of linear Bell inequalities. Moreover, our methodology enables the recovery of self-testing statements for Bell functions which are not only the mean value of a Hermitian operator. Specifically, to showcase the versatility of our methodology, we obtain self-testing statements for the maximal violation of N party Uffink's quadratic Bell inequalities, which form tight witnesses of genuine multipartite non-locality, and the novel Uffink's complex-valued N partite Bell expressions³⁵.

The paper is organized as follows. First, in the Results section we recall the formal definition of self-testing. Then, we present the requisite preliminaries and specify the families of multipartite Bell

¹Institute of Theoretical Physics and Astrophysics, Faculty of Mathematics, Physics and Informatics, University of Gdańsk, ul. Wita Stwosza 57, 80-308 Gdańsk, Poland.

²International Centre for Theory of Quantum Technologies, University of Gdańsk, ul. Wita Stwosza 63, 80-308 Gdańsk, Poland. ✉email: ekta.panwar@phdstud.ug.edu.pl

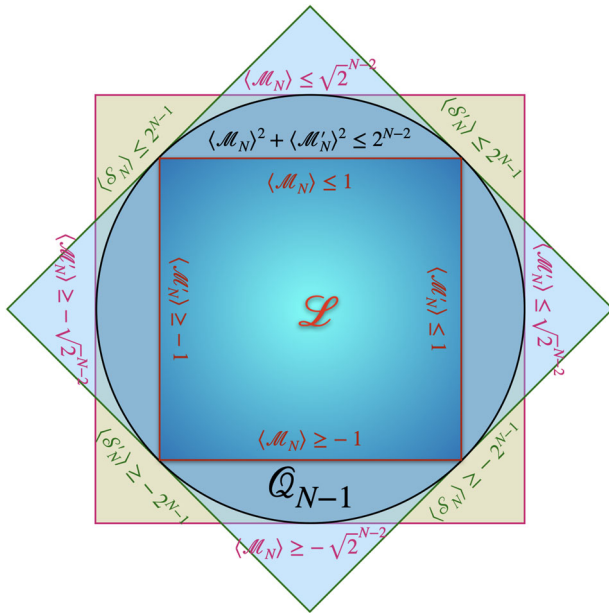


Fig. 1 Schematic representation of the correlations in multipartite Bell scenarios. This graphic is a schematic representation of the correlations in multipartite (involving arbitrary number N of spatially separated parties) Bell scenarios. Just like the bipartite Bell scenarios, the correlations which admit local hidden variable explanations form a convex polytope \mathcal{L} (shiny blue small horizontal square), whose facets are the N -party MABK inequalities [Eq. (2)] (red edges). However, the convex set of biseparable quantum correlations \mathcal{Q}_{N-1} (sky blue disk) does not form a polytope. Consequently, the linear inequalities such as the MABK [Eq. (2)] (pink edges of the large horizontal square) and Svetlichny inequalities [Eq. (3)] (green edges of the tilted square) do not form tight witness of genuine multipartite quantum non-locality. As the boundary of biseparable quantum correlations (black circle) is non-linear, Uffink’s quadratic inequalities [Eq. (4)] form tighter witnesses of genuine multipartite quantum non-locality.

inequalities we consider in this article. Next, we develop the mathematical preliminaries of the self-testing scheme. In particular, we show that the observables of each party in two-setting binary outcome multipartite Bell scenarios can always be simultaneously represented as anti-diagonal matrices. Next, we utilize this anti-diagonal matrix representation to obtain self-testing statements for the maximal violations of N party MABK and tripartite WWWZB family of linear (on correlators) Bell inequalities. While the former serves to benchmark our scheme, the latter demonstrates the spectrum of situations one can encounter. Finally, we obtain self-testing statements for the maximal violation of N party Uffink’s quadratic Bell inequalities and, at the very end of the Results section, we present the self-testing statements for the N partite Uffink’s complex-valued Bell expressions. Next, we provide a brief discussion about the robustness of the self-testing statements obtained in this work. Finally, we conclude by providing a brief summary of our work and potential application.

RESULTS

Before presenting our results, let us first introduce the requisite preliminaries.

Self-testing in Bell scenarios

A Bell scenario describes the operational setup of a Bell experiment by specifying the following three components: (1) the number of spatially separated parties, (2) the number of inputs of each party specifying their measurement settings, (3) the

number of outcomes corresponding to each input per party specifying the measurement outcomes for each measurement setting for each party. Each party performs measurements on a quantum system they share. As there are no assumptions on the internal working mechanism of the experimental devices, we may consider the devices to be mere black boxes, capable of receiving inputs (measurement settings) and generating outputs (measurement outcomes). The parties perform measurements based on their inputs and record the corresponding measurement outcomes, and estimate the conditional joint probability distributions governing their devices. Now, the question is, what can we deduce from these experimental statistics? Specifically, can we make statements describing the underlying physics, i.e., the quantum state and measurements? Such statements are broadly referred to as self-testing statements.

Formally, we say that a given Bell scenario entailing N parties, $\{A_j\}_{j=1}^N$, each measuring two observables, $\bar{A}^{(j)}, \bar{A}'^{(j)}$ and sharing a state $|\bar{\psi}\rangle\langle\bar{\psi}|$, self-tests, if the observation of the quantum maximal value B of a given Bell expression \mathcal{B} implies that the state $|\bar{\psi}\rangle$ used in the experiment can be transformed by local unitaries, $\bigotimes_j U_{A_j}$, to a reference state, $|\psi\rangle$, and a separable junk part, $|\Psi\rangle$, on which the observables act trivially, i.e,

$$\bigotimes_j U_{A_j} |\bar{\psi}\rangle = |\psi\rangle \otimes |\Psi\rangle.$$

Likewise, the local observables $\{\bar{A}^{(j)}\}_{j=1}^N$ and $\{\bar{A}'^{(j)}\}_{j=1}^N$, satisfy,

$$U_{A_j} \bar{A}^{(j)} (U_{A_j})^\dagger = A^{(j)} \otimes \mathbb{1},$$

$$U_{A_j} \bar{A}'^{(j)} (U_{A_j})^\dagger = A'^{(j)} \otimes \mathbb{1},$$

where the joint observables $\bigotimes_j O^{(j)}$ where $O^{(j)} \in \{A^{(j)}, A'^{(j)}\}$ act on the Hilbert space of $|\psi\rangle$, j and the tuple $\{|\psi\rangle, \{A^{(j)}, A'^{(j)}\}_j\}$ maximizes the given Bell expression, i.e., $\mathcal{B}(\{|\psi\rangle, \{A^{(j)}, A'^{(j)}\}_j\}) = B$.

The original idea of self-testing was presented in ref. ¹¹ by Mayers and Yao. Over the last few years, a great deal of work has been done in this area, primarily focused on bipartite Bell scenarios. However, self-testing in multipartite Bell scenarios remains relatively unexplored. In this paper, we obtain self-testing statements for multipartite Bell inequalities, introduced in the next section.

Two-setting N-party correlation Bell inequalities

This section presents the requisite preliminaries and specifies the families of Bell inequalities considered in this article. Specifically, here we consider multipartite Bell scenarios entailing N spatially separated (hence non-signaling) parties. We restrict ourselves to Bell scenarios where each party A_j , where $j \in \{1, \dots, N\}$, has two binary outcome observables $A^{(j)}, A'^{(j)}$ (Since there is no restriction on dimension, we can always take the measurements to be projective, in light of Naimark’s dilation Theorem. The projectivity of measurements is a distinguishing feature of a broadly subscribed viewpoint on quantum theory, namely, “The Church of the larger Hilbert space”). In contrast to the well-studied bipartite Bell scenarios, multipartite scenarios are substantially richer in complexity. While the notion of multipartite locality is an obvious extension of bipartite locality, multipartite behaviors can be non-local in many distinct ways. Apart from this, the most significant impediment in obtaining self-testing statements for multipartite Bell scenarios is that they do not admit simplifying characterizations such as Schmidt decomposition of the shared entangled state, unlike the bipartite Bell scenarios.

Typically, Bell inequalities comprise a Bell expression and a corresponding local causal bound. The violation of Bell inequalities witnesses the non-locality of the underlying behaviors. In the rest of this section, we introduce the families of multipartite Bell

inequalities, for which we demonstrate self-testing statements using our proof technique.

Linear inequalities

The most frequently used Bell inequalities comprise Bell expressions which are linear expressions of observed probabilities. Our self-testing argument is immediately applicable for any Bell inequality whose Bell expression is the mean of any linear combination of N party operators of the form $\bigotimes_{i=1}^N O^{(i)}$, where $O^{(i)} \in \{A^{(i)}, A'^{(i)}\}$. Among such linear Bell inequalities, we consider the Werner-Wolf-Weinfurter-Żukowski-Brukner (WWWŻB) families of correlation Bell inequalities for which there exists a well-defined systematic characterization³⁶. The Bell operator for the WWWŻB family of Bell inequalities has the following general form,

$$\mathcal{W}_N = \frac{1}{2^N} \sum_{s_1, \dots, s_N = \pm 1} S(s_1, \dots, s_N) \bigotimes_{j=1}^N (A^{(j)} + s_j A'^{(j)}), \quad (1)$$

where $S(s_1, \dots, s_N)$ is an arbitrary function of the indices $s_1, \dots, s_N \in \{-1, 1\}$ with binary outcomes ± 1 . Every tight (WWWŻB) inequality is given by $\langle \mathcal{W}_N \rangle \leq_{\mathcal{L}} 1$, where $\langle O \rangle = \text{Tr}\{\rho O\}$ is the expectation value of the linear operator O with respect to the quantum state ρ , and $\leq_{\mathcal{L}}$ signifies that the inequality holds for all correlations which admit local hidden variable explanations (\mathcal{L})³⁷.

Next, we introduce a sub-family of (WWWŻB) Bell inequalities, the Mermin-Ardehali-Belinskii-Klyshko (MABK) family of inequalities, featuring one inequality for any number N of parties^{30,31,38}. Moreover, in the following subsection, we introduce non-linear (quadratic) Bell inequalities composed of these MABK inequalities. The N -party MABK operators can be obtained recursively as,

$$\begin{aligned} \mathcal{M}_N &= \frac{1}{2} (\mathcal{M}_{N-1} \otimes (A^{(j)} + A'^{(j)}) \\ &\quad + \mathcal{M}'_{N-1} \otimes (A^{(j)} - A'^{(j)})) \\ &= \frac{1}{2^{\frac{N-1}{2}}} \left(\left(\frac{1+i}{\sqrt{2}} \right)^{(N-1) \bmod 2} \bigotimes_{j=1}^N (A^{(j)} + iA'^{(j)}) \right. \\ &\quad \left. + \left(\frac{1+i}{\sqrt{2}} \right)^{(N-1) \bmod 2} \bigotimes_{j=1}^N (A^{(j)} - iA'^{(j)}) \right), \end{aligned} \quad (2)$$

where the complimentary MABK Bell expression \mathcal{M}'_{N-1} has the same form as \mathcal{M}_{N-1} but with all $A^{(j)}$ and $A'^{(j)}$ interchanged. The corresponding Bell inequalities are of the form, $\langle \mathcal{M}_N \rangle \leq_{\mathcal{L}} 1$. Whereas the maximum attainable values of $\langle \mathcal{M}_N \rangle$ for biseparable \mathcal{Q}_{N-1} , and generic quantum correlations \mathcal{Q} are $2^{\frac{N-2}{2}}$, and $2^{\frac{N-1}{2}}$, respectively. The maximal quantum value can be attained with anti-commuting local observables and the maximally entangled N -partite GHZ state³⁹⁻⁴¹.

Finally, we present yet another relevant sub-family of the (WWWŻB) inequalities, referred to as Svetlichny inequalities³⁵, which were explicitly conceived to witness genuine N -partite non-locality. Moreover, the quadratic Bell inequalities featured in the following subsection can also be composed of N -partite Svetlichny-Bell inequalities. The Svetlichny operator can be formed of MABK operators [Eq. (2)] in the following way,

$$\mathcal{S}_N^{\pm} = \begin{cases} 2^{k-1} \left((-1)^{\frac{k(\pm 1)}{2}} \mathcal{M}_N^{\pm}, \right. \\ \quad \left. (\text{for } N = 2k); \right. \\ 2^{k \pm 1} \left((-1)^{\frac{k(k \pm 1)}{2}} \mathcal{M}_N \mp (-1)^{\frac{k(k \mp 1)}{2}} \mathcal{M}_N \right), \\ \quad \left. (\text{for } N = 2k + 1), \right. \end{cases} \quad (3)$$

where \mathcal{M}_N^+ is equivalent to \mathcal{M}_N [Eq. (2)] and \mathcal{M}_N^- is equivalent to \mathcal{M}_N . The corresponding Svetlichny inequalities are of the form, $\langle \mathcal{S}_N^{\pm} \rangle \leq_{\mathcal{Q}_{N-1}} 2^{N-1} \leq_{\mathcal{Q}} 2^{2N-1}$.

Quadratic inequalities

In bipartite Bell scenarios, without loss of generality, it is enough to consider linear Bell inequalities to witness non-locality as the set of behaviors that admit a local casual explanation form a convex polytope demarcated by linear facet inequalities. In contrast to the bipartite case, non-linear Bell inequalities form tighter witnesses of genuine multipartite non-locality. In multipartite Bell scenarios, the convex set of biseparable quantum behaviors does not form a polytope. Consequently, Uffink's quadratic Bell inequalities form stronger witnesses of genuine multipartite non-locality than the linear inequalities. There are two distinct families of N party quadratic Bell inequalities formed of the MABK [Eq. (2)] and Svetlichny [Eq. (3)], families of linear inequalities, \mathcal{U}_N^M and \mathcal{U}_N^S , respectively, which have the form

$$\mathcal{U}_N^M = \langle \mathcal{M}_N \rangle^2 + \langle \mathcal{M}'_N \rangle^2 \leq_{\mathcal{Q}_{N-1}} 2^{N-2} \leq_{\mathcal{Q}} 2^{N-1}, \quad (4)$$

$$\mathcal{U}_N^S = \langle \mathcal{S}_N^+ \rangle^2 + \langle \mathcal{S}_N^- \rangle^2 \leq_{\mathcal{Q}_{N-1}} 2^{2N-2} \leq_{\mathcal{Q}} 2^{2N-1}, \quad (5)$$

Characterizing local observables

In this section, we obtain a characterization for the binary outcome local observables $A = A^{(j)}$ and $A' = A'^{(j)}$ on an arbitrary Hilbert space $\mathcal{H} = \mathcal{H}^{(j)}$ for any given party \mathcal{A}_j , where $j \in \{1, \dots, N\}$. As in Bell scenarios, there is no restriction on the dimension of the underlying Hilbert space, using Naimark's dilation Theorem, without loss of generality, we can take the observables A and A' to be projective, i.e., $A^2 = A'^2 = \mathbb{1}$. First, via the following lemma, we demonstrate that the second observable A' can be split into two observables, one which commutes with the first observable A and one which anti-commutes with A ,

Lemma 1. Given any two binary outcome projective observables A and A' , A' can be decomposed as the sum of two observables $-1 \leq A'_- \leq 1$ and $-1 \leq A'_+ \leq 1$, such that $[A, A'_+] = 0$, $\{A, A'_-\} = 0$, $\{A'_+, A'_-\} = 0$ and $(A'_+)^2 + (A'_-)^2 = 1$.

Proof. Without loss of generality, the binary outcome projective observable A can be represented as a diagonal matrix with positive and negative eigenvalues grouped together,

$$A = \begin{pmatrix} \mathbb{1}_m & 0 \\ 0 & -\mathbb{1}_n \end{pmatrix}, \quad (6)$$

where $\mathbb{1}_m$ is the $m \times m$ identity operator. With respect to A , the binary outcome projective observable A' has the following generic matrix representation,

$$A' = \begin{pmatrix} D_1 & D_2 \\ D_2^\dagger & D_3 \end{pmatrix}. \quad (7)$$

such that,

$$A'_- = \begin{pmatrix} 0 & D_2 \\ D_2^\dagger & 0 \end{pmatrix}, \quad (8)$$

$$A'_+ = \begin{pmatrix} D_1 & 0 \\ 0 & D_3 \end{pmatrix}. \quad (9)$$

Clearly, $[A, A'_+] = 0$, and $\{A, A'_-\} = 0$. As A' is projective we have,

$$\begin{aligned} (A')^2 &= (A'_+)^2 + (A'_-)^2 + \{A'_+, A'_-\} \\ &= \begin{pmatrix} D_1^2 + D_2 D_2^\dagger & D_1 D_2 + D_2 D_3 \\ D_2^\dagger D_1 + D_3 D_2^\dagger & D_2^\dagger D_2 + D_3^2 \end{pmatrix} \end{aligned} \quad (10)$$

$$= \mathbb{1}, \quad (11)$$

which requires the off-diagonal blocks to be zero,

$$\begin{aligned} \{A'_+, A'_-\} &= \begin{pmatrix} 0 & D_1 D_2 + D_2 D_3 \\ D_2^\dagger D_1 + D_3 D_2^\dagger & 0 \end{pmatrix} \\ &= 0, \end{aligned} \quad (12)$$

and leaves $(A'_+)^2 + (A'_-)^2 = \mathbb{1}$, which completes the proof.

Using the above Lemma, the relation between the eigenvalues of A' , A'_- , and A'_+ can be ascertained to be $\lambda_{A'}^i = \pm \sqrt{(\lambda_{A'_-}^i)^2 + (\lambda_{A'_+}^i)^2} = \pm 1$, where λ^i denotes the i^{th} eigenvalue⁴². So that the eigenvalues can be without loss of generality taken as $\pm \sin \theta_i$ and $\pm \cos \theta_i$ for A'_- and A'_+ respectively.

Next, we show that the spectra of any two anti-commuting observables must be symmetric, and each observable maps the positive eigenspaces to the negative eigenspaces of the other.

Lemma 2. Given any two binary outcome anti-commuting projective observables, A and A'_- , such that $A^2 = \mathbb{1}$, their spectra must be symmetric (i.e., if $|\psi_\lambda\rangle$ is an eigenvector corresponding to the eigenvalue λ , then there exists a unique eigenvector $|\psi_{-\lambda}\rangle$ corresponding to the eigenvalue $-\lambda$). Moreover, A'_- acts on an effective even-dimensional Hilbert space $\bigoplus_i E_{\pm\lambda_i}^{A'_-}$ decomposed into the direct sum of the even-dimensional eigenspaces $E_{\pm\lambda_i}^{A'_-} = E_{\lambda_i}^{A'_-} \oplus E_{-\lambda_i}^{A'_-}$. Where, $E_{\lambda_i}^{A'_-}$ and $E_{-\lambda_i}^{A'_-}$ are eigenspaces corresponding to the non-zero eigenvalues λ_i and $-\lambda_i$, respectively.

Proof. From the anti-commutation relation it follows that, $AA'_- = -A'_-A$. As A is unitary and Hermitian, we can take A to the other side to sandwich A'_- , which leaves us with,

$$AA'_-A = -A'_-. \quad (13)$$

Further, taking trace on both sides of Eq. (13) yields,

$$\text{Tr}\{A'_-\} = 0. \quad (14)$$

This implies that the observable A'_- has a symmetric spectra, i.e., for each eigenvector corresponding to a non-zero eigenvalue λ_i there exists an eigenvector corresponding to the eigenvalue $-\lambda_i$, along with the null space or the kernel $\ker(A'_-)$. Without loss of generality, we can ignore the kernel as it does not contribute to the violation of Bell inequalities. Hence, we are left with the subspace, $\bigoplus_i E_{\pm\lambda_i}^{A'_-}$, where $E_{\pm\lambda_i}^{A'_-} = E_{\lambda_i}^{A'_-} \oplus E_{-\lambda_i}^{A'_-}$ is an even-dimensional subspace corresponding to the non-zero eigenvalues $\pm\lambda_i$. The diagonalizability of A'_- (Hermitian) implies that we can decompose this subspace into the direct sum of these eigenspaces (and the kernel $\ker(A'_-)$), which further implies that the effective subspace of such operators can be truncated to an even-dimensional subspace. Finally, as on this truncated subspace, $AA'_-|\psi_{\lambda_i}\rangle = -\lambda_i A'_-|\psi_{\lambda_i}\rangle$, where $|\psi_{\lambda_i}\rangle$ is an eigenvector of A corresponding to eigenvalue $\lambda_i = \pm 1$, we conclude that $m = n$, i.e., A is even-dimensional and has a similarly symmetric spectrum.

Now, as $A' = A'_+ + A'_-$, the effective subspaces of A'_+ , A' , can also be truncated to the same effective even-dimensional subspace as A'_- . Also, as on this truncated subspace, $A'_+A'_-|\psi_{\lambda_i}\rangle = -\lambda_i A'_-|\psi_{\lambda_i}\rangle$, where $|\psi_{\lambda_i}\rangle$ is an eigenvector of A'_+ corresponding to its eigenvalue λ_i , i.e., A'_+ has a similar symmetric spectrum. Moreover, Lemma 2 yields the following succinct parameterization of the two mutually anti-commuting components of any projective observable,

Corollary 2.1. Given two even-dimensional anti-commuting operators A_+ and A_- such that $(A'_+)^2 + (A'_-)^2 = \mathbb{1}$, they can be written in the form,

$$A'_{\pm|\theta_i} = \cos \theta_i B_{\pm|\theta_i}, \quad A'_{\mp|\theta_i} = \sin \theta_i B_{\mp|\theta_i}, \quad (15)$$

when restricted to the subspace $E_{+\theta_i}^{A'_+} \oplus E_{-\theta_i}^{A'_-}$ with corresponding eigenvalues $\pm \cos(\theta_i)$ for A_+ and $\pm \sin(\theta_i)$ for A_- , such that the operators $B_{\pm|\theta_i}$ are traceless and projective.

Proof. We have already shown the dimension of the combined eigenspaces $E_{\lambda_i}^{A'_+} \oplus E_{-\lambda_i}^{A'_-}$ is even. Then the two anti-commuting operators A'_+ and A'_- restricted to this eigenspace, denoted by $A'_{\pm|\theta_i}$ and $A'_{\mp|\theta_i}$, will only have eigenvalues $\pm \cos \theta_i$ and $\pm \sin \theta_i$, respectively, whilst still satisfying $(A'_{\pm|\theta_i})^2 + (A'_{\mp|\theta_i})^2 = \mathbb{1}$. It is then possible to write the same relation in terms of scaled operators, as

$$\cos^2 \theta_i B_{\pm|\theta_i}^2 + \sin^2 \theta_i B_{\mp|\theta_i}^2 = \mathbb{1}. \quad (16)$$

As a result, the operators $B_{\pm|\theta_i}$ have eigenvalues ± 1 that occur in pairs. Therefore, $\text{Tr}(B_{\pm|\theta_i}) = 0$ and $B_{\pm|\theta_i}^2 = \mathbb{1}$.

Using the above results, in such an even-dimensional subspace the following lemma holds.

Lemma 3. Given any two traceless and projective anti-commuting observables B_+ and B_- , the observable $\cos \alpha B_+ + \sin \alpha B_-$ is also traceless and projective.

Proof. Expanding the square,

$$\begin{aligned} &(\cos \alpha B_+ + \sin \alpha B_-)^2 \\ &= \cos^2 \alpha B_+^2 + \sin^2 \alpha B_-^2 + \cos \alpha \sin \alpha \{B_+, B_-\} \\ &= \mathbb{1}. \end{aligned} \quad (17)$$

And the trace is simply,

$$\cos \alpha \text{Tr}(B_+) + \sin \alpha \text{Tr}(B_-) = 0. \quad (18)$$

The above lemma shows that in the Bell scenarios considered here, the effective local dimension of any subsystem must be even-dimensional. Now, we present the main ingredient of our self-testing proof technique, i.e., the simultaneous anti-diagonal matrix representation for local observables of each party up to local isometries.

Theorem 4. Given any three binary outcome traceless and projective observables A , B_+ , and B_- , such that $[A, B_+] = 0$, $\{A, B_-\} = 0$, and $\{B_+, B_-\} = 0$, then these operators have a simultaneous anti-diagonal matrix representation.

Proof. As $[A, B_+] = 0$, we can take the dimension of the subspace for which the eigenvalues of A and B_+ are equal to be $2d_1$, and $2d_2$ for the subspace where the eigenvalues differ. Consequently, without loss of generality, by Lemma 2 the operators A , B_+ , and B_- have the following matrix representations,

$$\begin{aligned} A &= \begin{pmatrix} \mathbb{1}_{d_1} & & & \\ & \mathbb{1}_{d_2} & & \\ & & -\mathbb{1}_{d_2} & \\ & & & -\mathbb{1}_{d_1} \end{pmatrix}, \\ B_+ &= \begin{pmatrix} \mathbb{1}_{d_1} & & & \\ & -\mathbb{1}_{d_2} & & \\ & & \mathbb{1}_{d_2} & \\ & & & -\mathbb{1}_{d_1} \end{pmatrix}, \\ B_- &= \begin{pmatrix} & & & U_1 \\ & & U_2 & \\ & U_2^\dagger & & \\ U_1^\dagger & & & \end{pmatrix}. \end{aligned} \quad (19)$$

Since B_- is projective, U_1 and U_2 must be unitary. Thus, without altering A or B_+ we can take four unitaries V_1, V_2, V_3, V_4 , each acting on a different block, such that $V_1 U_1 V_4^\dagger = J_{d_1}$ and $V_2 U_2 V_3^\dagger = J_{d_2}$, where J_d is the row-reversed $d \times d$ identity matrix.

Consequently, we can now restrict ourselves to considering any one of the $d_1 + d_2$ two-dimensional subspaces, on which A and B_+ are represented by $\pm\sigma_z$, while B_- is projected onto σ_x . Finally, in each of these subspaces, we apply the following unitary transformation,

$$U = \frac{1}{2} \begin{pmatrix} -1 + i & 1 + i \\ -1 + i & -1 - i \end{pmatrix}, \quad (20)$$

which corresponds to a rotation by $\frac{2\pi}{3}$ with respect to axis $(1, 1, 1)$, and transforms $\sigma_z \rightarrow \sigma_x \rightarrow \sigma_y$, and bringing all three operators to strictly anti-diagonal form.

Summarizing, the Theorem 4, along with Lemmas 2 and 3 allow us to take the first observable of each party $A^{(j)}$ to be equivalent to σ_x on all relevant two-dimensional subspaces, while the second operator $A'^{(j)}$ can be taken to be $A'^{(j)} = \cos\theta_j\sigma_x + \sin\theta_j\sigma_y$.

We note here that the above thesis also follows from a well-known result, commonly referred to as Jordan's lemma^{43,44}, which states that any two dichotomic observables squaring to identity can be simultaneously brought into a block diagonal form with one and two-dimensional blocks. Discarding the one-dimensional blocks as they do not contribute to Bell non-locality, each pair of the remaining two-dimensional blocks, which act as dichotomic observables on the same Hilbert space can be unitarily rotated to σ_x and $\cos\theta_j\sigma_x + \sin\theta_j\sigma_y$. In fact, Jordan's lemma has already been used in this way to obtain self-testing statements⁴¹. Therefore, the contents of this section constitute an alternative proof of Jordan's lemma and the subsequent parametrization.

This theorem forms the key ingredient of our proof technique as it yields the following criterion for self-testing statements obtained in this work,

Lemma 5. The maximum quantum value B of any two-setting two outcome N -partite Bell expression \mathcal{B} composed of N party correlators, self-tests a generalized GHZ state, $\alpha \otimes_{j=1}^N |i_j\rangle + \beta \otimes_{j=1}^N |\bar{i}_j\rangle$, where $i_j \in \{0, 1\}$ and $\bar{i}_j = 1 \oplus i_j$, if the corresponding Bell operator has a non-degenerate maximum eigenvalue $\lambda_{max} = B$.

Proof. For two-setting binary outcome N partite Bell scenarios, Theorem 4 implies that the local observables of each party have simultaneous anti-diagonal matrix representations. Consequently, any N partite Bell expression \mathcal{B} composed only of N party correlators corresponds to a Bell operator on $(\mathbb{C}^2)^{\otimes N}$ which also has an anti-diagonal matrix representation. Clearly, the maximum value of the Bell expression \mathcal{B} corresponds to the maximum eigenvalue λ_{max} of the Bell operator. As the eigenvectors of any such anti-diagonal matrix are of the form of generalized GHZ states, $\alpha \otimes_{j=1}^N |i_j\rangle + \beta \otimes_{j=1}^N |\bar{i}_j\rangle$, where $i_j \in \{0, 1\}$ and $\bar{i}_j = 1 \oplus i_j$, the maximum value B of such a Bell expression self-tests such a state if the maximum eigenvalue λ_{max} of the Bell operator is non-degenerate.

In the next section, we demonstrate our proof technique and obtain self-testing statements for the MABK family of N party inequalities and tripartite Bell inequalities composed of three-party correlators.

Self-testing statements for multipartite inequalities

In this section, we use the tools developed in the previous section to obtain self-testing statements for linear MABK family of N party inequalities [Eq. (2)], and sketch the proofs for the self-testing statements for all distinct equivalence classes of tripartite WWWZB

facet inequalities [Eq. (1)]. Finally, we obtain self-testing statements for Uffink's family [Eq. (4)] of non-linear N party inequalities.

N party MABK inequalities

Theorem 6. In order to achieve maximal quantum violation of a N -party MABK inequality, $\langle \mathcal{M}_N \rangle = 2^{\frac{N-1}{2}}$, the parties must share a N qubit GHZ state $|\text{GHZ}_N\rangle = \frac{1}{\sqrt{2}}(|0\rangle^{\otimes N} + e^{i\phi(N)}|1\rangle^{\otimes N})$, where $\phi(N)$ is the relative phase, $\phi(N) = 0$ when N is odd, $\phi(N) = -\frac{\pi}{4}$ when N is even and perform maximally anti-commuting projective measurements $A^{(j)} = \sigma_x$ and $A'^{(j)} = \sigma_y$ (up to local isometries).

Proof. From Lemma 2 and Theorem 4, without loss of generality, the local observables of any party \mathcal{A}_j , where $j \in \{1, \dots, N\}$, can be taken to be,

$$\begin{aligned} A^{(j)} &= \sigma_x, \\ A'^{(j)} &= \cos\theta_j\sigma_x + \sin\theta_j\sigma_y, \end{aligned} \quad (21)$$

acting on the effective two-dimensional subspace. This parametrization implies that the MABK operator [Eq. (2)] \mathcal{M}_N has the following anti-diagonal matrix representation,

$$\mathcal{M}_N = \text{adiag} \begin{pmatrix} \frac{1}{2^{\frac{N-1}{2}}} \left(\left(\frac{1-i}{\sqrt{2}} \right)^{(N-1) \bmod 2} \prod_{j=1}^N (1 + ie^{-i\theta_j}) \right) \\ + \left(\frac{1+i}{\sqrt{2}} \right)^{(N-1) \bmod 2} \prod_{j=1}^N (1 - ie^{-i\theta_j}) \\ \vdots \\ \frac{1}{2^{\frac{N-1}{2}}} \left(\left(\frac{1-i}{\sqrt{2}} \right)^{(N-1) \bmod 2} \prod_{j=1}^N (1 + ie^{i\theta_j}) \right) \\ + \left(\frac{1+i}{\sqrt{2}} \right)^{(N-1) \bmod 2} \prod_{j=1}^N (1 - ie^{i\theta_j}) \end{pmatrix}, \quad (22)$$

where adiag represents a matrix with non-zero values only on the anti-diagonal. It is easy to see for any combination, $\forall j \in \{1, \dots, N\} : \theta_j = \pm \frac{\pi}{2}$, one of the anti-diagonal elements attains the maximum absolute value of $2^{\frac{N-1}{2}}$ while the others vanish.

Recall that the maximum expectation value of an operator corresponds to its highest eigenvalue, attained when the state corresponds to the associated eigenvector. Moreover, the eigenvectors of operators with an anti-diagonal matrix representation are of the generic form, $\alpha \otimes_{j=1}^N |i_j\rangle + \beta \otimes_{j=1}^N |\bar{i}_j\rangle$, where $i_j \in \{0, 1\}$ and $\bar{i}_j = 1 \oplus i_j$. Now, taking the expectation value of \mathcal{M}_N with respect to any one of these states selects the sum of a pair of (equidistant from the top and the bottom) anti-diagonal elements. As each such pair is equivalent to the rest up-to local rotations, we can, without loss of any generality, consider the state, $|\psi_N\rangle = \alpha|0\rangle^{\otimes N} + \beta|1\rangle^{\otimes N}$, which effectively yields a weighted sum of the top and bottom anti-diagonal elements of the matrix [Eq. (22)].

Specifically, the expectation value of the Hermitian operator \mathcal{M}_N for the state $|\psi_N\rangle$ has the expression,

$$\begin{aligned} \langle \psi_N | \mathcal{M}_N | \psi_N \rangle &= 2\text{Re} \left\{ \bar{\alpha} \frac{1}{2^{\frac{N-1}{2}}} \left(\left(\frac{1-i}{\sqrt{2}} \right)^{(N-1) \bmod 2} \prod_{j=1}^N (1 + ie^{-i\theta_j}) \right) \right. \\ &\quad \left. + \left(\frac{1+i}{\sqrt{2}} \right)^{(N-1) \bmod 2} \prod_{j=1}^N (1 - ie^{-i\theta_j}) \right\} \beta, \end{aligned} \quad (23)$$

Using the fact that $\forall \alpha, \beta \in \mathbb{C} : \text{Re} \alpha\beta \leq |\alpha\beta| = |\alpha||\beta|$ we bound $\langle \psi_N | \mathcal{M}_N | \psi_N \rangle$ from above in the following way,

$$\begin{aligned} \langle \psi_N | \mathcal{M}_N | \psi_N \rangle &\leq 2|\bar{\alpha}||\beta| \frac{1}{2^{\frac{N-1}{2}}} \left(\left(\frac{1-i}{\sqrt{2}} \right)^{(N-1) \bmod 2} \prod_{j=1}^N (1 + ie^{-i\theta_j}) \right) \\ &\quad + \left(\frac{1+i}{\sqrt{2}} \right)^{(N-1) \bmod 2} \prod_{j=1}^N (1 - ie^{-i\theta_j}) \Big|. \end{aligned} \quad (24)$$

As $|\alpha|^2 + |\beta|^2 = 1$, the maximum value of the above expression can only be attained for $|\alpha| = |\beta| = \frac{1}{\sqrt{2}}$, which picks out $|GHZ_N\rangle$ as the shared state. Consequently, we retrieve the following upper bound,

$$\langle \psi_N | \mathcal{M}_N | \psi_N \rangle \leq \left| \frac{1}{2^{\frac{N-1}{2}}} \left(\left(\frac{1-i}{\sqrt{2}} \right)^{(N-1) \bmod 2} \prod_{j=1}^N (1 + ie^{-i\theta_j}) + \left(\frac{1+i}{\sqrt{2}} \right)^{(N-1) \bmod 2} \prod_{j=1}^N (1 - ie^{-i\theta_j}) \right) \right|. \quad (25)$$

Now, as $|\frac{1+i}{\sqrt{2}}|^{(N-1) \bmod 2} = |\frac{1-i}{\sqrt{2}}|^{(N-1) \bmod 2} = 1$ and $|(1 + ie^{-i\theta_j})| = |2 \sin(\frac{\pi}{4} + \frac{\theta_j}{2})|$ and $|(1 - ie^{-i\theta_j})| = |2 \cos(\frac{\pi}{4} + \frac{\theta_j}{2})|$, we can further upper bound the above expression as,

$$\langle \psi_N | \mathcal{M}_N | \psi_N \rangle \leq 2^{\frac{N-1}{2}} \left(\prod_{j=1}^N \left| \sin\left(\frac{\pi}{4} + \frac{\theta_j}{2}\right) \right| + \prod_{j=1}^N \left| \cos\left(\frac{\pi}{4} + \frac{\theta_j}{2}\right) \right| \right).$$

As, $\forall j : |\sin(\frac{\pi}{4} + \frac{\theta_j}{2})| \leq 1, |\cos(\frac{\pi}{4} + \frac{\theta_j}{2})| \leq 1$, we can further upper bound the above expression by discarding all but three terms corresponding to any $i, j, k \in \{1, \dots, N\}$, such that,

$$\begin{aligned} \langle \psi_N | \mathcal{M}_N | \psi_N \rangle &\leq 2^{\frac{N-1}{2}} \left(\left| \sin\left(\frac{2\theta_i + \pi}{4}\right) \sin\left(\frac{2\theta_j + \pi}{4}\right) \sin\left(\frac{2\theta_k + \pi}{4}\right) \right| \right. \\ &\quad \left. + \left| \cos\left(\frac{2\theta_i + \pi}{4}\right) \cos\left(\frac{2\theta_j + \pi}{4}\right) \cos\left(\frac{2\theta_k + \pi}{4}\right) \right| \right) \\ &\leq 2^{\frac{N-1}{2}}, \end{aligned} \quad (26)$$

where the proof of the second inequality has been deferred to the Supplementary Note. In the Supplementary Note, we also show that this inequality can only be saturated when $\theta_i = \theta_j = \theta_k = \frac{\pi}{2}$. As the choice of $i, j, k \in \{1, \dots, N\}$ is completely arbitrary, the inequality can only be saturated when $\forall j \in \{1, \dots, N\} : \theta_j = \frac{\pi}{2}$, i.e., when for each party the local observables maximally anti-commute. As these settings maximize the value of \mathcal{M}_N only for a unique pair of equidistant anti-diagonal entries, the state must be $|GHZ_N\rangle \equiv \frac{1}{\sqrt{2}}(|0\rangle^{\otimes N} + e^{i\phi(N)}|1\rangle^{\otimes N})$, where $\phi(N) = 0$ when N is odd, and $\phi(N) = -\frac{\pi}{4}$ when N is even, up to auxiliary degrees of freedom on which the measurements act trivially, and local basis transformations. This further implies that the actual shared state could be of the form $|GHZ_N\rangle \otimes |\Psi\rangle$ up to local unitaries, where the arbitrary state $|\Psi\rangle$ on auxiliary degrees of freedom does not contribute to the operational Bell violation and thus is referred to as the junk state.

We note here that the same proof technique extends to the complimentary MABK inequalities, \mathcal{M}_N , defined in ‘‘Results: Two-setting N -party correlation Bell inequalities’’, as well, to yield the corresponding self-testing statements, summarized in the following Corollary.

Corollary 6.1. In order to achieve the maximal quantum violation of a N -party complimentary MABK inequality, $\langle \mathcal{M}_N \rangle = 2^{\frac{N-1}{2}}$, the parties must share a N qubit GHZ state $|GHZ_N\rangle = \frac{1}{\sqrt{2}}(|0\rangle^{\otimes N} + e^{i\phi(N)}|1\rangle^{\otimes N})$, where $\phi(N) = \frac{\pi}{2}$ when N is odd, $\phi(N) = \frac{\pi}{4}$ when N is even and perform maximally anti-commuting projective measurements $A^{(i)} = \sigma_x$ and $A^{(j)} = \sigma_y$ (up to local isometries).

The proof follows a relatively straightforward modification of the proof of Theorem 6. However, these self-testing statements will be used in the next section for obtaining self-testing of Uffink’s quadratic inequalities. Moreover, the proof technique readily applies to the Svetlichny family of N -party inequalities as they are composed of the N -party MABK inequalities. Furthermore, the proof technique enables self-testing of a much broader class of N -

party WWWZB inequalities. To demonstrate this, we sketch the proofs for self-testing of tripartite WWWZB inequalities [Eq. (1)].

Tripartite WWWZB inequalities

In the case of tripartite Bell scenarios where each party has two input and output respectively, we have a 26-dimensional local correlation polytope that has 64 vertices and 53,856 faces⁴⁵. These faces can be grouped into 46 equivalence classes of Bell inequalities listed in ref. ⁴⁶, and out of which, we consider the non-trivial facet inequalities, which are composed of only three-party correlators and can be grouped into the following four equivalence classes.

The first class is composed of correlation inequalities equivalent (up-to relabeling) to the *Mermin’s inequality* $\langle \mathcal{M}_3 \rangle \leq 1$,

$$\frac{1}{2} (\langle A^{(1)} A^{(2)} A^{(3)} \rangle + \langle A^{(1)} A^{(2)} A^{(3)} \rangle + \langle A^{(1)} A^{(2)} A^{(3)} \rangle - \langle A^{(1)} A^{(2)} A^{(3)} \rangle) \leq 1.$$

For these inequalities, the proof of Theorem 6 directly applies³⁷. As a consequence, we retrieve the tripartite GHZ state $|GHZ_3\rangle$ as well as maximally anti-commuting local observables as necessary ingredients for the maximal quantum violation 2.

The second equivalence class of tripartite inequalities is that of *unbalanced inequalities*, which can be found in the ref. ⁴⁷ as the seventh inequality in Table I, and also specified below,

$$\begin{aligned} &(3 \langle A^{(1)} A^{(2)} A^{(3)} \rangle + \langle A^{(1)} A^{(2)} A^{(3)} \rangle \\ &+ \langle A^{(1)} A^{(2)} A^{(3)} \rangle + \langle A^{(1)} A^{(2)} A^{(3)} \rangle \\ &- \langle A^{(1)} A^{(2)} A^{(3)} \rangle - \langle A^{(1)} A^{(2)} A^{(3)} \rangle \\ &- \langle A^{(1)} A^{(2)} A^{(3)} \rangle + \langle A^{(1)} A^{(2)} A^{(3)} \rangle) \leq 4. \end{aligned}$$

The corresponding operator has an anti-diagonal matrix representation with values of the form,

$$4 + (-1 + e^{ik_1\theta_1})(-1 + e^{ik_2\theta_2})(-1 + e^{ik_3\theta_3}), \quad (27)$$

where $(k_1, k_2, k_3 \in \{-1, 1\})$. Unlike the MABK class of inequalities the absolute values of these anti-diagonal terms are maximized when $\cos \theta_j = -\frac{1}{3}$. Thus, yet again, the tripartite GHZ state $|GHZ_3\rangle$ is distinguished, but non maximally anti-commuting local observables are required for maximal quantum violation, $\frac{20}{3}$, of these inequalities.

We will next discuss the equivalence class of the *extended CHSH inequalities* of the form given below, which is listed as the third inequality in Table I of the ref. ⁴⁶,

$$\frac{1}{2} (\langle A^{(1)} A^{(2)} A^{(3)} \rangle + \langle A^{(1)} A^{(2)} A^{(3)} \rangle + \langle A^{(1)} A^{(2)} A^{(3)} \rangle - \langle A^{(1)} A^{(2)} A^{(3)} \rangle) \leq 1.$$

For these inequalities, the operator in the anti-diagonal matrix representation has elements of the form,

$$\frac{1}{2} (1 + e^{ik_1\theta_1} + e^{i(k_2\theta_2 + k_3\theta_3)} - e^{i(k_1\theta_1 + k_2\theta_2 + k_3\theta_3)}). \quad (28)$$

Consequently, the corresponding absolute values are $2\sqrt{1 \pm \sin \theta_1 \sin(k_2\theta_2 \pm k_3\theta_3)}$. Clearly, for the maximal quantum violation, the operators $A^{(1)}$ and $A^{(1)}$ must maximally anti-commute, i.e., $\theta_1 = \pm \frac{\pi}{2}$. However, the maximal quantum violation only requires the sum $k_2\theta_2 \pm k_3\theta_3 = \pm \frac{\pi}{2}$, i.e., the optimal $A^{(2)}$ is defined only in reference to $A^{(3)}$. Clearly, for the maximal quantum violation $2\sqrt{2}$ the shared state must be equivalent to the bipartite maximally entangled state $|GHZ_2\rangle$. However, these inequalities do not satisfy the strict self-testing criterion as defined in section II, as the optimal local observables are not unique and specified only up-to a mutual relation.

Lastly, we have the equivalence class of the *CHSH-like inequalities* of the form given below, which correspond to the second

inequality listed in Table I of the ref. 47,

$$\frac{1}{2} (\langle A^{(1)} A^{(2)} A^{(3)} \rangle + \langle A^{(1)} A^{(2)} A^{(3)} \rangle) + \langle A^{(1)} A^{(2)} A^{(3)} \rangle - \langle A^{(1)} A^{(2)} A^{(3)} \rangle \leq 1.$$

These inequalities are equivalent to the CHSH or \mathcal{M}_2 inequality for which the proof of Theorem 6 directly applies. The non-zero elements of the anti-diagonal matrix representation of the corresponding Bell operator are of the form,

$$\left(1 + e^{ik_1\theta_1} + e^{ik_2\theta_2} - e^{i(k_1\theta_1+k_2\theta_2)}\right). \quad (29)$$

The modulo of these values is $2\sqrt{1 \pm \sin\theta_1 \sin\theta_2}$, which implies that for the maximum quantum violation $\sqrt{2}$ the observables for the first pair of parties must maximally anti-commute, i.e., $\pm\theta_1 = \pm\theta_2 = \frac{\pi}{2}$ and shared state must be equivalent to the bipartite maximally entangled state $|GHZ_2\rangle$.

Apart from the linear inequalities considered here, our proof technique, which relies on the anti-diagonal matrix representation of the Bell operator, is directly applicable to all two settings binary outcome linear (on correlators) multipartite Bell inequalities, either yielding perfect self-testing statements as defined in the beginning of the Results section, or pointing out the impossibility of them, as exemplified above. Next, we obtain self-testing statements using our proof technique for relevant classes of non-linear and complex-valued multipartite Bell expressions.

N party Uffink's quadratic Bell inequalities and complex Bell expression

As the convex set of biseparable multipartite quantum correlations does not form a polytope, linear inequalities like the Svetlichny inequalities [Eq. (3)] do not form tight, efficient witnesses of genuine multipartite non-locality. On the other hand, the non-linear inequalities such as the Uffink's family of $N \geq 3$ party quadratic (on correlators) inequalities [Eq. (4)] better capture the boundary of the quantum set of biseparable correlations and hence form better witnesses of genuine multipartite quantum non-locality. Here, we use our methodology to obtain self-testing statements for the maximum violation of Uffink's quadratic Bell inequalities. Specifically, we begin by linearizing Uffink's $N \geq 3$ party quadratic Bell expressions in the following way,

$$\langle \mathcal{U}_N^M \rangle = \langle \mathcal{M}_N \rangle^2 + \langle \mathcal{M}'_N \rangle^2 = |\langle \mathcal{M}_N \rangle \pm i \langle \mathcal{M}'_N \rangle|^2. \quad (30)$$

This follows from the simple observation that for any two real numbers $x_1, x_2 \in \mathbb{R}$, $x_1^2 + x_2^2 = |x_1 \pm ix_2|^2$, and the fact that the N -party MABK operator \mathcal{M}_N and the N -party complementary MABK operator \mathcal{M}'_N are Hermitian, such that $\langle \mathcal{M}_N \rangle, \langle \mathcal{M}'_N \rangle \in \mathbb{R}$. This linearization reduces our problem to considering a linear but non-Hermitian operator, $\tilde{\mathcal{U}}_N$, of the form,

$$\begin{aligned} \tilde{\mathcal{U}}_N &= (\mathcal{M}_N \pm i\mathcal{M}'_N) \\ &= \frac{1}{2^{\frac{N-1}{2}}} \left(\frac{1-i}{\sqrt{2}}\right)^{(N-1) \bmod 2} \bigotimes_{j=1}^N (A^{(j)} + iA'^{(j)}), \end{aligned} \quad (31)$$

where the second equality is either satisfied by $\tilde{\mathcal{U}}_N = (\mathcal{M}_N + i\mathcal{M}'_N)$ or $\tilde{\mathcal{U}}_N = (\mathcal{M}_N - i\mathcal{M}'_N)$, depending on N , for instance, for $N \in \{2, 5, 6\}$ we have the former while for $N \in \{3, 4, 7\}$ we require the latter form of $\tilde{\mathcal{U}}_N$. With the linear operator in hand, we can now obtain the self-testing statement for \mathcal{U}_N^M , essentially by maximizing the modulo of the possibly complex expectation value of $\tilde{\mathcal{U}}_N$.

Theorem 7. In order to achieve maximal quantum violation of a N party Uffink's quadratic inequality, $\mathcal{U}_N^M = 2^{N-1}$, the parties must share a $N \geq 3$ qubit GHZ state $|GHZ_N\rangle = \frac{1}{\sqrt{2}}(|0\rangle^{\otimes N} + e^{i\phi(N)}|1\rangle^{\otimes N})$, where $\phi(N) \in [-\frac{\pi}{2}, \frac{\pi}{2}]$, and perform maximally anti-commuting projective measurements $A^{(j)} = \sigma_x$ and $A'^{(j)} = \sigma_y$ (up to local isometries).

Proof. From Lemma 2 and Theorem 4, without loss of generality, the local observables of any party \mathcal{A}_j , where $j \in \{1, \dots, N\}$, can be taken to be,

$$\begin{aligned} A^{(j)} &= \sigma_x, \\ A'^{(j)} &= \cos\theta_j\sigma_x + \sin\theta_j\sigma_y, \end{aligned} \quad (32)$$

acting on the effective two-dimensional subspace. This parametrization implies that Uffink's non-Hermitian operator [Eq. (31)], $\tilde{\mathcal{U}}_N$, has the following anti-diagonal matrix representation,

$$\tilde{\mathcal{U}}_N = \frac{1}{2^{\frac{N-1}{2}}} \text{adiag} \left(\begin{array}{c} \left(\frac{1-i}{\sqrt{2}}\right)^{(N-1) \bmod 2} \prod_{j=1}^N (1 + ie^{-i\theta_j}) \\ \vdots \\ \left(\frac{1-i}{\sqrt{2}}\right)^{(N-1) \bmod 2} \prod_{j=1}^N (1 + ie^{i\theta_j}) \end{array} \right), \quad (33)$$

where *adiag* represents a matrix with non-zero values only on the anti-diagonal. It is easy to see for any combination, $\forall j \in \{1, \dots, N\} : \theta_j = \pm\frac{\pi}{2}$, one of the anti-diagonal element attains the maximum absolute value of $2^{\frac{N-1}{2}}$ while the others vanish.

Since, $\tilde{\mathcal{U}}_N$ has an anti-diagonal matrix representation, we know that the eigenvectors of such anti-diagonal matrices are of the generic form, $\alpha \bigotimes_{j=1}^N |i_j\rangle + \beta \bigotimes_{j=1}^N |\bar{i}_j\rangle$, where $i_j \in \{0, 1\}$ and $\bar{i}_j = 1 \oplus i_j$. Now, taking the expectation value of \mathcal{M}_N with respect to any one of these states selects the sum of a pair of (equidistant from the top and the bottom) anti-diagonal elements. As each such pair is equivalent to the rest up-to local rotations, we can, without loss of any generality, consider the state, $|\psi_N\rangle = \alpha|0\rangle^{\otimes N} + \beta|1\rangle^{\otimes N}$, which effectively yields a weighted sum of the top and bottom anti-diagonal elements of the matrix [Eq. (33)],

$$\begin{aligned} \mathcal{U}_N^M &= |\langle \psi_N | \tilde{\mathcal{U}}_N | \psi_N \rangle| \\ &= \frac{1}{2^{\frac{N-1}{2}}} \left| \left(\bar{\alpha} \left(\frac{1-i}{\sqrt{2}}\right)^{(N-1) \bmod 2} \prod_{j=1}^N (1 + ie^{-i\theta_j}) \beta \right. \right. \\ &\quad \left. \left. + \bar{\beta} \left(\frac{1-i}{\sqrt{2}}\right)^{(N-1) \bmod 2} \prod_{j=1}^N (1 + ie^{i\theta_j}) \alpha \right) \right| \\ &\leq \frac{1}{2^{\frac{N-1}{2}}} |\alpha| |\beta| \left(\left| \left(\frac{1-i}{\sqrt{2}}\right)^{(N-1) \bmod 2} \prod_{j=1}^N (1 + ie^{-i\theta_j}) \right| \right. \\ &\quad \left. + \left| \left(\frac{1-i}{\sqrt{2}}\right)^{(N-1) \bmod 2} \prod_{j=1}^N (1 + ie^{i\theta_j}) \right| \right), \end{aligned} \quad (34)$$

where for the inequality we employed the fact that $\forall \alpha, \beta \in \mathbb{C} : |\alpha + \beta| \leq |\alpha| + |\beta|$. Observe that, as $|\alpha|^2 + |\beta|^2 = 1$, the maximum value of the above expression can only be attained for $|\alpha| = |\beta| = \frac{1}{\sqrt{2}}$, which picks out $|GHZ_N\rangle$ as the shared state, $|GHZ_N\rangle = \frac{1}{\sqrt{2}}(|0\rangle^{\otimes N} + e^{i\phi(N)}|1\rangle^{\otimes N})$. We note here that the relative phase $\phi(N) \in [-\frac{\pi}{2}, \frac{\pi}{2}]$ is left completely unspecified, a fact that we explore thoroughly at the end of the proof in the following Corollary 7.1. Consequently, we retrieve the following upper bound,

$$\begin{aligned} |\langle \psi_N | \tilde{\mathcal{U}}_N | \psi_N \rangle| &\leq \frac{1}{2^{\frac{N-1}{2}}} \left| \left(\left(\frac{1-i}{\sqrt{2}}\right)^{(N-1) \bmod 2} \prod_{j=1}^N (1 + ie^{-i\theta_j}) \right) \right. \\ &\quad \left. + \left| \left(\frac{1-i}{\sqrt{2}}\right)^{(N-1) \bmod 2} \prod_{j=1}^N (1 + ie^{i\theta_j}) \right| \right). \end{aligned} \quad (35)$$

Now, as $\left| \left(\frac{1-i}{\sqrt{2}}\right)^{(N-1) \bmod 2} \right| = 1$ and $|(1 + ie^{-i\theta_j})| = |2 \sin(\frac{\pi}{4} + \frac{\theta_j}{2})|$ and $|(1 + ie^{i\theta_j})| = |2 \cos(\frac{\pi}{4} + \frac{\theta_j}{2})|$, we can further upper bound the above expression as,

$$\begin{aligned} |\langle \psi_N | \tilde{\mathcal{U}}_N | \psi_N \rangle| &\leq 2^{\frac{N-1}{2}} \left(\prod_{j=1}^N |\sin(\frac{\pi}{4} + \frac{\theta_j}{2})| \right. \\ &\quad \left. + \prod_{j=1}^N |\cos(\frac{\pi}{4} + \frac{\theta_j}{2})| \right). \end{aligned}$$

As, $\forall j : |\sin(\frac{\pi}{4} + \frac{\theta_j}{2})| \leq 1, |\cos(\frac{\pi}{4} + \frac{\theta_j}{2})| \leq 1$, we can further upper bound the above expression by discarding all but three terms

corresponding to $\forall i, j, k \in \{1, \dots, N\}$, such that,

$$\begin{aligned} & |\langle \psi_N | \tilde{\mathcal{U}}_N | \psi_N \rangle| \\ & \leq 2^{\frac{N-1}{2}} \left(\left| \sin\left(\frac{2\theta_i+\pi}{4}\right) \sin\left(\frac{2\theta_j+\pi}{4}\right) \sin\left(\frac{2\theta_k+\pi}{4}\right) \right| \right. \\ & \quad \left. + \left| \cos\left(\frac{2\theta_i+\pi}{4}\right) \cos\left(\frac{2\theta_j+\pi}{4}\right) \cos\left(\frac{2\theta_k+\pi}{4}\right) \right| \right) \\ & \leq 2^{\frac{N-1}{2}}, \end{aligned} \quad (36)$$

where the proof of the second inequality has been deferred to the Supplementary information. In the Supplementary information, we also show that this inequality can only be saturated when $\theta_i = \theta_j = \theta_k = \frac{\pi}{2}$, i.e., when for each party the local observables maximally anti-commute. Moreover, as these settings maximize a unique pair of equidistant anti-diagonal entries, while the others vanish, the state must be of the form, $|\text{GHZ}_N\rangle \equiv \frac{1}{\sqrt{2}}(|0\rangle^{\otimes N} + e^{i\phi(N)}|1\rangle^{\otimes N})$, specified only up to the relative phase $\phi(N)$, up to auxiliary degrees of freedom on which the measurements act trivially, and local basis transformations. This further implies that the actual shared state could be of the form $|\text{GHZ}_N\rangle \otimes |\Psi\rangle$ with the arbitrary relative phase $\phi(N)$ of the GHZ state and the arbitrary state $|\Psi\rangle$ on auxiliary degrees of freedom which does not contribute to the operational Bell violation and thus is referred to as the junk state.

We would now like to highlight the difference between the self-testing statements for N partite linear MABK inequalities (Theorem 6 and Corollary 6.1) and Uffink's quadratic Bell inequalities (Theorem 7). Like the linear Bell inequalities, maximal violation of quadratic Bell inequalities fixes the local observables of each party to be maximally anti-commuting, such that without loss of generality they can be taken to be $A^{(i)} = \sigma_x$ and $A^{(j)} = \sigma_y$. However, while in the case of N partite linear MABK inequalities fixing the measurements exhausts all freedom up to local isometries and completely specifies the optimal state, on the other hand, the maximal violation of Uffink's quadratic inequalities does not uniquely specifies the optimal state. Specifically, the maximal violation of Uffink's quadratic inequalities can be attained with $|\text{GHZ}(\phi(N))\rangle$ where the relative phase $\phi(N)$ could take any value in $[-\frac{\pi}{2}, \frac{\pi}{2}]$. Hence, Uffink's quadratic inequalities do not strictly self-test. Below we show that strict self-testing statements can nevertheless be obtained for the complex-valued N partite Bell expression corresponding to the expectation value of Uffink's non-Hermitian operator $\langle \tilde{\mathcal{U}}_N \rangle$ [Eq. (31)] whenever the corresponding Uffink's quadratic Bell inequalities is maximally violated.

Until now, we have used our methodology to obtain self-testing statements for real valued linear and quadratic (on correlators) Bell expressions. We now discuss the case when our Bell expression takes complex values. Specifically, in the following Corollary, we obtain self-testing statements for the complex-valued Bell expression corresponding to the complex expectation value of $\langle \tilde{\mathcal{U}}_N \rangle$, where the operator $\tilde{\mathcal{U}}_N$ is defined in Eq. (31), using our methodology.

Corollary 7.1. In order to achieve extremal quantum value of the complex-valued Bell expression, $\langle \tilde{\mathcal{U}}_N \rangle = \langle \mathcal{M}_N \pm i \mathcal{M}'_N \rangle$, such that $|\langle \tilde{\mathcal{U}}_N \rangle| = 2^{\frac{N-1}{2}}$, the parties must share a $N \geq 3$ qubit GHZ state $|\text{GHZ}_N\rangle = \frac{1}{\sqrt{2}}(|0\rangle^{\otimes N} + e^{i\phi(N)}|1\rangle^{\otimes N})$, where $\phi(N) = \text{arccot}\left(\frac{\langle \mathcal{M}_N \rangle}{\langle \mathcal{M}'_N \rangle}\right)$ when N is odd, $\phi(N) = \text{arccot}\left(\frac{\langle \mathcal{M}_N \rangle}{\langle \mathcal{M}'_N \rangle}\right) - \frac{\pi}{4}$ when N is even and perform maximally anti-commuting projective measurements $A^{(i)} = \sigma_x$ and $A^{(j)} = \sigma_y$ (up to local isometries).

Proof. From Theorem 7, we know that the maximal quantum value of $\tilde{\mathcal{U}}_N^M = |\langle \tilde{\mathcal{U}}_N \rangle|^2 = 2^{N-1}$, self-tests the state to be maximally entangled N partite GHZ state, $|\text{GHZ}_N\rangle = \frac{1}{\sqrt{2}}(|0\rangle^{\otimes N} + e^{i\phi(N)}|1\rangle^{\otimes N})$,

where the relative phase $\phi(N)$ can be chosen arbitrarily. However, here we show that this relative phase $\phi(N)$ can still be operationally determined from the complex-valued Bell expression,

$$\langle \tilde{\mathcal{U}}_N \rangle = \langle \mathcal{M}_N \pm i \mathcal{M}'_N \rangle, \quad (37)$$

where $\langle \mathcal{M}_N \rangle$ and $\langle \mathcal{M}'_N \rangle$ are real valued complementary MABK Bell expressions for N parties, such that $|\langle \tilde{\mathcal{U}}_N \rangle|$ is $2^{\frac{N-1}{2}}$. We know that $|\langle \tilde{\mathcal{U}}_N \rangle| = 2^{\frac{N-1}{2}}$ implies that the local observables of each party can always be taken to be $A^{(i)} = \sigma_x$, $A^{(j)} = \sigma_y$, such that the operator $\tilde{\mathcal{U}}_N$ has the matrix representation [Eq. (33)]. Consequently,

$$\begin{aligned} \langle \tilde{\mathcal{U}}_N \rangle & = \langle \text{GHZ}_N | \tilde{\mathcal{U}}_N | \text{GHZ}_N \rangle \\ & = 2^{\frac{N-1}{2}} \left(\bar{\alpha} \left(\frac{1-i}{\sqrt{2}} \right)^{(N-1) \bmod 2} \beta \right) \end{aligned} \quad (38)$$

Up to experimentally indeterminate global phase, we can always take $\alpha = \frac{1}{\sqrt{2}}$ and $\beta = \frac{e^{i\phi}}{\sqrt{2}}$, such that Eq. (38) is simplified to,

$$\begin{aligned} \langle \tilde{\mathcal{U}}_N \rangle & = 2^{\frac{N-1}{2}} \left(\left(\frac{1-i}{\sqrt{2}} \right)^{(N-1) \bmod 2} e^{i\phi} \right) \\ & = \begin{cases} 2^{\frac{N-1}{2}} e^{i\phi}, & \text{iff } N \text{ is odd,} \\ 2^{\frac{N-1}{2}} e^{i(\phi - \frac{\pi}{4})}, & \text{else.} \end{cases} \end{aligned} \quad (39)$$

Next, with the aid of Eqs. (37) and (39), we can finally uniquely specify the relative phase $\phi(N)$ operationally. When $|\langle \tilde{\mathcal{U}}_N \rangle| = 2^{\frac{N-1}{2}}$ and the number of parties, N , is odd, the relative phase $\phi(N)$, must be precisely $\text{arccot}\left(\frac{\langle \mathcal{M}_N \rangle}{\langle \mathcal{M}'_N \rangle}\right)$, else $\phi(N) = \text{arccot}\left(\frac{\langle \mathcal{M}_N \rangle}{\langle \mathcal{M}'_N \rangle}\right) - \frac{\pi}{4}$ up to local isometries.

We note here that $\langle \tilde{\mathcal{U}}_N \rangle$, although complex, is an operational quantity, i.e., just like the value of linear Bell expressions, it can be directly estimated from the experimental statistics. Corollary 7.1 allows us to infer the relative phase $\phi(N)$ of the $N \geq 3$ qubit GHZ state from $\langle \tilde{\mathcal{U}}_N \rangle$. This fact is illustrated in Fig. 2.

Robust self-testing

The criterion for self-testing of a Bell inequality used in this work relies strongly on the assumption that the considered Bell expression attains its maximal value. However, in real experiments, this assumption cannot be fulfilled due to various experimental imperfections. Therefore, the self-testing statements must be made robust.

To make the self-testing statements obtained in this work robust, one can use the numerical SWAP method, which utilizes the Navascues-Pironio-Acin hierarchy to obtain bounds on the closeness (fidelity) of the experimental measurements and the shared state to the ideal self-testing measurements and state. Here we detail the technique for bounding the fidelity between the actual state and the reference self-testing state; the same can be applied to retrieve corresponding bounds for the measurements. The main idea of this technique relies on the notion of local isometries, which map the actual physical state $|\bar{\psi}\rangle$ to our reference self-testing state $|\psi\rangle$ and a junk state $|\Psi\rangle$ on local auxiliary systems. In most of the self-testing cases, these local isometries act as partial SWAP gates, essentially swapping the actual physical state $|\bar{\psi}\rangle$ with the state $|0\rangle^{\otimes N}$ of the registers, such that the final state of the registers corresponds to the reference self-testing state $|\psi\rangle$. It is often instructive to visualize the action of these local isometries as a SWAP circuit, which only depends on the self-testing measurements. The particulars of such a SWAP circuit, specifically those of the local isometries, enable us to express the fidelity, $\mathcal{F}_n = \langle \psi | \rho_{\text{SWAP}}(\Gamma_n) | \psi \rangle$, of the final state of the register $\rho_{\text{SWAP}}(\Gamma_n)$ with the target state $|\psi\rangle$, as a function of the entries of the necessarily positive semi-definite NPA moment matrix Γ_n of level $n \in \mathbb{N}$, as well as of the target self-testing state $|\psi\rangle$. As some of the entries of the moment matrix Γ_n correspond to

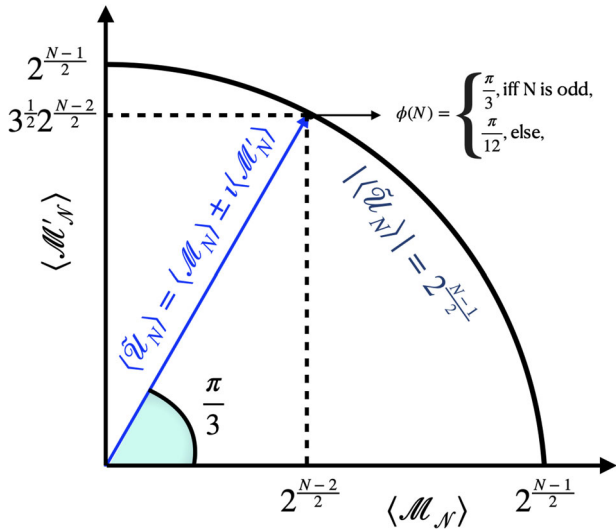


Fig. 2 Self-testing of the relative phase $\phi(N)$. This graphic schematically captures the self-testing statements for N partite Uffink’s quadratic Bell inequalities (Theorem 7), as well as the self-testing statements for the complex-valued Bell expressions corresponding to the mean value of Uffink’s non-Hermitian operator $\langle \tilde{\mathcal{U}}_N \rangle$ (Corollary 7.1). The figure depicts the complex plane on which the complex number $\langle \tilde{\mathcal{U}}_N \rangle = \langle \mathcal{M}_N \rangle \pm i \langle \mathcal{M}'_N \rangle$ lies, where $\langle \mathcal{M}_N \rangle$ is plotted on the real axis while $\langle \mathcal{M}'_N \rangle$ is plotted on the imaginary axis. The dark blue arc represents the boundary of the quantum set of correlations \mathcal{Q} characterized by the maximum violation of N partite Uffink’s quadratic Bell inequalities, $\mathcal{U}_N^M = |\langle \tilde{\mathcal{U}}_N \rangle|^2 = 2^{N-1}$. Crucially, for all points on the dark blue arc, Theorem 7 implies that the local observables of each party can be taken to be $A^{(j)} = \sigma_x$ and $A'^{(j)} = \sigma_y$, and the state to be maximally entangled N partite GHZ state, $|\text{GHZ}_N\rangle = \frac{1}{\sqrt{2}}(|0\rangle^{\otimes N} + e^{i\phi(N)}|1\rangle^{\otimes N})$, where the relative phase $\phi(N)$ can be chosen arbitrarily (up to local isometries). However, using Corollary 7.1, even the relative phase can be uniquely identified by the observed value of $\langle \tilde{\mathcal{U}}_N \rangle$ if it lies on this arc. To exemplify this, we plot the specific case of $\langle \tilde{\mathcal{U}}_N \rangle = \langle \mathcal{M}_N \rangle \pm i \langle \mathcal{M}'_N \rangle = 2^{\frac{N-2}{2}} e^{i\frac{\pi}{3}}$ (light blue arrow), which uniquely specifies the relative phase to be $\phi(N) = \arccot\left(\frac{\langle \mathcal{M}'_N \rangle}{\langle \mathcal{M}_N \rangle}\right) = \frac{\pi}{3}$ when N is odd, and $\phi(N) = \arccot\left(\frac{\langle \mathcal{M}'_N \rangle}{\langle \mathcal{M}_N \rangle}\right) - \frac{\pi}{4} = \frac{\pi}{12}$ when N is even.

experimental statistics, such as $[\Gamma_n]_{\bar{A}^{(1)}\bar{A}^{(2)}} = \langle \bar{\psi} | \bar{A}^{(1)} \bar{A}^{(2)} | \bar{\psi} \rangle$, the behavioral preconditions of a self-testing statement translate to linear constraints on the entries of the moment matrix Γ_n . Given a target self-testing state $|\psi\rangle$ and solving the consequent semi-definite minimization program with the fidelity, $\mathcal{F}_n = \langle \psi | \rho_{\text{SWAP}}(\Gamma_n) | \psi \rangle$ as the linear objective function, retrieves a converging sequence of lower bounds, $\mathcal{F}_1 \leq \mathcal{F}_2 \dots \mathcal{F}_n$ such that $\mathcal{F}_{n \rightarrow \infty} = \mathcal{F}$, where \mathcal{F} is the quantum fidelity.

In Fig. 3, we depict the SWAP circuit corresponding to the N party self-testing statements obtained in this work for MABK inequalities (Theorem 6), complimentary MABK inequalities (Corollary 6.1), Uffink’s quadratic inequalities (Theorem 7) and Uffink’s complex-valued Bell expressions (Corollary 7.1). As the self-testing measurements for all of these cases are the same, i.e., $A^{(j)} = \sigma_x$ and $A'^{(j)} = \sigma_y$, the circuit in Fig. 3 effectively swaps the actual state $|\bar{\psi}_N\rangle$ (which attains the respective preconditions of these self-testing statements) with the state $|0\rangle^{\otimes N}$ of the registers, such that the final state of the registers corresponds to their respective self-testing maximally entangled N partite GHZ state, $|\text{GHZ}_N\rangle = \frac{1}{\sqrt{2}}(|0\rangle^{\otimes N} + e^{i\phi(N)}|1\rangle^{\otimes N})$. This, in turn, allows us to retrieve a converging sequence of lower bounds on the fidelity, $\mathcal{F}_n = \langle \text{GHZ}_N | \rho_{\text{SWAP}}(\Gamma_n) | \text{GHZ}_N \rangle$, in the aforementioned fashion.

As the resultant semi-definite programs, although straightforward to implement^{22,23}, are too computationally hard to solve efficiently without additional symmetry-based simplifications, we leave this as a future direction.

We now highlight the advantage of Uffink’s quadratic Bell inequalities and Uffink’s complex-valued Bell expressions over the linear MABK inequalities for robust self-testing in noisy experimental scenarios. Heuristically, as Uffink’s quadratic Bell inequalities and Uffink’s complex Bell expressions take two experimentally observable quantities into account, namely, the value of linear MABK inequality, $\langle \mathcal{M}_N \rangle$, as well as the value of linear complementary MABK inequality $\langle \mathcal{M}'_N \rangle$, they provide more accurate robust self-testing than when the latter are considered on their own.

Specifically, consider an experiment E aimed at robust self-testing of the N qubit GHZ state using N party MABK Bell expression, $\langle \mathcal{M}_N \rangle$. Suppose that the experiment yields the value $\langle \mathcal{M}_N \rangle_E = 2^{\frac{N-1}{2}} - \epsilon$, the fidelity \mathcal{F}_1 of the experimental state with the N qubit GHZ state optimal for $\langle \mathcal{M}_N \rangle$ (Theorem 6) is proportional to $2^{\frac{N-1}{2}} - \epsilon$. However, the experimental imperfections will inevitably yield experimental behavior for which $\langle \mathcal{M}'_N \rangle_E \neq 0$. Consequently, the experimental behavior will always be closer to the extremal point which attains $\langle \tilde{\mathcal{U}}_N \rangle =$

$\frac{2^{\frac{N-1}{2}}}{\sqrt{\langle \mathcal{U}_N^M \rangle_E}} (\langle \mathcal{M}_N \rangle_E \pm i \langle \mathcal{M}'_N \rangle_E)$ as compared to the extremal point which attains $\langle \mathcal{M}_N \rangle = 2^{\frac{N-1}{2}}$ and $\langle \mathcal{M}'_N \rangle = 0$. Hence, the fidelity of the experimental state with the target GHZ state $|\text{GHZ}_N\rangle$ which realizes this extremal point (from Corollary 7.1) will yield a fidelity \mathcal{F}_2 proportional to $\sqrt{\langle \mathcal{U}_N^M \rangle_E} = \sqrt{(2^{\frac{N-1}{2}} - \epsilon)^2 + \langle \mathcal{M}'_N \rangle_E^2}$, such that, $\mathcal{F}_2 > \mathcal{F}_1$. Hence, in general taking into account, Uffink’s quadratic and complex-valued Bell expressions provide for a more accurate and robust DI self-testing of the N qubit GHZ state as compared to the MABK inequalities, especially in cases when the relative phase is irrelevant to the application and could be arbitrary.

Consequently, Uffink’s quadratic and complex-valued Bell expressions provide for a more accurate and robust DI characterization of quantum systems in multipartite Bell scenarios as compared to the MABK inequalities.

DISCUSSIONS

Quantum correlations that violate Bell inequalities can certify the shared entangled state and local measurements in an entirely device-independent manner. This feature of quantum non-local correlations is referred to as self-testing. In this work, we presented a simple and broadly applicable proof technique to obtain self-testing statements for the maximum quantum violation of a large relevant class of multipartite (involving an arbitrary number N of spatially separated parties) Bell inequalities. Unlike the relatively straightforward bipartite Bell scenarios, the multipartite scenarios are substantially richer in complexity owing to the various types of multipartite non-locality.

The traditionally employed sum-of-squares-like proof techniques rely on the Bell inequality’s specific structure and the hermiticity of the corresponding Bell operator. Moreover, we recall here that finding the sum-of-squares decomposition for a linear Bell expression is the semi-definite programming dual of finding the maximum quantum value of the Bell expression, which in turn can be cast as an instance of the moment-based formulation Navascues-Pironio-Acin hierarchy of semi-definite programming relaxations^{48,49}. It follows from this semi-definite programming duality that the level of the moment-based Navascues-Pironio-Acin hierarchy required for saturation of the maximal quantum value of a Bell expression corresponds to the degree of the

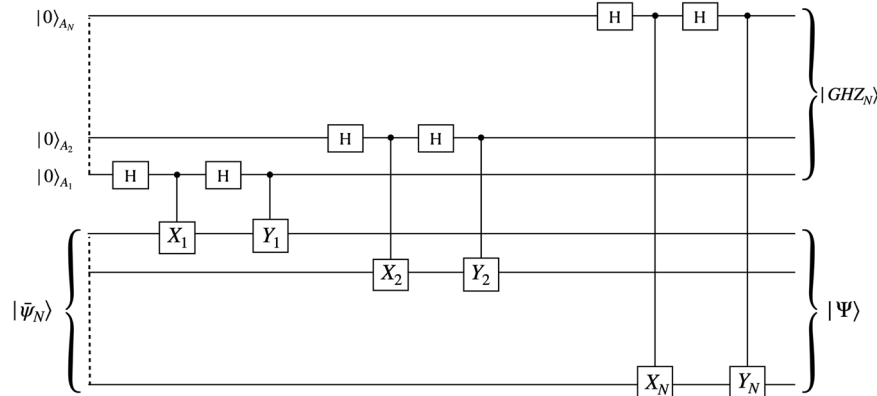


Fig. 3 Swap circuit. This graphic represents the partial SWAP gate isometry used to self-test maximally entangled N partite GHZ state $|\text{GHZ}_N\rangle = \frac{1}{\sqrt{2}}(|0\rangle^{\otimes N} + e^{i\phi(N)}|1\rangle^{\otimes N})$. After the application of the circuit, the $|\text{GHZ}_N\rangle$ state is extracted from the actual experimental state $|\tilde{\Psi}_N\rangle$ to the ancillary qubits. Here, H denotes a Hadamard gate, and $X_1, Y_1, X_2, Y_2, \dots, X_N, Y_N$ are the operators which act analogously to σ_x, σ_y on the actual state $|\tilde{\Psi}_N\rangle$. As the circuit only depends on the self-testing measurements, this circuit works for the N partite self-testing statements obtained in this work, namely, the self-testing statements for MABK inequalities (Theorem 6), complimentary MABK inequalities (Corollary 6.1), Uffink's quadratic inequalities (Theorem 7) and Uffink's complex-valued Bell expressions (Corollary 7.1). As the self-testing measurements for all of these cases are the same, i.e., $A^{(i)} = \sigma_x$ and $A^{(j)} = \sigma_y$, the circuit SWAPs the actual state $|\tilde{\Psi}_N\rangle$ (which attains the respective preconditions of these self-testing statements) with the state $|0\rangle^{\otimes N}$ of the registers, such that the final state of the registers corresponds to their respective self-testing maximally entangled N partite GHZ state.

polynomials in the sufficient sum-of-squares decomposition of the corresponding Bell operator. It is also easy to see that the minimum level $\lceil \frac{N}{2} \rceil$ of the moment-based Navascues-Pironio-Acin hierarchy degree required for the saturation of N party Bell inequalities, such as the MABK and the complimentary MABK family of Bell inequalities, increases with N , and so does the maximum degree of the polynomials in the corresponding sum-of-squares decomposition. Consequently, finding sum-of-squares decomposition becomes increasingly arduous for a large number N of spatially separated parties.

Although the Sum-of-Squares decomposition is applicable to any Bell scenario, more often than not, finding it can be challenging. In contrast, the technique presented in this paper offers a more state-forward approach. It is applicable to binary input and output Bell scenarios with an arbitrary number of spatially separated parties (N). It can derive self-testing statements for any Bell inequality in such Bell scenarios, as long as the associated Bell operator has an anti-diagonal matrix representation. In "Results: Characterizing local observables", we show that the observables of each party in two-setting binary outcome multipartite Bell scenarios can always be simultaneously represented as anti-diagonal matrices (Theorem 4). Consequently, in such scenarios, the Hermitian Bell operators corresponding to all Bell inequalities composed exclusively of N party correlators also have an anti-diagonal matrix representation. In "Results: Self-testing statements for multipartite inequalities", to demonstrate our proof technique, we obtain proofs of self-testing statements for the MABK family of N party inequalities (Theorem 6) (This constitutes a reproduction of the self-testing statements for MABK inequalities from ref. ³⁹, and hence serves as a preliminary certification of our proof technique.), followed by self-testing statements for the complimentary N party MABK inequalities (Corollary 6.1) and tripartite WWWZB inequalities ("Results: Tripartite WWWZB inequalities"). While the former self-testing statements demonstrate the relative simplicity and scalability (in the number of parties N) of our proof technique and serve as reliable benchmarks, the latter self-testing statements serve to exemplify all possible exceptions to perfect self-testing statements such as non-unique optimal states or observables, and non-anticommuting pairs of optimal measurements.

To further demonstrate the versatility of our proof technique which relies only on the anti-diagonal matrix representation of the

Bell operator and not even on its hermiticity, we obtain self-testing statements for Uffink's family of quadratic Bell inequalities (Theorem 7), as well as for the novel complex-valued Uffink's Bell expressions with corresponding non-Hermitian Bell operators (Corollary 7.1). As these quadratic and complex Bell expressions do not allow for sum-of-squares-like self-testing techniques, which rely on the linearity of the Bell expressions and on the hermiticity of the associated Bell operators, the self-testing statements obtained here form distinguishing applications of our proof technique.

One of the salient features of the multipartite self-testing statements obtained in this work, namely, for maximum quantum violation of MABK inequalities (Theorem 6), complimentary MABK inequalities (Corollary 6.1), Uffink's quadratic inequalities (Theorem 7) and extremal quantum values of Uffink's complex-valued Bell expressions (Corollary 7.1), is that they all uniquely single-out anti-commuting binary outcome observables for each party, which, without loss of generality, can be taken to be σ_x and σ_y , up to local isometries. On the other hand, these self-testing statements also pick out the maximally entangled N partite GHZ state $|\text{GHZ}_N\rangle = \frac{1}{\sqrt{2}}(|0\rangle^{\otimes N} + e^{i\phi(N)}|1\rangle^{\otimes N})$, where $\phi(N) \in [-\frac{\pi}{2}, \frac{\pi}{2}]$ is the relative phase. However, while the self-testing statements for the MABK and the complimentary MABK inequalities uniquely specify $\phi(N)$, the self-testing statements for Uffink's quadratic Bell inequalities do not uniquely specify the phase $\phi(N)$. These observations lead to the self-testing statements (Corollary 7.1) for the extremal values of the novel Uffink's complex-valued Bell expressions, which effectively summarize the former statements. Specifically, fixing the local observables of each party to be σ_x and σ_y , Corollary 7.1 brings forth the one-to-one correspondence between the experimentally accessible extremal values of Uffink's complex-valued Bell expressions and the relative phase $\phi(N)$ of the N partite GHZ state, essentially demonstrating the operational relevance of the latter.

The N -party MABK inequalities [Eq. (2)] form efficient witnesses of genuine N -partite non-locality and entanglement and hence find applications in tasks that require the participation of all parties, i.e., the tasks in which no subset of the parties can succeed without the others⁴⁷, for example, quantum secret sharing⁵⁰, social welfare games⁵¹, DI randomness generation and expansion⁵², and conference key distribution schemes^{53,54}. The advantage of the MABK inequalities over the other inequalities in N -partite DI information processing and cryptography task springs

from its permutational symmetry, which does not privilege one party at the expense of the other parties. Uffink's quadratic inequalities [Eq. (4)] and complex-valued Bell expression [Eq. (31)] also retain this permutational symmetry while being strictly better at witnessing genuine N -partite non-locality and entanglement. The DI information processing and cryptographic applications are essentially fueled by the characterization of the quantum devices, enabled by the values of respective Bell expressions, as exemplified by the self-testing statements presented in this work. Consequently, as Uffink's quadratic inequalities and complex-valued Bell expression allow for a more accurate and robust certification of quantum devices, using them instead of MABK in DI applications can only benefit the respective performance.

Note added: During the preparation of the current work, we have become aware of ref. ⁵⁵. While it presents similar results, our proof technique, which constitutes the main conceptual contribution of this work, is substantially different from their proof technique. In particular, the key contrasting feature of our proof technique is its applicability to non-linear Bell inequalities.

DATA AVAILABILITY

Data accessibility is not applicable to this manuscript.

Received: 1 March 2022; Accepted: 21 June 2023;

Published online: 17 July 2023

REFERENCES

- Bell, J. S. On the Einstein Podolsky Rosen paradox. *Phys. Phys. Fiz.* **1**, 195–200 (1964).
- Brunner, N. et al. Bell nonlocality. *Rev. Mod. Phys.* **86**, 419–478 (2014).
- Hensen, B. et al. Loophole-free Bell inequality violation using electron spins separated by 1.3 kilometres. *Nature* **526**, 682–686 (2015).
- Giustina, M. et al. Significant-loophole-free test of Bell's theorem with entangled photons. *Phys. Rev. Lett.* **115**, 250401 (2015).
- Shalm, L. K. et al. Strong loophole-free test of local realism. *Phys. Rev. Lett.* **115**, 250402 (2015).
- Vazirani, U. & Vidick, T. Fully device-independent quantum key distribution. *Phys. Rev. Lett.* **113**, 140501 (2014).
- Acín, A., Gisin, N. & Masanes, L. From Bell's theorem to secure quantum key distribution. *Phys. Rev. Lett.* **97**, 120405 (2006).
- Colbeck, R. Quantum and relativistic protocols for secure multi-party computation Preprint at <https://doi.org/10.48550/arXiv.0911.3814> (2011).
- Ekert, A. & Renner, R. The ultimate physical limits of privacy. *Nature* **507**, 443–447 (2014).
- Ekert, A. K. Quantum cryptography based on Bell's theorem. *Phys. Rev. Lett.* **67**, 661–663 (1991).
- Mayers, D. & Yao, A. Self testing quantum apparatus. *Quantum Inf. Comput.* **4**, 273–286 (2004).
- Mayers, D. & Yao, A. Quantum cryptography with imperfect apparatus. In *Proc. 39th Annual Symposium on Foundations of Computer Science (Cat. No.98CB36280)*, 503–509 (1998).
- Šupić, I. & Bowles, J. Self-testing of quantum systems: a review. *Quantum* **4**, 337 (2020).
- Colbeck, R. & Kent, A. Private randomness expansion with untrusted devices. *J. Phys. A Math. Theor.* **44**, 095305 (2011).
- Gheorghiu, A., Kapourniotis, T. & Kashefi, E. Verification of quantum computation: an overview of existing approaches. *Theory Comput. Syst.* **63**, 715–808 (2019).
- Bowles, J., Šupić, I., Cavalcanti, D. & Acín, A. Self-testing of Pauli observables for device-independent entanglement certification. *Phys. Rev. A* **98**, 042336 (2018).
- Sekatski, P., Bancal, J.-D., Wagner, S. & Sangouard, N. Certifying the building blocks of quantum computers from Bell's theorem. *Phys. Rev. Lett.* **121**, 180505 (2018).
- McKague, M. Self-testing graph states. *Theory of Quantum Computation, Communication, and Cryptography*, 104–120 (Springer, 2014).
- Greenberger, D. M., Zeilinger, A. & Horne, M. A. Going beyond Bell's theorem. *Bell's Theorem, Quantum Theory and Conceptions of the Universe* (ed Kafatos, M.) 73–76 (Kluwer Academic, 1989).
- Baccari, F., Augusiak, R., Šupić, I., Tura, J. & Acín, A. Scalable bell inequalities for qubit graph states and robust self-testing. *Phys. Rev. Lett.* **124**, 020402 (2020).
- Pál, K. F., Vértesi, T. & Navascués, M. Device-independent tomography of multipartite quantum states. *Phys. Rev. A* **90**, 042340 (2014).
- Bancal, J.-D., Navascués, M., Scarani, V., Vértesi, T. & Yang, T. H. Physical characterization of quantum devices from nonlocal correlations. *Phys. Rev. A* **91**, 022115 (2015).
- Yang, T. H., Vértesi, T., Bancal, J.-D., Scarani, V. & Navascués, M. Robust and versatile black-box certification of quantum devices. *Phys. Rev. Lett.* **113**, 040401 (2014).
- Wu, X. et al. Robust self-testing of the three-qubit W state. *Phys. Rev. A* **90**, 042339 (2014).
- Fadel, M. Self-testing Dicke states. Preprint at <https://doi.org/10.48550/arXiv.1707.01215> (2017).
- Šupić, I., Coladangelo, A., Augusiak, R. & Acín, A. Self-testing multipartite entangled states through projections onto two systems. *New J. Phys.* **20**, 083041 (2018).
- Buhrman, H. & Massar, S. Causality and Tsirelson's bounds. *Phys. Rev. A* **72**, 052103 (2005).
- Hayashi, M. & Hajdušek, M. Self-guaranteed measurement-based quantum computation. *Phys. Rev. A* **97**, 052308 (2018).
- Bamps, C. & Pironio, S. Sum-of-squares decompositions for a family of Clauser-Horne-Shimony-Holt-like inequalities and their application to self-testing. *Phys. Rev. A* **91**, 052111 (2015).
- Ardehali, M. Bell inequalities with a magnitude of violation that grows exponentially with the number of particles. *Phys. Rev. A* **46**, 5375–5378 (1992).
- Belinskii, A. V. & Klyshko, D. N. Interference of light and Bell's theorem. *Phys. Usp.* **36**, 653–693 (1993).
- Werner, R. F. & Wolf, M. M. All-multipartite Bell-correlation inequalities for two dichotomic observables per site. *Phys. Rev. A* **64**, 032112 (2001).
- Weinfurter, H. & Żukowski, M. Four-photon entanglement from down-conversion. *Phys. Rev. A* **64**, 010102 (2001).
- Żukowski, M. & Brukner, I. C. V. Bell's theorem for general n -qubit states. *Phys. Rev. Lett.* **88**, 210401 (2002).
- Uffink, J. Quadratic bell inequalities as tests for multipartite entanglement. *Phys. Rev. Lett.* **88**, 230406 (2002).
- Scarani, V. The device-independent outlook on quantum physics. *Acta Phys.* **62**, 347 (2012).
- Żukowski, M. & Brukner, I. C. V. Bell's theorem for general n -qubit states. *Phys. Rev. Lett.* **88**, 210401 (2002).
- Mermin, N. D. Extreme quantum entanglement in a superposition of macroscopically distinct states. *Phys. Rev. Lett.* **65**, 1838 (1990).
- Kaniewski, J. M. K. Self-testing of binary observables based on commutation. *Phys. Rev. A* **95**, 062323 (2017).
- Pál, K. F., Vértesi, T. & Navascués, M. Device-independent tomography of multipartite quantum states. *Phys. Rev. A* **90**, 042340 (2014).
- Kaniewski, J. Analytic and nearly optimal self-testing bounds for the Clauser-Horne-Shimony-Holt and Mermin inequalities. *Phys. Rev. Lett.* **117**, 070402 (2016).
- Ponomarenko, V. & Selstad, L. Eigenvalues of the sum and product of anti-commuting matrices. *J. Math.* **13**, 625–632 (2020).
- Pironio, S. et al. Device-independent quantum key distribution secure against collective attacks. *New J. Phys.* **11**, 045021 (2009).
- Irfan, A. A. M., Mayer, K., Ortiz, G. & Knill, E. Certified quantum measurement of Majorana fermions. *Phys. Rev. A* **101**, 032106 (2020).
- Pitowsky, I. & Svozil, K. Optimal tests of quantum nonlocality. *Phys. Rev. A* **64**, 014102 (2001).
- Śliwa, C. Symmetries of the Bell correlation inequalities. *Phys. Rev. Lett.* **317**, 165–168 (2003).
- Sami, S., Chakrabarty, I. & Chaturvedi, A. Complementarity of genuine multipartite Bell nonlocality. *Phys. Rev. A* **96**, 022121 (2017).
- Navascués, M., Pironio, S. & Acín, A. A convergent hierarchy of semidefinite programs characterizing the set of quantum correlations. *New J. Phys.* **10**, 073013 (2008).
- Ioannou, M. & Rosset, D. Noncommutative polynomial optimization under symmetry. Preprint at <https://doi.org/10.48550/arXiv.2112.10803> (2021).
- Hillery, M., Bužek, V. & Berthiaume, A. Quantum secret sharing. *Phys. Rev. A* **59**, 1829–1834 (1999).
- Banik, M. et al. Two-qubit pure entanglement as optimal social welfare resource in Bayesian game. *Quantum* **3**, 185 (2019).
- Grasselli, F., Murta, G., Kampermann, H. & Bruß, D. Entropy bounds for multiparty device-independent cryptography. *PRX Quantum* **2**, 010308 (2021).
- Murta, G., Grasselli, F., Kampermann, H. & Bruß, D. Quantum conference key agreement: a review. *QUTE* **3**, 2000025 (2020).
- Grasselli, F., Murta, G., Kampermann, H. & Bruß, D. Boosting device-independent cryptography with tripartite nonlocality. *Quantum* **7**, 980 (2023).
- Sarkar, S. & Augusiak, R. Self-testing of multipartite Greenberger-Horne-Zeilinger states of arbitrary local dimension with arbitrary number of measurements per party. *Phys. Rev. A* **105**, 032416 (2022).

ACKNOWLEDGEMENTS

We would like to thank Anubhav Chaturvedi, Nicolás Gigena, and Marek Żukowski for insightful discussions. This work is supported by the Institute of Information & Communications Technology Planning & Evaluation (IITP) grant funded by the Korean government (MSIT) (No.2022-0-00463, Development of a quantum repeater in optical fiber networks for quantum internet). E.P. acknowledges partial support by NCBiR through QuantEra grant (No. 2/2020), and P.P. acknowledges support by NCN SONATA-BIS grant No. 2017/26/E/ST2/01008.

AUTHOR CONTRIBUTIONS

All authors equally contributed to the conceptualization and preparation of the manuscript.

COMPETING INTERESTS

The authors declare no competing interests.

ADDITIONAL INFORMATION

Supplementary information The online version contains supplementary material available at <https://doi.org/10.1038/s41534-023-00735-3>.

Correspondence and requests for materials should be addressed to Ekta Panwar.

Reprints and permission information is available at <http://www.nature.com/reprints>

Publisher's note Springer Nature remains neutral with regard to jurisdictional claims in published maps and institutional affiliations.



Open Access This article is licensed under a Creative Commons Attribution 4.0 International License, which permits use, sharing, adaptation, distribution and reproduction in any medium or format, as long as you give appropriate credit to the original author(s) and the source, provide a link to the Creative Commons license, and indicate if changes were made. The images or other third party material in this article are included in the article's Creative Commons license, unless indicated otherwise in a credit line to the material. If material is not included in the article's Creative Commons license and your intended use is not permitted by statutory regulation or exceeds the permitted use, you will need to obtain permission directly from the copyright holder. To view a copy of this license, visit <http://creativecommons.org/licenses/by/4.0/>.

© The Author(s) 2023

Robust self-testing of Bell inequalities tilted for maximal loophole-free nonlocality

Nicolas Gigena,¹ Ekta Panwar,^{2,3} Giovanni Scala,^{4,3} Mateus Araújo,⁵ Máté Farkas,⁶ and Anubhav Chaturvedi^{7,*}

¹IFLP/CONICET–Departamento de Física, Universidad Nacional de La Plata, C.C. 67, La Plata (1900), Argentina

²Institute of Theoretical Physics and Astrophysics, Faculty of Mathematics, Physics and Informatics, University of Gdańsk, ul. Wita Stwosza 57, 80-308 Gdańsk, Poland

³International Centre for Theory of Quantum Technologies, University of Gdańsk, 80-308 Gdańsk, Poland

⁴Dipartimento Interateneo di Fisica, Politecnico di Bari, 70126 Bari, Italy

⁵Departamento de Física Teórica, Atómica y Óptica, Universidad de Valladolid, 47011 Valladolid, Spain

⁶Department of Mathematics, University of York, Heslington, York, YO10 5DD, United Kingdom

⁷Faculty of Applied Physics and Mathematics, Gdańsk University of Technology, Gabriela Narutowicza 11/12, 80-233 Gdańsk, Poland

The degree of experimentally attainable nonlocality, as gauged by the amount of loophole-free violation of Bell inequalities, remains severely limited due to inefficient detectors. We address an experimentally motivated question: Which quantum strategies attain the maximal loophole-free nonlocality in the presence of inefficient detectors? For *any* Bell inequality and *any* specification of detection efficiencies, the optimal strategies are those that maximally violate a *tilted* version of the Bell inequality in ideal conditions. In the simplest scenario, we demonstrate that the quantum strategies that maximally violate the tilted versions of *Clauser-Horne-Shimony-Holt* inequality are *unique* up to local isometries. However, self-testing via the standard sum of squares decomposition method turns out to be analytically intractable since even high levels of the *Navascués–Pironio–Acín* hierarchy are insufficient to saturate the maximum quantum violation of these inequalities. Instead, we utilize a novel Jordan’s lemma-based proof technique to obtain robust *analytical* self-testing statements for the *entire* family of tilted-Bell inequalities. These results allow us to unveil intriguing aspects of the effect of inefficient detectors and the complexity of characterizing the set of quantum correlations, in the simplest Bell scenario.

I. INTRODUCTION

Correlations born of local measurements performed on entangled quantum systems shared between distant observers resist local-causal explanations, a phenomenon known as *Bell nonlocality* [1, 2]. Apart from their foundational significance, nonlocal correlations enable several classically impossible information processing and cryptographic feats such as unconditionally secure Device-Independent Quantum Key Distribution (DIQKD) [3–7]. The efficacy of these applications relies on loophole-free certification of strong nonlocal correlations. In particular the *detection loophole*, which results of performing a Bell test with inefficient detectors, is the most persistent obstacle in the experimental realization of strong long-range loophole-free nonlocal correlations.

The detection efficiency of a measuring party is the ratio of particles detected to the total number of particles emitted by the source. The effective detection efficiency η depends on the detectors and the device’s distance from the source. For instance, in photonic Bell experiments, the effective detection efficiency decays exponentially with the length of the optical fiber, l , such that $\eta = \eta_0 10^{-\frac{\alpha l}{10}}$, where η_0 is the detection efficiency of the measuring apparatus due to the use of imperfect detectors, and α is the attenuation coefficient [8]. Closing the detection loophole in Bell experiments amounts to having an effective detection efficiency η higher than

a threshold value η^* , referred to as the *critical detection efficiency*. Typically, η^* is a characteristic of an ideal nonlocal correlation, below which it ceases to be nonlocal, and limits the distance across which nonlocality can be operationally certified to $l < \frac{10}{\alpha} \log\left(\frac{\eta^*}{\eta_0}\right)$.

In the simplest bipartite Bell scenario, the quantum strategy maximally violating the *Clauser-Horne-Shimony-Holt* (CHSH) inequality (in ideal conditions) ceases to yield nonlocal correlations for detector efficiencies below $\eta^* = 2\sqrt{2} - 2 \simeq 0.82$ [9]. However, for an almost product entangled state, this threshold efficiency can be lowered to $2/3 \simeq 0.66$ [10], which comes at the cost of very low robustness to background noise. Significant research efforts have been directed towards minimizing the critical detection efficiency requirement for loophole-free certification of nonlocality [11–14]. However, for real-world applications to be effective, mere violation of a Bell inequality is insufficient [15]. Instead, the efficacy of such applications [14] typically requires high degree of nonlocality and motivates the question:

Which quantum strategies yield the maximum loophole-free nonlocality in the presence of inefficient detectors?

As the extent of the violation of a (facet) Bell inequality corresponds to the distance of a nonlocal correlation from a facet of the local polytope, it translates to a reliable measure of nonlocality. Thus the question above boils down to finding the quantum strategies that yield the maximal loophole-free violation of a given Bell inequality for specified detection efficiencies. Since the

* anubhav.chaturvedi@pg.edu.pl

use of inefficient detectors results in the occurrence of “no-click” events, to decide whether a given inequality is violated these events must be included in the measurement statistics. The most general way to deal with them is to treat them as an additional outcome, which comes at the price of enlarging the Bell scenario. However, to analyse the violation of a given Bell inequality, we need to consider post-processing strategies which do not alter the Bell scenario. One such experimentally convenient post-processing, which avoids considering additional outcomes as well as the fair-sampling assumption, is to assign a valid outcome to the “no-click” event [16]. Moreover, such local *assignment* strategies were proven to be optimal in the CHSH scenario [17].

We use the assignment strategies described above to show that the quantum state and measurements maximally violating a given Bell inequality, in the presence of inefficient detectors, correspond to those maximally violating, in ideal conditions, a tilted version of the inequality. In the simplest Bell scenario, where up to a re-labeling of measurements and outcomes the only facet inequality is the CHSH inequality, attaining maximal loophole-free nonlocality amounts to maximally violating a doubly-tilted version of CHSH. Such inequalities can be thought of as a generalization of the ones considered in Ref. [18, 19], which correspond to the case of one party having access to ideal detectors, and for which both the maximal violation and the quantum realization attaining it are known. In fact, in Ref. [18] it is shown by means of *sum-of-squares* (SOS) decompositions that the optimal state and measurements are unique up to local unitaries, i.e., the maximal violation *self-tests* the optimal quantum strategy.

These self-testing results suggest that analogous results could be derived for the general doubly-tilted CHSH inequalities. However, for this general case self-testing via the standard SOS decomposition methods used in [18] turns out to be analytically intractable. On one hand, unlike the case of one imperfect detector, both the maximal quantum violation and the realization attaining it have a more intricate dependence on the detection efficiencies. This complexity translates to the coefficients of the polynomials in a tight SOS decomposition. On the other hand, most strikingly, for the general case, even higher levels (up to level 10) of the Navascués–Pironio–Acín (NPA) hierarchy are not enough to saturate the maximal violation of the doubly-tilted CHSH inequalities. This result highlights the complexity of characterizing the quantum set of correlations even in the simplest Bell scenario. In particular, as the degree of the polynomials in a tight SOS decomposition corresponds to the level of a tight NPA upper bound, finding such polynomials becomes a hard task.

Instead, we derive *analytical* self-testing statements and optimal quantum strategies for the entire family of doubly-tilted CHSH inequalities as a function of detection efficiencies, via a novel proof technique based on Gröbner basis reduction and Jordan’s lemma (Chapter

VII [20]). We find that the optimal quantum strategy entails a partially entangled two-qubit state and non-maximally incompatible observables for both parties. In particular, in contrast to the case of one imperfect detector, in general, the optimal observables of a party also depend on the detection efficiency of the other party. The analytical results allow us to reveal intriguing aspects of the set of quantum correlations in the simplest Bell scenario. Finally, we numerically demonstrate the robustness of these self-testing statements. We conclude by enlisting several implications of our findings to device independent processing with inefficient detectors and to the complexity of characterization of the set of quantum correlations.

II. NONLOCALITY WITH IMPERFECT DETECTORS

In this section we discuss how nonlocal correlations can be detected via violation of a Bell inequality in presence of non-ideal detectors. Building on these observations, we show that maximising the effective violation of a Bell inequality in the presence of imperfect detectors amounts to maximally violating a tilted version of the inequality in ideal conditions.

Consider a bipartite Bell experiment involving two parties, Alice and Bob. In each round of such experiment a source distributes a composite physical system to be shared between Alice and Bob. Alice performs one out of m_A possible measurements that we label with x , each of which has d_A possible outcomes labeled by a . Bob performs one out of m_B possible measurements, labeled by y , which results in one out of d_B outcomes, labeled by b . Together, the tuple (m_A, m_B, d_A, d_B) uniquely specifies a bipartite Bell scenario. In what follows we will denote by $p(ab|xy)$ the probability of Alice and Bob obtaining outcomes a and b conditioned on performing measurements x and y , respectively. We also denote by $\mathbf{p} \in \mathbb{R}^{m_A d_A m_B d_B}$, the vectors with entries $p(ab|xy)$, commonly referred to as a *behavior*.

Let us now recall that for any Bell scenario, the set \mathcal{L} of behaviors admitting local-causal explanations forms a convex polytope. The vertices of \mathcal{L} are local deterministic behaviors [21], for which $p(ab|xy) = p_A(a|x)p_B(b|y)$, with marginals $p_A(a|x), p_B(b|y) \in \{0, 1\}$. While any behavior \mathbf{p} in \mathcal{L} admits a quantum realization, i.e., there exists quantum strategies entailing a bipartite quantum state $\hat{\rho}_{AB}$ and local quantum measurement operators $\{\hat{M}_a^x, \hat{N}_b^y\}$ such that,

$$p(ab|xy) = \text{Tr} \left(\hat{\rho}_{AB} \hat{M}_a^x \otimes \hat{N}_b^y \right) \quad \forall a, b, x, y, \quad (1)$$

the converse does not hold. Specifically, there are behaviors admitting a quantum realization that cannot be expressed as a convex combination of local deterministic behaviors. Therefore, the set \mathcal{Q} of quantum behaviors strictly contains the local set, $\mathcal{L} \subset \mathcal{Q}$. We say that a quantum behavior \mathbf{p} is nonlocal if $\mathbf{p} \in \mathcal{Q} \setminus \mathcal{L}$.

Each facet of \mathcal{L} is associated with an inequality of the form

$$\beta(\mathbf{p}) := \sum_{a,b,x,y} c_{ab}^{xy} p(ab|xy) \leq \beta_{\mathcal{L}}, \quad (2)$$

with $c_{ab}^{xy}, \beta_{\mathcal{L}} \in \mathbb{R}$, which is satisfied by all local behaviors.

It follows then that a nonlocal behavior \mathbf{p} must violate at least one of these facet Bell inequalities, with the amount of the violation, $\beta(\mathbf{p}) - \beta_{\mathcal{L}}$, related to the distance of \mathbf{p} to the corresponding facet, which can be thought of as a measure on nonlocality [22].

Note that, up to this point, the experimental setups have been assumed to be ideal. In particular, the detectors are perfect as they always detect an incoming quantum system. In actual experiments, however, detectors are not perfect and will sometimes fail to click, which results in the occurrence of "no-click" events that so far were not considered in the measurement statistics. We describe in the following the effect of imperfect detectors on nonlocal quantum behaviors in Bell experiments, and in particular, on the violation of Bell inequalities.

The most general way of accounting for a "no-click" event is to consider it an additional outcome, say Φ , of the measurement, which enlarges the Bell scenario to $(m_A, m_B, d_A + 1, d_B + 1)$, significantly increasing the complexity of characterizing the sets \mathcal{L}, \mathcal{Q} . We can avoid this problem and the fair-sampling assumption, while remaining in the same scenario, by using a more convenient post-processing which assigns a pre-existing outcome to each "no-click" event. Besides the experimental benefits of a smaller Bell scenario, this method is well-suited for our purposes, since we are interested in gauging the effect of imperfect detectors on the value of a given Bell inequality and retrieving the optimal quantum strategies.

Let us suppose that Alice's and Bob's measurement devices click with efficiencies $\eta_A, \eta_B < 1$, respectively. Whenever Alice's device fails to click she assigns a pre-existing outcome a with probability $q_A(a|x)$. Similarly, Bob assigns b with probability $q_B(b|y)$ whenever his device fails to click. Together, the vector of probabilities $q(ab|xy) = q_A(a|x)q_B(b|y)$ specify a *local assignment strategy* \mathbf{q} . Let $p(ab|xy)$ be the *ideal* joint probabilities, then the *effective* measurement statistics $\tilde{p}(ab|xy)$ are determined by,

$$\begin{aligned} \tilde{p}(ab|xy) &= \eta_A \eta_B p(ab|xy) + \eta_A (1 - \eta_B) p_A(a|x) q_B(b|y) \\ &\quad + (1 - \eta_A) \eta_B q_A(a|x) p_B(b|y) \\ &\quad + (1 - \eta_A) (1 - \eta_B) q_A(a|x) q_B(b|y). \end{aligned} \quad (3)$$

Hence, for *any* local assignment strategy \mathbf{q} , the effect of inefficient detectors is a linear map $\tilde{\mathbf{p}} = \Omega_{\eta_A \eta_B}(\mathbf{p})$ such that,

$$\begin{aligned} \tilde{\mathbf{p}} &= \Omega_{\eta_A \eta_B}(\mathbf{p}) = \eta_A \eta_B \mathbf{p} + \eta_A (1 - \eta_B) \mathbf{p}^A \\ &\quad + (1 - \eta_A) \eta_B \mathbf{p}^B + (1 - \eta_A) (1 - \eta_B) \mathbf{q}, \end{aligned} \quad (4)$$

where the effective behavior $\tilde{\mathbf{p}}$ has entries $\tilde{p}(ab|xy)$, and the vectors $\mathbf{p}^A, \mathbf{p}^B$ linearly depend on the ideal marginal probabilities $p_A(a|x), p_B(b|y)$, and have entries $p_A(a|x)q_B(b|y), q_A(a|x)p_B(b|y)$, respectively, for *any* η_A, η_B and \mathbf{q} . Consequently, by linearity, the value of a given Bell functional β over this effective behavior takes the form,

$$\begin{aligned} \beta(\tilde{\mathbf{p}}) &= \eta_A \eta_B \beta(\mathbf{p}) + \eta_A (1 - \eta_B) \beta(\mathbf{p}^A) + (1 - \eta_A) \eta_B \beta(\mathbf{p}^B) \\ &\quad + (1 - \eta_A) (1 - \eta_B) \beta(\mathbf{q}). \end{aligned} \quad (5)$$

Since locally assigning a pre-existing outcome to the "no-click" is essentially a local post-processing, it cannot increase the local bound of a Bell inequality $\beta(\mathbf{p}) \leq \beta_{\mathcal{L}}$ (2). Hence, a Bell experiment with inefficient detectors is said to possess loophole-free nonlocality, if the effective behavior $\tilde{\mathbf{p}}$ violates the same Bell inequality, i.e.,

$$\beta(\tilde{\mathbf{p}}) \leq \beta_{\mathcal{L}}. \quad (6)$$

Consequently, we naturally arrive at the question of determining the maximum achievable loophole-free violation, $\beta(\tilde{\mathbf{p}}) - \beta_{\mathcal{L}}$, for a given Bell inequality. Note that the optimization problem involved in the computation of this maximal violation is twofold, since we need two optimize over both local assignments and quantum strategies. In the next Lemma, we greatly simplify this problem by showing that the optimal assignment strategy is necessarily deterministic, which results in a family of tilted Bell inequalities whose maximal violation in ideal circumstances corresponds to the maximum loophole-free violation of the Bell inequality in presence of inefficient detectors.

Lemma 1. *Consider a Bell experiment with inefficient detection with efficiencies η_A, η_B . For any given Bell inequality $\beta(\mathbf{p}) \leq \beta_{\mathcal{L}}$ (2), the optimal quantum strategies which yield the maximum loophole-free violation of the Bell inequality (6) are those that maximally violate a tilted Bell inequality of the form,*

$$\begin{aligned} \beta_{\eta_A \eta_B}(\mathbf{p}) &= \beta(\mathbf{p}) + \frac{1 - \eta_B}{\eta_B} \sum_{a,x} c_a^x p_A(a|x) \\ &\quad + \frac{1 - \eta_A}{\eta_A} \sum_{b,y} c_b^y p_B(b|y) \\ &\leq \frac{\beta_{\mathcal{L}}}{\eta_A \eta_B} - \frac{1 - \eta_A}{\eta_A} \frac{1 - \eta_B}{\eta_B} \left(\sum_{x,y} c_{a_x b_y}^{x,y} \right), \end{aligned} \quad (7)$$

where $p_A(a|x), p_B(b|y)$ are the ideal marginal probabilities of Alice and Bob, respectively, $q_A(a|x) = \delta_{a,a_x}, q_B(b|y) = \delta_{b,b_y}$ represent deterministic assignment strategies, and $c_a^x = \sum_y c_{a b_y}^{x,y}$ and $c_b^y = \sum_x c_{a_x b}^{x,y}$. The loophole-free value $\beta(\tilde{\mathbf{p}})$ of the Bell functional (5) is related to value of the Bell functional $\beta_{\eta_A \eta_B}(\mathbf{p})$ in the following way,

$$\beta(\tilde{\mathbf{p}}) = \eta_A \eta_B \beta_{\eta_A \eta_B}(\mathbf{p}) + (1 - \eta_A) (1 - \eta_B) \left(\sum_{x,y} c_{a_x b_y}^{x,y} \right). \quad (8)$$

Proof. Let us plug in the expression of the effective value of the Bell inequality (5) into (6) to obtain the Bell inequality,

$$\begin{aligned} \beta(\tilde{\mathbf{p}}) &= \eta_A \eta_B \beta(\mathbf{p}) + \eta_A (1 - \eta_B) \beta(\mathbf{p}^A) \\ &\quad + (1 - \eta_A) \eta_B \beta(\mathbf{p}^B) + (1 - \eta_A) (1 - \eta_B) \beta(\mathbf{q}) \\ &\leq \beta_{\mathcal{L}}. \end{aligned} \quad (9)$$

Now, for given detection efficiencies, η_A, η_B , to maximise the value of the Bell functional in (9), we need to optimize the ideal quantum behavior $\mathbf{p} \in \mathcal{Q}$ as well as the optimal local assignment strategy $\mathbf{q} \in \mathcal{L}$ for mitigating the “no-click” events. Because the latter is a local post-processing, the optimal assignment strategy can always be taken to be a local-deterministic strategy, wherein, $q_A(a|x) = \delta_{a,a_x}$ and $q_B(b|y) = \delta_{b,b_y}$ with $a_x \in \{0, \dots, d_A - 1\}$ and $b_y \in \{0, \dots, d_B - 1\}$. Plugging in the optimal deterministic assignment strategy (9), and moving the behavior independent terms to the right side, yields the tilted Bell inequality (7) on the ideal behavior as well as the relation (8). \square

Lemma 1 reduces the problem of retrieving the maximum quantum loophole-free violation for *any* given Bell inequality (2) to finding the maximum violation of the corresponding tilted Bell inequality with ideal detectors (6)¹. Specifically, for given efficiencies η_A, η_B , and a given local deterministic assignment strategy a_x, b_y , we need to optimize over quantum behaviors $\mathbf{p} \in \mathcal{Q}$ to find the maximum violation of the tilted Bell inequality (7), which can be tackled with standard numerical methods (such as the NPA hierarchy and see-saw semidefinite programming method [23]). Then, we consider all other local assignment deterministic strategies, $q_A(a|x) = \delta_{a,a_x}$ and $q_B(b|y) = \delta_{b,b_y}$, to find the maximum violation of the corresponding tilted Bell inequalities (7), and choose the optimal (*) local assignment strategy, say $q_A^*(a|x) = \delta_{a,a_x^*}$ and $q_B^*(b|y) = \delta_{b,b_y^*}$. Moreover, as we demonstrate in the next section, the expression of the tilted Bell inequality (7) also lets us infer the threshold detection efficiencies below which a loophole-free violation of the given Bell inequality is not possible.

In the next section, we exemplify the applications of Lemma 1 for the simplest bipartite Bell scenario, with two dichotomic measurements per party.

III. MAXIMAL DETECTION LOOPHOLE-FREE NONLOCALITY IN THE CHSH SCENARIO

We now consider the simplest bipartite Bell scenario, in which Alice and Bob perform one of the two distinct measurements, $x, y \in \{0, 1\}$ and obtain binary

outcomes, $a, b \in \{-1, +1\}$, respectively. It is convenient in this scenario to introduce *marginals* and *correlators* [2]: marginals are defined by $\langle A_x \rangle := \sum_a a p_A(a|x)$ and $\langle B_y \rangle := \sum_b b p_B(b|y)$, whereas correlators are defined by $\langle A_x B_y \rangle := \sum_{ab} ab p(ab|xy)$. We note that in a quantum realization these correlators are the expectation of binary observables, $\hat{A}_x = \hat{M}_{+1}^x - \hat{M}_{-1}^x$ and $\hat{B}_y = \hat{N}_{+1}^y - \hat{N}_{-1}^y$ with respect to a shared quantum state $\hat{\rho}_{AB}$.

Writing behaviors in terms of correlators and marginals, the nonlocality of a given behavior can be witnessed by a violation of the CHSH inequality,

$$C(\mathbf{p}) = \sum_{x,y} (-1)^{x \cdot y} \langle A_x B_y \rangle \leq 2, \quad (10)$$

which up to relabeling of measurements and outcomes is known to be the only tight and complete Bell inequality in this scenario [21, 24].

Let us now consider inefficient detectors with efficiencies η_A, η_B . Let \mathbf{p} be the ideal behavior corresponding to a quantum strategy. Then for *any* local assignment strategy \mathbf{q} , the condition for an the effective behavior $\tilde{\mathbf{p}} = \Omega_{\eta_A \eta_B}(\mathbf{p})$ in (5) to be nonlocal amounts to the ideal behavior \mathbf{p} violating the following inequality,

$$\begin{aligned} C(\tilde{\mathbf{p}}) &= \eta_A \eta_B C(\mathbf{p}) + (1 - \eta_A) (1 - \eta_B) C(\mathbf{q}) \\ &\quad + \eta_A (1 - \eta_B) C(\mathbf{p}^A) + (1 - \eta_A) \eta_B C(\mathbf{p}^B) \leq 2. \end{aligned} \quad (11)$$

We are particularly interested in the maximum possible loophole-free violation $C(\tilde{\mathbf{p}}) - 2$ of the CHSH inequality for given η_A, η_B . Therefore, we invoke Lemma 1 with an optimal² deterministic strategy, wherein $q(a|x) = \delta_{a,+1}$, $q(b|y) = \delta_{b,+1}$ for all x, y , to retrieve the following doubly-tilted CHSH inequality,

$$\begin{aligned} C_{\eta_A \eta_B}(\mathbf{p}) &= C(\tilde{\mathbf{p}}) + \frac{2}{\eta_B} (1 - \eta_B) \langle A_0 \rangle + \frac{2}{\eta_A} (1 - \eta_A) \langle B_0 \rangle \\ &\leq 2 \left[\frac{1}{\eta_A} + \frac{1}{\eta_B} - 1 \right] = c_{\mathcal{L}}(\eta_A, \eta_B). \end{aligned} \quad (12)$$

Consequently, for any given η_A, η_B , the maximum loophole-free violation of CHSH inequality corresponds to the maximum violation of the doubly-tilted CHSH inequality in (12). However, not all combinations η_A, η_B allow for loophole-free violation of the CHSH inequality. We now demonstrate that the expression of the doubly-tilted CHSH inequalities (12) allows us to infer the region of η_A, η_B that permits a loophole-free quantum violation of the CHSH inequality [25],

¹ We note that tilted Bell inequalities have been used to find optimal quantum strategies for maximum loophole-free violation of Bell inequalities in a case-by-case basis.

² We find that the assignment strategy considered above is one the family of optimal deterministic assignment strategies which achieve the maximum loophole-free violation of the CHSH inequality for all η_A, η_B (see Appendix A).

Observation 1. A quantum loophole-free violation of the CHSH inequality (11) is not possible if the detection efficiencies $\eta_A, \eta_B \in [0, 1]$ fail to satisfy,

$$\eta_B > \frac{\eta_A}{3\eta_A - 1} \quad (13)$$

Proof. First, let us note that while in general it is not guaranteed that tilted Bell inequalities obtained via Lemma 1 will be tight. Since local assignment strategy saturates the local value $\beta(\mathbf{q}) = 2$ of the CHSH inequality, the family of doubly-tilted CHSH inequalities (12) are indeed *tight*.

Next, we observe that the maximum no-signalling value $c_{\mathcal{NS}}$ of doubly-tilted CHSH functionals $C_{\eta_A \eta_B}(\mathbf{p})$ (12) is $c_{\mathcal{NS}}(\eta_A, \eta_B) = \max\{4, c_{\mathcal{L}}(\eta_A, \eta_B)\}$ for all $\eta_A, \eta_B \in [0, 1]$, where the value 4 corresponds to a nonlocal vertex of the no-signalling polytope (the PR-Box) [26]. Because of the strict inclusion relation between the sets of behaviors $\mathcal{L} \subset \mathcal{Q} \subset \mathcal{NS}$ (\mathcal{NS} denotes the no-signaling polytope), whenever $c_{\mathcal{NS}}(\eta_A, \eta_B) = c_{\mathcal{L}}(\eta_A, \eta_B)$, there is no room for quantum violation. Therefore, the region where a loophole-free violation of the CHSH inequality is possible is given by $c_{\mathcal{L}}(\eta_A, \eta_B) < 4$. This results in, $\frac{1}{\eta_A} + \frac{1}{\eta_B} < 3$. \square

Therefore, (13) provides lower bounds for Bob's critical detection efficiency $\eta_B^* \geq \frac{\eta_A}{3\eta_A - 1}$ given Alice's detection efficiency $\eta_A \in (\frac{1}{2}, 1]$, which turn out to be *tight* [27]. Hence, observation 1 effectively defines the region (13) of η_A, η_B , wherein we look for the maximum quantum violation of doubly-tilted CHSH inequalities, $c_{\mathcal{Q}}(\eta_A, \eta_B) = \max_{\mathbf{p} \in \mathcal{Q}}(C_{\eta_A, \eta_B}(\mathbf{p}))$ (12) to retrieve maximum loophole-free violation of CHSH inequality (11).

As discussed in the subsequent sections, retrieving the exact expression for the maximum violation of the doubly-tilted CHSH inequalities as a function of η_A, η_B , with the traditional methods, such as the NPA hierarchy and SOS decompositions, turns out to be intractable. Despite this, in FIG 1, we plot the *analytically* obtained value of maximum loophole-free violation of the CHSH inequality against $\eta_A, \eta_B \in [\frac{1}{2}, 1]$. Moreover, in FIG. 2, we use the optimal strategies to illustrate the effect of inefficient detectors with efficiency $\eta_A = \eta_B = 0.85$ on the violation of CHSH inequality as a consequence of Lemma 1.

In the following sections, we describe the technique to retrieve the analytical expression and the analytical form of the optimal quantum strategies, which are self-tested by the maximal violation.

IV. SELF-TESTING OF CHSH INEQUALITIES TILTED FOR INEFFICIENT DETECTORS

In this section, we derive *robust* self-testing statements for the family of doubly-tilted CHSH inequalities (12),

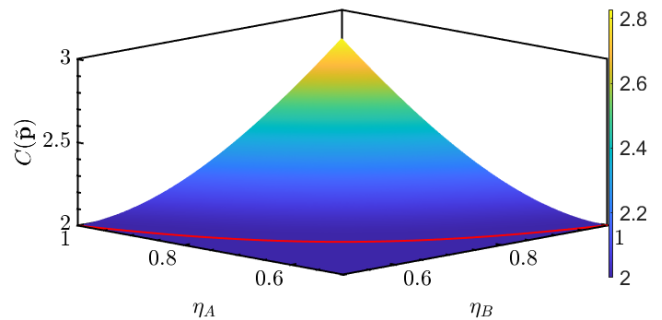


FIG. 1: *Maximum loophole-free violation of the CHSH inequality:*— A plot of the maximum loophole-free violation of the CHSH inequality, $C(\tilde{\mathbf{p}}) = \eta_A \eta_B c_{\mathcal{Q}}(\eta_A, \eta_B) + (1 - \eta_A)(1 - \eta_B)2$, against detection efficiencies $\eta_A, \eta_B \in [\frac{1}{2}, 1]$, where we used the analytical expression for maximum quantum violation of the doubly-tilted CHSH inequality (12), $c_{\mathcal{Q}}(\eta_A, \eta_B)$, derived in Section IV B. The solid red line represents Bob's critical detection efficiency $\eta_B^* = \frac{\eta_A}{3\eta_A - 1}$ (13), below which a loophole-free quantum violation of the CHSH inequality is not possible.

entailing the analytical expressions for the maximum violation, and the optimal quantum strategies. We briefly present the requisite preliminaries for self-testing by revisiting the already-solved sub-case of our problem, namely, CHSH inequalities tilted for one inefficient detector.

A. One inefficient detector

Let us consider an *ideal* scenario wherein Alice has access to perfect detectors, such that $\eta_A = 1$, while Bob's detector are imperfect and click with efficiency η_B . Consequently, we retrieve the following family of completely asymmetrically tilted CHSH inequalities from (12),

$$C_{\alpha}(\mathbf{p}) = \sum_{x,y} (-1)^{x \cdot y} \langle A_x B_y \rangle + \alpha \langle A_0 \rangle \leq 2 + \alpha, \quad (14)$$

where the tilting parameter $\alpha = \frac{2}{\eta_B}(1 - \eta_B)$ is determined by the detection efficiency on Bob's side. First, from Observation 1 and (13), for quantum violation we have that $\eta_B \in (\frac{1}{2}, 1]$, which restricts the tilting parameter to $\alpha \in [0, 2)$.

The maximum quantum value of the Bell functional in (14) is $c_{\mathcal{Q}}(\alpha) = \sqrt{8 + 2\alpha^2}$ [19]. Hence, from (8), the maximum loophole-free violation of CHSH inequality when $\eta_A = 1$ is $2\sqrt{2}\sqrt{\eta_B^2 + (1 - \eta_B)^2}$. Recall that, in terms of the state and measurements $\{|\psi'\rangle, \hat{A}'_x, \hat{B}'_y\}$ of an optimal quantum strategy, we can write the maximal

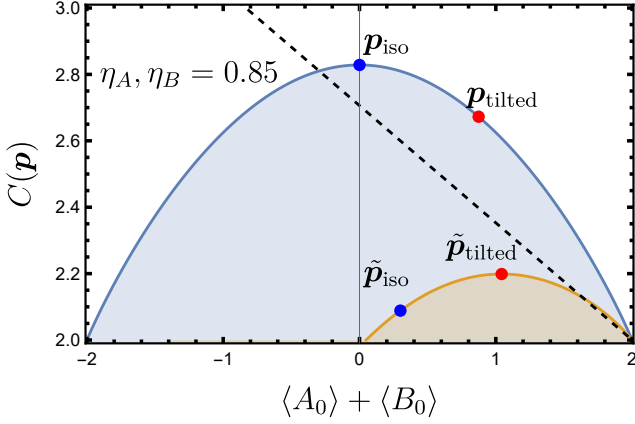


FIG. 2: *Effect of inefficient detectors on nonlocal correlations*:— This graphic illustrates the impact of detector inefficiencies on nonlocal quantum correlations within the simplest Bell scenario. The blue region represents the set of quantum correlations $\mathbf{p} \in \mathcal{Q}$ in ideal conditions. With the detection efficiencies $\eta_A = \eta_B = 0.85$, and the local assignment strategy $q_A(a|x) = \delta_{a,0}$, $q_B(b|y) = \delta_{b,0}$, the effective quantum correlations $\tilde{\mathbf{p}} = \Omega_{\eta_A \eta_B}(\mathbf{p})$ are constrained to the smaller orange subset. The blue dot on the blue curve corresponds to the isotropic behavior \mathbf{p}_{iso} that maximally violates the CHSH inequality, $C(\mathbf{p}_{iso}) = 2\sqrt{2}$, in ideal conditions, while the corresponding effective behavior (blue dot on the orange curve) $\tilde{\mathbf{p}} = \Omega_{\eta_A \eta_B}(\mathbf{p}_{iso})$ no longer attains the maximum loophole-free violation of the CHSH inequality, $C(\tilde{\mathbf{p}}_{tilted}) \approx 2.08854$. Instead, the red dot on the blue curve corresponds to the quantum behavior \mathbf{p}_{tilted} which maximally violates the doubly-tilted CHSH inequality (dashed black line), $C_{\eta_A \eta_B}(\mathbf{p}_{tilted}) = 2.98098$, (12), and attains the maximum loophole-free violation $C(\tilde{\mathbf{p}}_{tilted}) \approx 2.19876$ (red dot on the orange curve) of the CHSH inequality, thereby, exemplifying Lemma 1.

functional value as $c_{\mathcal{Q}}(\alpha) = \langle \psi' | \hat{C}_\alpha | \psi \rangle$, where \hat{C}_α is the CHSH Bell operator, given by

$$\hat{C}_\alpha = \sum_{x,y} (-1)^{x \cdot y} \hat{A}_x \otimes \hat{B}_y + \alpha \hat{A}_0. \quad (15)$$

In Ref. [18] it is shown that \hat{C}_α admits an SOS decompositions of the form

$$c_{\mathcal{Q}}(\alpha) \mathbb{1} - \hat{C}_\alpha = \sum_i P_i^\dagger P_i, \quad (16)$$

in terms of polynomials P_i in the operators $\{\mathbb{1}, \hat{A}'_x, \hat{B}'_y, \hat{A}'_x \otimes \hat{B}'_y\}$. These decompositions are then used to prove that $c_{\mathcal{Q}}(\alpha)$ self-tests the optimal strategy

$\{|\psi\rangle, \hat{A}_x, \hat{B}_y\}$ [18, 28], where

$$\begin{aligned} |\psi\rangle &= \cos \theta |00\rangle + \sin \theta |11\rangle, \\ \hat{A}_0 &= \sigma_z & \hat{B}_0 &= \cos \mu \sigma_z + \sin \mu \sigma_x \\ \hat{A}_1 &= \sigma_x & \hat{B}_1 &= \cos \mu \sigma_z - \sin \mu \sigma_x, \end{aligned} \quad (17)$$

with $\alpha = 2/\sqrt{1+2\tan^2 2\theta}$, $\tan(\mu) = \sin(2\theta)$ and $\sigma_{x(z)}$ denotes the $x(z)$ Pauli matrix.

The proof builds upon the observation that for *any* quantum strategy $\{|\psi'\rangle, \hat{A}'_x, \hat{B}'_y\}$ attaining the value $c_{\mathcal{Q}}(\alpha)$, the SOS decomposition (16) implies that $|\psi'\rangle$ must belong to the null space of the operators P_i , i.e., it must satisfy the conditions, $P_i |\psi'\rangle = 0$ for all i . From these conditions it is possible to infer the existence of operators $\{\hat{Z}_A, \hat{X}_A, \hat{Z}_B, \hat{X}_B\}$ [18], such that,

$$\begin{aligned} \hat{Z}_A |\psi'\rangle &= \hat{Z}_B |\psi'\rangle \\ \sin \theta \hat{X}_A (\mathbb{1} + \hat{Z}_B) |\psi'\rangle &= \cos \theta \hat{X}_A (\mathbb{1} - \hat{Z}_A) |\psi'\rangle. \end{aligned} \quad (18)$$

The conditions (18) ensure the existence of *local isometries*, Φ_A and Φ_B , mapping any optimal strategy $\{|\psi'\rangle, \hat{A}'_x, \hat{B}'_y\}$ to the reference strategy $\{|\psi\rangle, \hat{A}_x, \hat{B}_y\}$ in (17), that is,

$$\begin{aligned} \Phi_A \otimes \Phi_B (|\psi'\rangle) &= |\psi\rangle \otimes |\text{junk}\rangle \\ \Phi_A \otimes \Phi_B (\hat{A}'_x \otimes \hat{B}'_y |\psi'\rangle) &= \hat{A}_x \otimes \hat{B}_y |\psi\rangle \otimes |\text{junk}\rangle, \end{aligned} \quad (19)$$

where $|\text{junk}\rangle$ represents the arbitrary state of additional degrees of freedom on the which the measurements act trivially. Thus it is seen that the optimal quantum strategy is unique up to local isometries. We note that, while the proof of relations in Eq. (18) requires an ideal behavior, [18] demonstrates that the self-testing can be made robust. Recall, a Bell expression provides a robust self-test for a given quantum strategy, say R if, in a noise-tolerant manner, the expected value β in close to the maximum $\beta_{\mathcal{Q}}$ consistently corresponds to a strategy \tilde{R} in a close neighbourhood of the reference strategy R , up to local isometries.

Let us now proceed to the unsolved general case of inefficient detectors for both parties.

B. Two inefficient detectors

We now consider the most generic experimental setting, wherein the detectors of both parties may be imperfect and click with efficiencies $\eta_A, \eta_B \in [0, 1]$. We rewrite for convenience, the doubly-tilted CHSH inequalities (12) for the general case as,

$$C_{\alpha, \beta}(\mathbf{p}) = \sum_{x,y} (-1)^{x \cdot y} \langle A_x B_y \rangle + \alpha \langle A_0 \rangle + \beta \langle B_0 \rangle \leq 2 + \alpha + \beta, \quad (20)$$

where the tilting parameter $\alpha = \frac{2}{\eta_B} (1 - \eta_B)$ for Alice's term $\langle A_0 \rangle$ depends on the Bob's detection efficiency η_B , while Bob's tilting parameter $\beta = \frac{2}{\eta_A} (1 - \eta_A)$

is determined by Alice's efficiency η_A . Consequently, the boundary of the region of interest (13) translates to $0 < \alpha + \beta < 2$, in terms of the tilting parameters. We are interested in finding the maximal violation of the inequality in (20), as well as a quantum state and measurements attaining it, as a function of the tilting parameters α, β . However, we find the problem to be intractable via analytical techniques described above. In what follows we first describe in more detail the difficulties that arise when trying to obtain a tight SOS decomposition for the Bell operator on the left of (20), and then we show that obtaining an analytical solution is nonetheless possible by a different technique.

1. Impracticality of the SOS technique and NPA upper-bound convergence

Before we derive the analytical expression for the maximal quantum violation $c_Q(\alpha, \beta)$ of the doubly-tilted CHSH inequality (12) with an alternative technique, here we demonstrate that the standard SOS decomposition technique, though theoretically applicable, becomes impractical for these inequalities.

The problem of finding the maximum quantum violation β_Q of a Bell inequality (2) can be relaxed with the NPA hierarchy [29] of semi-definite programs. Specifically, the NPA hierarchy returns a converging sequence of upper-bounds β_{Q_L} on the maximum quantum violation β_Q . Here, $L \in \{1, 1 + AB, 2, \dots\}$ denotes the level of the hierarchy, which corresponds to the length of the monomials of the measurement operators $\{\hat{M}_a^x, \hat{N}_b^y\}$. We recall that finding a tight upper bound on the maximum quantum violation of Bell inequalities using NPA hierarchy, such that $\beta_{Q_L} = \beta_Q$, and retrieving a *tight* SOS decomposition $\sum_i P_i^\dagger P_i$ for the operator $\beta_Q \mathbb{I} - \hat{\beta}$ form a primal-dual pair of SDPs, where P_i are polynomials in the optimal measurement operators $\{\hat{M}_a^x, \hat{N}_b^y\}$. In particular, the level L of the NPA hierarchy at which $\beta_Q = \beta_Q$ corresponds to the degree of the polynomials P_i in a tight SOS decomposition. For instance, the degree polynomials in the tight SOS decompositions (16) of the completely asymmetrically doubly-tilted CHSH inequalities reflect the fact that the level $1 + AB$ of the NPA hierarchy is sufficient to retrieve the maximum quantum violation for these inequalities.

In FIG. 3, we chart the minimum level L of the NPA hierarchy against the tilting parameters α, β required to saturate the maximum quantum violation $c_Q(\alpha, \beta)$ (found in the next section) of doubly-tilted CHSH inequalities (20), up to machine precision. Remarkably, as the tilting parameters α, β approach the critical boundary (13), $\alpha + \beta = 2$, the level L of NPA hierarchy increases rapidly. In particular, we found that even the level 12 of the NPA hierarchy is not enough to saturate the maximum violation of the symmetrically doubly-

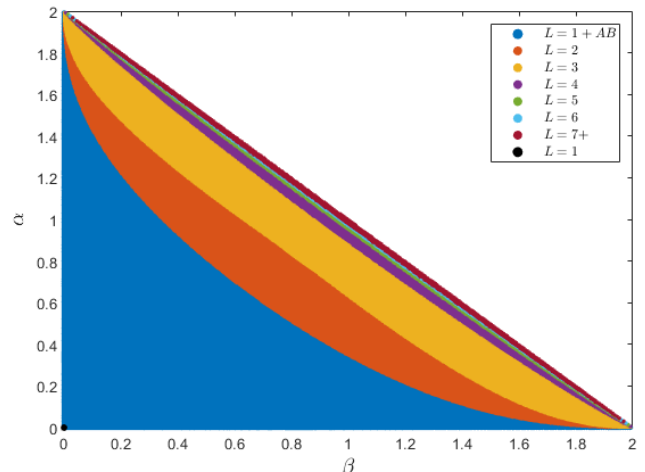


FIG. 3: Increasing levels for tight NPA upper bounds in the CHSH scenario:— A plot of the minimum level $L \in \{1, 1 + AB, 2, 3, 4, 5, 6, 7+\}$ of the NPA hierarchy required to saturate (up to machine precision) the maximum quantum violation $c_Q(\alpha, \beta)$ for $\alpha, \beta \in [0, 2]$. Notably, the required minimum level of the NPA-hierarchy rapidly increases as the tilting parameters the critical boundary $\alpha + \beta = 2$.

tilted CHSH inequality when³ $\alpha = \beta = 0.999$. This observation raises a critical question: is *any* finite level of the NPA hierarchy enough to saturate the maximum quantum violation of the doubly-tilted CHSH inequalities for all tilting parameters α, β ? The uncertainty surrounding this question implies that the degree of polynomials required for a tight analytical SOS decomposition for these inequalities remains elusive and potentially unbounded.

Nonetheless, for a significantly large range of the parameters α, β , the NPA level $1 + AB$ saturates the maximum quantum violation $c_Q(\alpha, \beta)$. This observation makes it tempting to apply the methodology from [18] to extend the analytical self-testing results by finding a Sum-of-Squares (SOS) decomposition for the Bell operator $\hat{C}_{\alpha\beta}$ associated with the general doubly-tilted CHSH inequalities. Indeed, it is possible to numerically retrieve SOS decompositions for fixed values of the tilting parameters, especially when lower levels of NPA hierarchy saturate the maximum quantum violation. However, unlike the simpler completely asymmetric where the SOS decomposition includes just *two* polynomials, even the simplest decompositions for the general case

³To a 12-digits approximation the analytical answer is 3.9980 0000 1333, whereas the NPA hierarchy gives the upper bound of 3.9980 0000 2190. The calculation was done using the toolkit for non-commutative polynomial optimization Moment [30], the modeller YALMIP [31], and the arbitrary-precision solver SDPA-GMP [32].

demand at least *five* polynomials. The task of deducing a generically applicable analytical SOS decomposition from the numerical results is significantly hindered due to the complex dependence of the maximal quantum violation and the optimal quantum strategy on the tilting parameters α, β . This complex interdependence translates into the SOS polynomials, rendering them overly convoluted and preventing any definitive statements about the optimal strategies based on the SOS decompositions. Interestingly, nonetheless, for the symmetric case with $\alpha = \beta = 2/\sqrt{13}$, it is possible to find the analytical expression of the polynomials of degree $1 + AB$ in the tight SOS decomposition and the optimal quantum strategy.

The derivation of the self-testing results presented in the section IV A, relied heavily on the existence of SOS decompositions from which relations of the form $P_i |\psi\rangle = 0$, where $\{P_i\}$ are polynomial functions on the measurement operators of an optimal realization $\{\hat{A}_x, \hat{B}_y, |\psi\rangle\}$. The increase in the minimum degree as well as the number of polynomials in tight SOS decomposition for the general tilted-Bell inequalities, makes self-testing with the SOS technique for general doubly-tilted CHSH inequalities too arduous to be practical. Nevertheless, as we show in the next section, it is still possible to retrieve the analytical expressions for the maximum quantum violation and the optimal quantum strategy for general doubly-tilted CHSH inequalities and demonstrate that the maximum violation self-tests the optimal quantum strategy.

2. Self-testing based on Jordan's lemma

Lacking tight analytical SOS decompositions for the general doubly-tilted CHSH inequalities (20), we present in this section an alternative approach based on Jordan's lemma [33–35].

Jordan's lemma provides a convenient characterization for the local observables of a party having two settings with two outputs each. In particular, in CHSH scenario, we can take Alice and Bob's observables A_x, B_y to be projective, à la *Naimark's dilation theorem*. Jordan's lemma then asserts that there exists local unitary transformations that simultaneously block-diagonalise the observables A_x, B_y , with one and two dimensional blocks. As we are interested in the expectation values $\langle \hat{A}_x \rangle, \langle \hat{B}_y \rangle$ of the observables with respect to a state $|\psi\rangle$, we can always add a projector $|\phi\rangle\langle\phi|$ onto the $\text{Ker}(\rho_A)$ of the respective reduced state $\rho_A = \text{Tr}_B |\psi\rangle\langle\psi|$ to each one dimensional block. Hence, we can, without loss of generality, take all Jordan blocks to be two-dimensional,

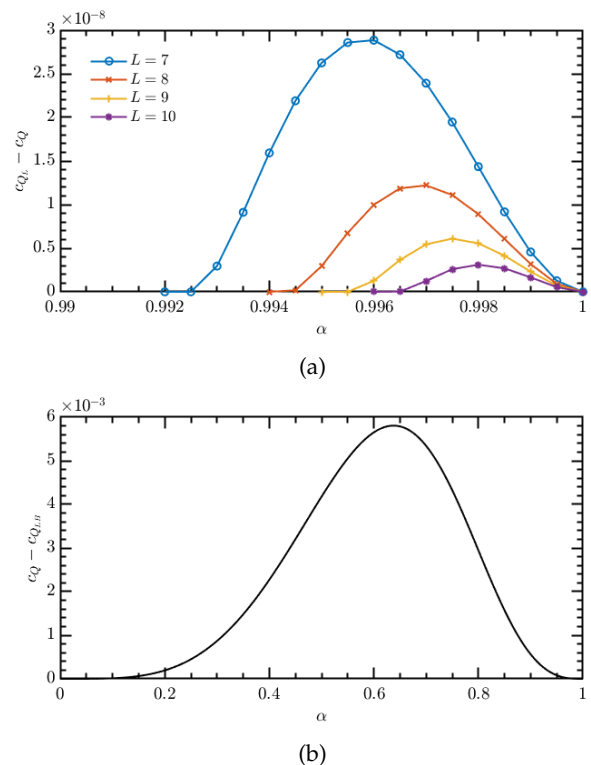


FIG. 4: *Error in estimation of maximum quantum violation*:— The curves in plot (a) correspond to the difference $c_{Q_L}(\alpha, \alpha) - c_Q(\alpha, \alpha)$ ($\times 10^{-8}$) between the upper-bounds from the levels $L \in \{7, 8, 9, 10\}$ of the NPA hierarchy and the maximum quantum violation $c_Q(\alpha, \alpha)$ of symmetrically tilted Bell inequalities (12), against $\alpha \in [0.99, 1]$, obtained with an arbitrary precision solver SDPA-GMP [32] and our analytical solution (Theorem 1), respectively. This plot demonstrates the insufficiency of high levels of the NPA hierarchy for obtaining tight bounds in the CHSH scenario. The curve in plot (b) corresponds to the difference $c_Q(\alpha, \alpha) - c_{Q_{LB}}(\alpha, \alpha)$ ($\times 10^{-3}$) between the maximum quantum violation $c_Q(\alpha, \alpha)$ and the lower-bound $c_{Q_{LB}}(\alpha, \alpha)$ corresponding to the sub-optimal analytical solutions presented in [13], against $\alpha \in [0, 1]$.

such that Alice's observables can now be expressed as,

$$\hat{A}_0 = \bigoplus_i \hat{A}_0^{(i)} = \bigoplus_i \sigma_Z \quad (21)$$

$$\hat{A}_1 = \bigoplus_i \hat{A}_1^{(i)} = \bigoplus_i (\cos \theta_i^A \sigma_Z + \sin \theta_i^A \sigma_X), \quad (22)$$

where the index i iterates runs over blocks and $\sigma_Z^{(i)}, \sigma_X^{(i)}$ denote the Pauli Z, X matrices on the i th two dimensional block. Similarly, Bob's observables can be ex-

pressed as,

$$\hat{B}_0 = \bigoplus_j \hat{B}_0^{(j)} = \bigoplus_j \sigma_Z \quad (23)$$

$$\hat{B}_1 = \bigoplus_j \hat{B}_1^{(j)} = \bigoplus_j (\cos \theta_j^B \sigma_Z + \sin \theta_j^B \sigma_X), \quad (24)$$

where again j runs over blocks. Consequently, the Bell operator $\hat{C}_{\alpha\beta}$ associated with the general doubly-tilted CHSH inequalities (20) also take a block diagonal form,

$$\hat{C}_{\alpha\beta} = \sum_{i,j} \hat{C}_{\alpha\beta}(\theta_i^A, \theta_j^B), \quad (25)$$

where $\hat{C}_{\alpha\beta}(\theta_i^A, \theta_j^B)$ is an operator with local dimension 2 given by

$$\begin{aligned} \hat{C}_{\alpha\beta}(\theta_i^A, \theta_j^B) &= \sum_{x,y} (-1)^{x \cdot y} \hat{A}_x^{(i)} \otimes \hat{B}_y^{(j)} \\ &\quad + \alpha (\hat{A}_0^{(i)} \otimes \mathbb{I}_2) + \beta (\mathbb{I}_2 \otimes \hat{B}_0^{(j)}). \end{aligned} \quad (26)$$

where \mathbb{I}_2 denotes the two-dimensional identity operator.

Let Π_i, Π_j be the projectors onto Alice's i th and Bob's j th blocks respectively, such that, $\hat{C}_{\alpha\beta}(\theta_i^A, \theta_j^B) = \Pi_i \otimes \Pi_j \hat{C}_{\alpha\beta} \Pi_i \otimes \Pi_j$. Consequently, the value of the Bell functional $C_{\alpha\beta}(\mathbf{p})$ is given by

$$C_{\alpha\beta}(\mathbf{p}) = \langle \hat{C}_{\alpha\beta} \rangle_{|\psi\rangle} = \sum_{i,j} p_{ij} \text{tr} \left\{ \rho_{ij} \hat{C}_{\alpha\beta}(\theta_i^A, \theta_j^B) \right\}, \quad (27)$$

where $p_{ij} \rho_{ij} = (\Pi_i \otimes \Pi_j) |\psi\rangle \langle \psi| (\Pi_i \otimes \Pi_j)$ are the (unnormalised) projections of $|\psi\rangle$ onto the i th and j th blocks of Alice and Bob, respectively. Since $C_{\alpha\beta}(\mathbf{p})$ is a convex combination of the values $\text{tr} \left\{ \rho_{ij} \hat{C}_{\alpha\beta}(\theta_i^A, \theta_j^B) \right\}$ in Alice's i th and Bob's j th blocks with weights p_{ij} , its maximum value $c_Q(\alpha, \beta)$ is attained when for all i, j , the value of the Bell functional is the optimal two-qubit value. Consequently, without loss of generality,

$$\hat{A}_0 = \sigma_Z, \quad \hat{A}_1 = c_A \sigma_Z + s_A \sigma_X \quad (28a)$$

$$\hat{B}_0 = \sigma_Z, \quad \hat{B}_1 = c_B \sigma_Z + s_B \sigma_X, \quad (28b)$$

where $c_A = \cos \theta_A$, $s_A = \sin \theta_A$, $c_B = \cos \theta_B$ and $s_B = \sin \theta_B$. Consequently, the maximum quantum violation $c_Q(\alpha, \beta)$ self-tests a quantum strategy if, up to local two-dimensional unitaries, the optimal two-qubit strategy is unique. Now we are prepared to present our main result, namely, the *analytical* self-testing statements for the symmetrically ($\alpha = \beta$) tilted CHSH inequality. We have differed the self-testing statements for the general case of $\alpha \neq \beta$ to the supplementary material (Sec. B) for brevity.

Theorem 1. [Self-testing of symmetrically tilted CHSH inequalities] *The maximum quantum violation $c_Q(\alpha, \alpha)$ of*

the symmetrically ($\alpha = \beta$) tilted CHSH inequality (12) is the largest root of the degree 4 polynomial,

$$\begin{aligned} f(\lambda) &= \lambda^4 + (4 - \alpha^2)\lambda^3 + \left(\frac{11}{4}\alpha^4 - 12\alpha^2 - 4 \right) \lambda^2 \\ &\quad + (2\alpha^6 - \alpha^4 - 20\alpha^2 - 32)\lambda + 5\alpha^6 - 21\alpha^4 + 16\alpha^2 - 32. \end{aligned} \quad (29)$$

$C_{\alpha\alpha}(\mathbf{p}) = c_Q(\alpha, \alpha)$ self-tests a two qubit quantum strategy with optimal ($*$) local observables of the form (28), such that the optimal cosines are equal, i.e., $c^*(\alpha) = c_A^*(\alpha) = c_B^*(\alpha) \in [0, 1]$, and satisfy the relation,

$$c^*(\alpha) = \frac{1}{8} \left[3\alpha^2 - 4 + \sqrt{16 + 9\alpha^4 + 8\alpha^2(2c_Q(\alpha, \alpha) - 1)} \right]. \quad (30)$$

Proof. Here, we present a comprehensive overview of the proof-technique while the complete proof is contained in the accompanying Mathematica notebook. As discussed above Jordan's lemma lets us express the Bell operator $\hat{C}_{\alpha\beta=\alpha}$ associated with the symmetrically ($\alpha = \beta$) tilted CHSH inequality (12) as a two qubit operator,

$$\hat{C}_{\alpha\alpha} = \sum_{x,y} (-1)^{x \cdot y} \hat{A}_x \otimes \hat{B}_y + \alpha (\hat{A}_0 \otimes \mathbb{I}_2 + \mathbb{I}_2 \otimes \hat{B}_0). \quad (31)$$

With the parametrization (28), the Bell operator $\hat{C}_{\alpha\alpha}$, now a function of just two cosines $c_A, c_B \in [0, 1]$, has the following four dimensional matrix representation:

$$\begin{pmatrix} \omega + 2\alpha & s_B - c_A s_B & s_A - c_B s_A & -s_A s_B \\ s_B - c_A s_B & -\omega & -s_A s_B & (c_B - 1)s_A \\ s_A - c_B s_A & -s_A s_B & -\omega & (c_A - 1)s_B \\ -s_A s_B & (c_B - 1)s_A & (c_A - 1)s_B & \omega - 2\alpha \end{pmatrix} \quad (32)$$

where $\omega = 1 + c_A + c_B - c_B c_A$. Now, for fixed cosines c_A, c_B , the maximum quantum violation $c_Q(\alpha, \alpha)$ of the symmetrically doubly-tilted CHSH inequality corresponds to the largest eigenvalue of the matrix (32), i.e., the largest root of its characteristic polynomial $q(\lambda, c_A, c_B, \alpha)$, which has the form,

$$\begin{aligned} q(\lambda, c_A, c_B, \alpha) &= \lambda^4 - (4\alpha^2 + 8)\lambda^2 \\ &\quad + 8\alpha^2(c_A c_B - c_A - c_B - 1)\lambda \\ &\quad + 8[2(c_B^2 + c_A^2(1 - c_B^2)) - \alpha^2(c_A^2(1 - c_B))] \\ &\quad + c_B(1 + c_B) - c_A s_B(1 - c_B^2)], \end{aligned} \quad (33)$$

where λ denotes the eigenvalue of the matrix (32). Thus, finding $c_Q(\alpha, \alpha)$ boils down to maximizing the largest root of $q(\lambda, c_A, c_B, \alpha)$ in (33) over the cosines c_A and c_B . While for any fixed value of the tilting parameter α , this optimization problem can be numerically solved, obtaining an analytical expression as a function of the α is a more arduous problem. We now describe how such expression can be obtained via Gröbner basis elimination for both the optimal quantum value $c_Q(\alpha, \alpha)$ and

the optimal measurement settings in terms of cosines $c_A^*(\alpha), c_B^*(\alpha)$.

Let us consider the Lagrangian for this problem,

$$L = \lambda + s \cdot q(\lambda, c_A, c_B, \alpha) \quad (34)$$

where s is a Lagrange multiplier. Consequently, the stationary points must satisfy the conditions, $\partial_{c_A} L = \partial_{c_B} L = \partial_s L = 0$, which in-turn imply the following polynomial conditions,

$$\begin{cases} q(\lambda, c_A, c_B, \alpha) = 0 \\ q_{c_A}(\lambda, c_A, c_B, \alpha) = \partial_{c_A} q(\lambda, c_A, c_B, \alpha) = 0 \\ q_{c_B}(\lambda, c_A, c_B, \alpha) = \partial_{c_B} q(\lambda, c_A, c_B, \alpha) = 0. \end{cases} \quad (35)$$

The cosines parameterizing the optimal observables $c_A^*(\alpha), c_B^*(\alpha)$ and the maximum quantum violation $c_Q(\alpha, \alpha) = \lambda^*(\alpha)$ are thus common roots of the polynomials q, q_{c_A}, q_{c_B} in (35). We now use the Gröbner basis elimination on q, q_{c_A}, q_{c_B} to eliminate the cosines c_A, c_B and retrieve a polynomial $f_0(\lambda)$ of degree 12. We then take the polynomial quotient of $f_0(\lambda)$ with respect to eight trivial and sub-optimal roots to retrieve the desired degree 4 polynomial $f(\lambda)$ (29). The expression for maximum quantum violation $c_Q(\alpha, \alpha)$ which corresponds to the largest real root of the polynomial $f(\lambda)$ as a function of α is contained in the accompanying Mathematica notebook⁴ (See FIG. 1 in the more general scenario $\eta_A \neq \eta_B$).

Similarly, to find the expression for Alice's optimal cosine $c_A^*(\alpha)$, we eliminate c_B, λ using Gröbner basis elimination on q, q_{c_A}, q_{c_B} . This results in a degree 11 polynomial $g(c)$. We then take the polynomial quotient of $g(c)$ with respect to seven trivial and sub-optimal roots to obtain the following degree 4 polynomial,

$$\begin{aligned} g(c) = & -16c^4 + (40\alpha^2 - 32)c^3 \\ & + (-33\alpha^4 + 48\alpha^2 - 16)c^2 + (8\alpha^6 - 10\alpha^4 + 8\alpha^2)c \\ & - 4\alpha^6 + 7\alpha^4 \quad (36) \end{aligned}$$

Repeating the same procedure for Bob's optimal cosine $c_B^*(\alpha)$, we end up with a degree 4 polynomial identical to $g(c)$ in (36). We find the expressions for the optimal cosines to be identical $c_A^*(\alpha) = c_B^*(\alpha) = c_\alpha^*$ and corresponding to the largest root c_α^* of $g(c)$ (contained accompanying Mathematica notebook and see FIG. 5 for the scenario $\alpha \neq \beta$). Furthermore, the simplification $c_A^*(\alpha) = c_B^*(\alpha) = c_\alpha^*$ allows us to derive the relation (30) between the maximum quantum violation $c_Q(\alpha, \alpha)$ and the optimal cosine c_α^* . Observe that in the interval $[0, \pi]$ the angle $\theta_A^* = \theta_B^* = \theta$ between optimal measurements is uniquely determined by $c_Q(\alpha, \alpha)$

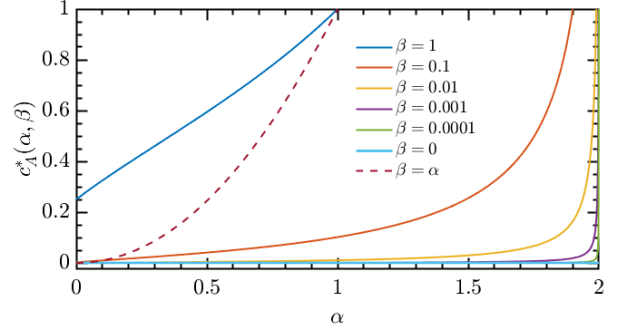


FIG. 5: *Self-testing of partially incompatible observables*:— A plot of the optimal cosines of Alice $c_A^*(\alpha, \beta)$ (28) with $\beta \in \{\alpha, 0.1, 0.01, 0.001, 0\}$ self-tested by the maximum quantum violation $C_{\alpha\beta}(\rho) = c_Q(\alpha, \beta)$ of the doubly-tilted CHSH inequalities (12) against the tilting parameter $\alpha \in [0, 1]$. Here, $c_A^*(\alpha, \beta) = 0$ implies maximally incompatible whereas $c_A^*(\alpha, \beta) = 1$ reflects compatible observables. Notice, that in contrast to the totally asymmetrically case $\beta = 0$ wherein Alice's optimal cosine $c_A^*(\alpha, \beta = 0)$ stays constant with respect to α [18], for the general case, whenever $\beta > 0$, Alice's optimal measurements change with $\alpha = \frac{2}{\eta_B}(1 - \eta_B)$ and in-turn depend on Bob's detection efficiency η_B , and tend towards compatible measurements as $\alpha \rightarrow 2 - \beta$.

via the relation (30), and therefore, the measurements in the optimal two-qubit realization are unique up to local unitaries. Thus, the maximum quantum violation of symmetrically doubly-tilted CHSH inequalities *self-tests* the optimal measurements. Since the largest eigenvalue of the Bell operator with the optimal measurements is non-degenerate, the maximum quantum violation $c_Q(\alpha, \alpha)$ also self-tests the state partially entangled two-qubit state which corresponding to eigenvector associated with the largest eigenvalue (see FIG. 6). \square

The presented self-testing results rely on ideal experimental conditions. In the next section, we demonstrate the robustness of these results, showing that small deviations from the maximal violation limit the variation from the optimal realization. In the last section, we discuss several key insights based on the self-testing results derived in this section.

3. Robust self-testing

The self-testing statements derived in this work rely on the assumption that the violation of the given Bell inequality is maximal, which is an theoretically idealization due to the inevitability of experimental imperfections. Therefore, the self-testing results must be made robust. The lack an analytical tight SOS decomposition prevents us from studying the robustness of

⁴ An open source version of the Mathematica Notebook can be downloaded from the public folder [GitHub](#).

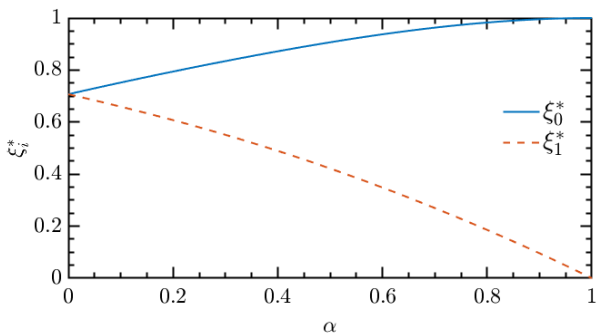


FIG. 6: *Self-testing of non-maximally entangled states:*— A plot of the Schmidt coefficients ζ_i^* of the optimal non-maximally entangled quantum state $|\psi\rangle = \zeta_0^*|00\rangle + \zeta_1^*|11\rangle$ (represented in the Schmidt basis) against $\alpha \in [0, 1]$ for attaining maximum quantum violation of the symmetrically ($\alpha = \beta$) tilted CHSH inequality (12). Notice, as $\alpha = \beta \rightarrow 1$ ($\eta \rightarrow \frac{2}{3}$) the optimal state becomes almost product.

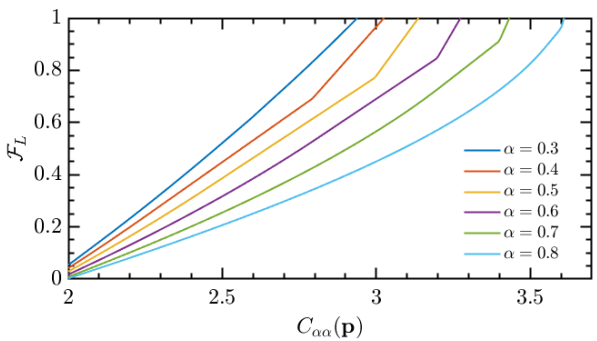


FIG. 7: *Robustness of the self-testing statements:*— A plot of lower bounds \mathcal{F}_L^* on the minimum quantum fidelity $\mathcal{F}_L^* \leq \mathcal{F}^*$ from the level $L = 3$ of NPA hierarchy between the actual state and the optimal self-testing state against the violation $C_{\alpha\alpha}(\mathbf{p})$ of the symmetrically ($\alpha = \beta$) tilted CHSH inequality (12) for tilting parameters $\alpha \in \{0.3, 0.4, 0.5, 0.6, 0.7, 0.8\}$.

these self-testing results analytically. Nevertheless, we can approach this problem by means of the numerical SWAP technique introduced in [36, 37]. The numerical SWAP method utilizes the NPA hierarchy to obtain lower bounds on the closeness (fidelity) of the experimental measurements and the shared state to the ideal self-testing measurements and state. Here we describe the technique for bounding the fidelity between *any* optimal state $|\psi'\rangle$ and the reference self-testing state $|\psi\rangle$. The main idea of this technique relies on the notion of local isometries, which map the actual physical state $|\psi'\rangle$ to our reference self-testing state $|\psi\rangle$ and a junk state $|\text{junk}\rangle$ on auxiliary local degrees of freedom. In particular, the local isometries act as partial SWAP gates, essentially swapping the actual physical

state $|\psi'\rangle$ with the state $|0\rangle^{\otimes N}$ of the registers, such that the final state of the registers corresponds to the reference self-testing state $|\psi\rangle$. The local isometries can be implemented through a SWAP circuit U_{SWAP} , such that the fidelity $\mathcal{F} = \langle \psi | U_{\text{SWAP}} |\psi'\rangle = 1$ for any state $|\psi'\rangle$ maximally violating the Bell inequality.

Consequently, we can cast the problem of certifying whether the behavior \mathbf{p} attaining maximum violation of a Bell inequality self-tests the optimal state $|\psi\rangle$, as that of minimising the fidelity \mathcal{F} , with the behavior subject to the behavior \mathbf{p} admitting a quantum strategy. While this optimisation problem is in general computationally hard, we can relax it as a semidefinite program (SDP) via the NPA hierarchy.

The SWAP circuit U_{SWAP} only depends on the self-testing measurements. The particulars of such U_{SWAP} , specifically those corresponding local isometries, enable us to express the fidelity, $\mathcal{F}_L = \langle \psi | \rho_{\text{SWAP}}(\Gamma_L) | \psi \rangle$, of the final state of the register $\rho_{\text{SWAP}}(\Gamma_L)$ with the reference state $|\psi\rangle$, as a function of the entries of the necessarily positive semi-definite NPA moment matrix Γ_L of level L , as well as of the reference self-testing state $|\psi\rangle$. As some of the entries of the moment matrix Γ_L correspond to experimental behavior, such as $[\Gamma_n]_{\hat{A}'_x, \hat{B}'_y} = \langle \psi' | \hat{A}'_x \hat{B}'_y | \psi' \rangle$, the behavioral preconditions of a self-testing statement translate to linear constraints on the entries of the moment matrix Γ_L . Given a target self-testing state $|\psi\rangle$ and solving the consequent semi-definite minimization program with the fidelity, $\mathcal{F}_L = \langle \psi | \rho_{\text{SWAP}}(\Gamma_L) | \psi \rangle$ as the linear objective function, retrieves a converging sequence of lower bounds, $\mathcal{F}_1^* \leq \mathcal{F}_2^* \leq \dots \leq \mathcal{F}_L^*$ such that $\mathcal{F}_{L \rightarrow \infty}^* = \mathcal{F}^*$, on the minimal quantum fidelity \mathcal{F}^* .

In the figure FIG. 7, we plot a lower bound of the minimal fidelity \mathcal{F}_L^* against the violation of the symmetrically tilted Bell inequality $C_{\alpha\alpha}(\mathbf{p})$, for $\alpha \in \{0.2, 0.4, 0.6, 0.8\}$ obtained with the numerical SWAP method. For these curves, for each α , we used the maximal violation of the doubly-tilted CHSH inequality (20), and the reference optimal state and measurements, derived in the previous section. Since the optimal observables \hat{A}_1 and \hat{B}_1 are given by some linear combination of gates \hat{Z} and \hat{X} in the SWAP circuit, to find the minimum fidelity \mathcal{F}_L , we introduce extra dichotomic operators \hat{A}_2 and \hat{B}_2 to account for the X gate on Alice's and Bob's side and impose the relevant extra constraints by means of localising matrices [36].

We find that level 3 of the NPA hierarchy is enough for producing the fidelity curves for $\alpha < 0.9$, but higher values of α require increasing levels of the hierarchy. We tentatively attribute this effect to the exploding levels of the NPA hierarchy described in the section IV B 1. Observe that the minimal fidelity becomes $\mathcal{F}_L = \mathcal{F} = 1$ when the inequality violation is maximal, indicating that the maximal quantum violation self-tests the optimal state, as expected from the discussion above. In particular, for $\alpha > 0.3$ a clear change in behavior in the fidelity curve is observed when the violation reaches the

maximal local value $C_{\alpha\alpha}(\mathbf{p}) = 2 + 2\alpha$, after which the dependence is almost linear.

V. DISCUSSIONS

The experimental realization of long-range loophole-free nonlocal correlations is a prerequisite for the large-scale adoption of device-independent quantum cryptography. However, a significant hurdle stands in our way: the inevitable loss of photons in optical fibers and the limited efficiencies of detectors. In particular, if the detection efficiencies fall below the critical value, the otherwise nonlocal quantum strategies cease to produce nonlocal correlations. Consequently, extensive research has thus far been devoted to identifying quantum strategies with minimal threshold detection efficiencies. Nonetheless, there is a distinct but significant unaddressed question: what quantum strategies maximize loophole-free nonlocality when detector efficiencies surpass these critical values?

In this work, we addressed the problem of finding the quantum strategies that maximize the loophole-free violation of a given Bell inequality in the presence of inefficient detectors. In Lemma 1, we demonstrate that for *any* Bell inequalities and *any* specification of detection efficiencies, the quantum strategies that yield the maximum loophole-free violation are the ones that maximally violate a tilted version of the Bell inequality. We then focus on the simplest case of the CHSH inequality (10) to retrieve a family of doubly-tilted CHSH inequalities (12). As our main results, we derive *analytical* self-testing statements (Theorem 1) for this family of Bell inequalities, entailing the analytical expressions for the maximum quantum violation and the ensuing optimal quantum strategy. In particular, we note that the maximum violation of the tilted CHSH inequality in Theorem 1 differs from that reported in [13] (see FIG. 4). Additionally, it is worth noting that the nonlocal correlations maximally violating the tilted inequalities in (7) also maximize the guessing probability $\langle A_0 \rangle + \langle B_0 \rangle$, subject to the given CHSH functional value $C(\mathbf{p})$. Consequently, the quantum strategies obtained via Theorem 1 allow us to recover the boundary of the set of quantum correlations on the slice $C(\mathbf{p})$ vs $\langle A_0 \rangle + \langle B_0 \rangle$, plotted in FIG. 2. Furthermore, these quantum strategies have found application in the recently introduced routed Bell experiments [14, 38, 39].

Besides providing a convenient way for finding quantum strategies that generate the maximum loophole-free nonlocality, Lemma 1, and in particular the expression of the tilted Bell inequalities (7), offers crucial insights into the how the optimal quantum behaviors move with the efficiencies of the detectors in the no-signaling polytope. Essentially, with decreasing efficiencies, the hyperplane corresponding to the Bell inequality (7) tilts about a local deterministic point specified by the assignment strategies, in turn moving the optimal strategies along

towards the local polytope \mathcal{L} , and specifically towards the local deterministic point. We exemplify this observation in FIG. 2.

The family of self-testing statements in Theorem 1 and 2 provide crucial insights into how decreasing detector efficiency affects optimal quantum strategies. As illustrated in figure 6, for inefficient detectors $\eta_A, \eta_B < 1$ ($\alpha, \beta > 0$), the optimal strategy requires partially entangled states for maximal loophole-free nonlocality. Observe that the degree of entanglement decreases as the efficiencies approach the critical values (13), as the state becomes almost product. While this finding is in line with observations from the known asymmetric case $\eta_A = 1$ ($\beta = 0$), the optimal measurements present an intriguing deviation. Specifically, in the asymmetric case $\eta_A = 1$ ($\beta = 0$) (17), Alice's optimal measurements remain maximally incompatible irrespective of Bob's detection efficiency $\eta_B \in (1/2, 1]$ ($\alpha \in [0, 2)$), while Bob requires partially incompatible measurements whose incompatibility decreases with his decreasing efficiency η_B (α), approaching almost compatible measurements as $\eta_B \rightarrow 1/2$ ($\alpha \rightarrow 1$). However, the situation changes significantly when both detectors are inefficient. As we illustrate in FIG. 5, in contrast to the asymmetric case, Alice's measurements depend non-trivially on Bob's detection efficiency η_B . Specifically, whenever $\eta_A < 1$ ($\beta > 0$), Alice's optimal measurement tends towards compatible measurements as η_B (α) approaches the critical boundary ($\alpha \rightarrow 2 - \beta$) (13). This observation highlights the natural importance of partially incompatible measurements in device independent cryptography [40]. Finally, as Bell scenarios are linked to prepare and measure scenarios [41], it would be interesting to investigate the implications of our results to prepare and measure experiments with inefficient detectors.

Besides the inferences concerning the maximum effective nonlocality in the presence of inefficient detectors, the analytical results in Theorem 1 and 2 allow us to reveal a fascinating complexity in the characterization of the set of nonlocal quantum correlations in the simplest Bell scenario with the NPA hierarchy. While it is a well-known fact that the NPA hierarchy converges to the set of quantum correlations, lower levels $1 + AB, 2, 3$ were widely believed to be sufficient to characterize extremal quantum correlations in the CHSH scenario. However, in striking contrast to the widely held belief, we demonstrate in FIG. 3 and 4, as the tilting parameters $\alpha, \beta > 0$ approach critical limit $\alpha + \beta \rightarrow 2$, the level of NPA hierarchy required for a tight upper bound increases drastically. This effect is the most pronounced for the symmetric case $\alpha = \beta$ where we find that even level 12 of the NPA hierarchy does not yield tight upper bounds on the maximal violation of the symmetrically tilted CHSH inequalities as $\alpha \rightarrow 1$ (FIG. 4). Crucially, it remains unclear if *any* finite level of NPA will be enough to characterize all extremal quantum correlations in the CHSH scenario. This effect renders the traditional SOS decomposition method impractical for deriving analytical self-

testing statements, and we rely on Jordan’s lemma to retrieve analytical self-testing statements in Theorem 1 and 2.

Even more strikingly, this unexpected feature is observed in those correlation points achieving maximal loophole free nonlocality with detection efficiencies near the critical value, as depicted in FIG. 3, which are realized with almost compatible measurements and almost product states. Since the level $1 + AB$ is enough for the asymmetric case $\beta = 0$ wherein Alice’s optimal measurement remains maximally incompatible, irrespective of the value of α , the effect of exploding NPA levels seems to be linked to the aforementioned complicated dependency of the optimal partially incompatible measurements on the tilting parameters $0 < \alpha, \beta < 2$, and which becomes sharper as the optimal measurements for both parties become almost compatible as $\alpha + \beta \rightarrow 2$. These results then raise the question of whether the complexity of the characterization extremal nonlocal quantum correlation, as measured by the minimum saturating level of the NPA hierarchy is related to the partial incompatibility of the quantum measurements realizing them.

ACKNOWLEDGEMENTS

We would like to thank Tamás Vértesi, Marcin Pawłowski, Jędrzej Kaniewski, Cosmo Lupo, Marcin Wieśniak and Marek Żukowski for insightful discussions. N.G. acknowledges support from CONICET and CIC (R.R.) of Argentina, CONICET PIP Grant No. 11220200101877CO. This project has received funding from the European Union’s Horizon Europe research and innovation program under the project “Quantum Secure Networks Partnership” (QSNP, grant agreement No 101114043), QuantERA/2/2020, an ERA-Net co-fund in Quantum Technologies, under the eDICT project, and INFN through the project “QUANTUM”. The research of M.A. was supported by the European Union–Next Generation UE/MICIU/Plan de Recuperación, Transformación y Resiliencia/Junta de Castilla y León. E.P. acknowledges support by NCN SONATA-BIS grant No. 2017/26/E/ST2/01008. AC acknowledges financial support by NCN grant SONATINA 6 (contract No. UMO-2022/44/C/ST2/00081).

-
- [1] J. S. Bell, On the Einstein Podolsky Rosen paradox, *Physics Physique Fizika* **1**, 195 (1964).
- [2] N. Brunner, D. Cavalcanti, S. Pironio, V. Scarani, and S. Wehner, Bell nonlocality, *Reviews of Modern Physics* **86**, 419 (2014).
- [3] A. K. Ekert, Quantum cryptography based on Bell’s theorem, *Phys. Rev. Lett.* **67**, 661 (1991).
- [4] D. Mayers and A. Yao, Quantum cryptography with imperfect apparatus, in *Proceedings 39th Annual Symposium on Foundations of Computer Science* (IEEE, Los Alamitos, CA, 1998) p. 503.
- [5] J. Barrett, L. Hardy, and A. Kent, No signaling and quantum key distribution, *Phys. Rev. Lett.* **95**, 010503 (2005).
- [6] A. Acín, N. Brunner, N. Gisin, S. Massar, S. Pironio, and V. Scarani, Device-independent security of quantum cryptography against collective attacks, *Phys. Rev. Lett.* **98**, 230501 (2007).
- [7] S. Pironio, A. Acín, N. Brunner, N. Gisin, S. Massar, and V. Scarani, Device-independent quantum key distribution secure against collective attacks, *New J. Phys.* **11**, 045021 (2009).
- [8] Optical fiber loss and attenuation, <https://www.fiberoptics4sale.com/blogs/archive-posts/95048006-optical-fiber-loss-and-attenuation> (2022).
- [9] A. Garg and N. D. Mermin, Detector inefficiencies in the Einstein-Podolsky-Rosen experiment, *Phys. Rev. D* **35**, 3831 (1987).
- [10] P. H. Eberhard, Background level and counter efficiencies required for a loophole-free Einstein-Podolsky-Rosen experiment, *Phys. Rev. A* **47**, R747 (1993).
- [11] S. Massar, Nonlocality, closing the detection loophole, and communication complexity, *Phys. Rev. A* **65**, 032121 (2002).
- [12] T. Vértesi, S. Pironio, and N. Brunner, Closing the detection loophole in Bell experiments using qudits, *Phys. Rev. Lett.* **104**, 060401 (2010).
- [13] N. Miklin, A. Chaturvedi, M. Bourennane, M. Pawłowski, and A. Cabello, Exponentially decreasing critical detection efficiency for any Bell inequality, *Phys. Rev. Lett.* **129**, 230403 (2022).
- [14] A. Chaturvedi, G. Viola, and M. Pawłowski, Extending loophole-free nonlocal correlations to arbitrarily large distances, *npj Quantum Information* **10**, 7 (2024).
- [15] M. Farkas, M. Balanzó-Juandó, K. Łukanowski, J. Kołodyński, and A. Acín, Bell nonlocality is not sufficient for the security of standard device-independent quantum key distribution protocols, *Phys. Rev. Lett.* **127**, 050503 (2021).
- [16] P. H. Eberhard and P. Rosset, Bell’s theorem based on a generalized EPR criterion of reality, *Found. Phys.* **25**, 91 (1995).
- [17] C. Branciard, Detection loophole in Bell experiments: How postselection modifies the requirements to observe nonlocality, *Phys. Rev. A* **83**, 032123 (2011).
- [18] C. Bamps and S. Pironio, Sum-of-squares decompositions for a family of Clauser-Horne-Shimony-Holt-like inequalities and their application to self-testing, *Phys. Rev. A* **91**, 052111 (2015).
- [19] A. Acín, S. Massar, and S. Pironio, Randomness versus nonlocality and entanglement, *Phys. Rev. Lett.* **108**, 100402 (2012).
- [20] R. Bhatia, *Matrix Analysis*, Graduate Texts in Mathematics (Springer New York, 2013).
- [21] N. Brunner, D. Cavalcanti, S. Pironio, V. Scarani, and S. Wehner, Bell nonlocality, *Rev. Mod. Phys.* **86**, 419 (2014).
- [22] M. Araújo, F. Hirsch, and M. T. Quintino, Bell nonlocality with a single shot, *Quantum* **4**, 353 (2020).

- [23] P. Mironowicz, Semi-definite programming and quantum information, *Journal of Physics A: Mathematical and Theoretical* (2023).
- [24] N. Gigena, G. Scala, and A. Mandarino, Revisited aspects of the local set in CHSH Bell scenario, *International Journal of Quantum Information* [10.1142/s0219749923400051](https://doi.org/10.1142/s0219749923400051) (2022).
- [25] A. Cabello and J.-A. Larsson, Minimum detection efficiency for a loophole-free atom-photon Bell experiment, *Phys. Rev. Lett.* **98**, 220402 (2007).
- [26] J. Barrett, N. Linden, S. Massar, S. Pironio, S. Popescu, and D. Roberts, Nonlocal correlations as an information-theoretic resource, *Phys. Rev. A* **71**, 022101 (2005).
- [27] T. Cope and R. Colbeck, Bell inequalities from no-signaling distributions, *Phys. Rev. A* **100**, 022114 (2019).
- [28] I. Šupić and J. Bowles, Self-testing of quantum systems: a review, *Quantum* **4**, 337 (2020).
- [29] M. Navascués, S. Pironio, and A. Acín, Bounding the set of quantum correlations, *Phys. Rev. Lett.* **98**, 010401 (2007).
- [30] A. Garner and M. Araújo, Moment, <https://github.com/ajpgarner/moment> (2023).
- [31] J. Löfberg, YALMIP: a toolbox for modeling and optimization in MATLAB, in *Proceedings of the CACSD Conference* (Taipei, Taiwan, 2004) pp. 284–289, <https://yalmip.github.io/>.
- [32] M. Nakata, A numerical evaluation of highly accurate multiple-precision arithmetic version of semidefinite programming solver: SDPA-GMP, -QD and -DD., in *2010 IEEE International Symposium on Computer-Aided Control System Design* (2010) pp. 29–34, <https://github.com/nakatamaho/sdpa-gmp>, <https://github.com/nakatamaho/sdpa-qd>, <https://github.com/nakatamaho/sdpa-dd>.
- [33] L. Masanes, Extremal quantum correlations for N parties with two dichotomic observables per site (2005), [arXiv:quant-ph/0512100](https://arxiv.org/abs/quant-ph/0512100) [quant-ph].
- [34] I. Šupić and J. Bowles, Self-testing of quantum systems: a review, *Quantum* **4**, 337 (2020).
- [35] E. Panwar, P. Pandya, and M. Wieśniak, An elegant scheme of self-testing for multipartite Bell inequalities, *npj Quantum Information* **9**, 71 (2023).
- [36] J.-D. Bancal, M. Navascués, V. Scarani, T. Vértesi, and T. H. Yang, Physical characterization of quantum devices from nonlocal correlations, *Phys. Rev. A* **91**, 022115 (2015).
- [37] T. H. Yang, T. Vértesi, J.-D. Bancal, V. Scarani, and M. Navascués, Robust and versatile black-box certification of quantum devices, *Phys. Rev. Lett.* **113**, 040401 (2014).
- [38] E. P. Lobo, J. Pauwels, and S. Pironio, Certifying long-range quantum correlations through routed Bell tests, *Quantum* **8**, 1332 (2024).
- [39] T. L. Roy-Deloison, E. P. Lobo, J. Pauwels, and S. Pironio, Device-independent quantum key distribution based on routed Bell tests (2024), [arXiv:2404.01202](https://arxiv.org/abs/2404.01202) [quant-ph].
- [40] M. Masini, M. Ioannou, N. Brunner, S. Pironio, and P. Sekatski, Joint-measurability and quantum communication with untrusted devices (2024), [arXiv:2403.14785](https://arxiv.org/abs/2403.14785) [quant-ph].
- [41] G. Scala, S. A. Ghoreishi, and M. Pawłowski, Advantages of quantum communication revealed by the reexamination of hyperbit theory limitations, *Phys. Rev. A* **109**, 022230 (2024).
- [42] R. Augusiak, M. Demianowicz, and P. Horodecki, Universal observable detecting all two-qubit entanglement and determinant-based separability tests, *Phys. Rev. A* **77**, 030301 (2008).

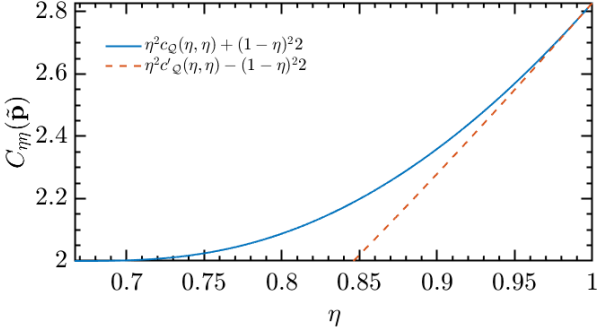


FIG. 8: *Optimal assignment strategy for maximum loophole-free violation of the CHSH inequality*:— A plot comparing the maximum effective violation of the CHSH inequality (solid blue line) with the assignment strategy considered in the main text

$C_{\eta\eta}(\tilde{\mathbf{p}}) = \eta^2 c_{\mathcal{Q}}(\eta, \eta) + (1 - \eta)^2 2$ (12), and the maximum effective violation of the CHSH inequality with the other representative assignment strategy $C_{\eta\eta}(\tilde{\mathbf{p}}) = \eta^2 c'_{\mathcal{Q}}(\eta, \eta) + (1 - \eta)^2 2$ (A4) (dashed orange curve). The plot demonstrates that the assignment strategy considered in the main text is optimal.

Appendix A: Optimal local assignment strategy for maximum loophole-free violation of the CHSH inequality

To any given Bell inequality $\beta(\mathbf{p}) \leq \beta_{\mathcal{L}}$ Lemma 1 associates a family of tilted Bell inequalities of the form (7),

$$\begin{aligned} \beta_{\eta_A \eta_B}(\mathbf{p}) &= \beta(\mathbf{p}) + \frac{1 - \eta_B}{\eta_B} \sum_{a,x} c_a^x p_A(a|x) \\ &\quad + \frac{1 - \eta_A}{\eta_A} \sum_{b,y} c_b^y p_B(b|y) \\ &\leq \beta_{\mathcal{L}}(\eta_A, \eta_B), \end{aligned} \quad (\text{A1})$$

As the coefficients $c_a^x = \sum_y c_{aby}^{xy}$, $c_b^y = \sum_x c_{axb}^{xy}$ depend on the deterministic assignment strategy $q_A(a|x) = \delta_{a,a_x}$, $q_B(b|y) = \delta_{b,b_y}$, to maximum the effective violation $\beta(\tilde{\mathbf{p}}) - \beta_{\mathcal{L}}$ an optimal assignment strategy must be chosen, such that for any specification of detection efficiencies η_A, η_B , the maximum effective violation of the original Bell inequality $\beta(\tilde{\mathbf{p}})$ corresponds to the maximum violation $\beta_{\mathcal{Q}}(\eta_A, \eta_B)$ of the corresponding tilted Bell inequality.

In the CHSH scenario, there are 16 such strategies, which can be labeled by four bits $s_A, s_B, r_A, r_B \in \{0, 1\}$ specifying the possible values of the marginals $\langle A_x \rangle = (-1)^{r_A x + s_A}$ and $\langle B_y \rangle = (-1)^{r_B y + s_B}$. For any such a deterministic strategy we obtain the following tilted family

of CHSH functionals,

$$\begin{aligned} C_{\eta_A \eta_B}^{(s_A, s_B, r_A, r_B)}(\mathbf{p}) &= \sum_{x,y} (-1)^{x \cdot y} \langle A_x B_y \rangle + \\ &\quad + \frac{2(1 - \eta_B)}{\eta_B} \sum_x (1 + (-1)^{r_B + x}) (-1)^{s_B} \langle A_x \rangle \\ &\quad + \frac{2(1 - \eta_A)}{\eta_A} \sum_y (1 + (-1)^{r_A + y}) (-1)^{s_A} \langle B_y \rangle \end{aligned} \quad (\text{A2})$$

Also, any such deterministic strategy the effective violation of the CHSH inequality for is given by,

$$\begin{aligned} C(\tilde{\mathbf{p}}) &= \eta_A \eta_B C_{\eta_A \eta_B}^{(s_A, s_B, r_A, r_B)}(\mathbf{p}) \\ &\quad + 2(1 - \eta_A)(1 - \eta_B) (-1)^{s_A + s_B + r_A r_B}. \end{aligned} \quad (\text{A3})$$

Consequently, for any specification of the efficiency, η_A, η_B , the optimal deterministic assignment strategy will be the one which yields maximum effective violation (A3) of the CHSH inequality. The same holds for the other 8 strategies satisfying $s_A + s_B + r_A r_B = 1 \pmod{2}$. Thus, to find the optimal strategy we need only to compare representatives of each class, namely, the cases $r_A = r_B = s_A = s_B = 0$ and $r_A = r_B = s_B = 0, s_A = 1$. While former strategy yields the doubly-tilted CHSH inequality (12) considered in the main text, the later corresponds to following distinct doubly-tilted CHSH inequality,

$$\begin{aligned} C'_{\eta_A \eta_B}(\mathbf{p}) &= C(\tilde{\mathbf{p}}) + \frac{2}{\eta_B} (1 - \eta_B) \langle A_0 \rangle \frac{2}{\eta_A} (1 - \eta_A) \langle B_0 \rangle \\ &\leq 2 \left[1 - \frac{1}{\eta_A} - \frac{1}{\eta_B} \right] = c'_{\mathcal{L}}(\eta_A, \eta_B). \end{aligned} \quad (\text{A4})$$

We use the proof technique described in Section IV B, to retrieve the analytical expression for the maximum violation $c'_{\mathcal{Q}}(\eta_A, \eta_B)$ of (A4) and compare corresponding effective violation of the CHSH inequality (A3) to the one obtained from the maximum violation $c_{\mathcal{Q}}(\eta_A, \eta_B)$ doubly-tilted CHSH inequality (12). We find that, for all η_A, η_B the doubly-tilted CHSH inequality considered in the main text (12) yields higher effective violation of the CHSH inequality (see FIG. 8).

Appendix B: Self-testing of doubly-tilted CHSH inequalities

In this section, we present the analytical self-testing statements for the entire family of doubly-tilted CHSH inequalities (12).

Theorem 2. [Self-testing of doubly-tilted CHSH inequalities] *The maximum quantum violation $c_{\mathcal{Q}}(\alpha, \beta)$ of the doubly-tilted CHSH inequality (12) is the largest root of the degree 6 polynomial,*

$$f(\lambda) = 4\lambda^6 - 4\alpha\beta\lambda^5 + \sum_{k=0}^4 \tau_k \lambda^k \quad (\text{B1})$$

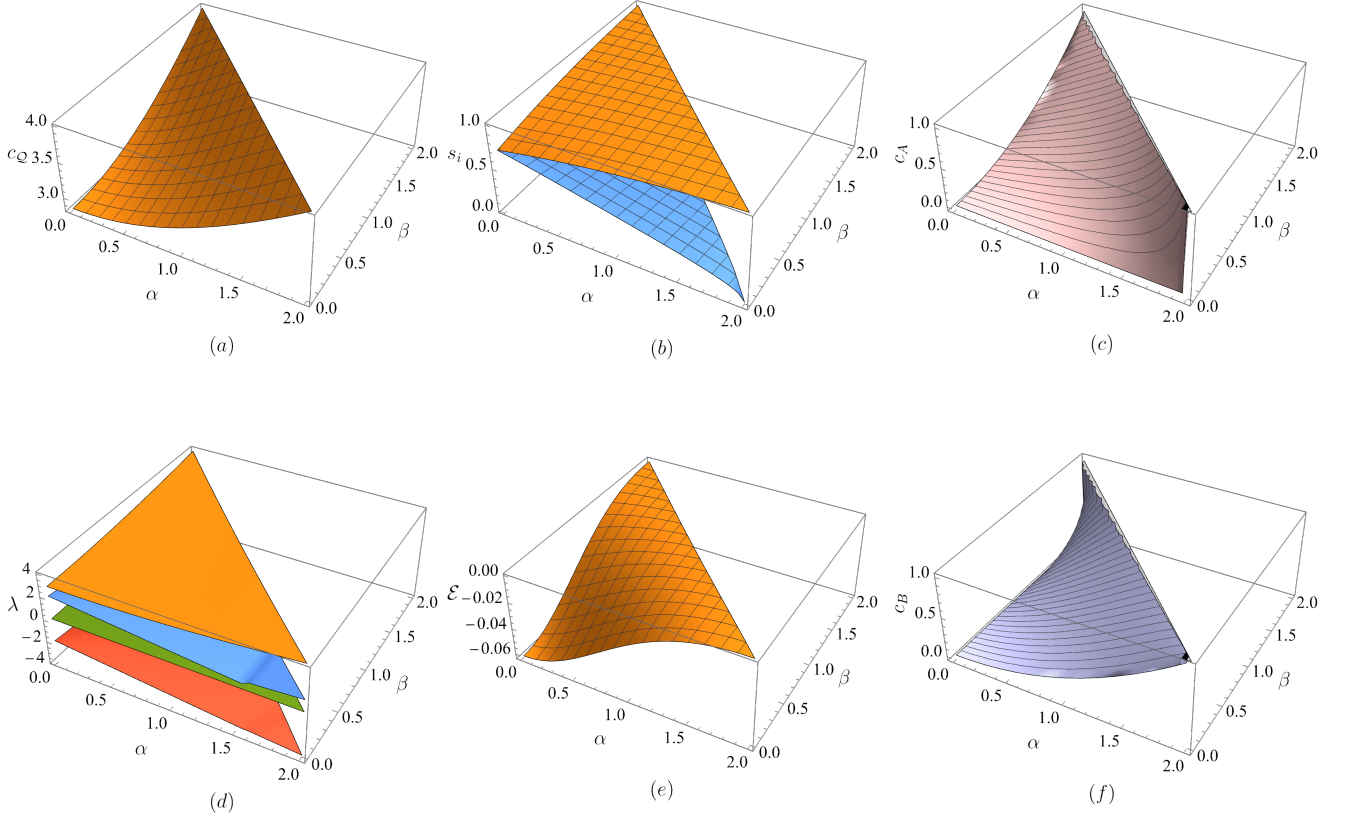


FIG. 9: Summary of result for not equal efficient detectors (α, β) . (a) Optimal quantum value as the largest eigenvalue of \hat{C} . (d) all the non-degenerate eigenvalues of \hat{C} (the largest is zoomed in (a)). (b) The Schmidt decomposition of the optimal quantum state $|\psi\rangle = s_0|00\rangle + s_1|11\rangle$ and a negative measure of entanglement in [42] on $|\psi\rangle$ in (e). In (c) and (f) respectively the (mirroring in $\alpha \leftrightarrow \beta$) optimal Alice and Bob's settings in terms of c_A (the mesh lines are detailed in FIG. 5) and c_B .

and $C_{\alpha\beta}(\mathbf{p}) = c_Q(\alpha, \beta)$ self-tests a two qubit quantum strategy with optimal (*) local observables of the form (28), such that, Alice's optimal cosine $c_A^*(\alpha, \beta)$ corresponds to the largest real root of the following degree 6 polynomial,

$$g_A(c) = 16(\alpha^2 - 4)^2 c^6 - 8(\alpha^2 - 4)^2 (5\beta^2 - 8) c^5 + \sum_{k=0}^4 \zeta_k c^k \quad (\text{B2})$$

and Bob's optimal cosine $c_B^*(\alpha, \beta)$ corresponds to the largest real root of a degree 6 polynomial $g_B(c)$ obtained from $g_A(c)$ by interchanging tilting parameters α, β . The remained coefficients of the polynomials are the following:

$$\begin{aligned} \tau_4 &= 11\alpha^2\beta^2 - 16(\alpha^2 + \beta^2) - 64 \\ \tau_3 &= 8\alpha^3\beta^3 - 24(\alpha^3\beta + \alpha\beta^3) + 96\alpha\beta \\ \tau_2 &= 20(\alpha^4 + \beta^4) - 6(\alpha^4\beta^2 + \alpha^2\beta^4) - 64\alpha^2\beta^2 \\ &\quad + 96(\alpha^2 + \beta^2) + 320 \end{aligned}$$

$$\begin{aligned} \tau_1 &= 60(\alpha^5\beta + \alpha\beta^5) - 168\alpha^3\beta^3 + 160(\alpha^3\beta + \alpha\beta^3) - 576\alpha\beta \\ \tau_0 &= 27(\alpha^6\beta^2 + \alpha^2\beta^6) - 54\alpha^4\beta^4 + 48(\alpha^4\beta^2 + \alpha^2\beta^4) \\ &\quad - 8(\alpha^6 + \beta^6) - 400\alpha^2\beta^2 + 32(\alpha^4 + \beta^4) \\ &\quad + 128(\alpha^2 + \beta^2) - 512 \end{aligned} \quad (\text{B3})$$

with

$$\begin{aligned} \zeta_4 &= (\alpha^2 - 4)[\alpha^2(33\beta^4 - 96\beta^2 + 96) \\ &\quad - 4(41\beta^4 - 128\beta^2 + 96)] \\ \zeta_3 &= -4(\alpha^2 - 4)[2(\alpha^2 - 11)\beta^6 - 5(\alpha^2 - 20)\beta^4 \\ &\quad + 12(\alpha^2 - 12)\beta^2 - 16(\alpha^2 - 4)] \\ \zeta_2 &= 2a^2[\alpha^4(3\beta^6 - 5\beta^4 + 8) - \alpha^2(9\beta^8 - 24\beta^6 + 8\beta^4 + 64) \\ &\quad + 4(\beta^2 - 2)^2(13\beta^4 - 24\beta^2 + 8)] \end{aligned}$$

$$\begin{aligned}
\zeta_1 &= -4\beta^2[\alpha^4(\beta^4 - 5\beta^2 + 10) + 4(\beta^2 - 2)^3(\beta^2 - 1) \\
&\quad + \alpha^2(-5\beta^6 + 34\beta^4 - 88\beta^2 + 80)] \\
\zeta_0 &= \beta^2[\alpha^4(\beta^6 - 10\beta^4 + 33\beta^2 - 32) \\
&\quad - 2\alpha^2(\beta^2 - 2)^2(\beta^4 - 7\beta^2 + 16) + \beta^2(\beta^2 - 2)^4]
\end{aligned} \tag{B4}$$

Proof. Here, we present a comprehensive overview of the proof-technique while the complete proof is contained in the accompanying Mathematica notebook. As discussed in above Section IV B, Jordan's lemma lets us express the Bell operator $\hat{C}_{\alpha\beta}$ associated with the family of doubly-tilted CHSH inequalities (12) as a two-qubit operator,

$$\hat{C}_{\alpha\beta} = \sum_{x,y} (-1)^{x \cdot y} \hat{A}_x \otimes \hat{B}_y + \alpha(\hat{A}_0 \otimes \mathbb{I}_2) + \beta(\mathbb{I}_2 \otimes \hat{B}_0). \tag{B5}$$

With the parametrization (28), the Bell operator $\hat{C}_{\alpha\beta}$, now a function of just two cosines $c_A, c_B \in [0, 1]$, has the following four dimensional matrix representation:

$$\begin{pmatrix}
\omega + s_+ & s_B - c_A s_B & s_A - c_B s_A & -s_A s_B \\
s_B - c_A s_B & -\omega + s_- & -s_A s_B & (c_B - 1)s_A \\
s_A - c_B s_A & -s_A s_B & -\omega - s_- & (c_A - 1)s_B \\
-s_A s_B & (c_B - 1)s_A & (c_A - 1)s_B & \omega - s_+
\end{pmatrix} \tag{B6}$$

with $s_{\pm} = \alpha \pm \beta$ and $\omega = 1 + c_A + c_B - c_B c_A$. Now, for fixed cosines c_A, c_B , the maximum quantum violation corresponds to the largest eigenvalue of the matrix (B6), i.e., the largest root of its characteristic polynomial $q(\lambda, c_A, c_B, \alpha, \beta) \equiv \sum_{k=0}^4 \gamma_k \lambda^k$ with,

$$\gamma_0 = (\alpha^2 - \beta^2)^2 - 8[\alpha^2(a^2(-b) + a^2 + b) + \beta^2(-ab^2 + a + b^2) - 2(b^2 + a^2) - a^2 b^2] \tag{B7}$$

$$\gamma_1 = 8\alpha\beta(ab - a - b - 1) \tag{B8}$$

$$\gamma_2 = -2(4 + \alpha^2 + \beta^2), \quad \gamma_3 = 0, \quad \gamma_4 = 1. \tag{B9}$$

where λ denotes the eigenvalue of the matrix (32). Thus, finding $c_Q(\alpha, \beta)$ boils down to maximizing the largest root of the characteristic polynomial (33) over the cosines c_A and c_B . We now employ the self-testing proof technique described in Section IV B, which utilizes Gröbner basis elimination to retrieve the analytical solutions (B1),(B2) for the maximum violation $c_Q(\alpha, \beta)$ and the optimal cosines $c_A^*(\alpha, \beta), c_B^*(\alpha, \beta)$, respectively.

Following the proof-technique in Section IV B, we use the Lagrange multipliers method. The Lagrangian for this problem reads,

$$L = \lambda + s \cdot q(\lambda, c_A, c_B, \alpha, \beta) \tag{B10}$$

where s is a Lagrange multiplier. Consequently, the stationary points must satisfy the conditions, $\partial_{c_A} L = \partial_{c_B} L = \partial_s L = 0$, which in-turn imply the following polynomial conditions,

$$\begin{cases}
q(\lambda, c_A, c_B, \alpha, \beta) = 0 \\
q_{c_A}(\lambda, c_A, c_B, \alpha, \beta) = \partial_{c_A} q(\lambda, c_A, c_B, \alpha, \beta) = 0 \\
q_{c_B}(\lambda, c_A, c_B, \alpha, \beta) = \partial_{c_B} q(\lambda, c_A, c_B, \alpha, \beta) = 0
\end{cases} \tag{B11}$$

Consequently, the cosines parameterizing the optimal observables $c_A^*(\alpha, \beta), c_B^*(\alpha, \beta)$ and the maximum quantum violation $c_Q(\alpha, \beta) = \lambda^*(\alpha, \beta)$ are common roots of the polynomials q, q_{c_A}, q_{c_B} in (B11). We now use the Gröbner basis elimination on q, q_{c_A}, q_{c_B} to eliminate the cosines c_A, c_B and retrieve a polynomial $f_0(\lambda)$ of degree 12. We then take the polynomial quotient of $f_0(\lambda)$ with respect to the polynomials corresponding to six trivial and sub-optimal roots to retrieve the desired degree six polynomial $f(\lambda)$ (B1). The maximum quantum violation $c_Q(\alpha, \beta)$ corresponds to the largest real root of the polynomial $f(\lambda)$. Similarly, to find the analytical solution for Alice's optimal cosine $c_A^*(\alpha, \beta)$, we eliminate c_B, λ using Gröbner basis elimination on q, q_{c_A}, q_{c_B} . This results in a degree 13 polynomial $g_0(c)$. We then take the polynomial quotient of $g_0(c)$ with respect to the polynomials corresponding to seven trivial and sub-optimal roots to obtain the degree 6 polynomial $g_A(c)$ (B2). Repeating the same procedure for Bob, we end up with a degree 6 polynomial $g_B(c)$ which equivalent to $g_A(c)$ in (36) up on interchanging the tilting parameters α, β . We find that optimal cosines $c_A^*(\alpha, \beta), c_B^*(\alpha, \beta)$ correspond to the largest real root of the polynomials $g_A(c)$ and $g_B(c)$, respectively.

Observe that in the interval $[0, \pi]$ the angles θ_A^*, θ_B^* between optimal measurements is uniquely determined by $c_Q(\alpha, \alpha)$ via the relation (30), and therefore, the measurements in the optimal two-qubit realization are unique up to local unitaries. Thus, the maximum quantum violation of doubly-tilted CHSH inequalities $\hat{C}_{\alpha\beta}(\mathbf{p}) = c_Q(\alpha, \beta)$ self-tests the optimal measurements. Alternatively, once g_A and g_B are determined the c_A and c_B depend only on α and β . Therefore the optimal quantum value can be also obtained as roots of the quartic characteristic polynomial q of $\hat{C}_{\alpha, \beta}$ that reads as

$$\lambda = \pm_t \frac{\sqrt{\zeta}}{2} \pm_s \sqrt{\kappa \mp_t \frac{\gamma_1}{2\sqrt{\zeta}}}, \tag{B12}$$

where

$$\zeta = 2\gamma_2^3 - 72\gamma_0\gamma_2 + 27\gamma_1^2 + \sqrt{(2\gamma_2^3 - 72\gamma_0\gamma_2 + 27\gamma_1^2)^2 - 4(\gamma_2^2 + 12\gamma_0)^3}$$

$$\zeta = \frac{1}{3} \left((\gamma_2^2 + 12\gamma_0) \sqrt[3]{\frac{2}{\zeta}} - 2\gamma_2 + \sqrt[3]{\frac{\zeta}{2}} \right)$$

$$\kappa = -\frac{\sqrt[3]{\zeta}}{12\sqrt[3]{2}} - \frac{\gamma_2}{3} - \frac{\gamma_2^2 + 12\gamma_0}{3\sqrt[3]{32\zeta}}$$

The two \pm_t both have the same sign, while the sign of \pm_s is independent. Given that $\gamma_1 < 0$, the maximum quantum violation $c_Q(\alpha, \beta)$ has the expression,

$$c_Q(\alpha, \beta) = \frac{\sqrt{\zeta}}{2} + \sqrt{\kappa - \frac{\gamma_1}{2\sqrt{\zeta}}}. \tag{B13}$$

Since the largest eigenvalue of the Bell operator with the optimal measurements is non-degenerate (see FIG. 9), the maximum quantum violation $c_Q(\alpha, \beta)$ also self-tests the state partially entangled two-qubit state $|\psi\rangle$ (the eigenvector corresponding to the largest eigen-

value). FIG. 9.b shows its Schmidt coefficients. \square

All the results for the generalized case $\alpha \neq \beta$ are summarized in the FIG. 9.

Quantitative Nonclassicality of Mediated Interactions

Ray Ganardi^{1,2,*}, Ekta Panwar,^{1,3} Mahasweta Pandit,^{1,4} Bianka Woloncewicz,^{1,3,5}
and Tomasz Paterek^{1,6}

¹*Institute of Theoretical Physics and Astrophysics, Faculty of Mathematics, Physics and Informatics,
University of Gdańsk, Gdańsk 80-308, Poland*

²*Centre for Quantum Optical Technologies, Centre of New Technologies, University of Warsaw,
Warsaw 02-097, Poland*

³*International Centre for Theory of Quantum Technologies, University of Gdańsk, Gdańsk 80-308, Poland*

⁴*Departamento de Física, Universidad de Murcia, Murcia E-30071, Spain*

⁵*Quantum Research Center, Technology Innovation Institute, Masdar City, Abu Dhabi, United Arab Emirates*

⁶*School of Mathematics and Physics, Xiamen University Malaysia, Sepang 43900, Malaysia*



(Received 24 March 2023; accepted 30 November 2023; published 6 February 2024)

In a plethora of physical situations, one can distinguish a mediator—a system that couples other, non-interacting, systems. Often, the mediator itself is not directly accessible to experimentation, yet it is interesting and sometimes crucial to understand if it admits nonclassical properties. An example of this sort that has recently been enjoying considerable attention is that of two quantum masses coupled via a gravitational field. It has been argued that the gain of quantum entanglement between the masses indicates nonclassicality of the states of the whole tripartite system. Here, we focus on the nonclassical properties of the involved interactions rather than the states. We derive inequalities the violation of which indicates noncommutativity and nondecomposability (open-system generalization of noncommuting unitaries) of interactions through the mediators. The derivations are based on properties of general quantum formalism and make minimalistic assumptions about the studied systems; in particular, the interactions can remain uncharacterized throughout the assessment. Furthermore, we also present conditions that solely use correlations between the coupled systems, excluding the need to measure the mediator. Next, we show that the amount of violation places a lower bound on suitably defined degree of nondecomposability. This makes the methods quantitative and at the same time experiment ready. We give applications of these techniques in two different fields: for detecting the nonclassicality of gravitational interaction and in bounding the Trotter error in quantum simulations.

DOI: [10.1103/PRXQuantum.5.010318](https://doi.org/10.1103/PRXQuantum.5.010318)

I. INTRODUCTION

Mediated interactions are very common and often the mediators are practically inaccessible to direct experimentation. For example, consider a system of unpaired spins interacting via spin chains in solids [1]. The bulk measurements of magnetic properties are argued to be solely determined by the unpaired spins at the end of the chain, making the chain experimentally inaccessible. As another example, consider light modes interacting via mechanical membranes [2]. In this case, usually it is only the light that

is being monitored. Furthermore, fundamentally electric charges are coupled via an electromagnetic field, etc. All these scenarios share a common structure in which systems A and B do not interact directly but are solely coupled via a mediator system, M (see Fig. 1). Already at this general level, one can ask about the properties of the mediator that can be deduced from the dynamics of the coupled systems.

In this line of study, methods have been proposed to witness the nonclassicality of the state of the mediator from the correlation dynamics of the coupled probes. In particular, conditions have been derived under which the gain of quantum entanglement implies that the mediator must have explored nonorthogonal states during the dynamics [3,4]. Similar ideas, applied to more general models than the canonical quantum formalism, have been used to argue that the entanglement gain between quantum masses witnesses nonclassical gravity [5,6] and have motivated a number of concrete proposals aimed at experimental demonstration of

*ray@ganardi.xyz

Published by the American Physical Society under the terms of the [Creative Commons Attribution 4.0 International](https://creativecommons.org/licenses/by/4.0/) license. Further distribution of this work must maintain attribution to the author(s) and the published article's title, journal citation, and DOI.

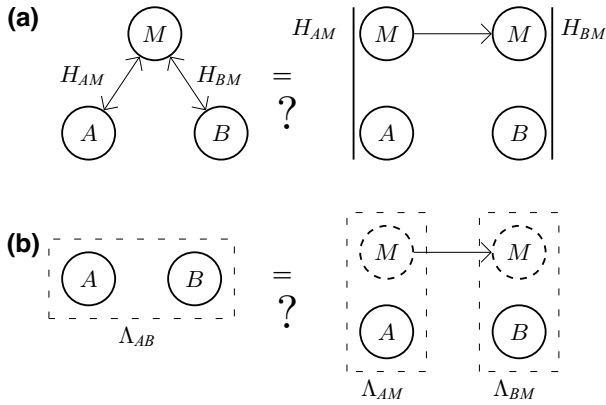


FIG. 1. Mediated interactions. (a) Systems A and B are coupled via mediator M , i.e., the underlying Hamiltonian is $H_{AM} + H_{BM}$ and it explicitly excludes direct coupling between the systems, i.e., H_{AB} . We present methods based on correlations showing that the interaction Hamiltonians do not commute, i.e., the tripartite dynamics cannot be understood as a sequence of interactions via H_{AM} and then H_{BM} or in reverse order. We also quantify this noncommutativity by providing a lower bound on a suitable norm of the commutator $[H_{AM}, H_{BM}]$. These notions are generalized to open systems and we emphasize that the tools make minimalistic assumptions about the whole setup. (b) We extend these techniques to cases in which the mediator is nonaccessible. They are based on correlations in system AB only and show that the tripartite dynamics cannot be understood as a sequence of interactions described by dynamical maps Λ_{AM} and Λ_{BM} or in reverse order. We also quantify this form of nondecomposability.

gravity-induced entanglement (see, e.g., Refs. [7–17]). A considerable advantage of these methods is due to the minimalistic assumptions that they make about the physical systems involved. They are independent of the initial state, the dimensions of the involved systems, or the explicit form of interactions and they also work in the presence of local environments. Accordingly, they are applicable in a variety of fields (see, e.g., Refs. [18,19] for examples in quantum biology and solid-state physics, respectively).

Here, we move on from the nonclassicality of states and develop tools to quantify the amount of nonclassicality of mediated *interactions*, while retaining minimalistic assumptions about the considered physical systems. The notion of nonclassicality that we employ is given by the commutativity of interaction Hamiltonians in the case of closed dynamics, which generalizes to the decomposability of dynamical maps, which also encompasses open systems. Arguments supporting this choice are given in Sec. II. A method to detect the presence of such nonclassicality was first presented in Ref. [20] but it was only qualitative, i.e., it could only witness the presence of noncommutativity. It is intriguing that the methods mentioned earlier, aimed at the nonclassicality of states, are also at this qualitative level at the present moment. Our main contribution here

is the development of methods to quantify the amount of nonclassicality. We derive conditions that lower bound the norm of the commutator as well as a suitably defined distance to decomposable maps. These conditions are of two types and the structure of the paper reflects this division. In Sec. III, we assume that the mediator is accessible to experimentation and in Sec. IV, the derived conditions use only data measured on the probes. Nontrivial bounds are derived for any continuous correlation measure. Hence, it is again expected that the methods presented are applicable in a variety of fields. We provide two examples.

The first one is in the field of quantum simulations. Suzuki-Trotter expansion is a common way to simulate arbitrary sums of local Hamiltonians (see, e.g., Refs. [21,22]). It has recently been shown that the number of Trotter steps needed to obtain the required simulation error scales with the spectral norm of the commutator [23]. We link this norm to the correlations in the system, showing a quantitative relation between the complexity of the simulation and the amount of correlations.

As the second example, the methods detect and measure the noncommutativity of the gravitational interaction coupling two quantum masses. The idea of detecting the nonclassicality of gravitational interaction has been discussed very recently in Ref. [24] but there the notion of nonclassicality is different, based on the impossibility of simulating the dynamics via local operations and classical communication. Within the quantum formalism, local operations are modeled by arbitrary local channels and classical communication by sequences of dephasing channels connecting the communicating parties. In the tripartite setting of two masses and gravitational field, this means the following sequence: λ_{AM} , DEPHASING(M), λ_{BM} , DEPHASING(M), etc. In principle, different dephasing maps could even be performed in different bases. In contradistinction, the definition that we adopt in the present work deals with dynamics that are continuous in time and defines classicality at the level of Hamiltonians, as their commutativity. This implies an effective picture in which a *quantum* mediator is transmitted between “communicating” parties, but only one way. So, in the tripartite setting, this means $U_{AM}U_{BM}$ or in reverse order. For other ways of revealing that the evolution cannot be understood in terms of classical (gravitational) field, see also Refs. [25,26], and for general arguments that any system capable of coupling to a quantum system must itself be quantized, see, e.g., Ref. [27]. Our tools show that correlations between the masses exclude gravity as a form of interaction with commuting particle-field couplings.

II. CLASSICALITY AND DECOMPOSABILITY

Let us start with closed systems and explain our choice of the notion of classicality and its relation to the properties

of dynamical maps. In this work, classical mediated interactions are defined by commuting Hamiltonians H_{AM} and H_{BM} (see Fig. 1). A high-level motivation for this choice comes from the fact that in classical mechanics, all observables commute; hence a classical mediator would have all its couplings to other systems commuting. The commutativity can also be motivated starting with the notion of classical states as those admitting vanishing quantum discord [28], or vanishing coherence in the case of a single system [29], and asking for the evolution that preserves this form of classicality. The vanishing discord means that the whole tripartite state can be measured on the mediator without disturbing the total state. Mathematically, the state has a block-diagonal form and we assume that at all times there exists a single “preferred” basis of the mediator. We show in Appendix A that such dynamics are generated if and only if the Hamiltonian has a block-diagonal form too, with the same basis on the mediator. Since, here, we consider systems with global Hamiltonian $H = H_{AM} + H_{BM}$, the state classicality is preserved when both H_{AM} and H_{BM} are block diagonal with the same basis on system M , i.e., both Hamiltonians commute $[H_{AM}, H_{BM}] = 0$. Furthermore, for commuting nondegenerate H_{AM} and H_{BM} , the total Hamiltonian admits only product eigenstates and out-of-time-ordered correlators vanish at all times, as shown in Appendix A.

A closely related notion is that of decomposability. A tripartite unitary U is decomposable if there exist unitaries U_{AM} and U_{BM} such that

$$U = U_{BM}U_{AM}. \quad (1)$$

Intuitively, decomposable unitaries are those that can be simulated by first coupling one of the systems to the mediator M and then coupling the other. One can picture that the mediator particle is being transmitted between A and B , which are in separate laboratories, making this setting similar to that in Refs. [30–36]. Although the Suzuki-Trotter formula shows that any unitary can be approximated by a sequence of Trotter steps, decomposable unitaries are special because we can implement the exact unitary with only a single Trotter step. For its relation to the notion of locality in quantum field theory, see Ref. [37].

Clearly, for classical interactions $[H_{AM}, H_{BM}] = 0$, the unitary operator $U(t) = e^{-itH}$ is decomposable for all t . But there exist unitaries that are decomposable and yet are not generated by a classical interaction. A concrete example is given in Appendix A 4 and relies on the fact that the unitary can be written as $U = U_{BM}U_{AM}$, but there exist no unitaries V_{AM} and V_{BM} such that the sequence $V_{AM}V_{BM}$ would be equal to U . This example already suggests that decomposability has to be augmented with commutativity of decompositions to be equivalent to the classicality of interactions, a fact that we prove in Appendix A 5. Therefore,

the unitary generated by classical interactions is continuously decomposable, with the added property that the decomposition must commute, i.e., $[U_{AM}(t), U_{BM}(t)] = 0$ for all t . Accordingly, it is irrelevant whether we define the decomposition order as $U_{BM}U_{AM}$ or $U_{AM}U_{BM}$.

Decomposability naturally extends to open systems. In this case, the evolution is described by a map λ giving the state of the system at time t , i.e., $\rho = \lambda(\rho_0)$. We say that a tripartite map λ is decomposable if there exist maps λ_{AM} and λ_{BM} such that

$$\lambda(\rho) = \lambda_{BM}\lambda_{AM}(\rho), \quad (2)$$

for every ρ . In Appendix A 6, we discuss the consistency of this definition and the one based on unitaries. As expected, a unitary operator is decomposable if and only if the corresponding unitary map is decomposable (general maps are not required).

It is this general notion of decomposability that we will exclude and measure the degree of its exclusion in the coming sections. A number of similar concepts have been introduced before and it is instructive to compare the decomposability with them and note where the novelty is. So-called divisibility asks whether map Λ can be written as $\Lambda_1\Lambda_2$, where neither Λ_1 nor Λ_2 are unitaries [38]. A stronger notion of completely positive (cp) divisibility, studied in the context of Markovian dynamics [39,40], asks whether map Λ_t can be written as the sequence of completely positive maps $\Lambda_t = V_{t,s}\Lambda_s$. Interestingly, the set of cp-divisible maps is not convex [38]. The decomposability that we study here has a specific multipartite structure that has been considered only in Refs. [20,41], which is clearly significant from a physics perspective.

III. ACCESSIBLE MEDIATOR

We first present methods that utilize correlations measured on all three subsystems and devote Sec. IV to eliminating measurements on the mediator. The basic idea is that correlations between subsystem A and subsystems MB together should be bounded in the case of decomposable dynamics because they are effectively established via a process in which the mediator is being transmitted from A to B only *once*. It is therefore expected that the correlations are bounded by the “correlation capacity” of the mediator, i.e., maximal correlations to the mediator alone. Such inequalities for distance-based correlation measures have been derived in Ref. [20] and could also be obtained by manipulating the results of Refs. [3,41]. Our contribution in this section is a generalization to any continuous correlation measure and then quantification of nondecomposability based on the amount of violation of the derived criterion.

A. Detecting nondecomposability

Let us take a correlation quantifier Q that is monotonic under local operations. In Appendix B, we show that the bound in terms of the correlation capacity holds when we additionally assume that the initial state is of the form $\rho_0 = \rho_{AM} \otimes \rho_B$. For such an initial state, the correlations generated by a decomposable map λ admit

$$Q_{A:MB}(\lambda(\rho_0)) \leq \sup_{\sigma_{AM}} Q_{A:M}(\sigma_{AM}), \quad (3)$$

where the bound is derived for any correlation measure Q that is monotonic under local processing. Here, σ_{AM} ranges over all possible joint states of AM . Exchanging the roles of A and B gives rise to another inequality, and the experimenter should choose the one that is violated to detect nondecomposability. This bound is already nontrivial, as we now demonstrate by showing that the maximally entangling map cannot be decomposable. Consider the initial product state $|000\rangle$ and assume that systems A and B are of higher dimension than the mediator, i.e., $d_A = d_B > d_M$. As an exemplary entanglement measure, take the relative entropy of entanglement, E . It is known that its maximum depends on the dimension of the smaller Hilbert space, i.e., $\sup_{\sigma_{AM}} E_{A:M}(\sigma_{AM}) = \log d_M$. According to Eq. (3), no decomposable evolution can produce more entanglement than $\log d_M$. This holds for entanglement $E_{A:MB}$ as well as for $E_{A:B}$ due to the monotonicity of relative entropy under partial trace. Since the dimensions of A and B are larger than the dimension of the mediator, a maximally entangled state between AB cannot be produced by any decomposable map.

Of course, we are interested in extending Eq. (3) to an arbitrary initial state, making the method independent of it. To achieve this aim, we use continuity arguments. Many correlation measures, including relative-entropy-based quantifiers [42], all distance-based measures [43], or convex-roof extensions of asymptotically continuous functions [44], admit a version of continuity in which there exists an invertible monotonically nondecreasing function, g , such that $|Q(x) - Q(y)| \leq g(d(x, y))$, where d is a contractive distance and $\lim_{s \rightarrow 0} g(s) = 0$. This is a refinement of the notion of uniform continuity, where we can bound how much the function varies when we perturb the input. A notable example is logarithmic negativity [45], which is not asymptotically continuous and yet fulfills this notion of continuity. For simplicity, we shall call such functions gd continuous. We prove in Appendix B that correlation quantifiers that are gd continuous are bounded in decomposable dynamics as follows:

$$Q_{A:MB}(\lambda(\rho_0)) \leq \sup_{\sigma_{AM}} Q_{A:M}(\sigma_{AM}) + I_{AM:B}(\rho_0), \quad (4)$$

where $I_{AM:B}(\rho) = \inf_{\sigma_{AM} \otimes \sigma_B} g(d(\rho, \sigma_{AM} \otimes \sigma_B))$ is a measure of the total correlations in the state ρ across the

partition $AM : B$. Indeed, from the properties of g and d , it is easy to verify that this quantity is monotonic under local operations and that it is zero if and only if ρ is a product state across the $AM : B$ partition. Again, an independent inequality is obtained by exchanging A and B .

This bound is also nontrivial and its violation has been demonstrated in Ref. [46], which focused on negativity as a concrete correlation (entanglement) measure. The system under consideration involved two cavity modes, A and B , coupled via two-level atom M . This scenario is particularly well suited to demonstrate the violation, because the dimension of the mediator is as small as it can be, whereas the dimensions of the probes are in principle unbounded.

B. Measuring nondecomposability

Having established witnesses of nondecomposability, we now argue that the amount of violation of Eq. (4) quantifies the nondecomposability. As a measure of nondecomposability, we propose a minimal operator distance from an arbitrary map Λ to the set of decomposable maps, which we denote as DEC:

$$d^{\text{DEC}}(\Lambda) = \inf_{\lambda \in \text{DEC}} D(\Lambda, \lambda). \quad (5)$$

We shall refer to this quantity as the ‘‘degree of nondecomposability.’’ The operator distance D in its definition could be chosen as the one induced by the distance on states

$$D(\Lambda_1, \Lambda_2) = \sup_{\sigma} d(\Lambda_1(\sigma), \Lambda_2(\sigma)), \quad (6)$$

where Λ_1 and Λ_2 are arbitrary maps and σ is any state from the domain of the map. In Appendix B, we demonstrate that violation of Eq. (4) lower bounds the degree of nondecomposability as follows:

$$d^{\text{DEC}}(\Lambda) \geq g^{-1}(Q_{A:MB}(\Lambda(\rho_0)) - B(\rho_0)), \quad (7)$$

where $B(\rho_0)$ is the right-hand side of Eq. (4). Accordingly, any violation of the decomposability criterion in terms of correlations sets a nontrivial lower bound on the distance between the dynamical map and the set of decomposable maps.

C. Quantum simulations

As the first application of the introduced measure, suppose that we would like to simulate the dynamics generated by the Hamiltonian $H = H_{AM} + H_{BM}$. (In fact, this analysis can be generalized to any 2-local Hamiltonian.) Quantum simulators implement a dynamic close to the desired one by truncating the Suzuki-Trotter formula to r Trotter

steps

$$e^{-itH} \approx \left(e^{-i\frac{t}{r}H_{AM}} e^{-i\frac{t}{r}H_{BM}} \right)^r. \quad (8)$$

The error of this approximation can be quantified by the spectral norm (the largest singular value),

$$\left\| e^{-itH} - \left(e^{-i\frac{t}{r}H_{AM}} e^{-i\frac{t}{r}H_{BM}} \right)^r \right\|_{\infty}, \quad (9)$$

and it has been shown in Ref. [23] that in order to make this error smaller than ϵ , the number of Trotter steps has to scale with the norm of the commutator,

$$r = O\left(\frac{t^2}{\epsilon} \|[H_{AM}, H_{BM}]\|_{\infty}\right). \quad (10)$$

Our aim is to provide a lower bound on the commutator norm in terms of correlations and in this way bound the number of required Trotter steps. Recall, after Ref. [23], that for a single Trotter step, we have

$$\|U - U_{AM}U_{BM}\|_{\infty} \leq \frac{t^2}{2} \|[H_{AM}, H_{BM}]\|_{\infty},$$

where $U = e^{-itH}$ and, e.g., $U_{AM} = e^{-itH_{AM}}$. We need to link our methods to the spectral norm. For finite-dimensional systems, all metrics generate the same topology [47], i.e., for any two distances d_1 and d_2 , there exists a constant C such that

$$\frac{1}{C} d_2(\rho, \sigma) \leq d_1(\rho, \sigma) \leq C d_2(\rho, \sigma). \quad (11)$$

In particular, there exists a constant that relates any distance to the trace distance $d_{\text{tr}}(\rho, \sigma) = \frac{1}{2} \|\rho - \sigma\|_1$. Therefore, if a correlation quantifier on finite-dimensional systems is gd continuous with respect to the trace distance, it is also gd continuous with respect to any other distance d . Furthermore, since the trace distance is contractive, Eq. (4) holds for any distance on finite-dimensional systems, at the cost of constants in function g . Accordingly, let us consider the distance induced by the spectral norm $d_{\infty}(\rho, \sigma) = \|\rho - \sigma\|_{\infty}$. We call the corresponding operator distance $D_{\infty}(\Lambda_1, \Lambda_2)$ and the degree of nondecomposability $d_{\infty}^{\text{DEC}}(\Lambda)$. For the connection to the Trotter error, we note the following:

$$d_{\infty}^{\text{DEC}}(U) \leq D_{\infty}(U, U_{AM}U_{BM}) \leq 2\|U - U_{AM}U_{BM}\|_{\infty}, \quad (12)$$

where the first inequality follows from the fact that $d_{\infty}^{\text{DEC}}(U)$ is the shortest distance to the set of decomposable maps and $U_{AM}U_{BM}$ is a particular decomposable map. The second inequality is proven in Appendix B 1. Combining the

two inequalities, we obtain $d_{\infty}^{\text{DEC}}(U) \leq t^2 \|[H_{AM}, H_{BM}]\|_{\infty}$. A concrete example relating the mutual information in a state to the number of Trotter steps is provided in Appendix B 2.

We have therefore shown a direct link between correlations in the system and the number of Trotter steps that one needs to keep the simulation error small. The amount of violation of Eq. (4) lower bounds the degree of nondecomposability and hence the spectral norm of the commutator and, accordingly, sets the number of required Trotter steps. Conversely, if it is possible to simulate U with r Trotter steps to precision ϵ , Eq. (10) shows that the commutator norm is bounded and consequently Eq. (12) implies that the correlations $Q_{A:MB}$ admit an upper bound.

IV. INACCESSIBLE MEDIATOR

An interesting opportunity arises where the nonclassicality of evolution through a mediator could be witnessed without measuring the mediator. Here, we show that this is indeed possible. We start by introducing the necessary concepts and the related mathematical tools and then we present witnesses of nondecomposable evolution based on measurements on AB only. Finally, we establish measures of nondecomposability together with their experimentally friendly lower bounds.

A. Marginal maps

In order to detect nonclassicality of interactions solely through the correlations between the coupled objects, we need the notion of ‘‘marginals’’ of decomposable maps. We propose to introduce it via a related concept of dilation. A dilation of a map $\Lambda : X \rightarrow X$ is an ancillary state σ_R and a map $\tilde{\Lambda} : XR \rightarrow XR$ acting on the system and ancilla, such that

$$\Lambda(\rho) = \text{Tr}_R(\tilde{\Lambda}(\rho \otimes \sigma_R)), \quad (13)$$

for all ρ . Accordingly, our aim is to exclude the existence of a decomposable dilation of the dynamics that are observed on systems AB . In principle, the existence of dilations may depend on the dimension of the Hilbert space of the mediator, which motivates us to introduce *decomposable m -dilation* as follows. A map $\Lambda : AB \rightarrow AB$ has a decomposable m -dilation if there exists a dilation $\tilde{\Lambda} : ABM \rightarrow ABM$ such that $\tilde{\Lambda}$ is decomposable and the dimension of the mediator satisfies $d_M \leq m$. We denote the set of all maps with a decomposable m -dilation as $\overline{\text{DEC}}(m)$.

With these definitions, we can state our goal precisely: we wish to infer whether a map on AB admits any decomposable m -dilation and we wish to do this via measurements of correlations only. If no decomposable dilation exists, we conclude that the interaction generating the map is nonclassical.

B. Detecting nondecomposability

It turns out that one can obtain an interesting condition that witnesses nondecomposability as a simple corollary to Eq. (4). In Appendix C, we prove that any gd -continuous correlation measure Q admits the following bound under the evolution generated by $\lambda \in \overline{\text{DEC}}(m)$:

$$Q_{A:B}(\rho_t) \leq \sup_{\sigma_{XM}} Q_{X:M}(\sigma_{XM}) + I_{A:B}(\rho_0), \quad (14)$$

where $\rho_t = \lambda(\rho_0)$ and we emphasize that $\lambda \in \overline{\text{DEC}}(m)$ acts on AB only. The supremum on the right-hand side runs over all AM or BM states with $d_M \leq m$ and $I_{A:B}(\rho_{AB}) = \inf_{\sigma_A \otimes \sigma_B} g(d(\rho_{AB}, \sigma_A \otimes \sigma_B))$ measures the total correlations across $A : B$. Note that if the correlation measure that we use is not gd continuous, we can still obtain a witness of nondecomposability assuming that we start with a product state. For example, this could be ensured without having access to M by preparing the AB systems in a pure product state.

As an example of using this criterion, note that the maximally entangling maps we have discussed before cannot have any decomposable m -dilation for $m < \min(d_A, d_B)$. A question emerges as to whether there exist evolutions that do not admit decomposable m -dilation even when the dimension of the mediator is unbounded. This is indeed the case. We show in Appendix C 1 that a SWAP operation on two objects (even two qubits) has no decomposable m -dilation for any m . This leads to the conclusion that classical interactions cannot produce a SWAP. The intuitive reason behind this statement is that it takes at least *two* steps to implement swapping with $d_A = d_B = d_M$. We first exchange A and M , then we exchange B and M , and we still must exchange A and M again to complete the implementation. In fact, any AB interaction can be implemented in two steps by first exchanging A and M , applying the interaction on BM , and finally swapping A and M back. The conclusion becomes less unexpected once we realize that SWAP is a highly entangling operation. For example, Alice and Bob can entangle their laboratories by starting with each having local Bell pairs $|\psi_{AA'}^-\rangle \otimes |\psi_{BB'}^-\rangle$ and swapping the AB subsystems.

We wish to give a little more insight into the structure of maps with decomposable dilations. Clearly, the sets are nested: $\overline{\text{DEC}}(m) \subseteq \overline{\text{DEC}}(m+1)$. In fact, the inclusions are strict, as we show in Appendix C 2.

C. Measuring nondecomposability

In the spirit of Sec. III B, we would like to extend Eq. (7) to bound the distance to $\overline{\text{DEC}}(m)$ based solely on correlations measured on systems AB . Of course, the ABM operator distance to DEC and the AB operator distance to $\overline{\text{DEC}}(m)$ are closely related. For contractive distances d on states, we have $D(\Lambda_{ABM}, \lambda_{ABM}) \geq D(\Lambda_{AB}, \lambda_{AB})$, which unfortunately is the opposite of what we need. To overcome this,

we use the so-called completely bounded variant of the operator distance [48]:

$$\mathcal{D}(\Lambda_1, \Lambda_2) = \sup_{\sigma_{XY}} d((\Lambda_1 \otimes \mathbb{1}_Y)(\sigma), (\Lambda_2 \otimes \mathbb{1}_Y)(\sigma)), \quad (15)$$

where $\Lambda_1, \Lambda_2 : X \rightarrow X$ and Y is a finite-dimensional system. The benefit of the completely bounded operator distance is that it behaves nicely on dilations. This makes it easier to jump from the distance to DEC to the distance to $\overline{\text{DEC}}(m)$. Indeed, the completely bounded distance can be written in terms of the dilations as follows:

$$\mathcal{D}(\Lambda_1, \Lambda_2) = \inf_{\tilde{\Lambda}_i} \mathcal{D}(\tilde{\Lambda}_1, \tilde{\Lambda}_2). \quad (16)$$

On the one hand, for contractive distances on states, the left-hand side cannot be larger than the right-hand side. On the other, the bound can be achieved by an exemplary dilation $\tilde{\Lambda}_i = \Lambda_i \otimes \mathbb{1}$.

As a measure of nondecomposability that we will link to the violation of Eq. (14), we propose the analogue of the degree of nondecomposability written in terms of the completely bounded distance:

$$\mathcal{D}^{\overline{\text{DEC}}(m)}(\Lambda_{AB}) = \inf_{\lambda_{AB} \in \overline{\text{DEC}}(m)} \mathcal{D}(\Lambda_{AB}, \lambda_{AB}). \quad (17)$$

With these concepts and tools, it is proven in Appendix C that the amount of violation of Eq. (14) lower bounds the quantity just introduced:

$$\mathcal{D}^{\overline{\text{DEC}}(m)}(\Lambda_{AB}) \geq g^{-1}(Q_{A:B}(\rho_t) - \mathcal{B}(\rho_0)), \quad (18)$$

where \mathcal{B} is the right-hand side of Eq. (14). Note that all these quantities involve states and maps on AB only.

D. Nonclassical gravity

Our second application of these methods is in foundations. A prime example of an inaccessible mediator is a mediating field. The methods described above allow us to make conclusions about the field from the behavior of objects coupled through it. Gravitational interaction is especially interesting from this perspective, as there is no direct experimental evidence of its quantum properties today. As discussed in Sec. I, observation of quantum entanglement between gravitationally coupled masses is a plausible near-future experiment closing this gap [49]. In this section, we show that our methods allow a concise derivation of the nonclassicality witnesses presented in the literature [3,5,6] and lead to new conclusions about the interactions that can be drawn from the observation of considerable gravitational entanglement.

Assume first a completely classical situation in which both states and interactions are classical. Recall that within our framework, this means a zero-discord state at all times,

$D_{AB|M} = 0$ (with one and the same basis on the mediator at all times), and dynamical maps admitting decomposable dilations. As the correlation measure, consider quantum entanglement, measured by the relative entropy of entanglement. Then, the amount of entanglement $A : B$ that can be produced via these classical maps is

$$E_{A:B}(\rho_t) \leq \sup_{\sigma_{XM}} E_{X:M}(\sigma_{X:M}) + I_{A:B}(\rho_0), \quad (19)$$

where the supremum is over all the states of AM or BM allowed in the theory; here, $d_M \leq m$ and $D_{AB|M} = 0$. It is reasonable to assume that the initial state in the laboratory will be close to a product state and we therefore take $I_{A:B}(\rho_0) = 0$. Furthermore, all states admitting $D_{AB|M} = 0$ are disentangled across $A : M$ and $B : M$ and therefore the supremum is also zero. We therefore arrive at the conclusion that entanglement $A : B$ cannot grow and hence observation of any gain implies nonclassical states or nonclassical interactions or both.

If we assume that the interactions are classical (decomposable) but the state might have nonzero discord, then entanglement still satisfies the bound in Eq. (19). Therefore, the observation of a nonzero value of $E_{A:B}$ means that the supremum on the right-hand side is at least equal to this observed value, i.e., the mediator must be capable of being entangled to A or B , and in fact to AB due to monotonicity, to at least the degree that has been measured. Note that this is stronger than saying that the mediator needs to be discarded.

Finally, by violating the bound in Eq. (19), it is possible to demonstrate in the laboratory that unknown interactions are not decomposable. We stress that it is not sufficient to demonstrate that entanglement grows: we have to demonstrate that the entanglement is above a certain threshold. This threshold depends on the dimension of the mediator and we therefore ask how high entanglement can be generated by gravity. The answer depends on the concrete setup via which gravitational interaction is studied. If we take two nearby harmonically trapped masses initially prepared in squeezed states with squeezing parameters s_A and s_B , it has been shown that the gravitational entanglement in terms of logarithmic negativity can be as large as $E_{A:B}^{\max} = |s_A + s_B| / \ln 2$, which holds for large squeezing [8]. Since, in principle, $s_i \rightarrow \infty$, this already shows that gravity cannot be understood as a classical interaction with any finite-dimensional mediator. More practically, the highest optical squeezing achieved today is $s_{A,B} = 1.73$ [50] and assuming that it can be transferred to mechanical systems gives entanglement $E_{A:B}^{\max} \approx 5$ ebits (entangled bits), which would restrict still possible decomposable dilations to use mediators with dimension $m > 2^5$. It is rather unlikely that this amount of entanglement will be observed in the near future, as the time it takes the discussed system to reach $E_{A:B}^{\max}$ in the absence of dissipation

is $t_{\max} = \pi \omega L^3 / 4Gm$, independently of high squeezing, where L is the separation between the masses and ω is the frequency of the trapping potential [8]. For Laser Interferometer Gravitational Wave Observatory (LIGO)–like parameters of masses in the order of $m \sim 1$ kg, $\omega \sim 0.1$ Hz and $L \sim 1$ cm, this time is already in the order of hours and dissipation pushes it further, to tens of hours. Yet, a violation of the unit bound, and hence disproval of classical interactions via a two-level system, which would already be interesting, could be achieved within a second [5, 8, 11, 50].

Another route would be to use gravity to execute dynamics that by other means are known to be nondecomposable. For example, we have shown below Eq. (14) that maximally entangling maps do not admit decomposable dilations for $d_M \leq \min(d_A, d_B)$. The schemes in Refs. [5, 6] indeed use gravity to implement maximal entanglement but only between two-level quantum systems encoded in the path degree of freedom. It would therefore be interesting to determine whether gravity could be used to maximally entangle masses in more paths. Along the same line, we have shown that SWAP does not admit any decomposable dilation, even with an infinite-dimensional mediator. Interestingly, Ref. [24] argues that gravity could implement the SWAP gate. In addition, the time it takes to implement the gate is twice as long as the time it takes to implement the maximally entangling unitary, showing that it is not much more demanding than the entanglement-based method. This provides an alternative witness of quantum properties of gravitational interaction that does not rely on the dimension of the mediator.

V. CONCLUSIONS

We have proposed notions of classicality of mediated interactions (commutativity of Hamiltonians and decomposability of dynamical maps) and introduced their mathematical measures. Our main results are inequalities in terms of any continuous correlation quantifiers with the property that their violations place lower bounds on the amount of introduced nonclassicality. These quantitative methods are therefore experiment ready and applicable in a variety of physical situations due to the minimalistic assumptions under which they are derived. As examples, we have shown that accurate simulations of dynamics with high correlations necessarily require a large number of Trotter steps and that gravitational interaction cannot be understood with the help of commuting particle-field couplings.

ACKNOWLEDGMENTS

We are grateful to the anonymous referees for comments that have allowed us to strengthen the

conclusion about the nonclassicality of gravitational interaction. This work is supported by the Polish National Agency for Academic Exchange NAWA Project No. PPN/PPO/2018/1/00007/U/00001 and the Xiamen University Malaysia Research Fund (Grant No. XMUMRF/2022-C10/IPHY/0002). R.G. is supported by the National Science Centre, Poland, within the QuantERA II program (Grant No. 2021/03/Y/ST2/00178, acronym ExTRaQT) that has received funding from the European Union Horizon 2020 research and innovation program under Grant Agreement No. 101017733. E.P. acknowledges funding from QuantERA/2/2020, an ERA-Net cofund in Quantum Technologies, under the project eDICT. This work is also supported by the Foundation for Polish Science (FNP), IRAP project ICTQT, Contract No. 2018/MAB/5, cofinanced by the EU Smart Growth Operational Programme. M.P. is supported by European Commission via the Horizon Europe research and innovation programme ASPECTS (Grant Agreement No. 101080167).

APPENDIX A: CLASSICALITY AND DECOMPOSABILITY

1. Classical states

For completeness, let us start with elementary relations. A state is said to be classical (or incoherent) if it is diagonal in a preferred basis $\{|m\rangle\}$. A multipartite state is called quantum classical (qc)—or admits vanishing discord, $D_{AB|M} = 0$ —if it can be written as $\rho_{qc} = \sum_m \rho_{AB|m} \otimes \Pi_m$, where $\Pi_m = |m\rangle\langle m|$ is the projector on the preferred basis and the systems are enumerated as in Fig. 1. In words, the whole tripartite state explores only one basis in the Hilbert space of the mediator. Let us introduce a measurement map along the preferred basis, Π , the action of which on an arbitrary input state is to produce an average postmeasurement state: $\Pi(\rho) = \sum_m \Pi_m \rho \Pi_m$. A state ρ is qc if and only if $\rho = \Pi(\rho)$. Alternatively, the definition of classicality can be phrased in terms of commutation with the basis elements.

Proposition 1.—Let $\Pi(X) = \sum_m \Pi_m X \Pi_m$ be a projection map, where $\Pi_m \Pi_{m'} = \delta_{mm'} \Pi_m$. Then,

$$X = \Pi(X) \iff \forall m, [X, \Pi_m] = 0. \quad (\text{A1})$$

Proof.—The “if” direction is trivial. For the “only if” direction, consider the following argument:

$$X \Pi_m = \Pi_m X, \quad (\text{A2})$$

$$X \Pi_m = \Pi_m X \Pi_m, \quad (\text{A3})$$

$$X = \sum_m \Pi_m X \Pi_m = \Pi(X), \quad (\text{A4})$$

where we have multiplied the first equation by Π_m from the right and used $\Pi_m^2 = \Pi_m$, and then we have summed the

second equation over m and used the completeness relation $\sum_m \Pi_m = \mathbb{1}$. ■

2. Classical interactions

The definition of classicality of interactions in terms of commutativity is justified by the following proposition. It shows that the Hamiltonians preserving classicality of states are invariant under dephasing in the preferred basis. The commutativity is then a corollary.

Proposition 2.—Let H be a time-independent Hamiltonian. Then, $H = \Pi(H)$, if and only if for any classical initial state ρ_0 , $\rho_t = e^{-itH} \rho_0 e^{itH}$ is also classical.

Proof.—For the “only if” direction, let us write the assumption explicitly:

$$e^{-itH} \rho_0 e^{itH} = \Pi(e^{-itH} \rho_0 e^{itH}), \quad (\text{A5})$$

$$e^{-itH} [\rho_0, H] e^{itH} = \Pi(e^{-itH} [\rho_0, H] e^{itH}), \quad (\text{A6})$$

where the second line is the time derivative of the first one and ρ_0 denotes the initial (classical) state. By evaluating at $t = 0$, we find that the commutator is invariant:

$$[\rho_0, H] = \Pi([\rho_0, H]). \quad (\text{A7})$$

In particular, taking $\rho_0 = \Pi_m$ shows that for all the basis states:

$$[\Pi_m, H] = \Pi([\Pi_m, H]) = 0, \quad (\text{A8})$$

where the last equation is simple to verify. Applying Proposition 1 proves the claim.

For the “if” direction, from the assumption, the Hamiltonian has the block form $H = \sum_m h_m \otimes \Pi_m$, where h_m acts on all the systems other than the mediator. In this case, the orthonormality of the preferred basis implies

$$e^{\pm itH} = \sum_m e^{\pm it h_m} \otimes \Pi_m. \quad (\text{A9})$$

Accordingly, the initially classical mediator stays classical at all times and the remaining systems evolve conditionally depending on the state of the mediator. ■

In the case of the tripartite systems that we consider, where $H = H_{AM} + H_{BM}$, this shows that classicality is preserved when both H_{AM} and H_{BM} are block diagonal with the same basis on system M , i.e., they commute.

3. Simple eigenstates

As another argument to justify our definition of classicality, we show that it constrains the eigenstates of the Hamiltonian to be fully product, at least when the local terms are nondegenerate.

Proposition 3.—Let H_{AM}, H_{BM} be nondegenerate Hamiltonians. Then, $[H_{AM}, H_{BM}] = 0$ implies that $H = H_{AM} + H_{BM}$ can be diagonalized with fully product states.

Proof.—Let us assume that $[H_{AM}, H_{BM}] = 0$. Note that when a Hermitian matrix A has a nondegenerate spectrum, then all eigenvectors of $A \otimes \mathbb{1}$ must be of the form $|\psi_A\rangle \otimes |\psi_B\rangle$, where $|\psi_A\rangle$ is an eigenvector of A and $|\psi_B\rangle$ is an arbitrary vector. Since $[H_{AM}, H_{BM}] = 0$ implies that there is a common eigenbasis between H_{AM} and H_{BM} , this means that there exists a common eigenbasis for $H = H_{AM} + H_{BM}$ that is a product on $A : MB$ and $AM : B$ at the same time, which proves the claim. ■

4. One-way decomposability

The following proposition gives an example of decomposable unitary that nevertheless cannot be generated by classical interactions.

Proposition 4.—There are no two-qubit unitaries V_{AM}, V_{BM} such that $U_{AM}U_{BM} = V_{BM}V_{AM}$, where

$$U_{AM} = \frac{1}{\sqrt{2}} (\mathbb{1} + iZ_A X_M), \quad (\text{A10})$$

$$U_{BM} = \frac{1}{\sqrt{2}} (\mathbb{1} + iZ_B Z_M), \quad (\text{A11})$$

and Z and X denote Pauli matrices.

Proof.—We prove by contradiction. Suppose that there exist unitaries V_{AM}, V_{BM} such that $U_{AM}U_{BM} = V_{BM}V_{AM}$. Note that we can write U_{AM}, U_{BM} as

$$\begin{aligned} U_{AM} &= |0\rangle\langle 0|_A \otimes \frac{1}{\sqrt{2}} (\mathbb{1}_M + iX_M) \\ &\quad + |1\rangle\langle 1|_A \otimes \frac{1}{\sqrt{2}} (\mathbb{1}_M - iX_M), \end{aligned} \quad (\text{A12})$$

$$\begin{aligned} U_{BM} &= |0\rangle\langle 0|_B \otimes \frac{1}{\sqrt{2}} (\mathbb{1}_M + iZ_M) \\ &\quad + |1\rangle\langle 1|_B \otimes \frac{1}{\sqrt{2}} (\mathbb{1}_M - iZ_M). \end{aligned} \quad (\text{A13})$$

Therefore, the product $U_{AM}U_{BM}$ is given by

$$\begin{aligned} &|00\rangle\langle 00|_{AB} \otimes \frac{1}{2} (\mathbb{1} + iX_M + iY_M + iZ_M) \\ &+ |01\rangle\langle 01|_{AB} \otimes \frac{1}{2} (\mathbb{1} + iX_M - iY_M - iZ_M) \\ &+ |10\rangle\langle 10|_{AB} \otimes \frac{1}{2} (\mathbb{1} - iX_M - iY_M + iZ_M) \\ &+ |11\rangle\langle 11|_{AB} \otimes \frac{1}{2} (\mathbb{1} - iX_M + iY_M - iZ_M). \end{aligned} \quad (\text{A14})$$

Observe that we can always write $V_{AM} = \sum_{i,j=0}^1 |i\rangle\langle j|_A \otimes V_M^{A,ij}$ for some matrices $V_M^{A,ij}$ and similarly for V_{BM} . However, because we have assumed $V_{BM}V_{AM} = U_{AM}U_{BM}$ and

the AB part in Eq. (A14) is expressed solely in terms of projectors, we can express $V_{BM}V_{AM}$ as

$$V_{BM}V_{AM} = \sum_{i,j} |ij\rangle\langle ij|_{AB} \otimes V_M^{B,ij} V_M^{A,ii}, \quad (\text{A15})$$

where each product $V_M^{B,ij} V_M^{A,ii}$ is a unitary on M . Comparing Eqs. (A14) and (A15), we find that

$$V_M^{B,00} V_M^{A,00} = \frac{1}{2} (\mathbb{1} + iX_M + iY_M + iZ_M), \quad (\text{A16})$$

$$V_M^{B,11} V_M^{A,00} = \frac{1}{2} (\mathbb{1} + iX_M - iY_M - iZ_M), \quad (\text{A17})$$

$$V_M^{B,00} V_M^{A,11} = \frac{1}{2} (\mathbb{1} - iX_M - iY_M + iZ_M), \quad (\text{A18})$$

$$V_M^{B,11} V_M^{A,11} = \frac{1}{2} (\mathbb{1} - iX_M + iY_M - iZ_M). \quad (\text{A19})$$

However, this leads to the contradiction

$$\begin{aligned} \begin{pmatrix} 0 & 1 \\ -1 & 0 \end{pmatrix} &= \left(V_M^{B,00} V_M^{A,00} \right) \left(V_M^{B,11} V_M^{A,00} \right)^\dagger \\ &= \left(V_M^{B,00} V_M^{A,11} \right) \left(V_M^{B,11} V_M^{A,11} \right)^\dagger = \begin{pmatrix} 0 & -1 \\ 1 & 0 \end{pmatrix}, \end{aligned} \quad (\text{A20})$$

which completes the proof. ■

5. Classicality and commuting decompositions

Here, we show the relation between the classicality of an interaction and decomposability of the corresponding unitary. In particular, we show the equivalence between the classicality $[H_{AM}, H_{BM}] = 0$ and the existence of a continuous commuting decomposition $U(t) = U_{AM}(t)U_{BM}(t) = U_{BM}(t)U_{AM}(t)$.

Proposition 5.—A one-parameter continuous group of unitaries $U(t) = e^{-itH}$ has a commuting decomposition $U(t) = U_{BM}(t)U_{AM}(t) = U_{AM}(t)U_{BM}(t)$ such that the map $t \mapsto (U_{AM}(t), U_{BM}(t))$ is continuous if and only if there exist Hamiltonians H_{AM} and H_{BM} such that $H = H_{AM} + H_{BM}$ and $[H_{AM}, H_{BM}] = 0$.

Proof.—Using the Baker-Campbell-Hausdorff (BCH) formula [52], one easily sees that if such H_{AM}, H_{BM} exists, then $U(t) = e^{-itH_{AM}} e^{-itH_{BM}} = e^{-itH_{BM}} e^{-itH_{AM}}$, showing that the unitary has a continuous commuting decomposition.

To show the other direction, suppose that the unitary e^{-itH} has a continuous commuting decomposition. Now, let us take t small enough such that $\|U_{AM}(t) - \mathbb{1}\|_\infty, \|U_{BM}(t) - \mathbb{1}\|_\infty < 1$. This ensures that $H_{AM} = i \log U_{AM}(t)/t, H_{BM} = i \log U_{BM}(t)/t$ can be defined through the power series for a matrix logarithm. Using the series representation $\log(\mathbb{1} - X) =$

$-\sum_{n=1}^{\infty} (1/n)X^n$, we note that these interaction Hamiltonians must commute:

$$\begin{aligned}
 [H_{AM}, H_{BM}] &= -\frac{1}{t^2} [\log U_{AM}, \log U_{BM}] \\
 &= -\frac{1}{t^2} \left[\sum_{n=1}^{\infty} \frac{(\mathbb{1} - U_{AM})^n}{n}, \sum_{m=1}^{\infty} \frac{(\mathbb{1} - U_{BM})^m}{m} \right] \\
 &= 0.
 \end{aligned} \tag{A21}$$

Using the BCH formula, we obtain

$$e^{-itH} = e^{-itH_{AM}} e^{-itH_{BM}} = e^{-it(H_{AM}+H_{BM})}. \tag{A22}$$

Differentiating the above expression with respect to t and using the identity $(d/dt)e^{(tA)}|_{t=0} = A$ shows that $H = H_{AM} + H_{BM}$, which proves the claim. ■

6. Consistency

Let us start by recalling the two definitions of decomposability given in the main text.

Definition 1 (unitary).—Let U be a unitary acting on a tripartite system $\mathcal{H}_A \otimes \mathcal{H}_B \otimes \mathcal{H}_M$. U is decomposable if there exist unitaries U_{AM}, U_{BM} such that

$$U_{ABM} = U_{BM}U_{AM}. \tag{A23}$$

Definition 2 (map).—Let λ be a map acting on a tripartite system $\mathcal{H}_A \otimes \mathcal{H}_B \otimes \mathcal{H}_M$. λ is decomposable if there exist maps λ_{AM} and λ_{BM} such that

$$\lambda(\rho) = \lambda_{BM}\lambda_{AM}(\rho). \tag{A24}$$

The following proposition shows that these two definitions are consistent.

Proposition 6.—A unitary U is decomposable if and only if the map $\lambda(\rho) = U\rho U^\dagger$ is decomposable.

Proof.—If U is decomposable, choosing $\lambda_{AM}(\rho) = U_{AM}\rho U_{AM}^\dagger$ and $\lambda_{BM}(\rho) = U_{BM}\rho U_{BM}^\dagger$ shows that λ is also decomposable.

To show the other implication, suppose that there exist two maps λ_{AM} and λ_{BM} such that $U\rho U^\dagger = \lambda_{BM}\lambda_{AM}(\rho)$. It is enough to show that we can choose the maps λ_{AM} and λ_{BM} to be unitaries. This is indeed possible by the following argument. Since $U\rho U^\dagger = \lambda_{BM}\lambda_{AM}(\rho)$, we see that $\sigma \mapsto U^\dagger\lambda_{BM}(\sigma)U$ is a completely positive trace-preserving (CPTP) inverse of λ_{AM} . Since the only CPTP maps that have a CPTP inverse are unitaries [53], we conclude that λ_{AM} must be a unitary map. The fact that λ_{BM} is also unitary follows from $\lambda_{BM}(\rho) = U\lambda_{AM}^\dagger(\rho)U^\dagger$. ■

Another question regarding the consistency between the two definitions concerns unitary dilations: is decomposability of a map equivalent to the existence of a decomposable unitary dilation? This would be desirable, since this

would imply that any decomposable map is generated by some ‘‘classical’’ interaction on a larger system. Here, we show that the implication holds in at least one direction.

Proposition 7.—Let λ be a decomposable map. Then, there exists a Stinespring dilation of λ ,

$$\lambda(\rho_{ABM}) = \text{Tr}_R U_{ABMR}(\rho_{ABM} \otimes \sigma_R) U_{ABMR}^\dagger, \tag{A25}$$

such that U_{ABMR} is decomposable.

Proof.—Since λ is decomposable, there exist maps λ_{AM} and λ_{BM} such that $\lambda = \lambda_{BM}\lambda_{AM}$. Let us denote a Stinespring dilation of λ_{AM} as

$$\lambda_{AM}(\rho_{AM}) = \text{Tr}_{R_A} U_{AMR_A}(\rho_{AM} \otimes \sigma_{R_A}) U_{AMR_A}^\dagger, \tag{A26}$$

where R_A is the purifying system for λ_{AM} . Similarly, λ_{BM} must have a dilation with purifying system R_B . We prove the claim by identifying $R = R_A R_B$, $U_{ABMR} = U_{BMR_B} U_{AMR_A}$, and $\sigma_R = \sigma_{R_A} \otimes \sigma_{R_B}$. ■

7. Out-of-time-ordered correlator

Finally, we comment on the notion of the out-of-time-ordered correlator (OTOC) and its relation to the decomposability. The OTOC is often used to study the spread of correlations in a many-body system [54,55]. Given two observables V and W (usually chosen to be commuting at time $t = 0$), the OTOC is defined as

$$C(t) = -\text{Tr}(\rho_\beta ([V, W(t)]^2)), \tag{A27}$$

where ρ_β is the thermal state at inverse temperature β and $W(t) = e^{-iHt} W e^{iHt}$. Intuitively, it measures the effect of time evolution on the commutator between two initially commuting observables. We show that the OTOC witnesses the nondecomposability, providing an alternative to our methods. In particular, let us choose V as an observable on system A and W on system B . Let us assume that the dynamics are decomposable, i.e., for any t , there exist U_{AM} and U_{BM} such that $e^{-iHt} = U_{BM}U_{AM}$. Noting that $[W, U_{AM}] = 0$, an explicit calculation shows that

$$[V, W(t)] = [V, U_{BM} W U_{BM}^\dagger] \tag{A28}$$

$$= U_{BM} [V, W] U_{BM}^\dagger, \tag{A29}$$

which is zero, since V and W act on different subsystems. Therefore, the measurement of a nonzero OTOC can witness the nondecomposability of the dynamics. It remains to be shown whether such an approach can be extended to quantify the degree of nondecomposability.

APPENDIX B: ACCESSIBLE MEDIATOR

The following proposition proves the ‘‘correlation-capacity’’ bound when the initial state is product $\rho_0 = \rho_{AM} \otimes \rho_B$.

Proposition 8.—Let λ be a decomposable map. Any correlation measure satisfies

$$Q_{A:MB}(\lambda(\rho_{AM} \otimes \rho_B)) \leq \sup_{\sigma_{AM}} Q_{A:M}(\sigma_{AM}). \quad (\text{B1})$$

Proof.—By assumption, $\lambda = \lambda_{BM}\lambda_{AM}$. The bound follows solely from monotonicity of correlations under local operations:

$$\begin{aligned} Q_{A:MB}(\lambda(\rho_{AM} \otimes \rho_B)) &= Q_{A:MB}(\lambda_{BM}\lambda_{AM}(\rho_{AM} \otimes \rho_B)) \\ &\leq Q_{A:MB}(\lambda_{AM}(\rho_{AM} \otimes \rho_B)). \end{aligned} \quad (\text{B2})$$

Since Q is monotonic under local operations, it must be invariant under invertible local operations. In particular, adding or discarding an uncorrelated system does not change the value of Q . In our case, system B is completely uncorrelated and therefore $Q_{A:MB}(\lambda_{AM}(\rho_{AM} \otimes \rho_B)) = Q_{A:M}(\lambda_{AM}(\rho_{AM}))$. Of course, the last quantity is upper bounded by the supremum over all states. ■

For a general initial state, we have the following bound by continuity.

Proposition 9.—Let λ be a decomposable map and let ρ be any tripartite quantum state. Any gd -continuous correlation measure satisfies

$$Q_{A:MB}(\lambda(\rho)) \leq \sup_{\sigma_{AM}} Q_{A:M}(\sigma_{AM}) + I_{AM:B}(\rho), \quad (\text{B3})$$

where $I_{AM:B}(\rho) = \inf_{\sigma_{AM} \otimes \sigma_B} g(d(\rho, \sigma_{AM} \otimes \sigma_B))$ is a measure of total correlations in the state ρ across the partition $AM : B$.

Proof.—We bound the difference in correlations between an arbitrary state and the product state using gd -continuity:

$$\begin{aligned} |Q_{A:MB}(\lambda(\rho)) - Q_{A:MB}(\lambda(\sigma_{AM} \otimes \sigma_B))| \\ \leq g(d(\lambda(\rho), \lambda(\sigma_{AM} \otimes \sigma_B))) \\ \leq g(d(\rho, \sigma_{AM} \otimes \sigma_B)), \end{aligned} \quad (\text{B4})$$

where in the last line we have used the fact that g is monotonic and d contractive. The derived inequality holds for any $\sigma_{AM} \otimes \sigma_B$ —in particular, for the one achieving the infimum of $I_{AM:B}(\rho)$ —leading to

$$Q_{A:MB}(\lambda(\rho)) \leq Q_{A:MB}(\lambda(\sigma_{AM} \otimes \sigma_B)) + I_{AM:B}(\rho). \quad (\text{B5})$$

In the last step, we use Proposition 8 to bound the first term on the right. ■

In order to simplify the notation, let us denote the bound on correlations due to decomposable dynamics as $B(\rho) = \sup_{\sigma_{AM}} Q_{A:M}(\sigma_{AM}) + I_{AM:B}(\rho)$ and the state at time t as $\rho_t = \Lambda(\rho_0)$.

Proposition 10.—The degree of nondecomposability $d^{\text{DEC}}(\Lambda)$ is lower bounded as follows:

$$d^{\text{DEC}}(\Lambda) \geq g^{-1}(Q_{A:MB}(\rho_t) - B(\rho_0)). \quad (\text{B6})$$

Proof.—We will prove the theorem by combining the continuity bounds with the statement of Proposition 9. Consider a fixed, but arbitrary, decomposable map λ . Due to gd -continuity, we write

$$\begin{aligned} Q_{A:MB}(\rho_t) - Q_{A:MB}(\lambda(\rho_0)) &\leq |Q_{A:MB}(\rho_t) - Q_{A:MB}(\lambda(\rho_0))| \\ &\leq g(d(\rho_t, \lambda(\rho_0))). \end{aligned} \quad (\text{B7})$$

We rearrange and use the bound in Proposition 9:

$$\begin{aligned} Q_{A:MB}(\rho_t) &\leq Q_{A:MB}(\lambda(\rho_0)) + g(d(\rho_t, \lambda(\rho_0))) \\ &\leq B(\rho_0) + g(d(\rho_t, \lambda(\rho_0))). \end{aligned} \quad (\text{B8})$$

The amount of violation is now brought to the left-hand side and below we use the fact that g is invertible and take the supremum over states ρ_0 to identify the degree of nondecomposability:

$$\begin{aligned} Q_{A:MB}(\rho_t) - B(\rho_0) &\leq g(d(\rho_t, \lambda(\rho_0))) \\ g^{-1}(Q_{A:MB}(\rho_t) - B(\rho_0)) &\leq d(\rho_t, \lambda(\rho_0)), \\ g^{-1}(Q_{A:MB}(\rho_t) - B(\rho_0)) &\leq d^{\text{DEC}}(\Lambda), \end{aligned} \quad (\text{B9})$$

which proves the claim. ■

1. Spectral norm

We link the operator norm of unitary maps with the spectral distance between them.

Lemma 1.—Let U, V be unitaries. Then $D_\infty(U, V) \leq 2 \|U - V\|_\infty$.

Proof.—By simple algebra, we verify

$$U\rho U^\dagger - V\rho V^\dagger = \frac{1}{2}(U - V)\rho(U + V)^\dagger \quad (\text{B10})$$

$$+ \frac{1}{2}(U + V)\rho(U - V)^\dagger, \quad (\text{B11})$$

where ρ is a density matrix. Taking the spectral norm on both sides, we obtain

$$\|U\rho U^\dagger - V\rho V^\dagger\|_\infty \quad (\text{B12})$$

$$= \left\| \frac{1}{2}(U - V)\rho(U + V)^\dagger + \frac{1}{2}(U + V)\rho(U - V)^\dagger \right\|_\infty \quad (\text{B13})$$

$$\leq \frac{1}{2} \|(U - V)\rho(U + V)^\dagger\|_\infty + \frac{1}{2} \|(U + V)\rho(U - V)^\dagger\|_\infty \quad (\text{B14})$$

$$\leq \|U - V\|_\infty \|\rho\|_\infty \|U + V\|_\infty \quad (\text{B15})$$

$$\leq 2 \|U - V\|_\infty, \quad (\text{B16})$$

where we have used the triangle inequality and submultiplicativity of the spectral norm, $\|AB\|_\infty \leq \|A\|_\infty \|B\|_\infty$. Using the bounds $\|\rho\|_\infty \leq \|\rho\|_1 = 1$ and $\|U + V\|_\infty \leq \|U\|_\infty + \|V\|_\infty = 2$ on the last inequality finishes the proof. ■

2. Correlations and the number of Trotter steps

As a concrete illustration, let us relate the mutual information in a state to number of Trotter steps needed. In this case, we can use continuity bounds for von Neumann entropy to conclude that if $\frac{1}{2} \|\rho - \sigma\|_1 = \epsilon$, then [56,57]

$$|I_{A:MB}(\rho) - I_{A:MB}(\sigma)| \leq 2\epsilon \log(d_A d_M d_B - 1) + 3\eta(\epsilon), \quad (\text{B17})$$

where $\eta(x) = -x \log x - (1-x) \log(1-x)$ is the binary entropy. We now bound the first term using $\epsilon \leq \sqrt{\epsilon}$, recalling that ϵ is small, and the second term using $\eta(\epsilon) \leq \sqrt{\epsilon}$ to arrive at

$$|I_{A:MB}(\rho) - I_{A:MB}(\sigma)| \leq 5 \log(d_A d_M d_B) \sqrt{\epsilon}. \quad (\text{B18})$$

Furthermore, since $\|X\|_1 \leq \text{rank} X \cdot \|X\|_\infty$, we have

$$|I_{A:MB}(\rho) - I_{A:MB}(\sigma)| \leq C \sqrt{\|\rho - \sigma\|_\infty}, \quad (\text{B19})$$

where $C = 5\sqrt{2} \log(d_A d_M d_B) \sqrt{d_A d_M d_B}$ is a dimension-dependent constant. This means that we can choose $g(s) = C\sqrt{s}$ to show that mutual information is *gd* continuous with respect to the spectral distance and the inverse is $g^{-1}(s) = (s/C)^2$ when $s \geq 0$. Combining this with the discussion in Sec. III C and Proposition 10, we finally obtain

$$\left(\frac{I_{A:MB}(e^{-itH} \rho_0 e^{itH}) - B(\rho_0)}{C} \right)^2 \leq t^2 \| [H_{AM}, H_{BM}] \|_\infty, \quad (\text{B20})$$

when $I_{A:MB}(e^{-itH} \rho_0 e^{itH}) \geq B(\rho_0)$. This means that the number of Trotter steps needed to guarantee an ϵ error is

$$r \geq O \left(\frac{(I_{A:MB}(e^{-itH} \rho_0 e^{itH}) - B(\rho_0))^2}{\epsilon} \right). \quad (\text{B21})$$

Note that while we have used some relaxations to derive this bound, we still obtain nontrivial quantitative statements relating the correlations in the system and the commutator norm. In particular, while the quadratic power in the mutual information is suboptimal, a linear bound cannot exist due to the tightness of the entropic continuity bounds.

APPENDIX C: INACCESSIBLE MEDIATOR

First, we derive a necessary condition on maps admitting a decomposable *m*-dilation.

Proposition 11.—A *gd*-continuous correlation measure Q admits the following bound under the evolution generated by $\lambda \in \overline{\text{DEC}}(m)$:

$$Q_{A:B}(\lambda(\rho_{AB})) \leq \sup_{\sigma_{AM}} Q_{A:M}(\sigma_{AM}) + I_{A:B}(\rho_{AB}), \quad (\text{C1})$$

where the supremum is over all *AM* states with the dimension $d_M \leq m$ and $I_{A:B}(\rho_{AB}) = \inf_{\sigma_A \otimes \sigma_B} g(d(\rho_{AB}, \sigma_A \otimes \sigma_B))$ measures the total correlations across $A : B$.

Proof.—Consider the following argument:

$$\begin{aligned} Q_{A:B}(\lambda(\rho_{AB})) &\leq Q_{A:MB}(\tilde{\lambda}(\rho_{AB} \otimes \sigma_M)) \\ &\leq \sup_{\sigma_{AM}} Q_{A:M}(\sigma_{AM}) + I_{AM:B}(\rho_{AB} \otimes \sigma_M) \\ &= \sup_{\sigma_{AM}} Q_{A:M}(\sigma_{AM}) + I_{A:B}(\rho_{AB}), \end{aligned} \quad (\text{C2})$$

where the first line follows from the monotonicity of Q and the existence of a decomposable *m*-dilation, the second line restates Proposition 9 restricted to an *m*-dimensional mediator, and the last line follows from the fact that tracing out an uncorrelated particle is a reversible process and hence we have equality. ■

Note that we have assumed that any map with a decomposable dilation starts with the joint *ABM* state of a product form $\rho_{AB} \otimes \sigma_M$. Although this is a restrictive condition, it has been shown that this is essentially the only consistent choice if we require that the dynamics can start from any *AB* state and the assignment is linear [58].

Next, we show that the violation of the inequality provides a bound on the degree of nondecomposability.

Proposition 12.—The degree of nondecomposability satisfies the following lower bound:

$$\mathcal{D}^{\overline{\text{DEC}}(m)}(\Lambda_{AB}) \geq g^{-1}(Q_{A:B}(\Lambda_{AB}(\rho_{AB})) - \mathcal{B}(\rho_{AB})),$$

where \mathcal{B} is the two-particle version of the bound B ,

$$\mathcal{B}(\rho_{AB}) = \sup_{\sigma_{AM}} Q_{A:M}(\sigma_{AM}) + I_{A:B}(\rho_{AB}),$$

and the supremum over σ_{AM} assumes that the dimension of the mediator satisfies $d_M \leq m$.

Proof.—Consider a fixed but arbitrary dilation $\tilde{\Lambda}$ of the map Λ_{AB} and a decomposable map $\tilde{\lambda}$ (acting on all subsystems) that is a dilation of the map $\lambda_{AB} \in \overline{\text{DEC}}(m)$. The same steps as in Proposition 10 and Eqs. (B7) and (B8) lead to

the following inequality:

$$g^{-1}(Q_{A:B}(\Lambda(\rho_{AB})) - \mathcal{B}(\rho_{AB})) \leq d(\tilde{\Lambda}(\rho_{AB} \otimes \sigma_M), \tilde{\lambda}(\rho_{AB} \otimes \sigma_M)), \quad (C3)$$

where we have used monotonicity and the definition of dilation to write $Q_{A:B}(\Lambda(\rho_{AB})) \leq Q_{A:MB}(\tilde{\Lambda}(\rho_{AB} \otimes \sigma_M))$ and invariance of total correlations under tracing out an uncorrelated system in the bound B , which therefore becomes \mathcal{B} . The left-hand side is accordingly fully expressed in terms of bipartite quantities and we now similarly bound the right-hand side.

To show the claim, it is enough to show that the distance on the right-hand side gives a lower bound to the degree of nondecomposability. By taking the supremum over ρ_{AB} , the right hand side is upper bounded by the operator distance:

$$\sup_{\rho_{AB}} d(\tilde{\Lambda}(\rho_{AB} \otimes \sigma_M), \tilde{\lambda}(\rho_{AB} \otimes \sigma_M)) \leq D(\tilde{\Lambda}, \tilde{\lambda}), \quad (C4)$$

where the inequality is due to the optimization over states of AB only, not over all three systems. Analogous reasons show that the operator distance is upper bounded by the completely bounded distance

$$D(\tilde{\Lambda}, \tilde{\lambda}) \leq \mathcal{D}(\tilde{\Lambda}, \tilde{\lambda}). \quad (C5)$$

This time, because the right-hand side involves additional optimization over the ancillary states. Finally, note that this reasoning holds for any dilation and the best bound is obtained by taking the dilations producing the infimum: $\inf_{\lambda_{AB} \in \overline{\text{DEC}}(m)} \inf_{\tilde{\Lambda}, \tilde{\lambda}} \mathcal{D}(\tilde{\Lambda}, \tilde{\lambda}) = \inf_{\lambda_{AB} \in \overline{\text{DEC}}(m)} \mathcal{D}(\Lambda_{AB}, \lambda_{AB})$. ■

With these tools, we now investigate the structure of maps that admit decomposable m -dilations.

1. Nondecomposability of swapping

Proposition 13.—The map SWAP on two qubits has no decomposable m -dilation, for any m .

Proof.—We will prove this by contradiction. Suppose that SWAP has a decomposable m -dilation. Let us compare the action of SWAP on $|00\rangle_{AB}$ and on $|01\rangle_{AB}$. By definition, there exist two maps, λ_{AM} and λ_{BM} , and some initial state σ_M such that

$$|00\rangle\langle 00|_{AB} = \text{SWAP}(|00\rangle\langle 00|_{AB}) = \text{Tr}_M \lambda_{BM} \lambda_{AM} (|00\rangle\langle 00|_{AB} \otimes \sigma_M), \quad (C6)$$

$$|10\rangle\langle 10|_{AB} = \text{SWAP}(|01\rangle\langle 01|_{AB}) = \text{Tr}_M \lambda_{BM} \lambda_{AM} (|01\rangle\langle 01|_{AB} \otimes \sigma_M). \quad (C7)$$

Let us define $\sigma_{AM}^0 = \lambda_{AM}(|0\rangle\langle 0|_A \otimes \sigma_M)$. By Eqs. (C6) and (C7), we have

$$|0\rangle\langle 0|_A = \text{Tr}_B \text{SWAP}(|00\rangle\langle 00|_{AB}) = \text{Tr}_{BM} \lambda_{BM} (|0\rangle\langle 0|_B \otimes \sigma_{AM}^0), \quad (C8)$$

$$|1\rangle\langle 1|_A = \text{Tr}_B \text{SWAP}(|01\rangle\langle 01|_{AB}) = \text{Tr}_{BM} \lambda_{BM} (|1\rangle\langle 1|_B \otimes \sigma_{AM}^0). \quad (C9)$$

But because λ_{BM} is trace preserving and Tr_B factors out when applied to product states, we have

$$\begin{aligned} \text{Tr}_{BM} \lambda_{BM} (|0\rangle\langle 0|_B \otimes \sigma_{AM}^0) &= \text{Tr}_{BM} (|0\rangle\langle 0|_B \otimes \sigma_{AM}^0) \\ &= \text{Tr}_M \sigma_{AM}^0 \\ &= \text{Tr}_{BM} \lambda_{BM} (|1\rangle\langle 1|_B \otimes \sigma_{AM}^0). \end{aligned} \quad (C10)$$

Combining this with Eqs. (C8) and (C9), we obtain

$$|0\rangle\langle 0|_A = \text{Tr}_{BM} \lambda_{BM} (|0\rangle\langle 0|_B \otimes \sigma_{AM}^0) \quad (C11)$$

$$= \text{Tr}_{BM} \lambda_{BM} (|1\rangle\langle 1|_B \otimes \sigma_{AM}^0) \quad (C12)$$

$$= |1\rangle\langle 1|_A, \quad (C13)$$

which is clearly a contradiction. ■

2. Strict inclusions

Proposition 14.—The inclusion $\overline{\text{DEC}}(m) \subsetneq \overline{\text{DEC}}(m+1)$ is strict for all m .

Proof.—Let us fix m and take $d_A = d_B > d_M = m$. Let $\lambda_m(\rho_{AB}) = \text{Tr}_M \text{SWAP}_{BM} \lambda_{AM}(\rho_{AB} \otimes |0\rangle\langle 0|_M)$, where λ_{AM} is a maximally entangling map. By this construction, λ_m has a decomposable m -dilation, i.e., $\lambda_m \in \overline{\text{DEC}}(m)$. Choosing $\rho_{AB} = |00\rangle\langle 00|_{AB}$ and \mathcal{Q} to be the relative entropy of entanglement, we obtain $E_{A:B}(\lambda_m(\rho_{AB})) = \log m$, whereas by Proposition 11, for all maps $\lambda \in \overline{\text{DEC}}(m-1)$ we have (recall that ρ_{AB} is product)

$$E_{A:B}(\lambda(\rho_{AB})) \leq \sup_{\sigma_{AM}} E_{A:M}(\sigma_{AM}) + I_{A:B}(\rho_{AB}) \quad (C14)$$

$$= \log(m-1). \quad (C15)$$

Therefore, $\lambda_m \notin \overline{\text{DEC}}(m-1)$, and the claim is shown. ■

-
- [1] S. Sahling, G. Remenyi, C. Paulsen, P. Monceau, V. Saligrama, C. Marin, A. Revcolevschi, L. P. Regnault, S. Raymond, and J. E. Lorenzo, Experimental realization of long-distance entanglement between spins in antiferromagnetic quantum spin chains, *Nat. Phys.* **11**, 255 (2015).
 [2] J. D. Thompson, B. M. Zwickl, A. M. Jayich, F. Marquardt, S. M. Girvin, and J. G. E. Harris, Strong dispersive coupling

- of a high-finesse cavity to a micromechanical membrane, *Nature* **452**, 72 (2008).
- [3] T. Krisnanda, M. Zuppardo, M. Paternostro, and T. Paterek, Revealing nonclassicality of inaccessible objects, *Phys. Rev. Lett.* **119**, 120402 (2017).
- [4] S. Pal, P. Batra, T. Krisnanda, T. Paterek, and T. S. Mahesh, Experimental localisation of quantum entanglement through monitored classical mediator, *Quantum* **5**, 478 (2021).
- [5] S. Bose, A. Mazumdar, G. W. Morley, H. Ulbricht, M. Toroš, M. Paternostro, A. A. Geraci, P. F. Barker, M. S. Kim, and G. Milburn, Spin entanglement witness for quantum gravity, *Phys. Rev. Lett.* **119**, 240401 (2017).
- [6] C. Marletto and V. Vedral, Gravitationally induced entanglement between two massive particles is sufficient evidence of quantum effects in gravity, *Phys. Rev. Lett.* **119**, 240402 (2017).
- [7] A. Al Balushi, W. Cong, and R. B. Mann, Optomechanical quantum Cavendish experiment, *Phys. Rev. A* **98**, 043811 (2018).
- [8] T. Krisnanda, G. Y. Tham, M. Paternostro, and T. Paterek, Observable quantum entanglement due to gravity, *npj Quantum Inf.* **6**, 12 (2020).
- [9] S. Qvarfort, S. Bose, and A. Serafini, Mesoscopic entanglement through central-potential interactions, *J. Phys. B: At., Mol. Opt. Phys.* **53**, 235501 (2020).
- [10] T. W. van de Kamp, R. J. Marshman, S. Bose, and A. Mazumdar, Quantum gravity witness via entanglement of masses: Casimir screening, *Phys. Rev. A* **102**, 062807 (2020).
- [11] S. Rijavec, M. Carlesso, A. Bassi, V. Vedral, and C. Marletto, Decoherence effects in non-classicality tests of gravity, *New J. Phys.* **23**, 043040 (2021).
- [12] K. Kustura, C. Gonzalez-Ballester, A. D. L. R. Sommer, N. Meyer, R. Quidant, and O. Romero-Isart, Mechanical squeezing via unstable dynamics in a microcavity, *Phys. Rev. Lett.* **128**, 143601 (2022).
- [13] T. Weiss, M. Roda-Llodes, E. Torrontegui, M. Aspelmeyer, and O. Romero-Isart, Large quantum delocalization of a levitated nanoparticle using optimal control: Applications for force sensing and entangling via weak forces, *Phys. Rev. Lett.* **127**, 023601 (2021).
- [14] D. Carney, H. Müller, and J. M. Taylor, Using an atom interferometer to infer gravitational entanglement generation, *PRX Quantum* **2**, 030330 (2021).
- [15] J. S. Pedernales, K. Streltsov, and M. B. Plenio, Enhancing gravitational interaction between quantum systems by a massive mediator, *Phys. Rev. Lett.* **128**, 110401 (2022).
- [16] R. J. Marshman, A. Mazumdar, R. Folman, and S. Bose, Constructing nano-object quantum superpositions with a Stern-Gerlach interferometer, *Phys. Rev. Res.* **4**, 023087 (2022).
- [17] M. Christodoulou, A. Di Biagio, M. Aspelmeyer, Č. Brukner, C. Rovelli, and R. Howl, Locally mediated entanglement in linearized quantum gravity, *Phys. Rev. Lett.* **130**, 100202 (2023).
- [18] T. Krisnanda, C. Marletto, V. Vedral, M. Paternostro, and T. Paterek, Probing quantum features of photosynthetic organisms, *npj Quantum Inf.* **4**, 60 (2018).
- [19] W. Y. Kon, T. Krisnanda, P. Sengupta, and T. Paterek, Nonclassicality of spin structures in condensed matter: An analysis of $\text{Sr}_{14}\text{Cu}_{24}\text{O}_{41}$, *Phys. Rev. B* **100**, 235103 (2019).
- [20] T. Krisnanda, R. Ganardi, S.-Y. Lee, J. Kim, and T. Paterek, Detecting nondecomposability of time evolution via extreme gain of correlations, *Phys. Rev. A* **98**, 052321 (2018).
- [21] S. Lloyd, Universal quantum simulators, *Science* **273**, 1073 (1996).
- [22] D. Poulin, M. B. Hastings, D. Wecker, N. Wiebe, A. C. Doberty, and M. Troyer, The Trotter step size required for accurate quantum simulation of quantum chemistry, *Quantum Inf. Comput.* **15**, 361 (2015).
- [23] A. M. Childs, Y. Su, M. C. Tran, N. Wiebe, and S. Zhu, Theory of Trotter error with commutator scaling, *Phys. Rev. X* **11**, 011020 (2021).
- [24] L. Lami, J. S. Pedernales, and M. B. Plenio, Testing the quantumness of gravity without entanglement, *ArXiv:2302.03075* (2023).
- [25] R. Howl, V. Vedral, D. Naik, M. Christodoulou, C. Rovelli, and A. Iyer, Non-Gaussianity as a signature of a quantum theory of gravity, *PRX Quantum* **2**, 010325 (2021).
- [26] P. Sidajaya, W. Cong, and V. Scarani, Possibility of detecting the gravity of an object frozen in a spatial superposition by the Zeno effect, *Phys. Rev. A* **106**, 042217 (2022).
- [27] C. Marletto and V. Vedral, The quantum totalitarian property and exact symmetries, *AVS Quantum Sci.* **4**, 015603 (2022).
- [28] K. Modi, A. Brodutch, H. Cable, T. Paterek, and V. Vedral, The classical-quantum boundary for correlations: Discord and related measures, *Rev. Mod. Phys.* **84**, 1655 (2012).
- [29] A. Streltsov, G. Adesso, and M. B. Plenio, Colloquium: Quantum coherence as a resource, *Rev. Mod. Phys.* **89**, 041003 (2017).
- [30] T. S. Cubitt, F. Verstraete, W. Dür, and J. I. Cirac, Separable states can be used to distribute entanglement, *Phys. Rev. Lett.* **91**, 037902 (2003).
- [31] A. Streltsov, H. Kampermann, and D. Bruß, Quantum cost for sending entanglement, *Phys. Rev. Lett.* **108**, 250501 (2012).
- [32] T. K. Chuan, J. Maillard, K. Modi, T. Paterek, M. Paternostro, and M. Piani, Quantum discord bounds the amount of distributed entanglement, *Phys. Rev. Lett.* **109**, 070501 (2012).
- [33] X.-D. Yang, A.-M. Wang, X.-S. Ma, F. Hu, H. You, and W.-Q. Niu, Experimental creation of entanglement using separable states, *Chin. Phys. Lett.* **22**, 279 (2015).
- [34] A. Fedrizzi, M. Zuppardo, G. G. Gillett, M. A. Broome, M. P. Almeida, M. Paternostro, A. G. White, and T. Paterek, Experimental distribution of entanglement with separable carriers, *Phys. Rev. Lett.* **111**, 230504 (2013).
- [35] C. E. Vollmer, D. Schulze, T. Eberle, V. Händchen, J. Fiurášek, and R. Schnabel, Experimental entanglement distribution by separable states, *Phys. Rev. Lett.* **111**, 230505 (2013).
- [36] C. Peuntinger, V. Chille, L. Mišta, N. Korolkova, M. Förtsch, J. Korger, C. Marquardt, and G. Leuchs, Distributing entanglement with separable states, *Phys. Rev. Lett.* **111**, 230506 (2013).

- [37] A. D. Biagio, R. Howl, C. Brukner, C. Rovelli, and M. Christodoulou, Relativistic locality can imply subsystem locality, [ArXiv:2305.05645](#) (2023).
- [38] M. M. Wolf and J. I. Cirac, Dividing quantum channels, *Commun. Math. Phys.* **279**, 147 (2008).
- [39] G. Lindblad, On the generators of quantum dynamical semigroups, *Commun. Math. Phys.* **48**, 119 (1976).
- [40] V. Gorini, A. Kossakowski, and E. C. G. Sudarshan, Completely positive dynamical semigroups of N -level systems, *J. Math. Phys.* **17**, 821 (1976).
- [41] A. Streltsov, R. Augusiak, M. Demianowicz, and M. Lewenstein, Progress towards a unified approach to entanglement distribution, *Phys. Rev. A* **92**, 012335 (2015).
- [42] M. J. Donald and M. Horodecki, Continuity of relative entropy of entanglement, *Phys. Lett. A* **264**, 257 (1999).
- [43] K. Modi, T. Paterek, W. Son, V. Vedral, and M. Williamson, Unified view of quantum and classical correlations, *Phys. Rev. Lett.* **104**, 080501 (2010).
- [44] B. Synak-Radtke and M. Horodecki, On asymptotic continuity of functions of quantum states, *J. Phys. A: Math. Gen.* **39**, L423 (2006).
- [45] M. B. Plenio, Logarithmic negativity: A full entanglement monotone that is not convex, *Phys. Rev. Lett.* **95**, 090503 (2005).
- [46] R. Ganardi, M. Miller, T. Paterek, and M. Żukowski, Hierarchy of correlation quantifiers comparable to negativity, *Quantum* **6**, 654 (2022).
- [47] W. Rudin, ed. *Functional Analysis* (McGraw-Hill, New York, 1991).
- [48] V. Paulsen, *Completely Bounded Maps and Operator Algebras* (Cambridge University Press, New York, 2003).
- [49] M. Aspelmeyer, in *From Quantum to Classical: Essays in Honour of H.-Dieter Zeh*, edited by C. Kiefer (Springer International Publishing, Cham, 2022), p. 85.
- [50] H. Vahlbruch, M. Mehmet, K. Danzmann, and R. Schnabel, Detection of 15 dB squeezed states of light and their application for the absolute calibration of photoelectric quantum efficiency, *Phys. Rev. Lett.* **117**, 110801 (2016).
- [51] A. Kumar, T. Krisnanda, P. Arumugam, and T. Paterek, Continuous-variable entanglement through central forces: Application to gravity between quantum masses, *Quantum* **7**, 1008 (2023).
- [52] B. C. Hall, *Lie Groups, Lie Algebras, and Representations* (Springer International Publishing, Cham, 2015).
- [53] A. Nayak and P. Sen, Invertible quantum operations and perfect encryption of quantum states, *Quantum Inf. Comput.* **7**, 103 (2007).
- [54] B. Swingle, Unscrambling the physics of out-of-time-order correlators, *Nat. Phys.* **14**, 988 (2018).
- [55] A. I. Larkin and Y. N. Ovchinnikov, Quasiclassical method in the theory of superconductivity, *Sov. Phys. JETP* **28**, 1200 (1969).
- [56] K. M. R. Audenaert, A sharp continuity estimate for the von Neumann entropy, *J. Phys. A: Math. Theor.* **40**, 8127 (2007).
- [57] A. Winter, Tight uniform continuity bounds for quantum entropies: Conditional entropy, relative entropy distance and energy constraints, *Commun. Math. Phys.* **347**, 291 (2016).
- [58] P. Pechukas, Reduced dynamics need not be completely positive, *Phys. Rev. Lett.* **73**, 1060 (1994).